Electronic supporting information for:

Shedding light on the copper-catalysed diboron(4) reduction of nitrous oxide

Thomas M. Hood,[a] Andrew C. C. Ward,[a] Tobias Krämer,[b,*] and Adrian B. Chaplin[a,*]

[a] *Department of Chemistry, University of Warwick, Gibbet Hill Road, Coventry, CV4 7AL, UK*
E-mail: a.b.chaplin@warwick.ac.uk
[b] *School of Chemistry, Trinity College Dublin, The University of Dublin, Dublin 2, Ireland*
E-mail: kraemert@tcd.ie

Table of contents

1 General methods

All manipulations were performed under an atmosphere of argon using Schlenk and glove box techniques unless otherwise stated. Room temperature is approximately 293 K. Glassware was oven dried at 150 °C overnight and flame-dried under vacuum prior to use. Molecular sieves were activated by heating at 300 °C *in vacuo* overnight. Hexane was sparged with Ar for two hours, dried and stored over 3 Å molecular sieves. Benzene and toluene were dried over sodium, distilled, freeze-pump-thaw degassed and stored over 3 Å molecular sieves. C_6D_6 and d_8-toluene were dried over sodium, distilled, freeze-pump-thaw degassed and stored over a potassium mirror. Diethyl ether and THF were dried over sodium/benzophenone overnight, vacuum distilled and stored over 3 Å molecular sieves. d_8-THF was dried over sodium overnight, vacuum distilled, freeze-pump-thaw degassed and stored over 3 Å molecular sieves. $SiMe_4$ and C_6D_{12} were dried over Na/K_2 alloy overnight, vacuum distilled, freeze-pump-thaw degassed and stored over a potassium mirror. [Rh(PEt$_3$)$_3$(OPh)] **1***,[1] [Cu(SIPr)(O*t*Bu)] **2***,[2] [Cu(IPr)(O*t*Bu)] **3***,[3] [Cu(SIMes)(O*t*Bu)] **4***,[4] [Cu(IMes)(O*t*Bu)] **5***,[3,5] copper(I) *tert*-butoxide **6***,[6] [Rh(PNP-*i*Pr)Cl],[7] [Rh(COE)$_2$Cl]$_2$,[8] and Xantphos-*i*Pr (POP-*i*Pr)[9] were prepared using published procedures. The preparation of **2***–**5*** typically involved reaction of the corresponding formamidinium salt with copper(I) chloride in the presence of base, followed by salt metathesis with potassium *tert*-butoxide. TMEDA and 2,6-lutidine were dried over CaH_2 overnight, vacuum distilled, freeze-pump-thaw degassed and stored over 3 Å molecular sieves. The concentration of *n*BuLi was determined by titration using ^{1}H NMR spectroscopy.[10] Bis(pinacolato)diboron, bis(catecholato)diboron and bis(neopentyl glycolato)diboron were purchased from ABCR and stored under argon. Pinacolborane was purchased from Merck, distilled, and stored under argon. Nitrous oxide was purchased from BOC Ltd and used as supplied. NMR spectra were recorded on Bruker spectrometers (300–600 MHz) under argon at 298 K unless otherwise stated. Chemical shifts are quoted in ppm and coupling constants in Hz. Virtual coupling constants are reported as the separation between the first and third lines.[11] NMR spectra in proteo solvents were recorded using an internal capillary of C_6D_6. Analysis of samples by gas chromatography (GC) was carried out anaerobically using an Agilent technologies 7820A instrument fitted with a thermal conductivity detector (TCD) with a He makeup flow (250 °C, 5 mL/min He flow) and manual injector, connected to a 3-way Swagelok valve. The sample was passed through an Agilent HP-PLOT Molesieve column (19095P-MS6) held at 50 °C for 5 min then ramped to 200 °C over a 10 min period.

2 Preparation of rhodium (pre)catalysts

2.1 Preparation of PNP-*i*Pr

Adapted from a literature procedure.[12] To a solution of 2,6-lutidine (1.00 mL, 8.59 mmol) and TMEDA (2.60 mL, 17.2 mmol) in diethyl ether (20 mL) was added *n*-butyllithium (10.8 mL of a 1.6 M solution in hexane, 17.3 mmol), dropwise at 0 °C. The resulting dark orange mixture was allowed to warm to room temperature and stirred for 5 h. A solution of diisopropylchlorophosphine (2.74 mL, 17.2 mmol) in diethyl ether (20 mL) was then added dropwise at –78 °C. Following addition, the reaction mixture was stirred for 30 min at this temperature and then allowed to warm to room temperature and stirred for a further 18 h. The solution was filtered and the filtrate washed with degassed water (3×30 mL). The organic layer was dried over anhydrous sodium sulfate, filtered and the solvent removed in vacuo to afford the product as a light-yellow oil. Yield: 2.71 g (7.98 mmol, 93%). Spectroscopic data are consistent with the literature.

^{1}H NMR (400 MHz, hexane/C_6D_6): δ 7.84 (t, $^{3}J_{HH}$ = 7.7, 1H, *p*-py), 7.52 (d, $^{3}J_{HH}$ = 7.7, 2H, *m*-py), 3.43 (s, 4H, CH_2), 2.29 (app. septd, $^{3}J_{HH}$ = 7.1, $^{2}J_{PH}$ = 1.6, 4H, *i*Pr{CH}), 1.62 (dd, $^{3}J_{PH}$ = 11.2, $^{3}J_{HH}$ = 7.1, 12H, *i*Pr{CH_3}), 1.57 (dd, $^{3}J_{PH}$ = 13.1, $^{3}J_{HH}$ = 7.1, 12H, *i*Pr{CH_3}).

^{31}P{^{1}H} NMR (163 MHz, hexane/C_6D_6): δ 13.4 (s).

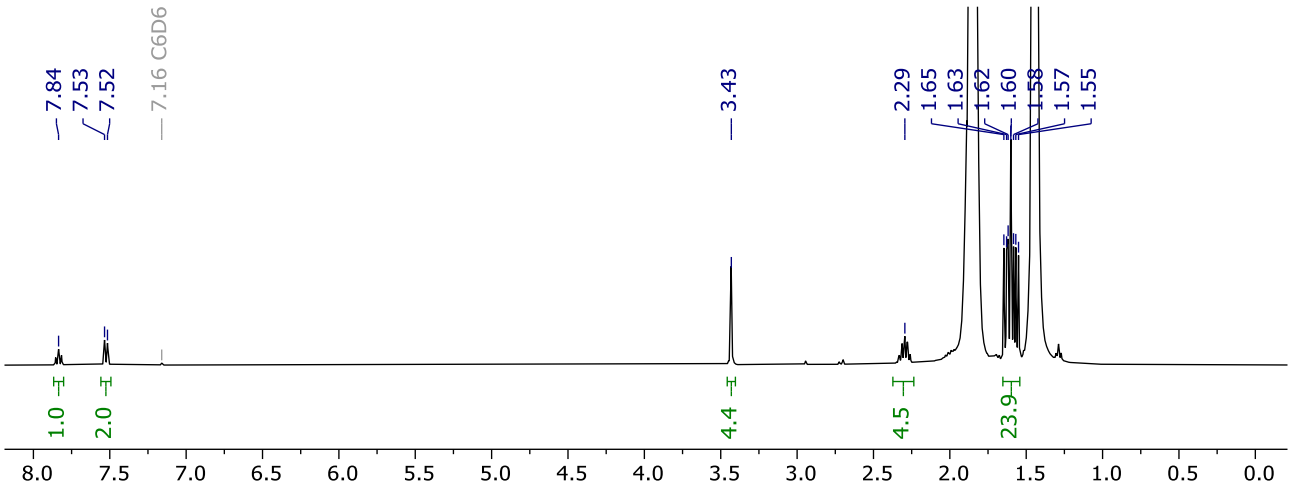

Figure S1. ^{1}H NMR spectrum of PNP-*i*Pr (400 MHz, hexane/C_6D_6).

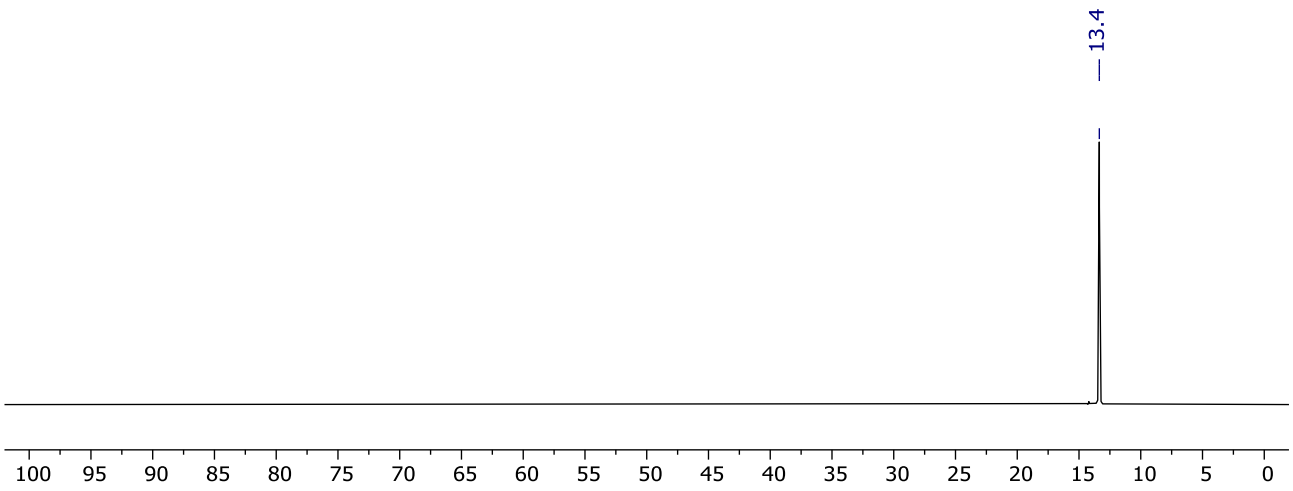

Figure S2. $^{31}P\{^{1}H\}$ NMR spectrum of PNP-*i*Pr (163 MHz, hexane/C_6D_6).

2.2 Preparation of [Rh(PNP-*i*Pr)(OPh)] 7*

A solution of [Rh(PNP-*i*Pr)Cl] (200 mg, 0.42 mmol) and NaOPh (53.6 mg, 0.46 mmol) in THF (20 mL) was stirred at 80 °C for 19 h. The reaction was cooled to room temperature, the solvent removed in vacuo, and the residue extracted with toluene (3×20 mL). The combined extracts were concentrated and layered with excess hexane to afford the product as burgundy crystals upon diffusion at –30 °C, some of which were suitable for analysis by X-ray diffraction. Yield: 96.0 mg (0.18 mmol, 43%).

^{1}H NMR (500 MHz, C_6D_6): *δ* 7.40–7.43 (m, 2H, *o*-Ph), 7.34–7.39 (m, 2H, *m*-Ph), 6.85 (t, $^{3}J_{HH}$ = 7.6, 1H, *p*-py), 6.71 (tt, $^{3}J_{HH}$ = 7.0, $^{4}J_{HH}$ = 1.4, 1H, *p*-Ph), 6.24 (d, $^{3}J_{HH}$ = 7.6, 2H, *m*-py), 2.43 (vt, J_{PH} = 7.3, 4H, CH_2), 1.91 (app. septvt, $^{3}J_{HH}$ = 7.1, J_{PH} = 4.7, 4H, *i*Pr{CH}), 1.29 (app. q, *J* = 7.3, 12H, *i*Pr{CH_3}), 1.08 (app. q, *J* = 6.9, 12H, *i*Pr{CH_3}).

^{13}C{^{1}H} NMR (126 MHz, C_6D_6): *δ* 174.2 (s, *i*-Ph), 164.2 (vt, J_{PC} = 12, *o*-py), 129.1 (s, *p*-py), 128.4 (s, *m*-Ph), 121.5 (s, *o*-Ph), 119.7 (vt, J_{PC} = 10, *m*-py), 111.6 (s, *p*-Ph), 35.0 (vt, J_{PC} = 13, CH_2), 24.6 (vt, J_{PC} = 18, *i*Pr{CH}), 18.9 (vt, J_{PC} = 7, *i*Pr{CH_3}), 18.0 (vt, J_{PC} = 3, *i*Pr{CH_3}).

^{31}P{^{1}H} NMR (163 MHz, C_6D_6): *δ* 44.3 (d, $^{1}J_{RhP}$ = 157).

Anal. Calcd. for $C_{25}H_{40}NOP_2Rh$ (535.45 g·mol^{-1}): C, 56.08; H, 7.53; N, 2.62. Found: 56.17; H, 7.50; N, 2.48.

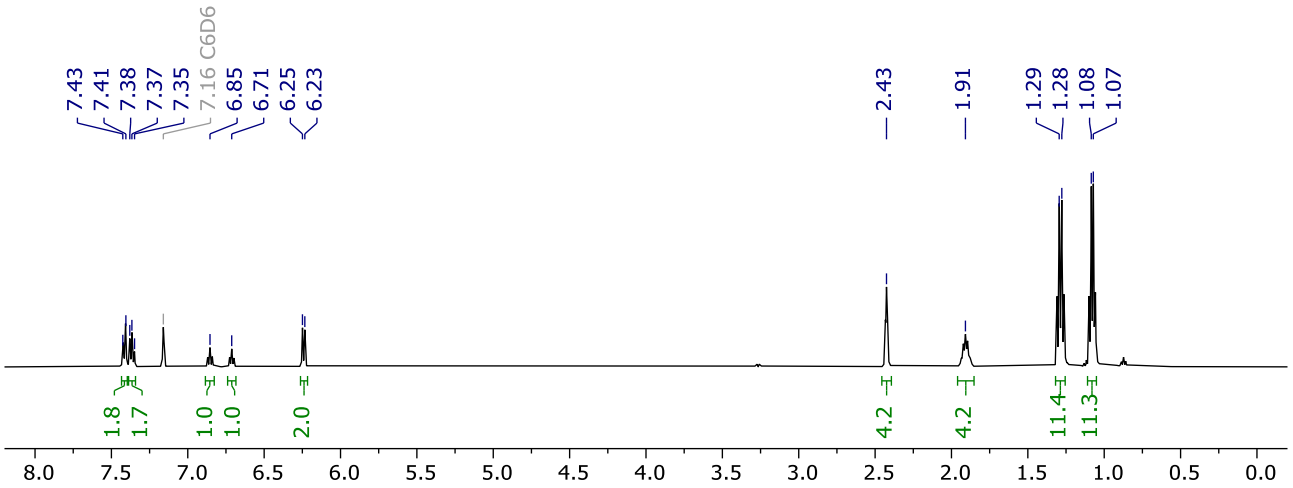

Figure S3. ^{1}H NMR spectrum of **7*** (500 MHz, C_6D_6).

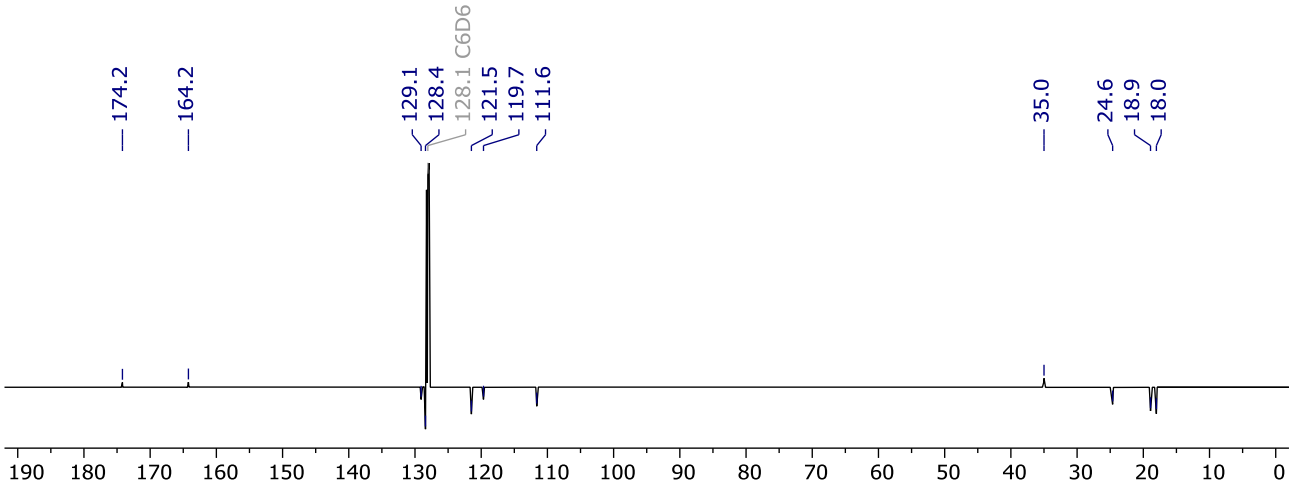

Figure S4. ^{13}C{^{1}H} NMR spectrum of **7*** (126 MHz, C_6D_6).

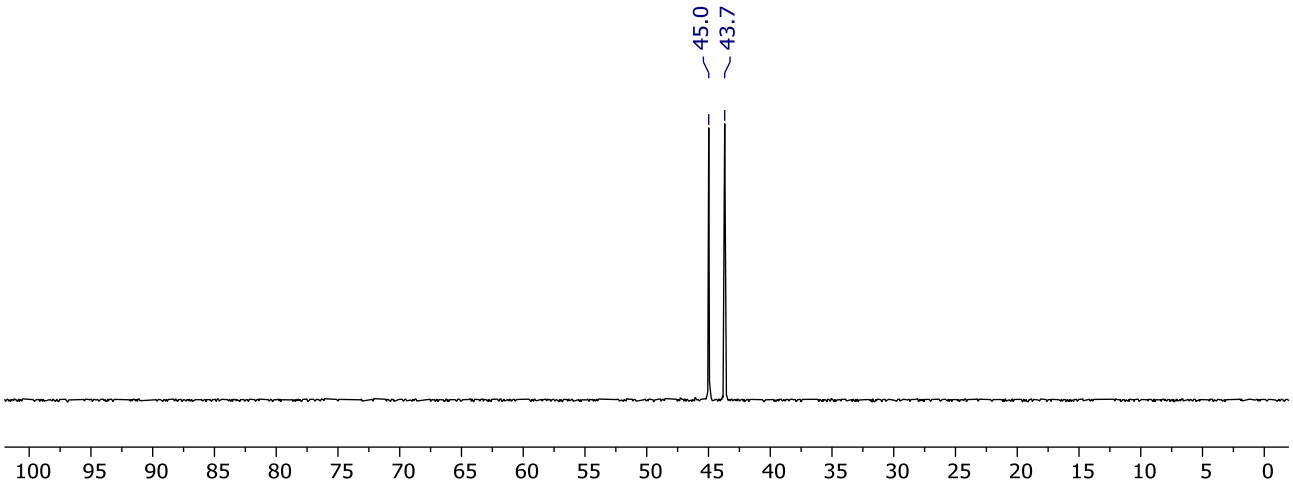

Figure S5. ^{31}P{^{1}H} NMR spectrum of **7*** (163 MHz, C_6D_6).

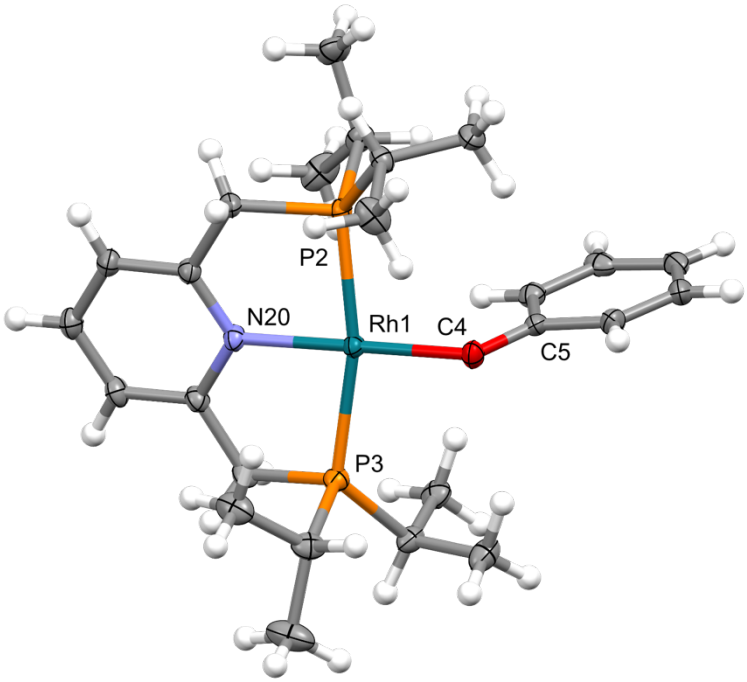

Figure S6. Solid-state structure of **7*** (CCDC 2549087). Only one of the two structurally similar but crystallographically unique complexes shown (Z′ = 2). Thermal ellipsoids at 30% probability. Selected bond lengths (Å) and angles (°): Rh1–P2, 2.2643(11); Rh1–P3, 2.2605(12); Rh1–N20, 2.035(3); Rh1–O4, 2.061(3); P2–Rh1–P3, 166.82(4); N20–Rh1–O4, 176.75(13); Rh1–O4–C5, 124.5(3); Rh1A–P2A, 2.2722(11); Rh1A–P3A, 2.2785(12); Rh1A–N20A, 2.026(3); Rh1A–O4A, 2.057(3); P2A–Rh1A–P3A, 165.53(4); N20A–Rh1A–O4A, 178.57(16); Rh1A–O4A–C5A, 122.8(3).

2.3 Synthesis of [Rh(PNP-*i*Pr)(Bpin)] 7

A mixture of [Rh(PNP-*i*Pr)(OPh)] (3.5 mg, 6.5 µmol) and B_2pin_2 (1.7 mg, 6.5 µmol) was dissolved in C_6D_{12} (0.5 mL) within a J. Young valve NMR tube at room temperature forming a dark red solution. Analysis by NMR spectroscopy indicated quantitative spectroscopic conversion into a mixture of the desired rhodium(I) boryl **7** and PhOBpin (δ_{11B} 21.8). The formation of **7** has previously been invoked in the reaction between [Rh(PNP-*i*Pr)(Ph)] and B_2pin_2 at 150 °C in C_6D_6.[13] The limited spectroscopic data provided are consistent with our characterisation data.

^{1}H NMR (500 MHz, C_6D_{12}, selected data): δ 7.27 (t, $^3J_{HH}$ = 7.6, 1H, *p*-py), 6.92 (d, $^3J_{HH}$ = 7.6, 2H, *m*-py), 3.09 (vt, J_{PH} = 5.8, 4H, CH_2), 2.08 (app. sept, $^3J_{HH}$ = 6.7, 4H, *i*Pr{CH}), 1.30 (app. q, $^3J_{HH}$ = 7.7, 12H, CH_3{*i*Pr}), 1.07 (s, 12H, pin), 1.04 (app. q, 12H, $^3J_{HH}$ = 6.7, *i*Pr{CH_3}).
^{13}C{^{1}H} NMR (126 MHz, C_6D_{12}, selected data): δ 161.5 (vtd, J_{PC} = 14, $^2J_{RhC}$ = 1, *o*-py), 132.0 (s, *p*-py), 119.4 (vt, J_{PC} = 8, *m*-py), 79.1 (d, $^2J_{RhC}$ = 1, pin{C}), 40.1 (s, CH_2), 26.7 (obscured, *i*Pr{CH}), 26.2 (s, pin{CH_3}), 20.3 (vtd, J_{PC} = 10, $^3J_{RhC}$ = 1, *i*Pr{CH_3}), 18.7 (app. q, J = 1, *i*Pr{CH_3}).
^{31}P{^{1}H} NMR (163 MHz, C_6D_{12}): δ 57.1 (d, $^1J_{RhP}$ = 171).
^{11}B{^{1}H} NMR (128 MHz, C_6D_{12}, selected data): δ 46.4 (vbr, fwhm = 510 Hz).

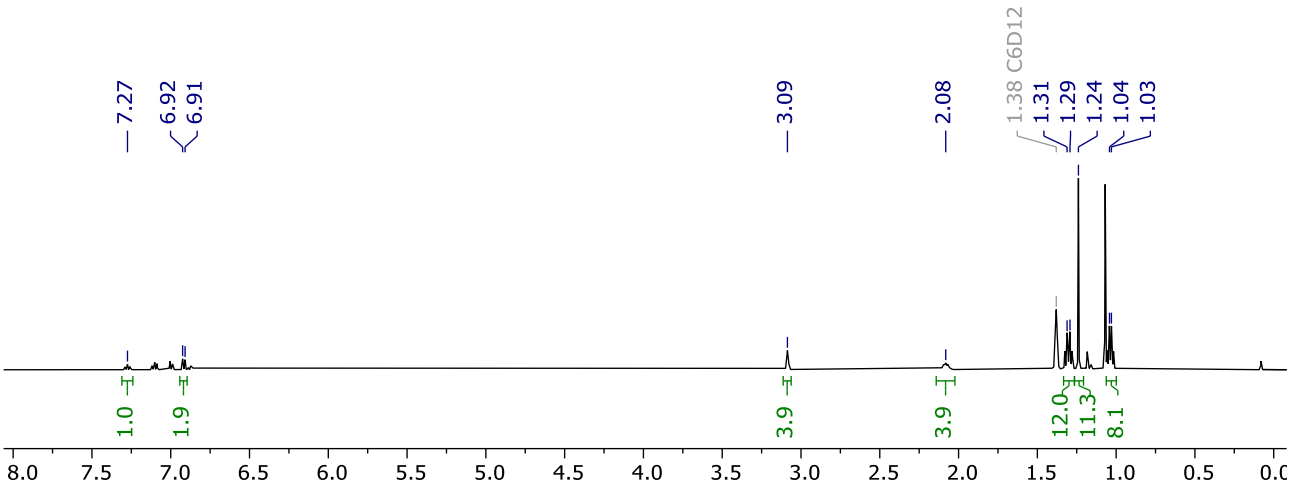

Figure S7. ^{1}H NMR spectrum of **7** (500 MHz, C_6D_{12}).

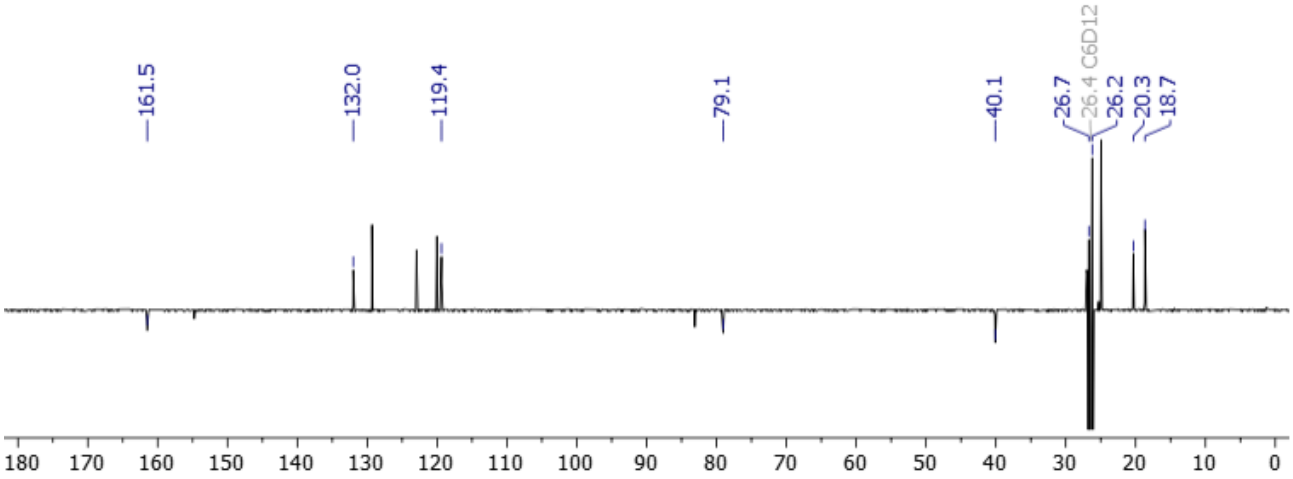

Figure S8. ^{13}C{^{1}H} NMR spectrum of **7** (126 MHz, C_6D_{12}).

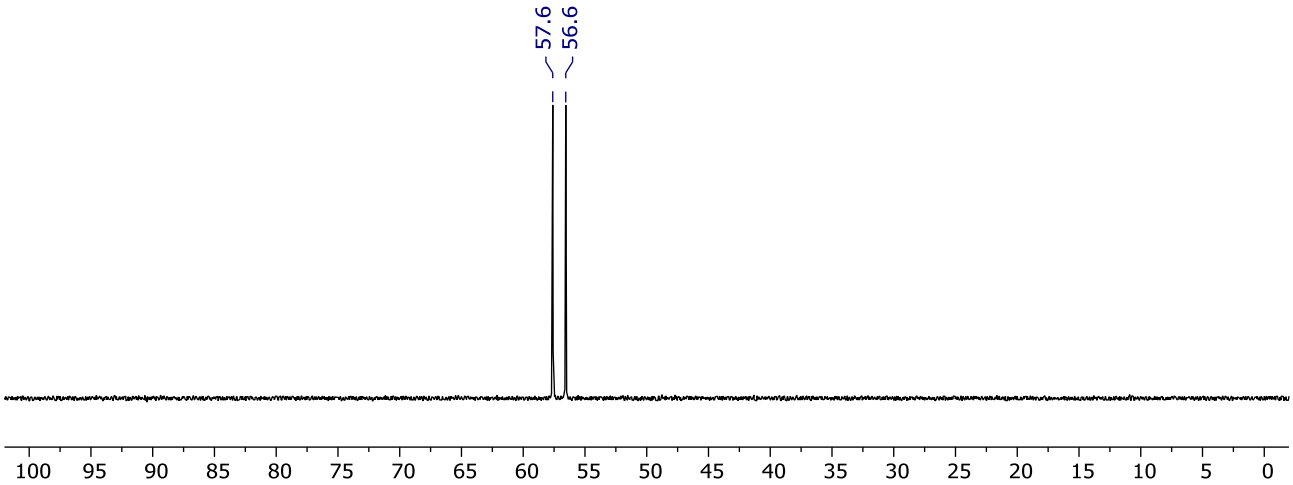

Figure S9. ^{31}P{^{1}H} NMR spectrum of **7** (163 MHz, C_6D_{12}).

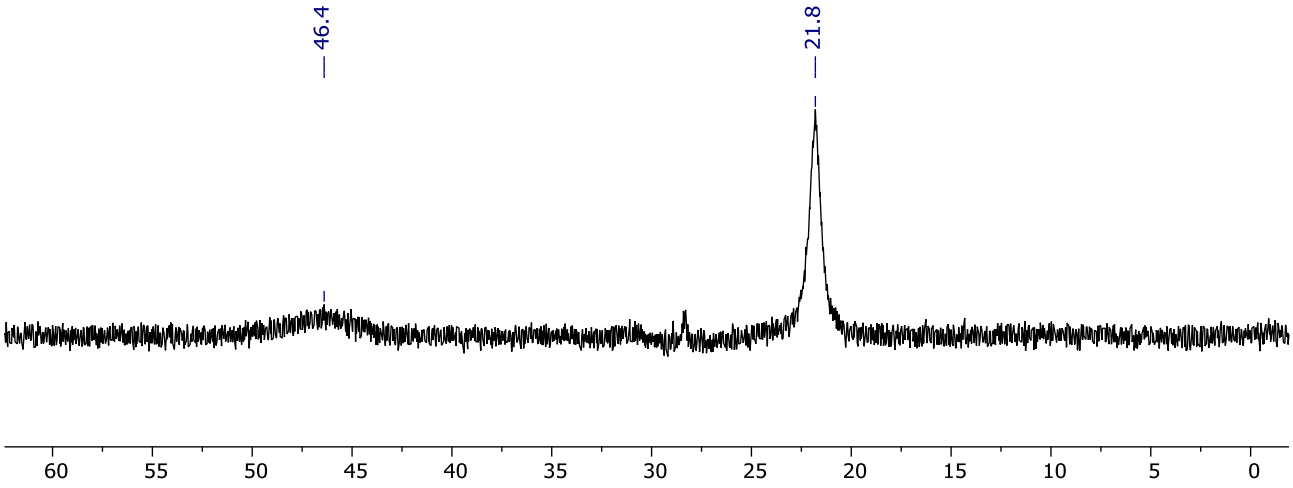

Figure S10. $^{11}B\{^{1}H\}$ NMR spectrum of **7** (128 MHz, C_6D_{12}).

2.4 Preparation of [Rh(POP-*i*Pr)Cl]

Adapted from a literature procedure.[14] To a solution of $[Rh(COE)_2Cl]_2$ (0.341 g, 0.47 mmol) in benzene (20 mL) was added a solution of POP-*i*Pr in hexane (10.0 mL of a 0.095 M solution, 0.95 mmol) at room temperature, immediately forming a brick-red solution. The solution was stirred for 1 h, the solvent removed in vacuo, and the residue washed with $SiMe_4$ (2×10 mL) at –78 °C to afford the product as a brick red powder which was dried in vacuo. Yield: 0.511 g (0.88 mmol, 93%). Spectroscopic data are consistent with the literature.[14]

^{1}H NMR (400 MHz, C_6D_6): δ 7.24 (br d, $^{3}J_{HH}$ = 7.0, 2H, Ar), 6.95 (d, $^{3}J_{HH}$ = 7.7, 2H, Ar), 6.80 (app. t, $^{3}J_{HH}$ = 7.5, 2H, Ar), 2.48 (app. sept, $^{3}J_{HH}$ = 7.0, 4H, *i*Pr{CH}), 1.67 (app. q, *J* = 7.7, 12H, *i*Pr{CH_3}), 1.26 (app. q, *J* = 7.1, 12H, *i*Pr{CH_3}), 1.14 (s, 6H, CH_3).

^{31}P{^{1}H} NMR (163 MHz, C_6D_6): δ 35.9 (d, $^{1}J_{RhP}$ = 142).

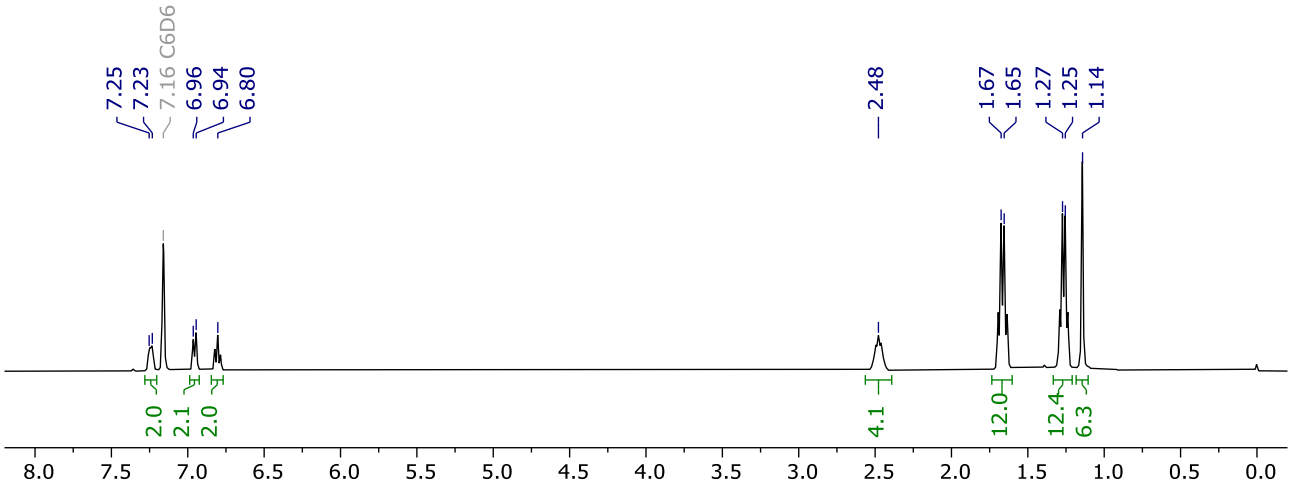

Figure S11. ^{1}H NMR spectrum of [Rh(POP-*i*Pr)Cl] (400 MHz, C_6D_6).

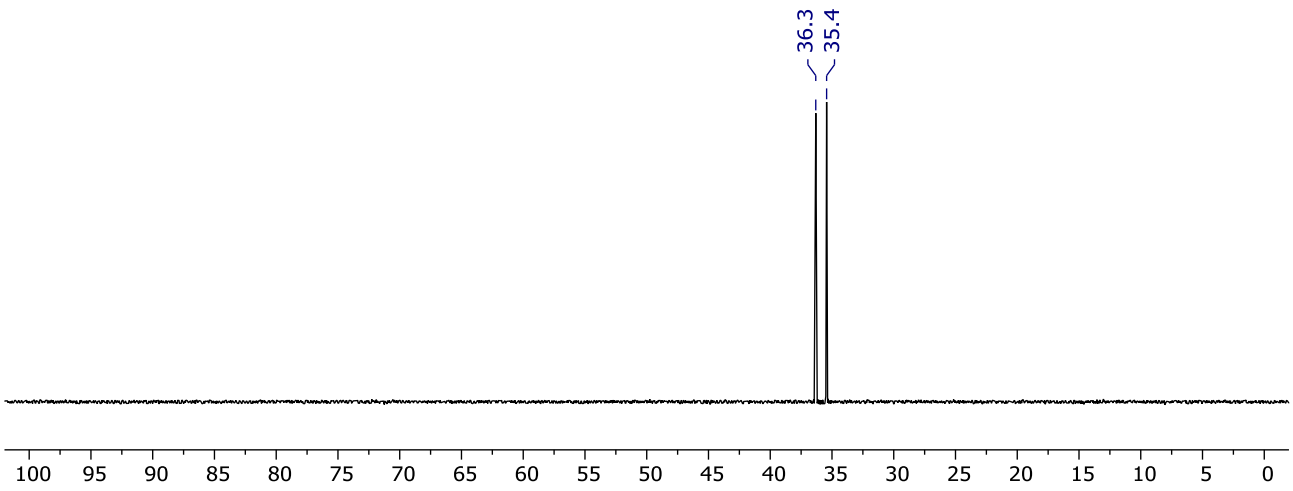

Figure S12. $^{31}P\{^{1}H\}$ NMR spectrum of [Rh(POP-*i*Pr)Cl] (163 MHz, C_6D_6).

2.5 NMR scale reaction of [Rh(POP-*i*Pr)Cl] with NaOPh

A mixture of [Rh(POP-*i*Pr)Cl] (5.8 mg, 10 µmol) and NaOPh (1.4 mg, 12 µmol) was dissolved in THF (0.5 mL) within a J. Young valve NMR tube and the resulting solution heated to 80 °C. Analysis by NMR spectroscopy indicated complete conversion of [Rh(POP-*i*Pr)Cl] into a new organometallic product, which was subsequently identified as [Rh(POP-*i*Pr)(2-(OH)Ph)] (δ_{31P} 40.3). No intermediate species were observed. Subsequently attention turned to examination of [Rh(POP-*i*Pr)(Bpin)] **8** in catalysts rather than [Rh(POP-*i*Pr)(OPh)] or [Rh(POP-*i*Pr)(2-(OH)Ph)].

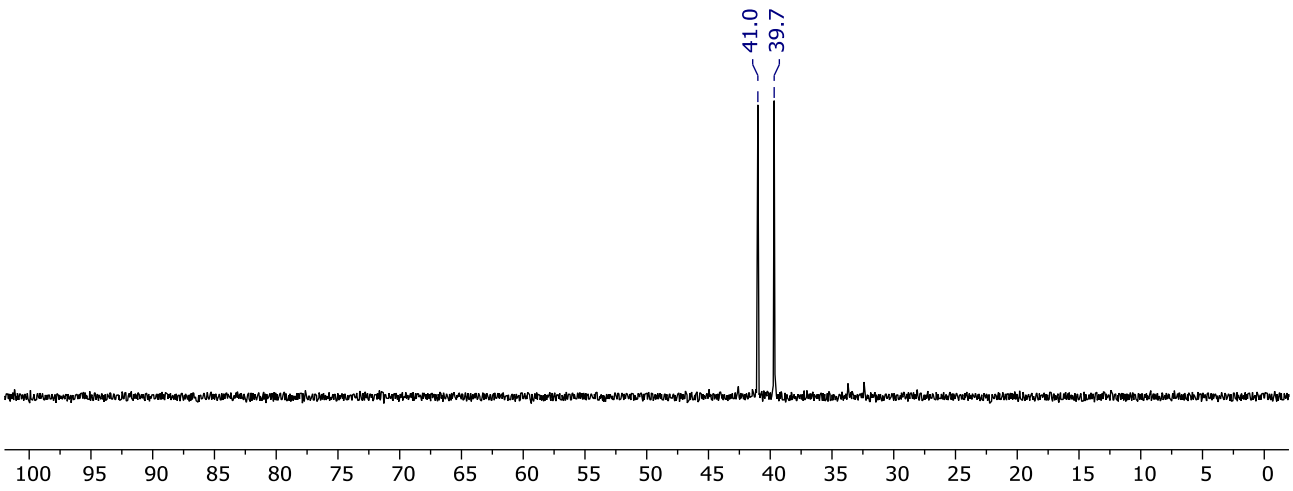

Figure S13. $^{31}P\{^{1}H\}$ NMR spectrum of the reaction between [Rh(POP-*i*Pr)Cl] and NaOPh recorded after 72 h at 80 °C (121 MHz).

2.6 Isolation of [Rh(POP-*i*Pr)(2-(OH)Ph)]

A stirred solution of [Rh(POP-*i*Pr)Cl] (100 mg, 172 µmol) and NaOPh (22.0 mg, 190 µmol) in THF (10 mL) was heated at 80 °C for 16 h. The reaction was cool to room temperature and the solvent removed in vacuo. The residue was extracted into a minimal amount of Et_2O, the solution filtered, and the crude product obtained upon removal of the solvent. Recrystallisation from hexane afforded

the product as an orange crystalline solid, with some of the crystals suitable for analysis by X-ray diffraction. Yield: 87.0 mg (136 μmol, 79%).

^{1}H NMR (500 MHz, C_6D_6): δ 8.06 (s, 1H, OH), 7.77 (br d, $^{3}J_{HH}$ = 5.8, 1H, 6-Ph), 7.12–7.15 (m, 4H, 3-Ph, 4-Ph, Ar), 7.05–7.08 (m, 1H, 5-Ph), 7.03 (dd, $^{3}J_{HH}$ = 7.7, $^{4}J_{HH}$ = 1.6, 2H, Ar), 6.83 (app t, J = 7.6, 2H, Ar), 2.37 (app. sept, $^{3}J_{HH}$ = 7.0, 2H, *i*Pr{CH}), 2.28–2.4 (obscured m, 2H, *i*Pr{CH}), 1.26 (s, 3H, CH_3), 1.26 (app. q, J = 7.6, 6H, *i*Pr{CH_3}), 1.22 (s, 3H, CH_3), 1.15 (app. q, J = 7.3, 6H, *i*Pr{CH_3}), 1.11 (app. q, J = 7.7, 6H, *i*Pr{CH_3}), 1.07 (app. q, J = 6.7, 6H, *i*Pr{CH_3}).

^{13}C{^{1}H} NMR (126 MHz, C_6D_6): δ 159.4 (br, 2-Ph), 156.0 (vt, J_{PC} = 16, Ar{C}), 142.2 (dt, $^{1}J_{RhC}$ = 41, $^{2}J_{PC}$ = 13, 1-Ph), 137.6 (vt, J_{PC} = 5, 6-Ph), 131.3 (s, Ar{CH}), 130.7 (vt, $^{3}J_{PC}$ = 5, Ar{C}), 128.4 (s, Ar{CH}), 124.9 (vtd, J_{PC} = 16, $^{2}J_{RhC}$ = 2, Ar{C}), 124.3 (vt, J_{PC} = 2, Ar{CH}), 121.4 (br, 4-Ph), 119.1 (s, 5-Ph), 108.8 (s, 3-Ph), 34.0 (s, $\underline{C}(CH_3)_2$), 33.4 (s, CH_3), 32.9 (s, CH_3), 25.7 (vtd, J_{PC} = 20, $^{2}J_{RhC}$ = 3, *i*Pr{CH}), 25.4 (vtd, J_{PC} = 18, $^{2}J_{RhC}$ = 2, *i*Pr{CH}), 19.8 (vt, J_{PC} = 7, *i*Pr{CH_3}), 18.7 (vtd, J_{PC} = 5, $^{3}J_{RhC}$ = 1, *i*Pr{CH_3}), 18.4 (vt, J_{PC} = 8, *i*Pr{CH_3}), 18.1 (br, *i*Pr{CH_3}).

^{31}P{^{1}H} NMR (163 MHz, C_6D_6): δ 40.3 (d, $^{1}J_{RhP}$ = 160).

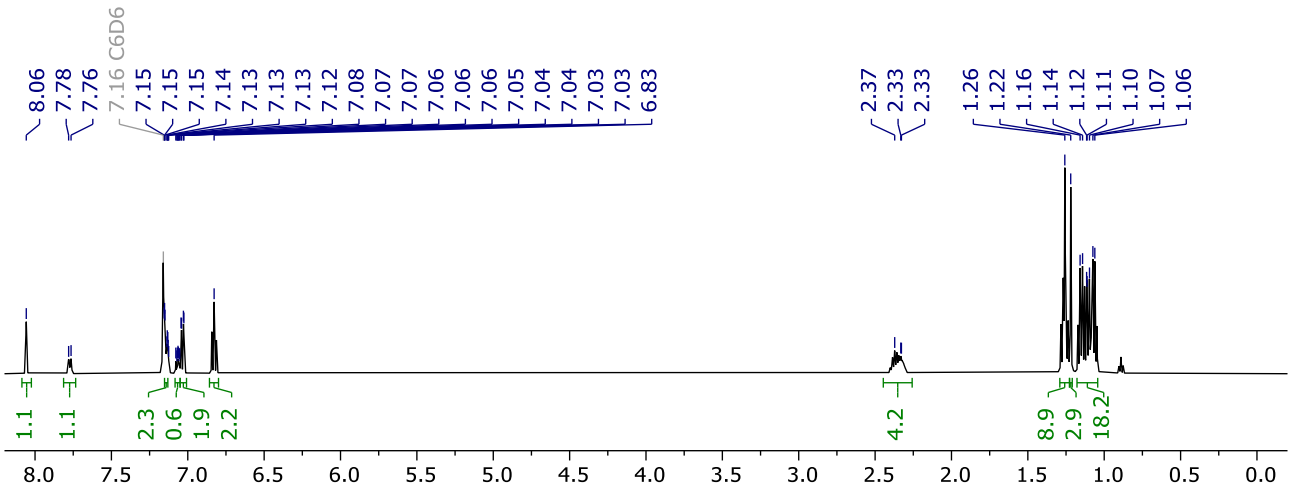

Figure S14. ^{1}H NMR spectrum of [Rh(POP-*i*Pr)(2-(OH)Ph)] (500 MHz, C_6D_6).

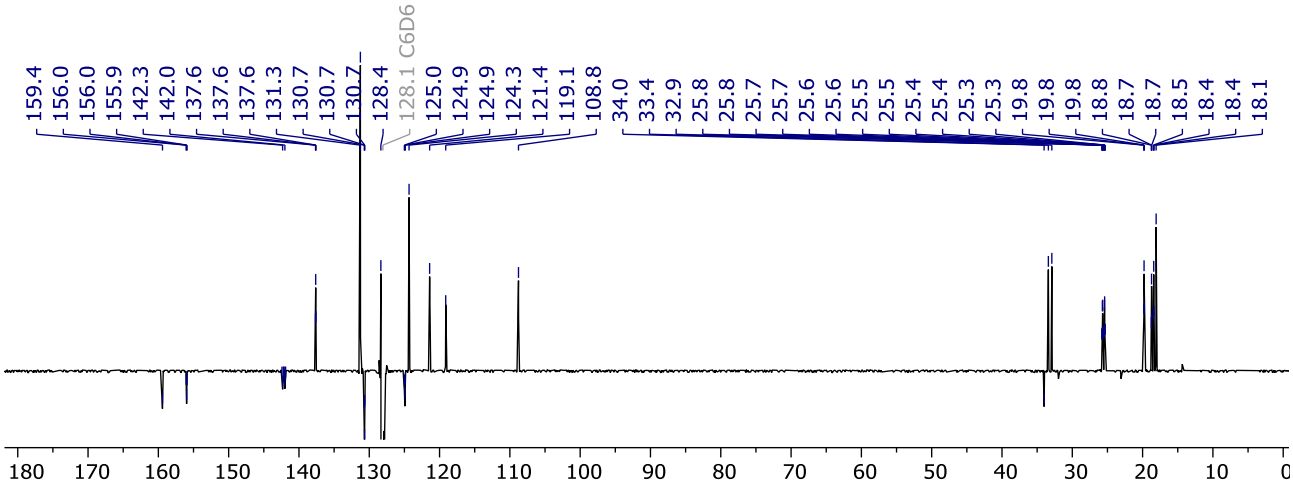

Figure S15. ^{13}C{^{1}H} NMR spectrum of [Rh(POP-*i*Pr)(2-(OH)Ph)] (126 MHz, C_6D_6).

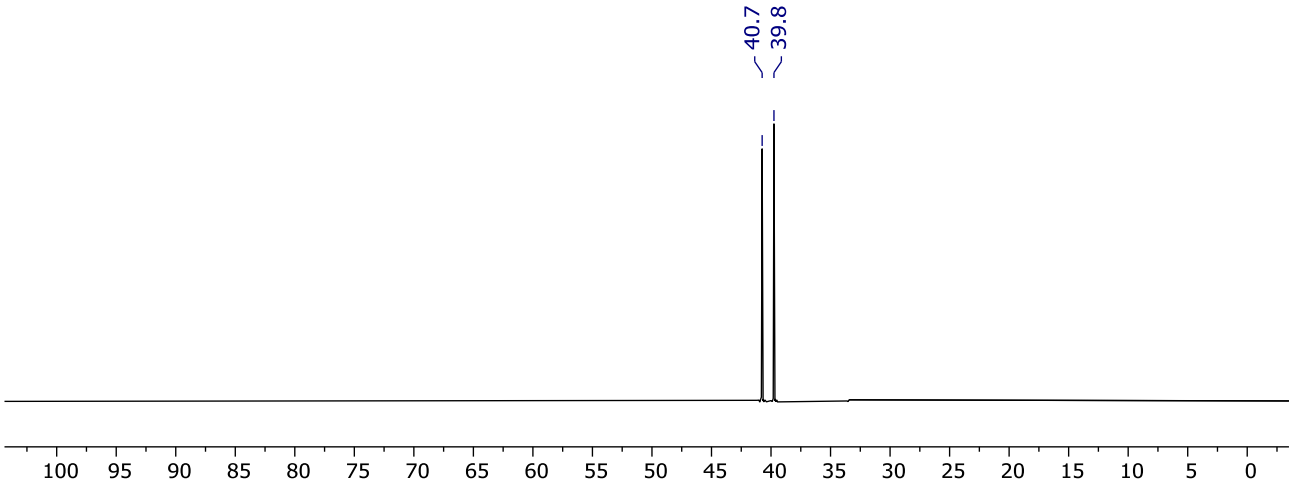

Figure S16. $^{31}P\{^{1}H\}$ NMR spectrum of [Rh(POP-*i*Pr)(2-(OH)Ph)] (163 MHz, C_6D_6).

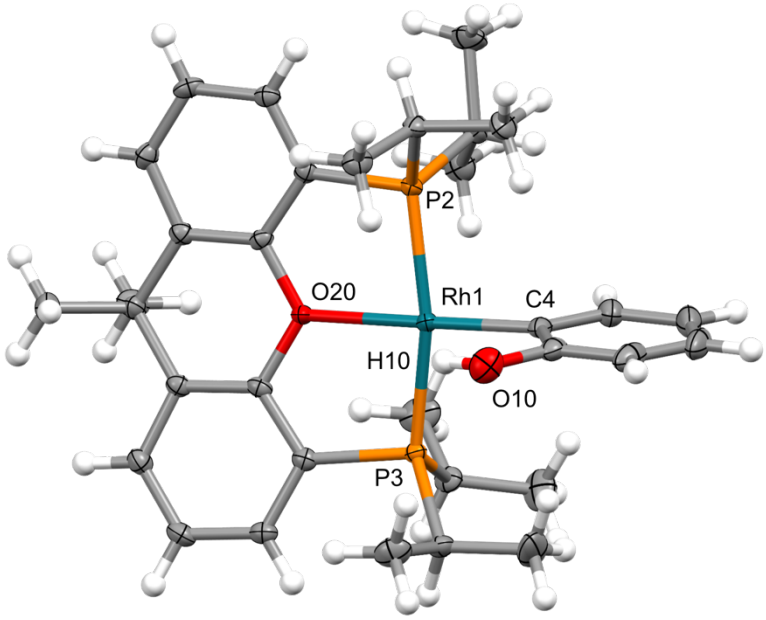

Figure S17. Solid-state structure of [Rh(POP-*i*Pr)(2-(OH)Ph)] (CCDC 2549088). Thermal ellipsoids at 50% probability. Selected bond lengths (Å) and angles (°): Rh1–P2, 2.2461(4); Rh1–P3, 2.2464(4); Rh1–O20, 2.2084(11); Rh1–C4, 1.9986(17); Rh1–H10, 2.4823(3); P2–Rh1–P3, 163.625(16); O20–Rh1–C4, 178.81(6).

2.7 NMR scale reaction of [Rh(POP-*i*Pr)(2-(OH)Ph)] with B_2pin_2

A mixture of [Rh(POP-*i*Pr)(2-(OH)Ph)] (6.4 mg, 10.0 µmol) and B_2pin_2 (2.5 mg, 9.84 µmol) was dissolved in THF (0.5 mL) within a J. Young valve NMR tube at room temperature, resulting in slow and unselective formation of [Rh(POP-*i*Pr)(Bpin)] **8** (δ_{31P} 51.8) at room temperature. Complete consumption of [Rh(POP-*i*Pr)(2-(OH)Ph)] was observed within 6 days at room temperature, with **8** the major organometallic product (ca. 75%).

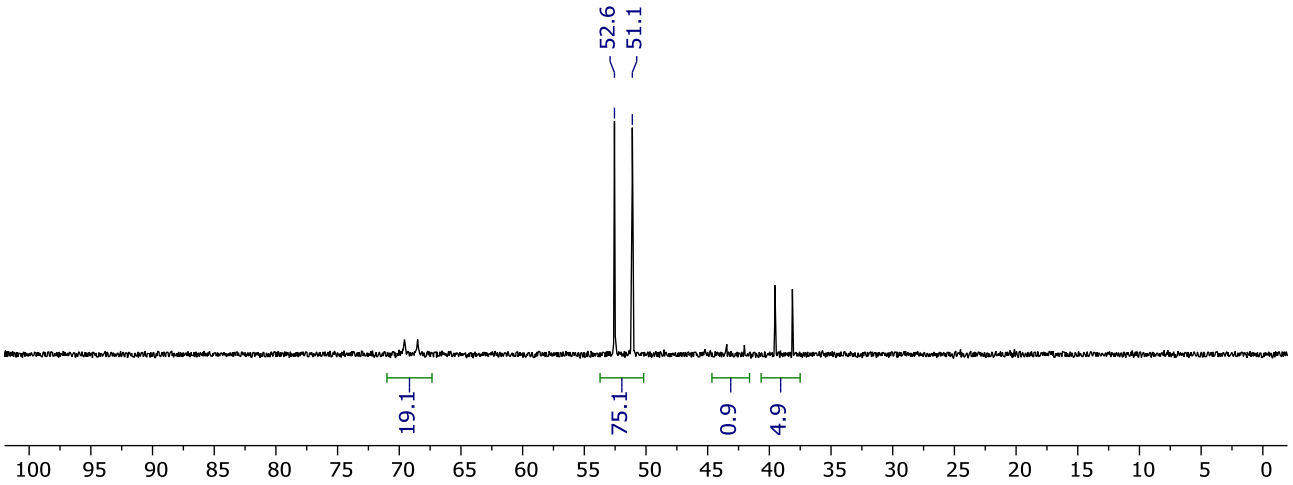

Figure S18. $^{31}P\{^{1}H\}$ NMR spectrum of the reaction between [Rh(POP-*i*Pr)(2-(OH)Ph)] and B_2pin_2 recorded after 6 days at room temperature (121 MHz, THF/C_6D_6).

2.8 Preparation of [Rh(POP-*i*Pr)(Bpin)] 8

To a solution of [Rh(POP-*i*Pr)Cl] (300 mg, 0.52 mmol) in THF (10 mL) was added a solution of Na[BEt_3H] in toluene (570 µL of a 1 M solution, 0.57 mmol) at 0 °C. The reaction was warmed to room temperature and stirred for 6 h and the volatiles removed in vacuo. The resulting black oil was repeatedly dissolved in hexane (5 mL) and the volatiles removed in vacuo until a very dark solid was obtained: [Rh(POP-*i*Pr)H]. The residue was taken up in hexane (2.5 mL) and a solution of B_2pin_2 (132 mg, 0.52 mmol) in hexane (2.5 mL) added at room temperature and the resulting solution stirred for 10 min. Volatiles were removed in vacuo and the residue washed with $SiMe_4$ (2 mL) at –30 °C to afford the product as a deep red microcrystalline solid. Yield: 251 mg (0.37 mmol, 72%). Spectroscopic data are consistent with the literature.[15]

^{1}H NMR (400 MHz, C_6D_{12}) δ 7.46 (br d, $^{3}J_{HH}$ = 7.2, 2H, Ar), 7.35 (d, $^{3}J_{HH}$ = 7.6, 2H, CH{Ar}), 7.04 (app. t, $^{3}J_{HH}$ = 7.6, 2H, Ar), 2.42 (app. sept, $^{3}J_{HH}$ = 7.5, 4H, *i*Pr{CH}), 1.56 (s, 6H, CH_3), 1.35 (app. q, J = 8.2, 12H, *i*Pr{CH_3}), 1.14 (s, 12H, pin), 1.06 (app. q, J = 7.0, 12H, *i*Pr{CH_3}).
^{31}P{^{1}H} NMR (162 MHz, C_6D_{12}) δ 51.4 (d, $^{1}J_{RhP}$ = 178).
^{11}B{^{1}H} NMR (128 MHz, C_6D_{12}) δ 43.4 (vbr, fwhm = 590 Hz).

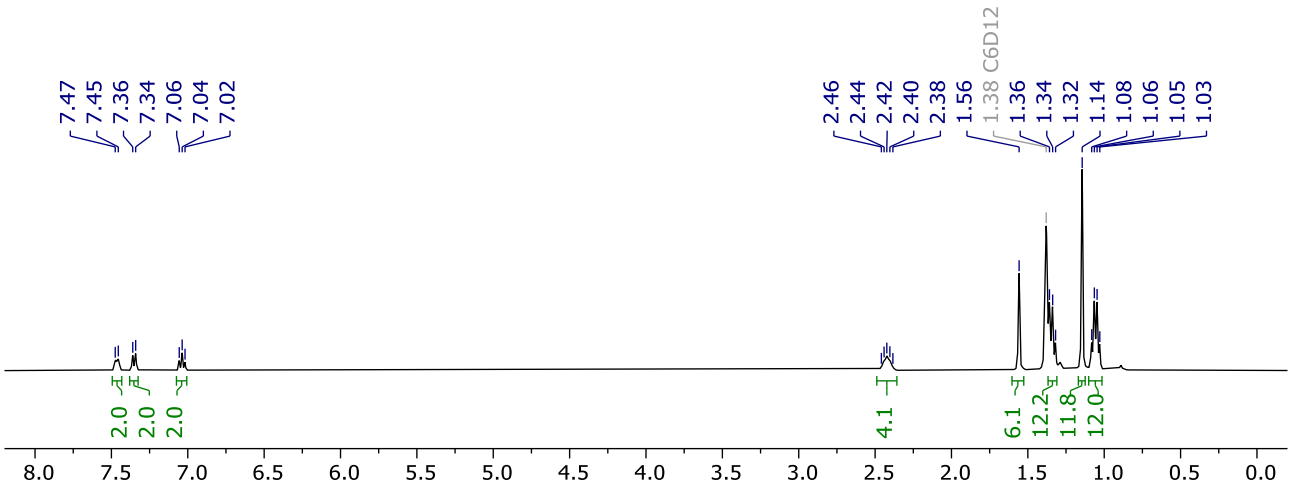

Figure S19. ^{1}H NMR spectrum of **8** (400 MHz, C_6D_{12}).

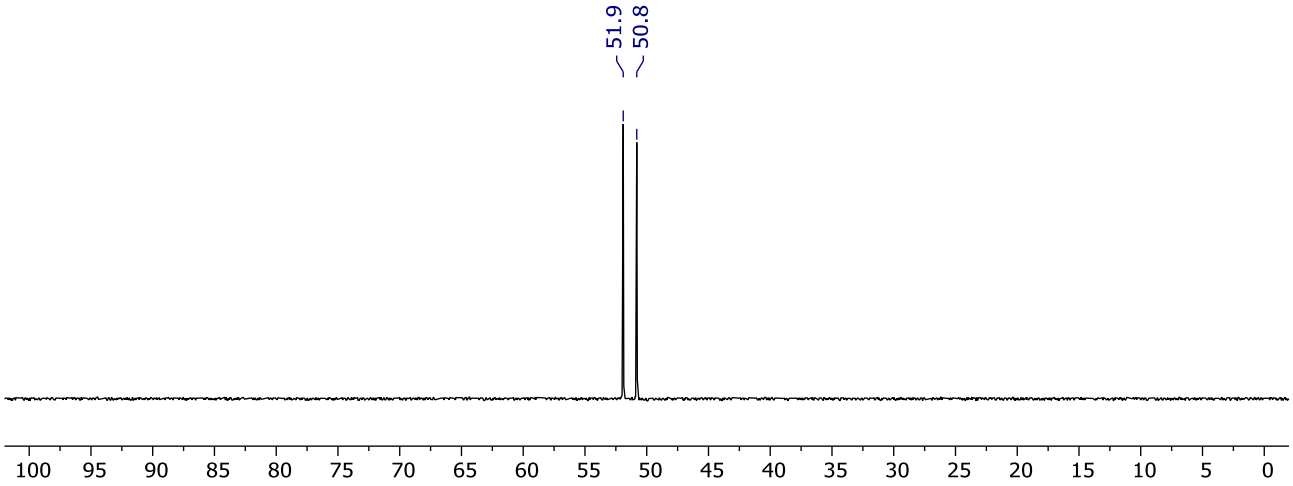

Figure S20. $^{31}P\{^{1}H\}$ NMR spectrum of **8** (162 MHz, C_6D_{12}).

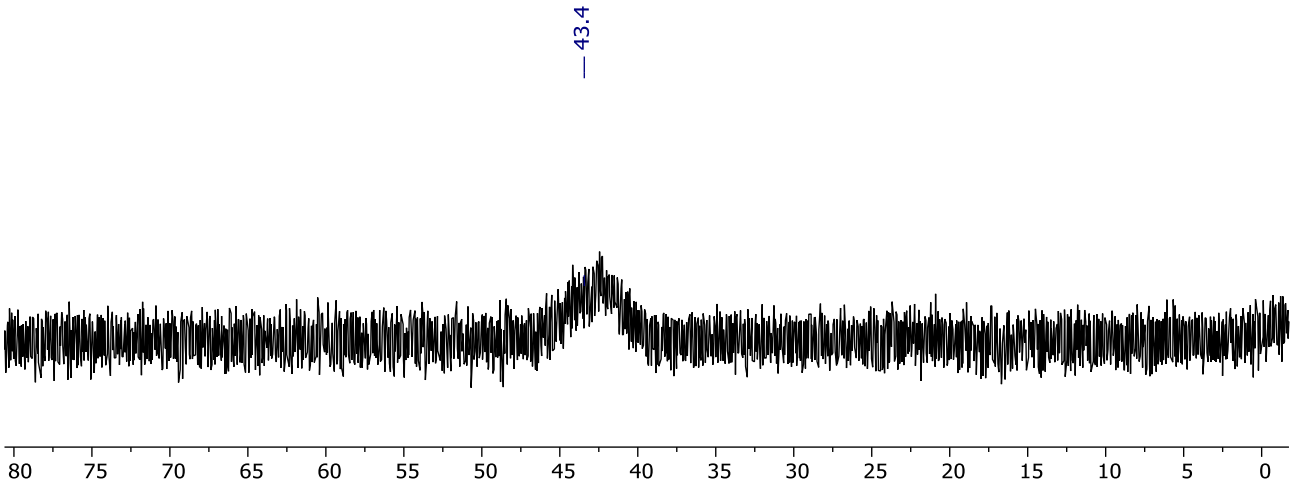

Figure S21. $^{11}B\{^{1}H\}$ NMR spectrum of **8** (128 MHz, C_6D_{12}).

3 Catalyst evaluation

3.1 General procedure

In an argon-filled glovebox, amberised vials were charged with precatalyst (5 μmol) and a solution of diboron[4] (100 μmol) in THF or toluene (1 mL) in the dark. The vials were sealed in a stainless-steel reactor within an 18-well aluminium insert, pressurised with N_2O (1 or 3 bar gauge), and stirred for 120 or 10 min at room temperature in the dark. The reactor was depressurised, opened to air and exposed to light. Aliquots were quickly taken from each vial (0.5 mL), loaded into a J. Young valve NMR tube, and immediately frozen (77 K) before being analysed by $^{11}B\{^1H\}$ NMR spectroscopy at room temperature. Conversion was calculated by line fitting of the $^{11}B\{^1H\}$ NMR spectra.

Table S1. Evaluation of catalysts for the diboron(4) reduction of N_2O.

Entry	**Conditions**				**Conversion %**								
	Diborane(4)	Solvent	p_{N2O} / bar	time / min	**-**	**1***	**2***	**3***	**4***	**5***	**6***	**7***	**8**
1a	B_2pin_2	THF	3	120	0	6	33	82	100	100	23	13	25
1b	B_2pin_2	THF	3	120	0	6	34	92	100	100	21	10	22
2a	B_2pin_2	THF	3	10					98	92			
2b	B_2pin_2	THF	3	10					99	92			
3a	B_2pin_2	THF	1	120			30	89	100	100			
3b	B_2pin_2	THF	1	120			36	90	100	100			
4a	B_2pin_2	THF	1	10					93	90			
4b	B_2pin_2	THF	1	10					99	95			
5a	B_2pin_2	toluene	3	120	0		77	100	100	100	25		
5b	B_2pin_2	toluene	3	120	0		84	100	100	100	17		
6a	B_2pin_2	toluene	3	10					48	85			
6b	B_2pin_2	toluene	3	10					68	83			
7a	B_2pin_2	toluene	1	120			78	100	100	100			
7b	B_2pin_2	toluene	1	120			83	100	100	100			
8a	B_2pin_2	toluene	1	10					42	66			
8b	B_2pin_2	toluene	1	10					42	60			
9a	B_2neop_2	THF	3	120	0	33	72	76	45	63	7	4	11
9b	B_2neop_2	THF	3	120	0	36	81	89	58	63	16	3	7
10a	B_2neop_2	toluene	3	120	0		84	69	40	37	15		
10b	B_2neop_2	toluene	3	120	0		90	78	41	35	17		
11a	B_2cat_2	THF	3	120	0	87	24	32	< 5	< 5	0	44	85
11b	B_2cat_2	THF	3	120	0	89	26	26	< 5	< 5	0	48	82
12a	B_2cat_2	toluene	3	120	0		18	17	24	14	2		
12b	B_2cat_2	toluene	3	120	0		20	9	16	12	3		

3.2 Data collected for entry 1a

3.2.1 No catalyst

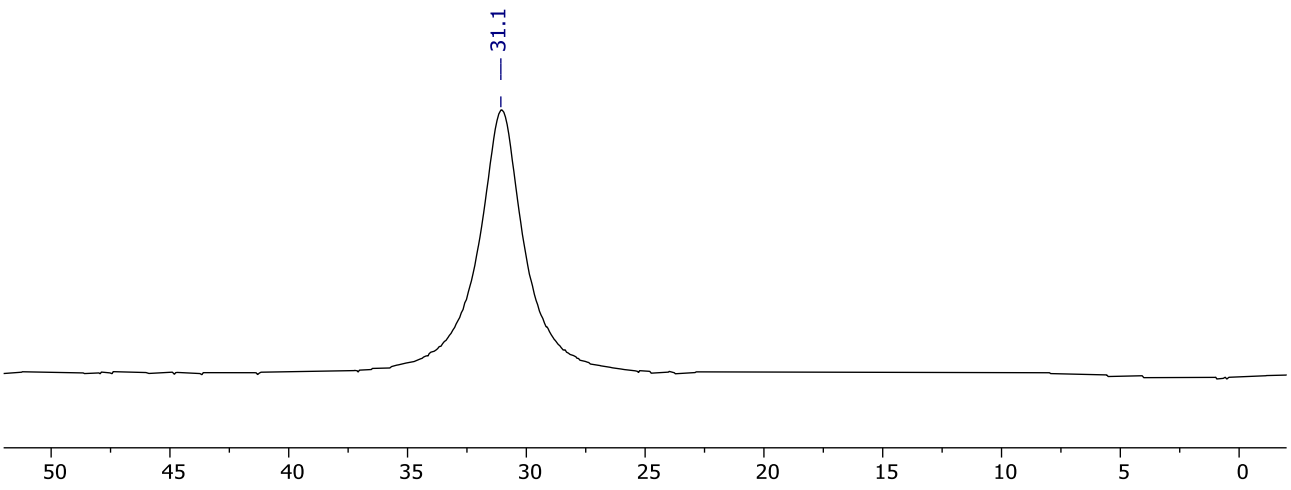

Figure S22. $^{11}B\{^{1}H\}$ NMR spectrum collected following the attempted B_2pin_2 reduction of N_2O (3 bar gauge) in THF with no catalyst after 120 min (128 MHz, THF/C_6D_6).

3.2.2 [$Rh(PEt_3)_3(OPh)$] **1***

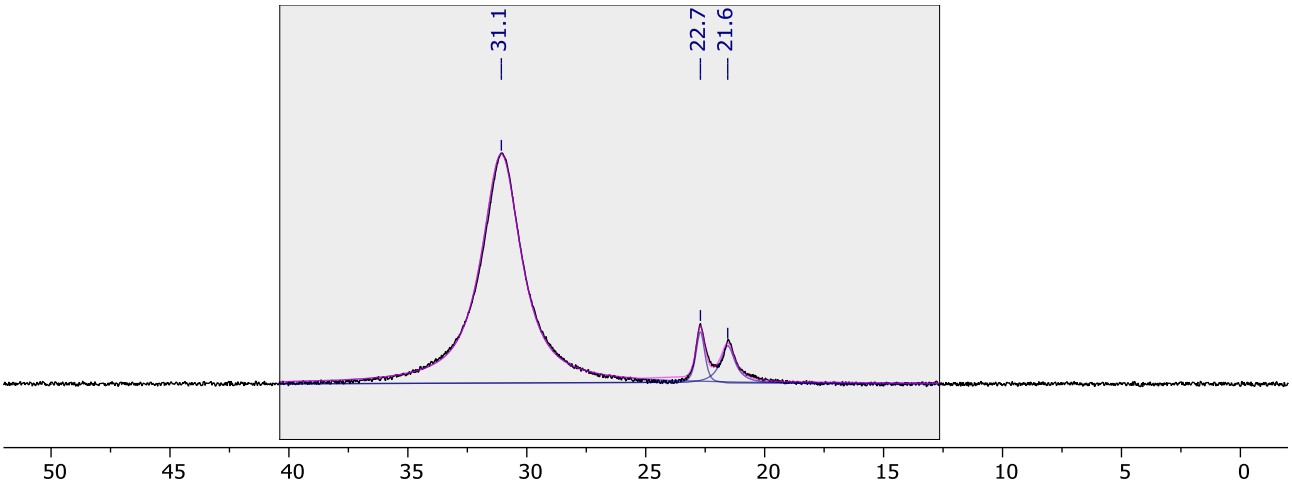

Figure S23. $^{11}B\{^{1}H\}$ NMR spectrum collected following the B_2pin_2 reduction of N_2O (3 bar gauge) using 5 mol% **1*** in THF after 120 min (128 MHz, THF/C_6D_6).

3.2.3 [Cu(SIPr)(O*t*Bu)] **2***

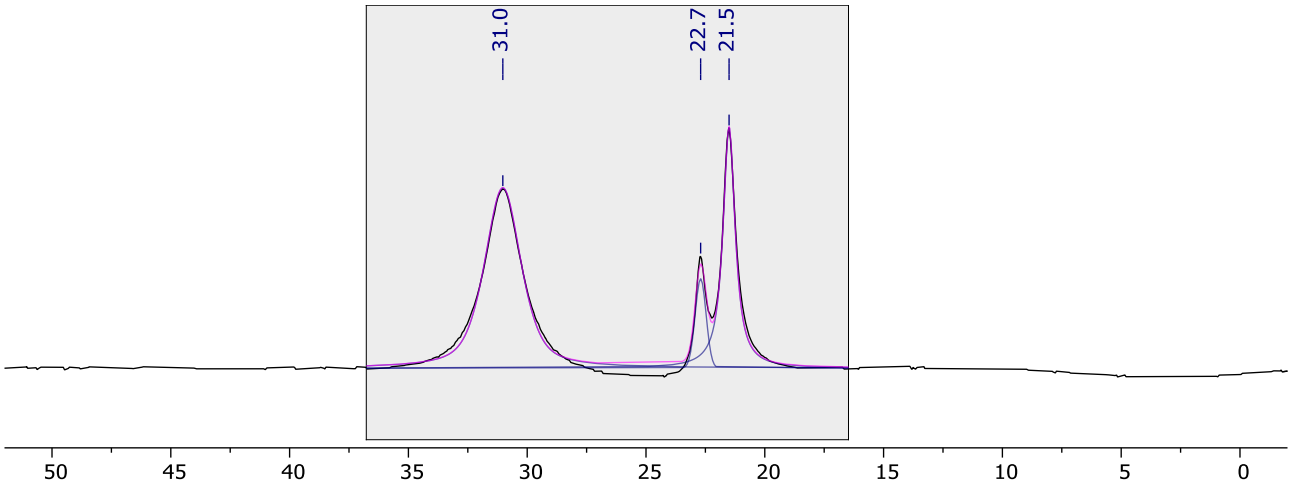

Figure S24. $^{11}B\{^{1}H\}$ NMR spectrum collected following the B_2pin_2 reduction of N_2O (3 bar gauge) using 5 mol% **2*** in THF after 120 min (128 MHz, THF/C_6D_6).

3.2.4 [Cu(IPr)(O*t*Bu)] **3***

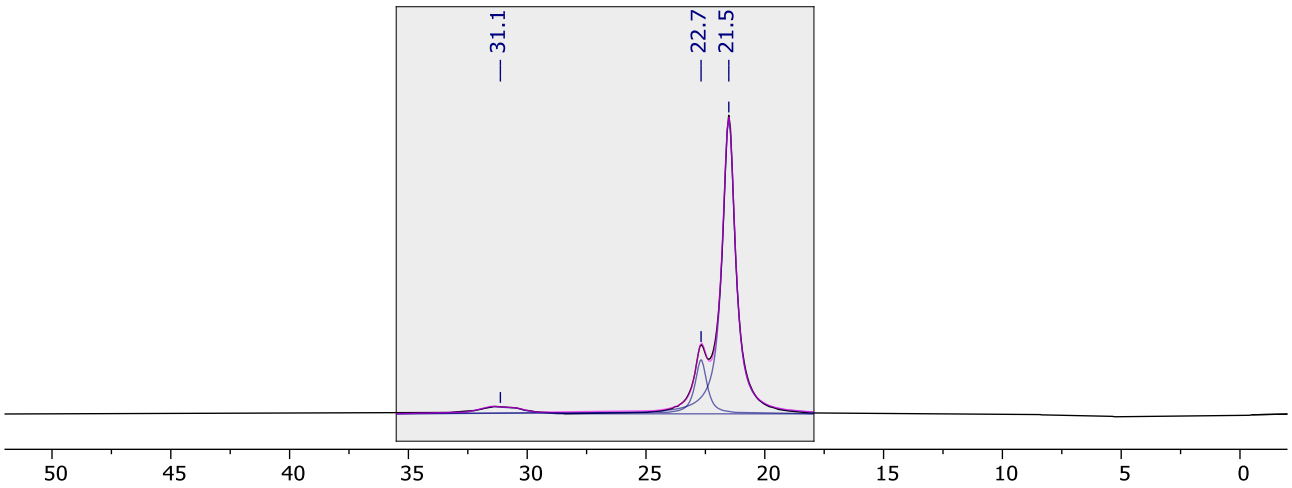

Figure S25. $^{11}B\{^{1}H\}$ NMR spectrum collected following the B_2pin_2 reduction of N_2O (3 bar gauge) using 5 mol% **3*** in THF after 120 min (128 MHz, THF/C_6D_6).

3.2.5 [Cu(SIMes)(O*t*Bu)] **4***

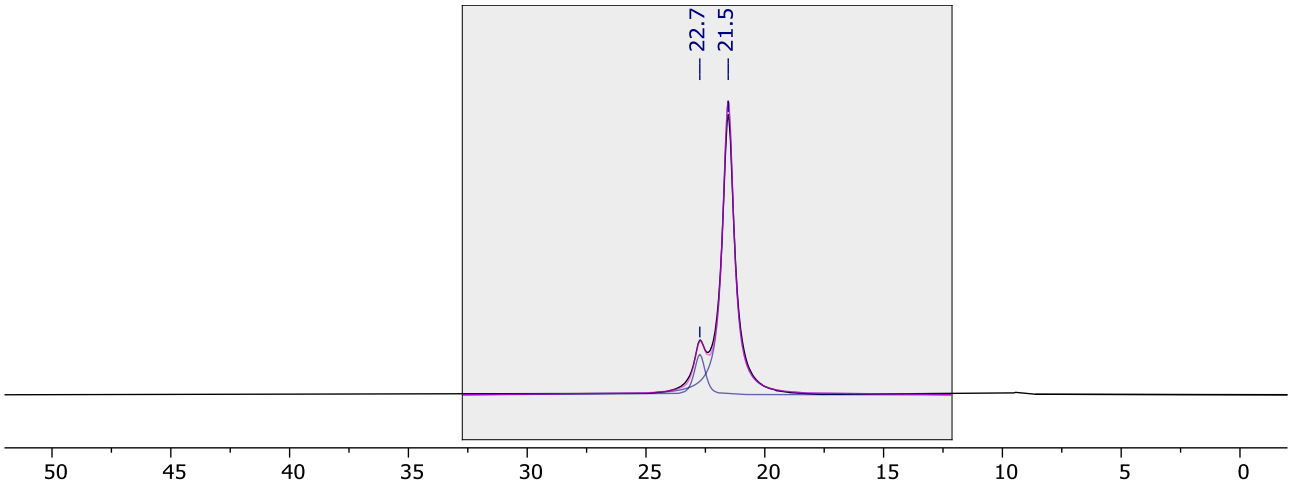

Figure S26. $^{11}B\{^{1}H\}$ NMR spectrum collected following the B_2pin_2 reduction of N_2O (3 bar gauge) using 5 mol% **4*** in THF after 120 min (128 MHz, THF/C_6D_6).

3.2.6 [Cu(IMes)(O*t*Bu)] **5***

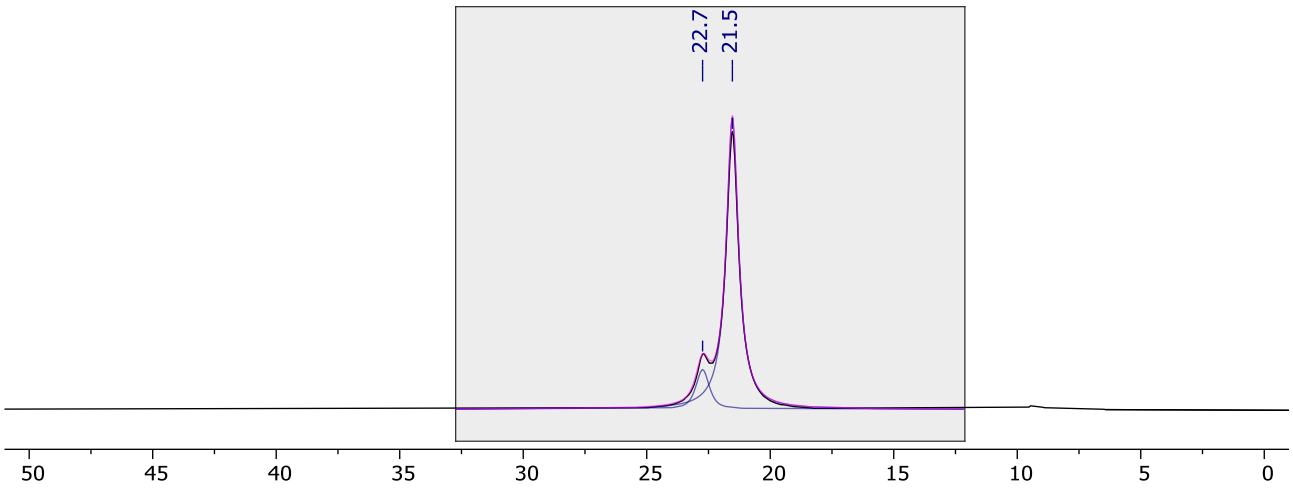

Figure S27. $^{11}B\{^{1}H\}$ NMR spectrum collected following the B_2pin_2 reduction of N_2O (3 bar gauge) using 5 mol% **5*** in THF after 120 min (128 MHz, THF/C_6D_6).

3.2.7 [CuO*t*Bu] **6***

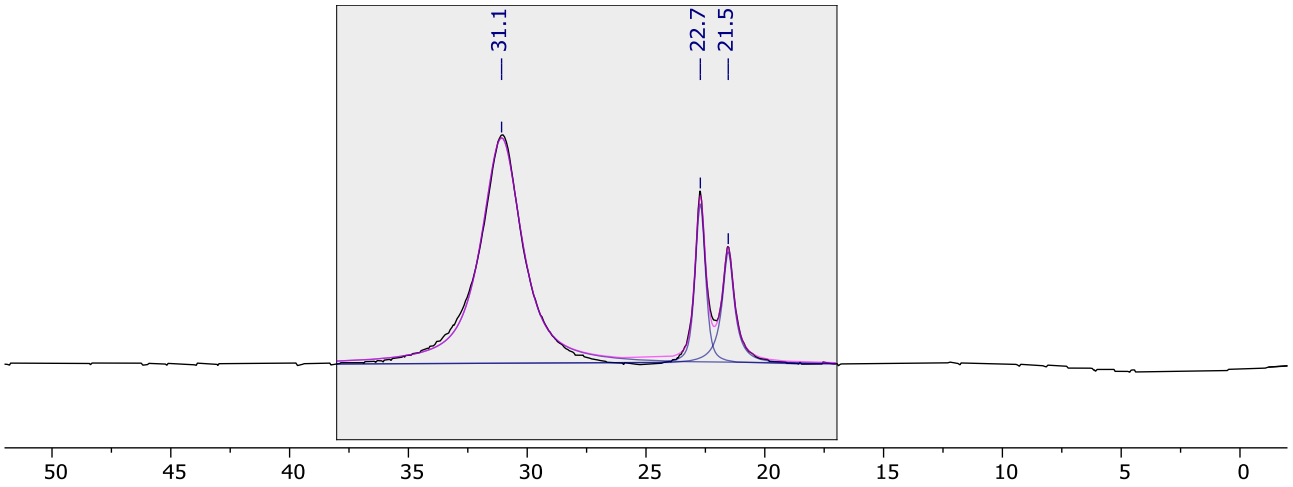

Figure S28. $^{11}B\{^{1}H\}$ NMR spectrum collected following the B_2pin_2 reduction of N_2O (3 bar gauge) using 5 mol% **6*** in THF after 120 min (128 MHz, THF/C_6D_6).

3.2.8 [Rh(PNP-*i*Pr)(OPh)] **7***

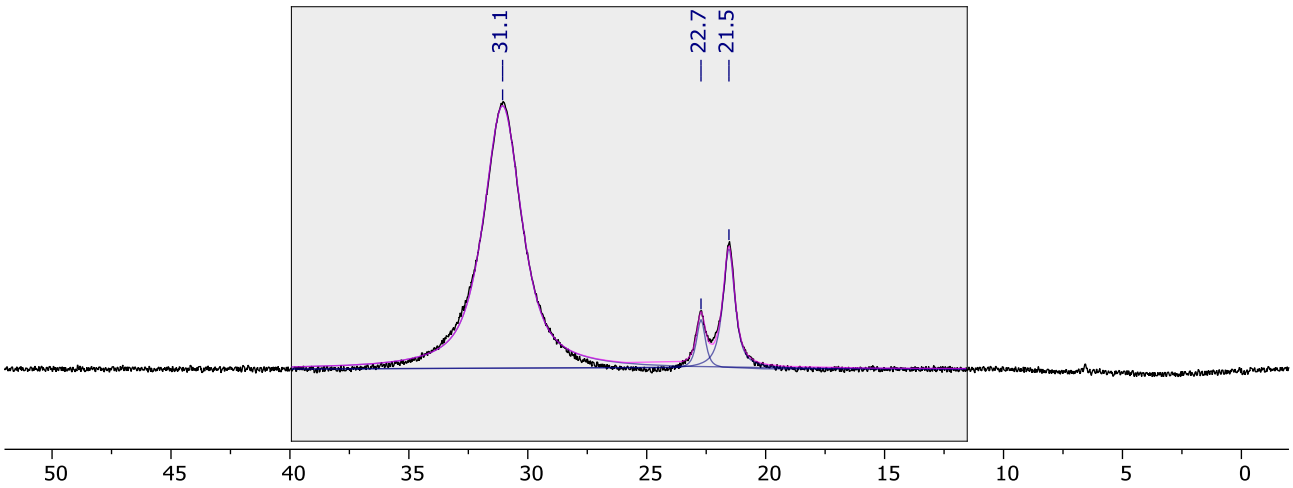

Figure S29. $^{11}B\{^{1}H\}$ NMR spectrum collected following the B_2pin_2 reduction of N_2O (3 bar gauge) using 5 mol% **7*** in THF after 120 min (128 MHz, THF/C_6D_6).

3.2.9 [Rh(POP-*i*Pr)(Bpin)] **8**

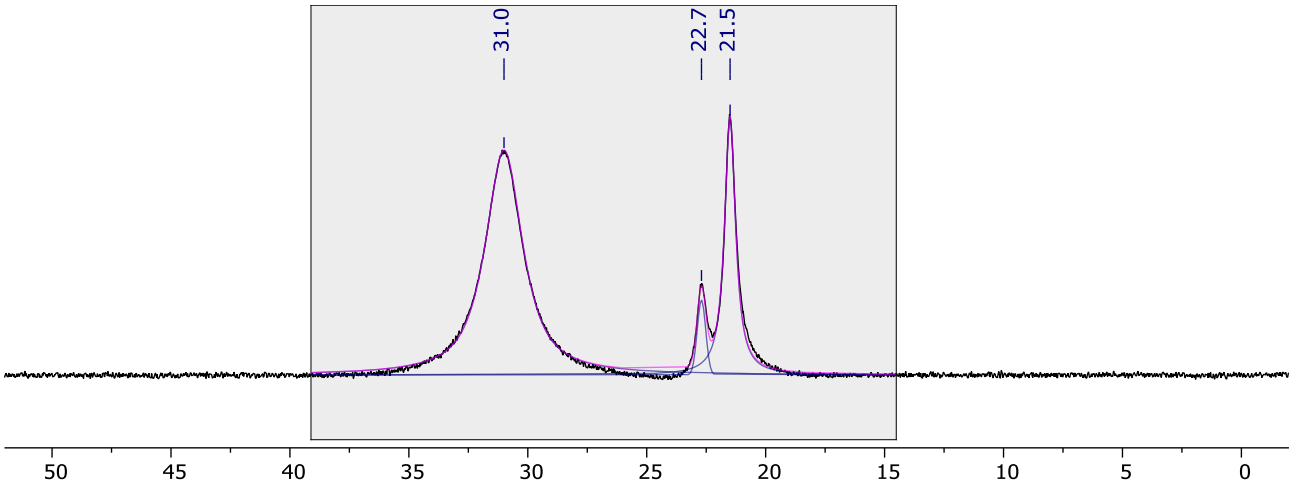

Figure S30. $^{11}B\{^{1}H\}$ NMR spectrum collected following the B_2pin_2 reduction of N_2O (3 bar gauge) using 5 mol% **8** in THF after 120 min (128 MHz, THF/C_6D_6).

3.3 Data collected for entry 1b

3.3.1 No catalyst

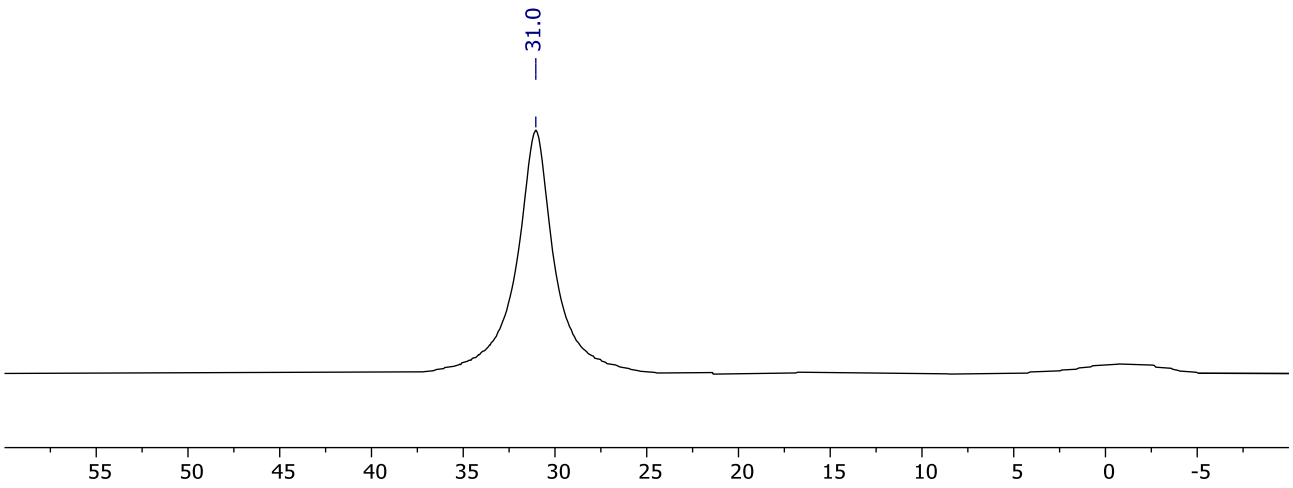

Figure S31. $^{11}B\{^{1}H\}$ NMR spectrum collected following the attempted B_2pin_2 reduction of N_2O (3 bar gauge) in THF with no catalyst after 120 min (128 MHz, THF/C_6D_6).

3.3.2 [Rh(PEt$_3$)$_3$(OPh)] (**1***)

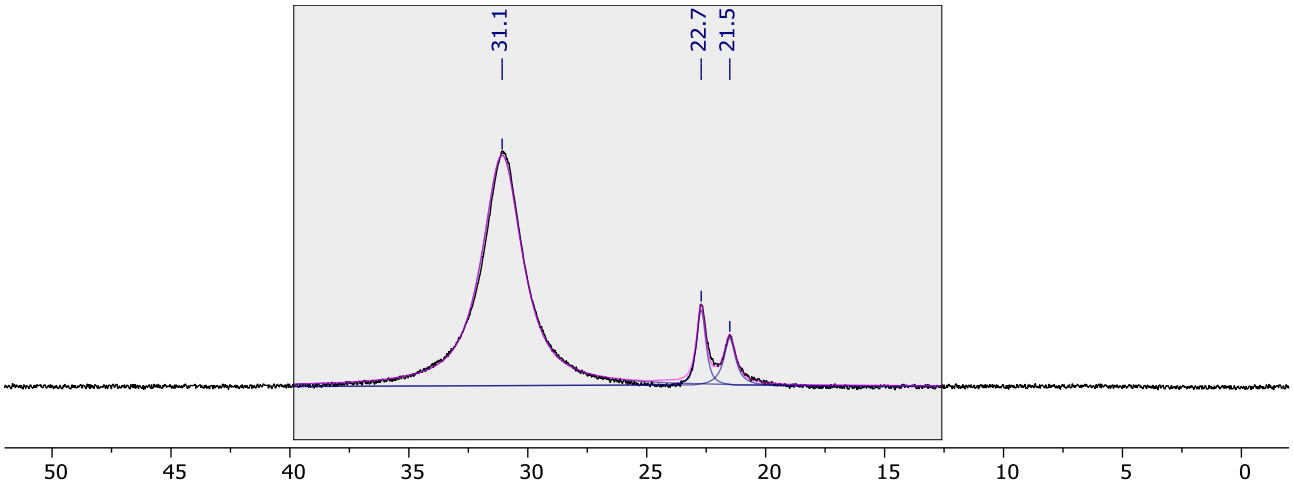

Figure S32. $^{11}B\{^1H\}$ NMR spectrum collected following the B_2pin_2 reduction of N_2O (3 bar gauge) using 5 mol% **1*** in THF after 120 min (128 MHz, THF/C_6D_6).

3.3.3 [Cu(SIPr)(O*t*Bu)] **2***

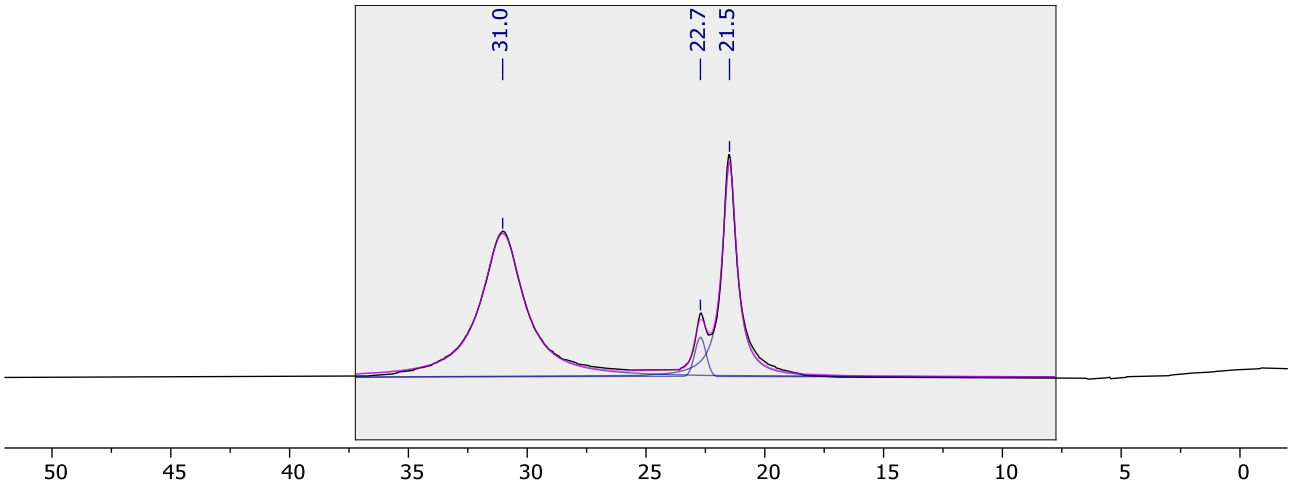

Figure S33. $^{11}B\{^1H\}$ NMR spectrum collected following the B_2pin_2 reduction of N_2O (3 bar gauge) using 5 mol% **2*** in THF after 120 min (128 MHz, THF/C_6D_6).

3.3.4 [Cu(IPr)(O*t*Bu)] **3***

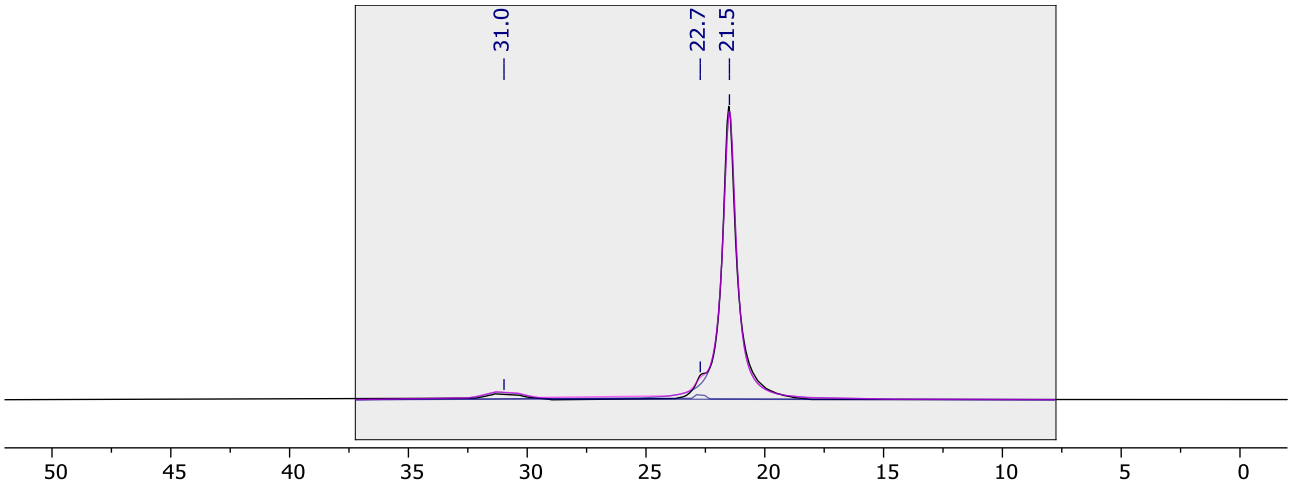

Figure S34. $^{11}B\{^{1}H\}$ NMR spectrum collected following the B_2pin_2 reduction of N_2O (3 bar gauge) using 5 mol% **3*** in THF after 120 min (128 MHz, THF/C_6D_6).

3.3.5 [Cu(SIMes)(O*t*Bu)] **4***

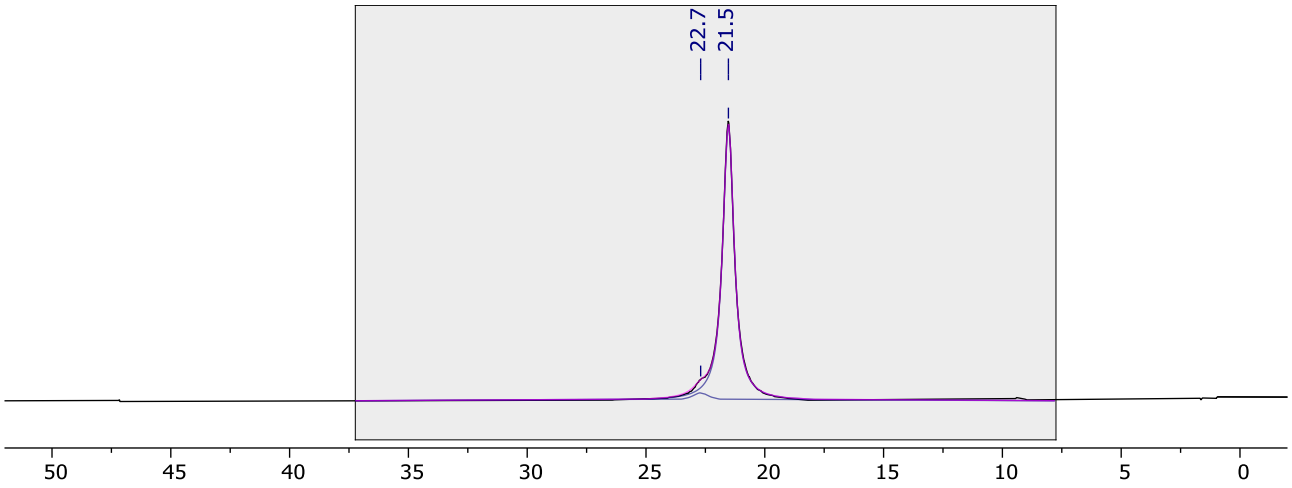

Figure S35. $^{11}B\{^{1}H\}$ NMR spectrum collected following the B_2pin_2 reduction of N_2O (3 bar gauge) using 5 mol% **4*** in THF after 120 min (128 MHz, THF/C_6D_6).

3.3.6 [Cu(IMes)(O*t*Bu)] **5***

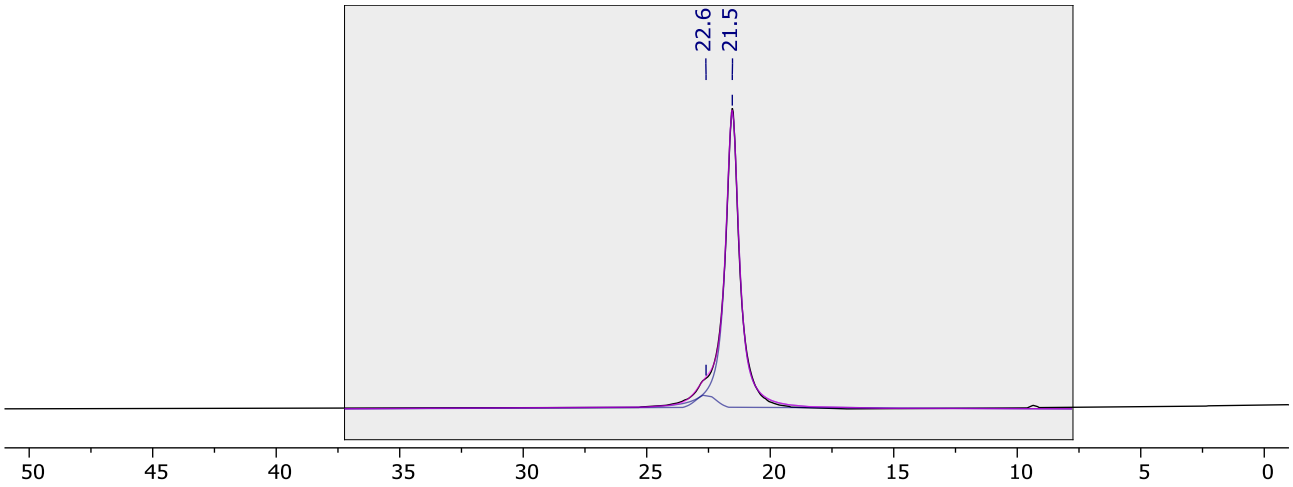

Figure S36. $^{11}B\{^{1}H\}$ NMR spectrum collected following the B_2pin_2 reduction of N_2O (3 bar gauge) using 5 mol% **5*** in THF after 120 min (128 MHz, THF/C_6D_6).

3.3.7 [CuO*t*Bu] **6***

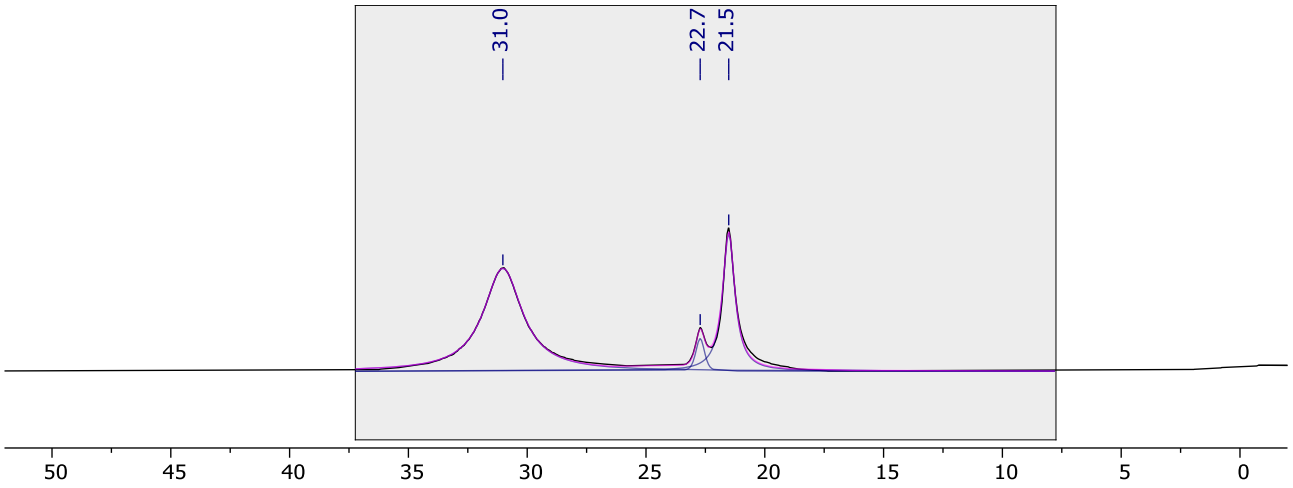

Figure S37. $^{11}B\{^{1}H\}$ NMR spectrum collected following the B_2pin_2 reduction of N_2O (3 bar gauge) using 5 mol% **6*** in THF after 120 min (128 MHz, THF/C_6D_6).

3.3.8 [Rh(PNP-*i*Pr)(OPh)] **7***

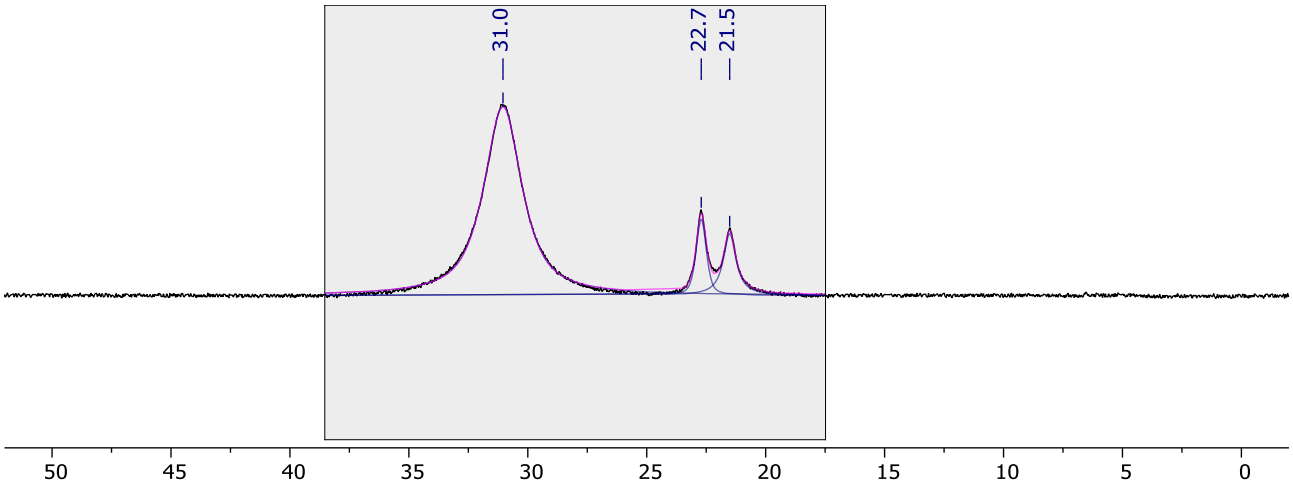

Figure S38. $^{11}B\{^{1}H\}$ NMR spectrum collected following the B_2pin_2 reduction of N_2O (3 bar gauge) using 5 mol% **7*** in THF after 120 min (128 MHz, THF/C_6D_6).

3.3.9 [Rh(POP-*i*Pr)(Bpin)] **8**

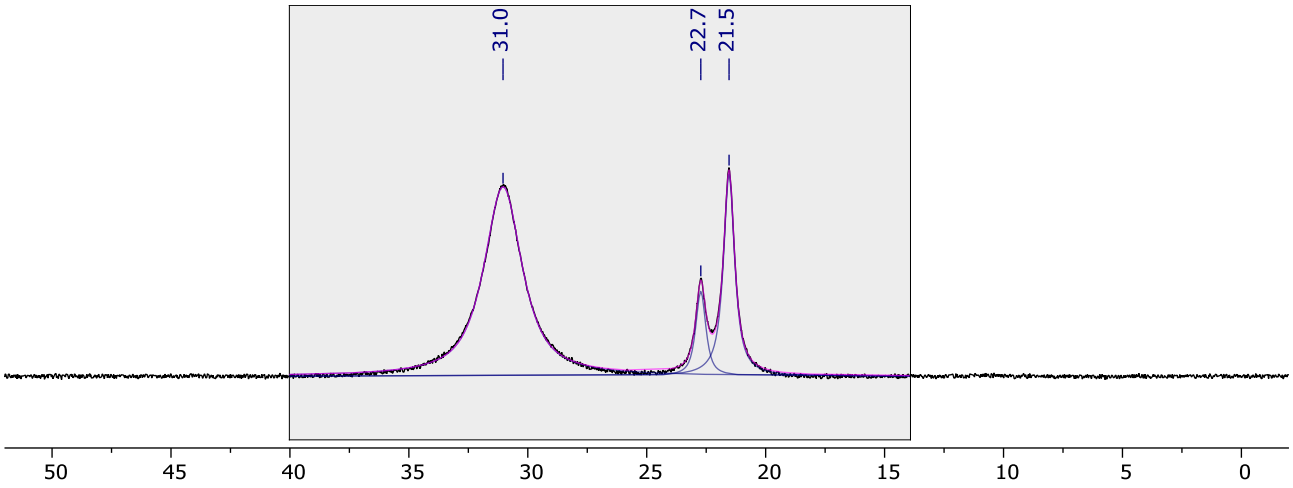

Figure S39. $^{11}B\{^{1}H\}$ NMR spectrum collected following the B_2pin_2 reduction of N_2O (3 bar gauge) using 5 mol% **8** in THF after 120 min (128 MHz, THF/C_6D_6).

3.4 Data collected for entry 2a

3.4.1 [Cu(SIMes)(O*t*Bu)] **4***

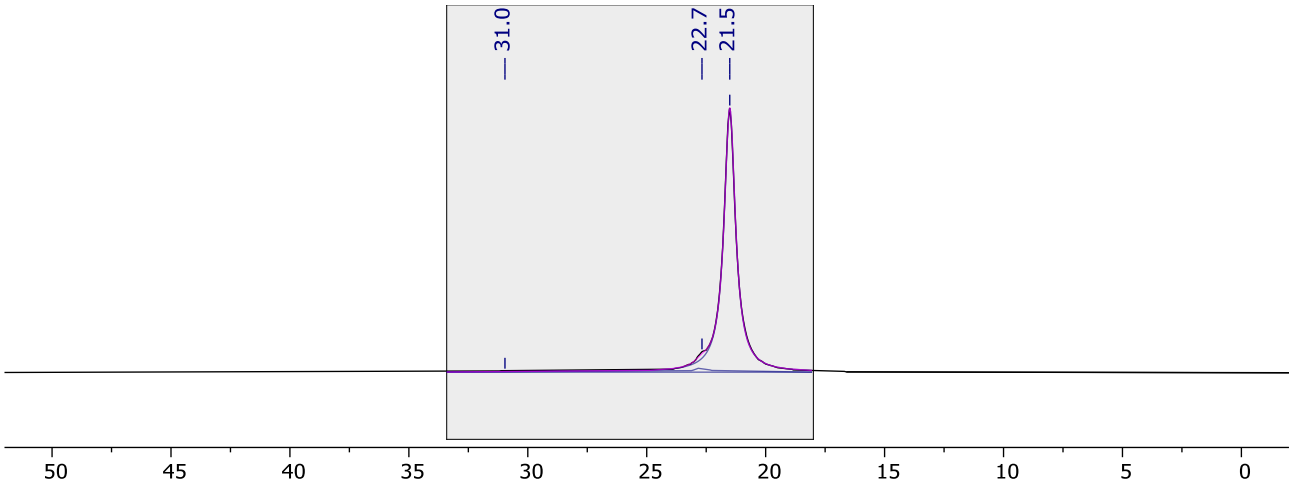

Figure S40. $^{11}B\{^{1}H\}$ NMR spectrum collected following the B_2pin_2 reduction of N_2O (3 bar gauge) using 5 mol% **4*** in THF after 10 min (128 MHz, THF/C_6D_6).

3.4.2 [Cu(IMes)(O*t*Bu)] **5***

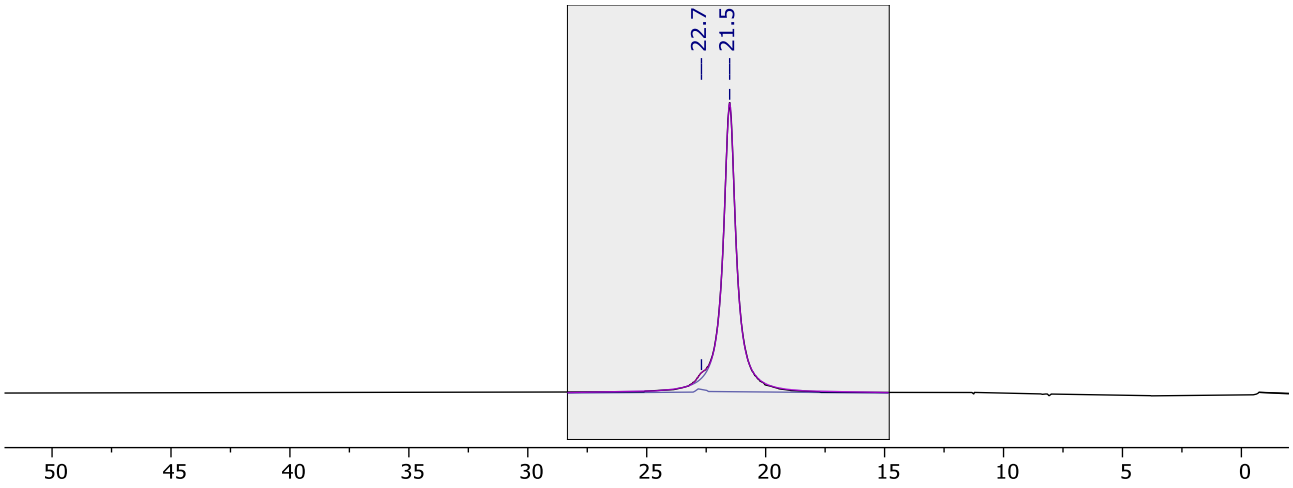

Figure S41. $^{11}B\{^{1}H\}$ NMR spectrum collected following the B_2pin_2 reduction of N_2O (3 bar gauge) using 5 mol% **5*** in THF after 10 min (128 MHz, THF/C_6D_6).

3.5 Data collected for entry 2b

3.5.1 [Cu(SIMes)(O*t*Bu)] **4***

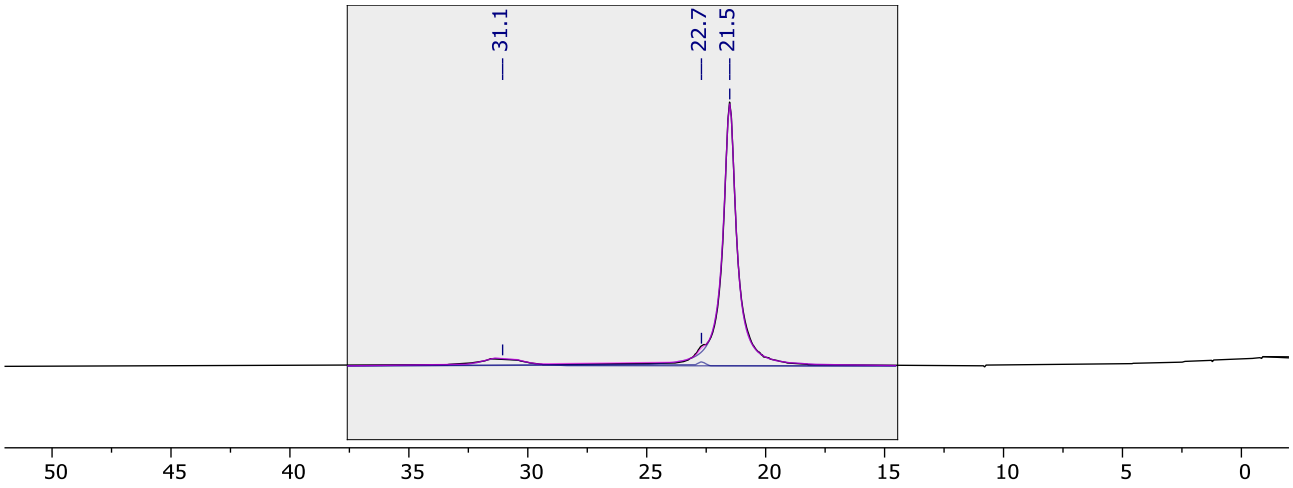

Figure S42. $^{11}B\{^{1}H\}$ NMR spectrum collected following the B_2pin_2 reduction of N_2O (3 bar gauge) using 5 mol% **4*** in THF after 10 min (128 MHz, THF/C_6D_6).

3.5.2 [Cu(IMes)(O*t*Bu)] **5***

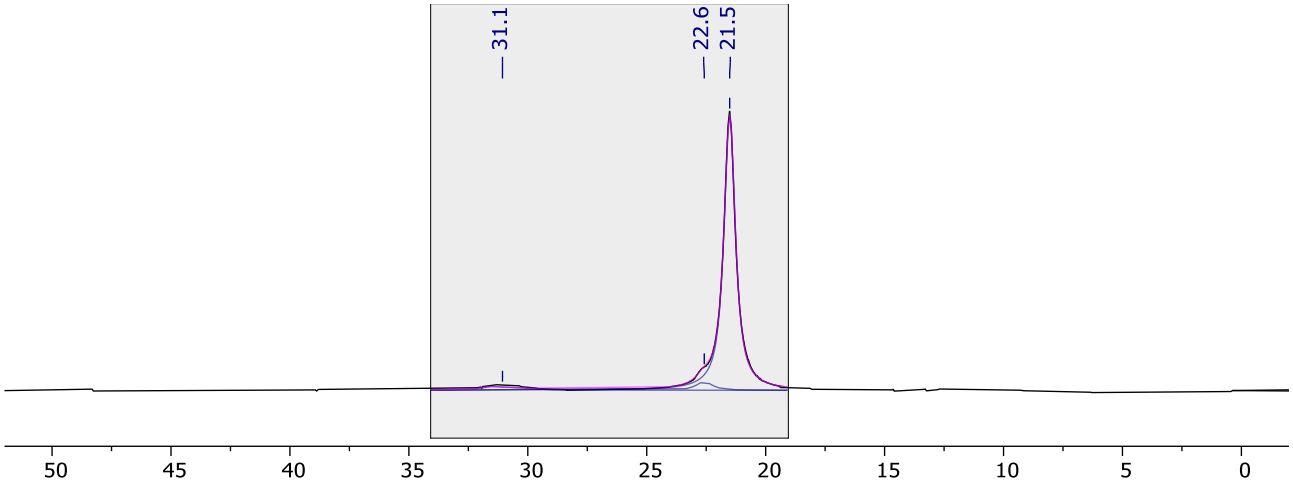

Figure S43. $^{11}B\{^{1}H\}$ NMR spectrum collected following the B_2pin_2 reduction of N_2O (3 bar gauge) using 5 mol% **5*** in THF after 10 min (128 MHz, THF/C_6D_6).

3.6 Data collected for entry 3a

3.6.1 [Cu(SIPr)(O*t*Bu)] **2***

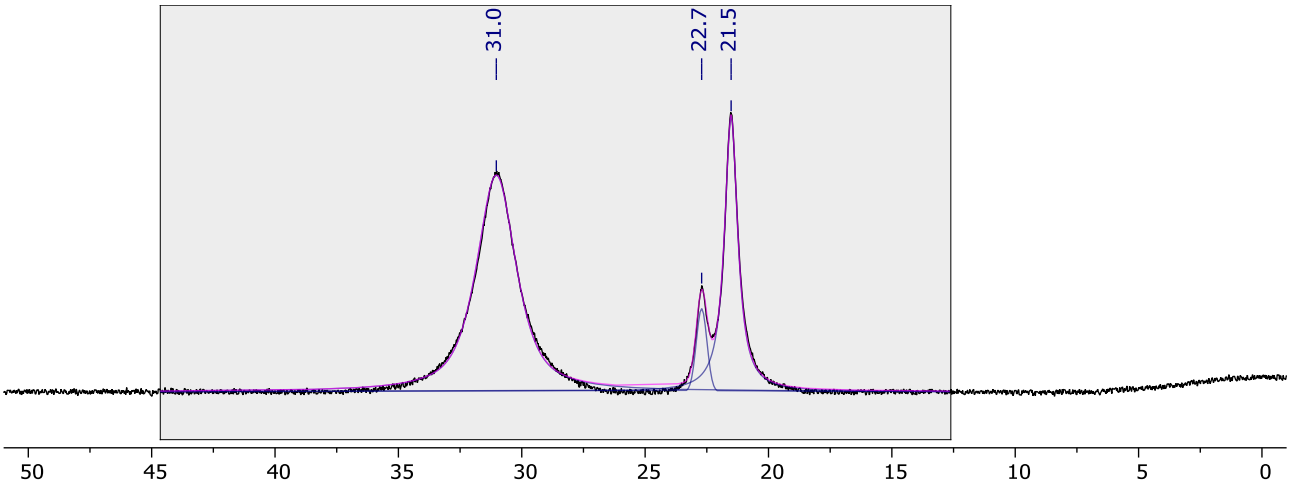

Figure S44. $^{11}B\{^{1}H\}$ NMR spectrum collected following the B_2pin_2 reduction of N_2O (1 bar gauge) using 5 mol% **2*** in THF after 120 min (128 MHz, THF/C_6D_6).

3.6.2 [Cu(IPr)(O*t*Bu)] **3***

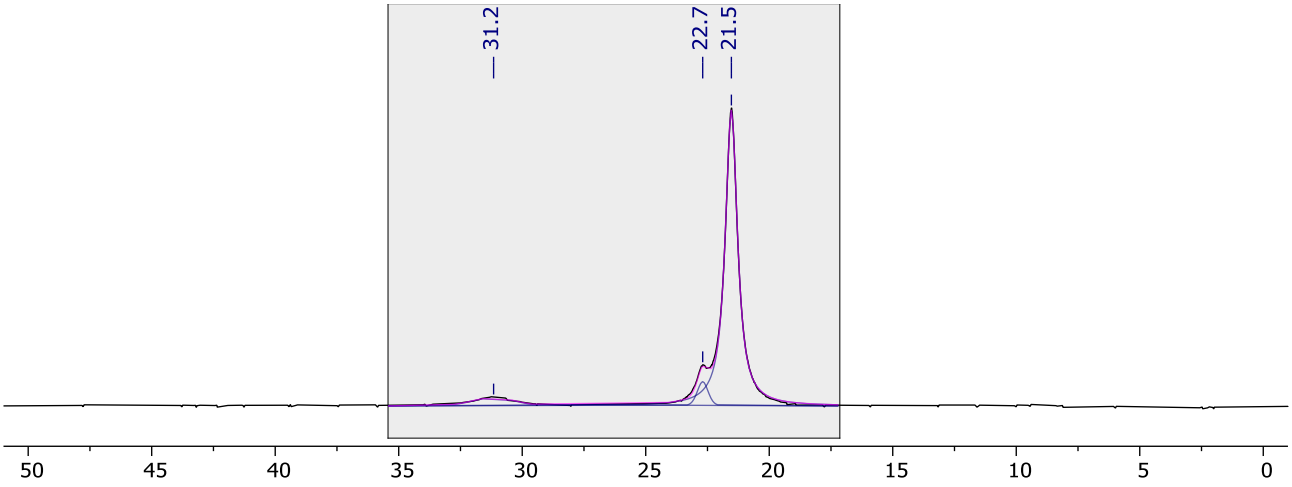

Figure S45. $^{11}B\{^{1}H\}$ NMR spectrum collected following the B_2pin_2 reduction of N_2O (1 bar gauge) using 5 mol% **3*** in THF after 120 min (128 MHz, THF/C_6D_6).

3.6.3 [Cu(SIMes)(O*t*Bu)] **4***

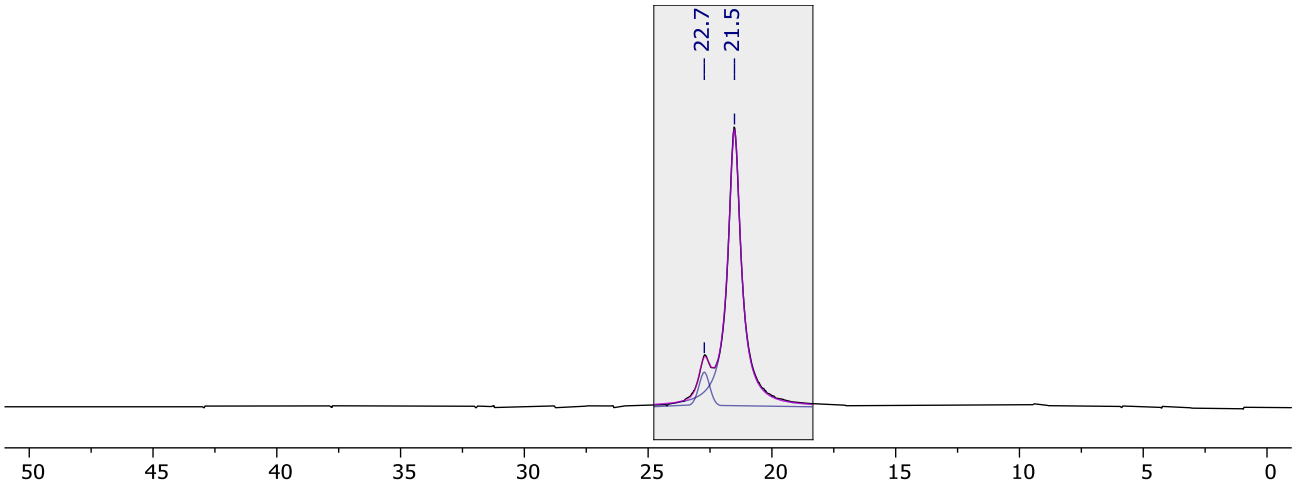

Figure S46. $^{11}B\{^{1}H\}$ NMR spectrum collected following the B_2pin_2 reduction of N_2O (1 bar gauge) using 5 mol% **4*** in THF after 120 min (128 MHz, THF/C_6D_6).

3.6.4 [Cu(IMes)(O*t*Bu)] **5***

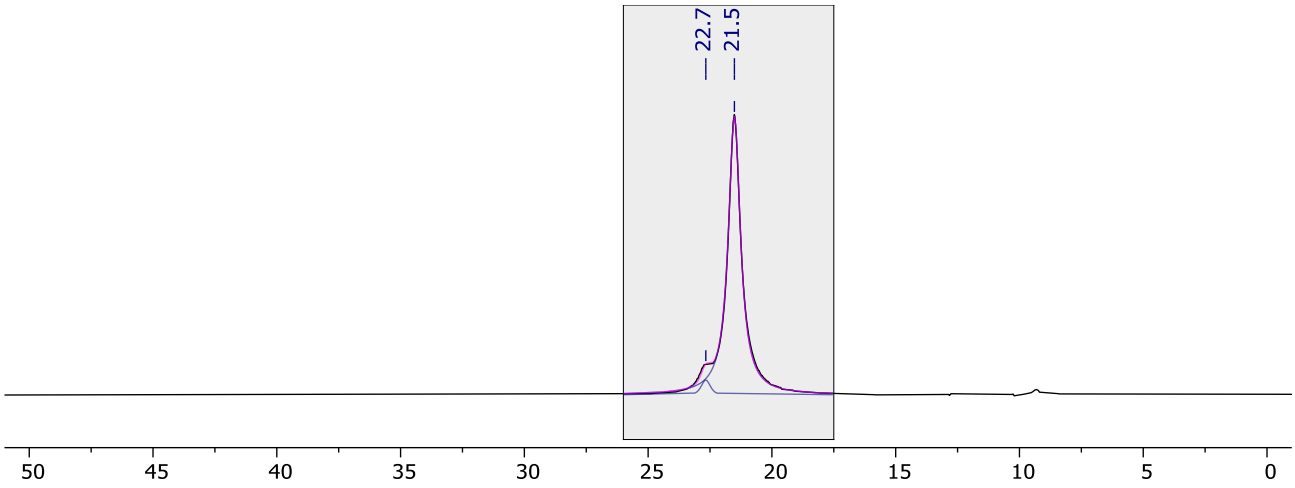

Figure S47. $^{11}B\{^{1}H\}$ NMR spectrum collected following the B_2pin_2 reduction of N_2O (1 bar gauge) using 5 mol% **5*** in THF after 120 min (128 MHz, THF/C_6D_6).

3.7 Data collected for entry 3b

3.7.1 [Cu(SIPr)(O*t*Bu)] **2***

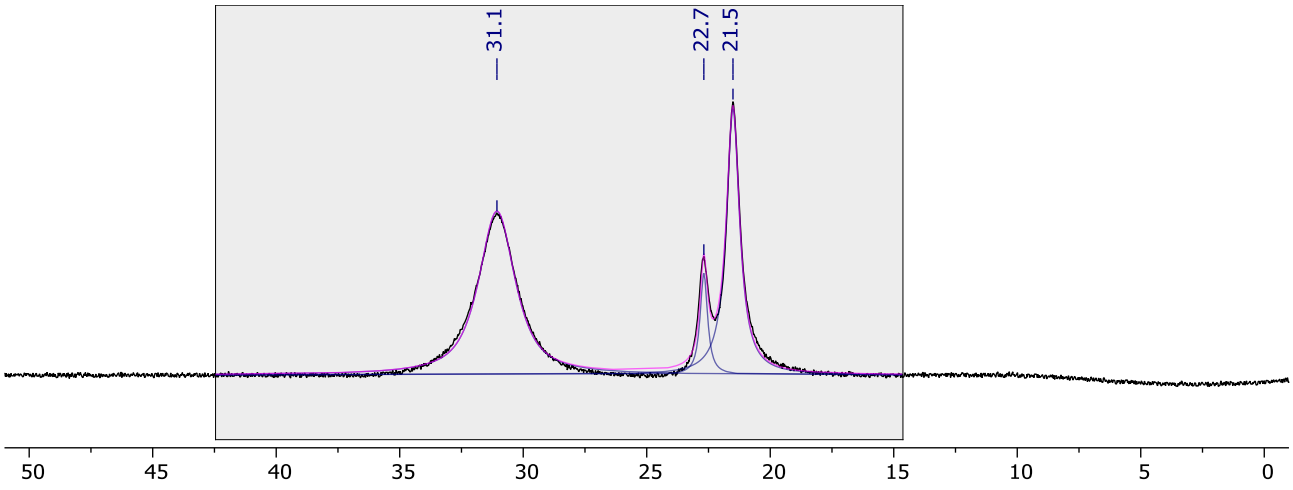

Figure S48. $^{11}B\{^{1}H\}$ NMR spectrum collected following the B_2pin_2 reduction of N_2O (1 bar gauge) using 5 mol% **2*** in THF after 120 min (128 MHz, THF/C_6D_6).

3.7.2 [Cu(IPr)(O*t*Bu)] **3***

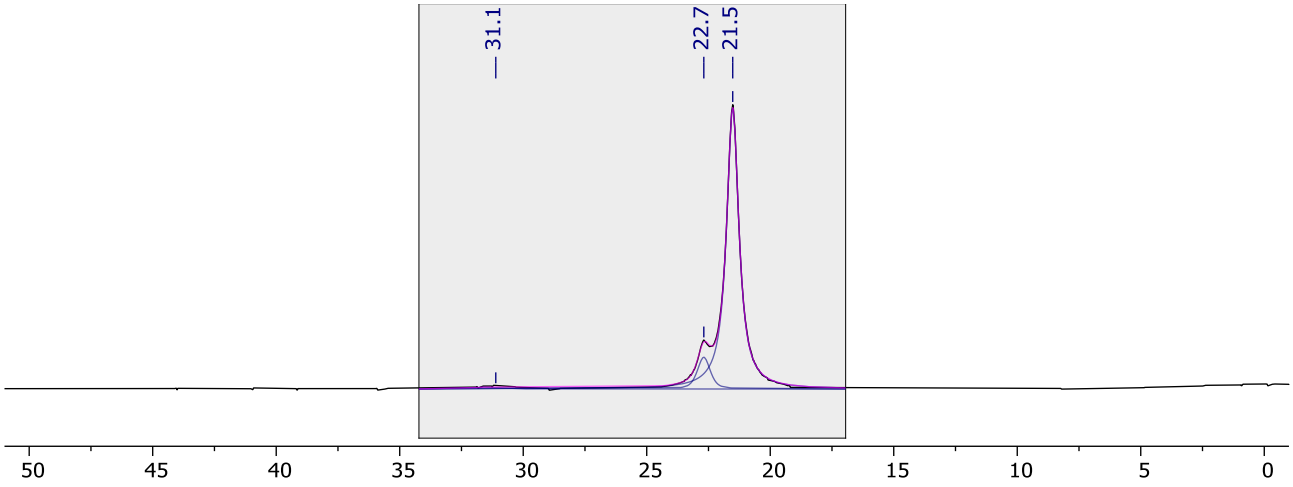

Figure S49. $^{11}B\{^{1}H\}$ NMR spectrum collected following the B_2pin_2 reduction of N_2O (1 bar gauge) using 5 mol% **3*** in THF after 120 min (128 MHz, THF/C_6D_6).

3.7.3 [Cu(SIMes)(O*t*Bu)] **4***

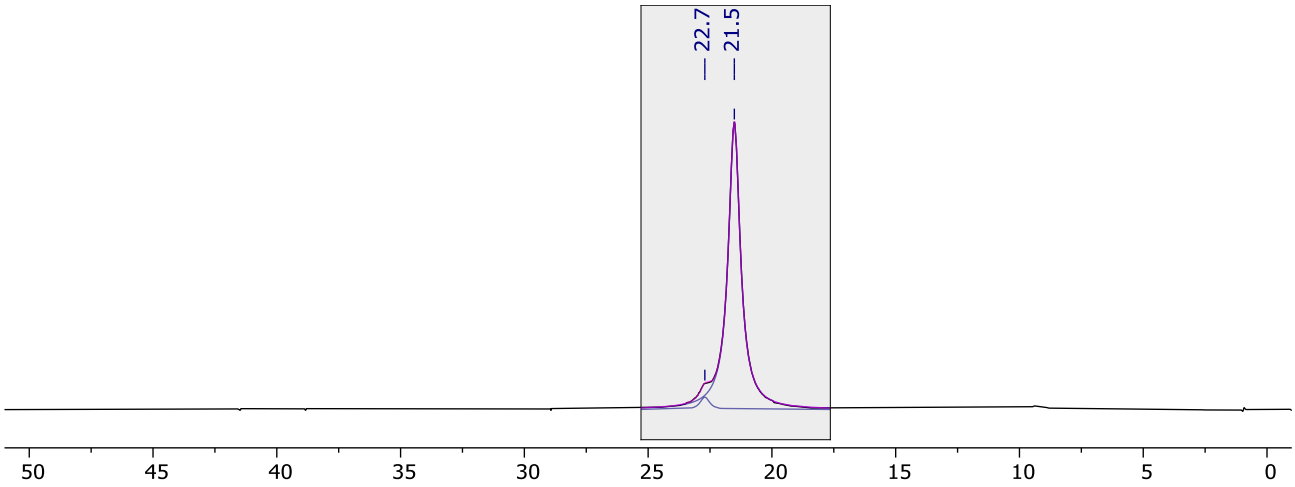

Figure S50. $^{11}B\{^{1}H\}$ NMR spectrum collected following the B_2pin_2 reduction of N_2O (1 bar gauge) using 5 mol% **4*** in THF after 120 min (128 MHz, THF/C_6D_6).

3.7.4 [Cu(IMes)(O*t*Bu)] **5***

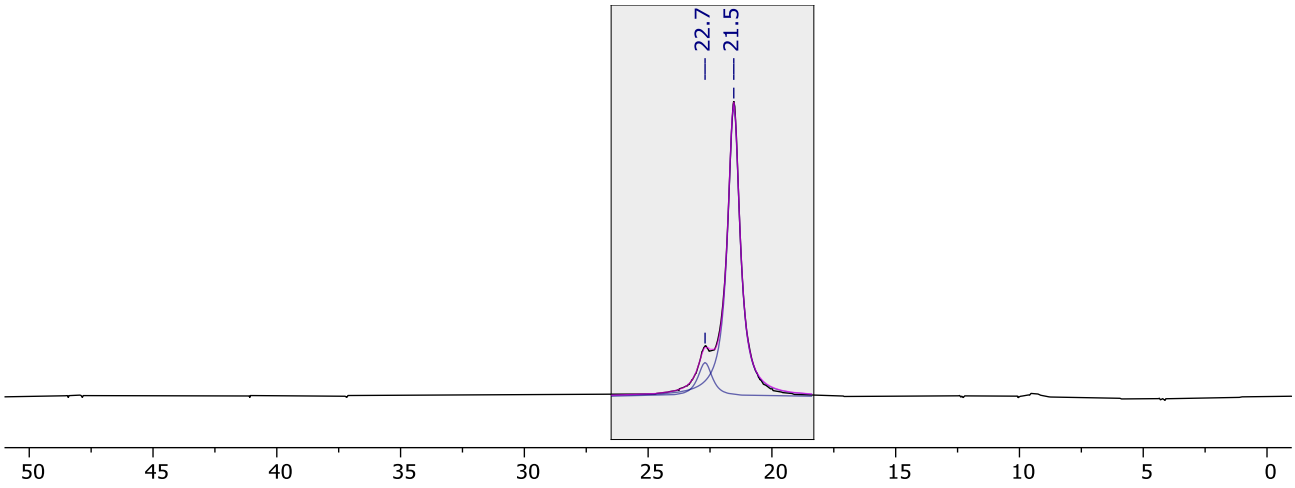

Figure S51. $^{11}B\{^{1}H\}$ NMR spectrum collected following the B_2pin_2 reduction of N_2O (1 bar gauge) using 5 mol% **5*** in THF after 120 min (128 MHz, THF/C_6D_6).

3.8 Data collected for entry 4a

3.8.1 [Cu(SIMes)(O*t*Bu)] **4***

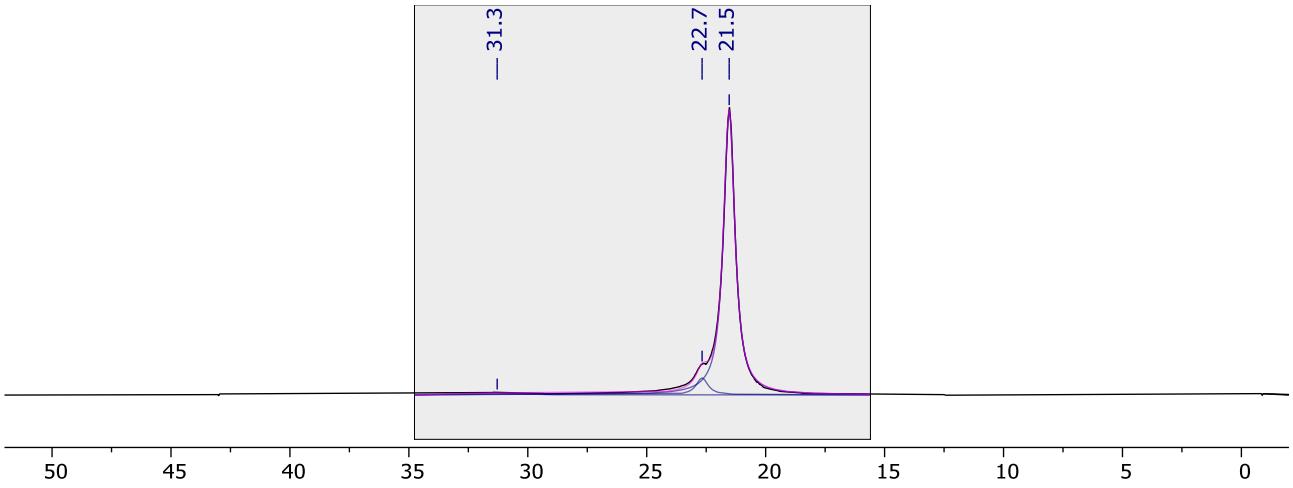

Figure S52. $^{11}B\{^{1}H\}$ NMR spectrum collected following the B_2pin_2 reduction of N_2O (1 bar gauge) using 5 mol% **4*** in THF after 10 min (128 MHz, THF/C_6D_6).

3.8.2 [Cu(IMes)(O*t*Bu)] **5***

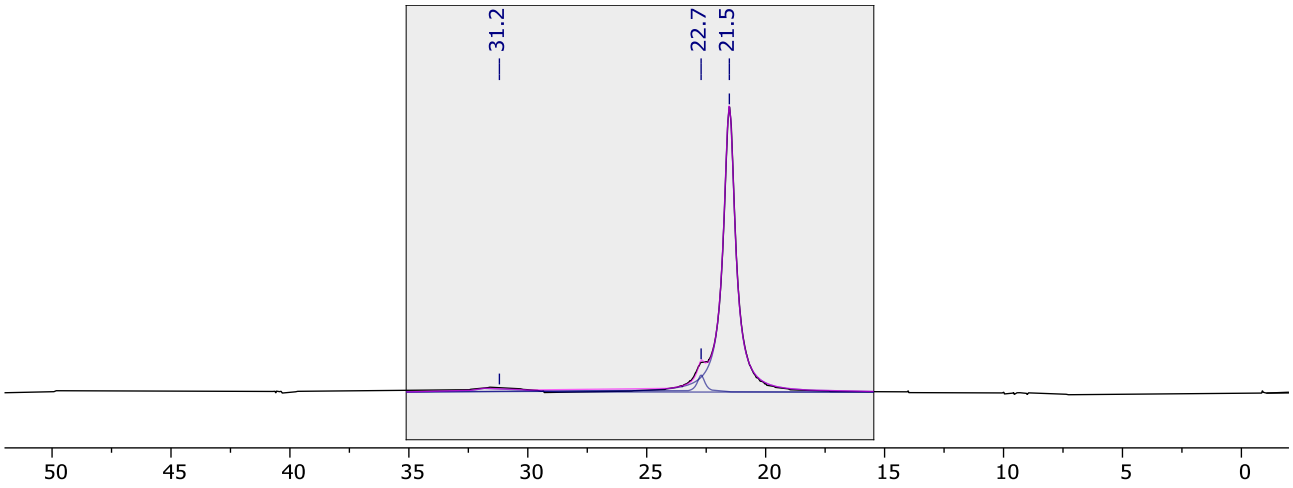

Figure S53. $^{11}B\{^{1}H\}$ NMR spectrum collected following the B_2pin_2 reduction of N_2O (1 bar gauge) using 5 mol% **5*** in THF after 10 min (128 MHz, THF/C_6D_6).

3.9 Data collected for entry 4b

3.9.1 [Cu(SIMes)(O*t*Bu)] **4***

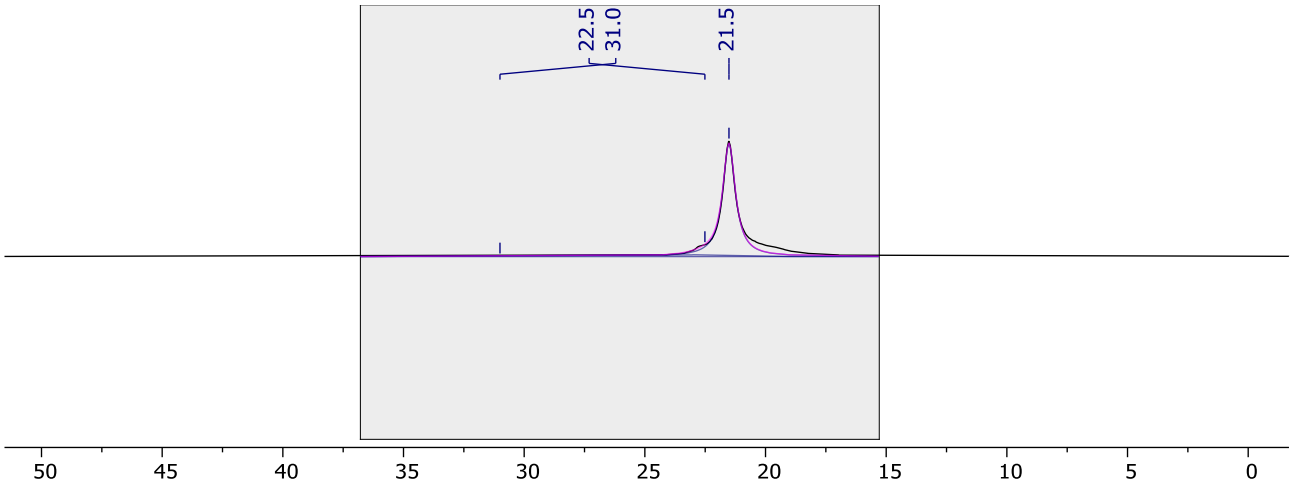

Figure S54. $^{11}B\{^{1}H\}$ NMR spectrum collected following the B_2pin_2 reduction of N_2O (1 bar gauge) using 5 mol% **4*** in THF after 10 min (128 MHz, THF/C_6D_6).

3.9.2 [Cu(IMes)(O*t*Bu)] **5***

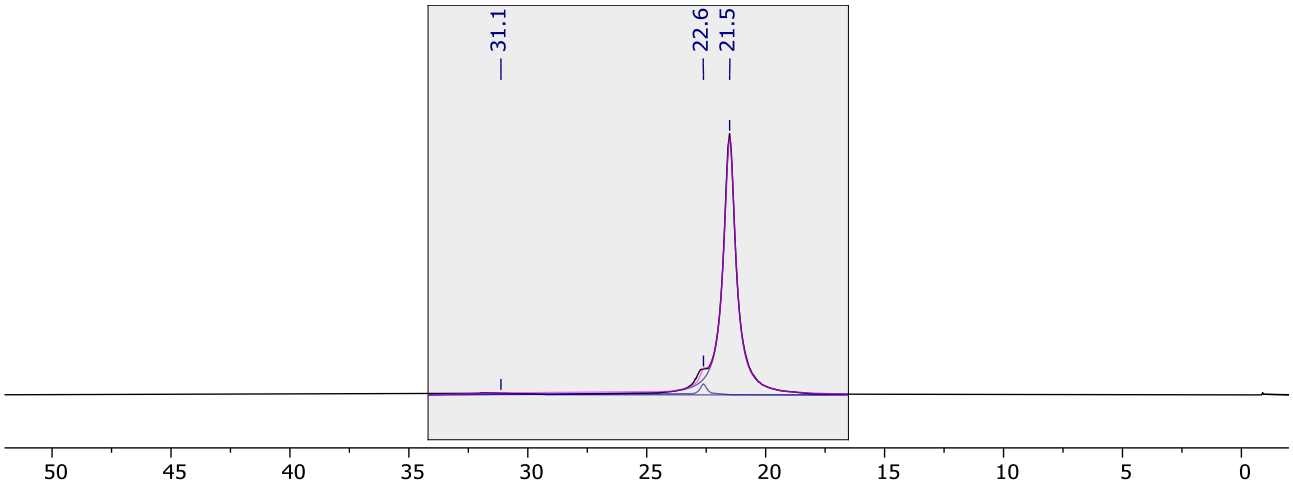

Figure S55. $^{11}B\{^{1}H\}$ NMR spectrum collected following the B_2pin_2 reduction of N_2O (1 bar gauge) using 5 mol% **5*** in THF after 10 min (128 MHz, THF/C_6D_6).

3.10 Data collected for entry 5a

3.10.1 No catalyst

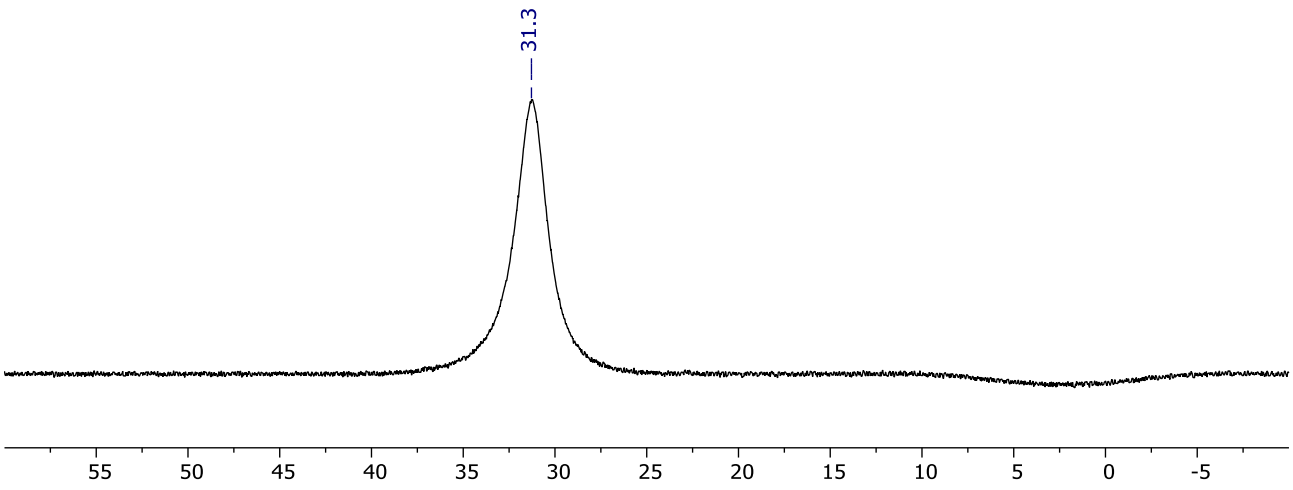

Figure S56. $^{11}B\{^{1}H\}$ NMR spectrum collected following the attempted B_2pin_2 reduction of N_2O (3 bar gauge) in toluene with no catalyst after 120 min (128 MHz, toluene/C_6D_6).

3.10.2 [Cu(SIPr)(O*t*Bu)] **2***

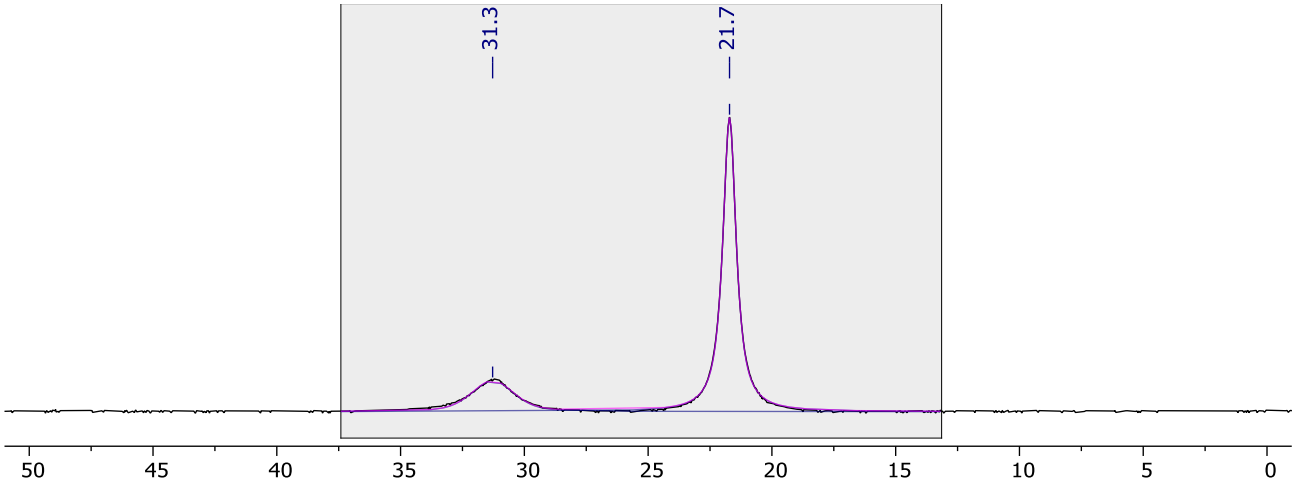

Figure S57. $^{11}B\{^{1}H\}$ NMR spectrum collected following the B_2pin_2 reduction of N_2O (3 bar gauge) using 5 mol% **2*** in toluene after 120 min (128 MHz, toluene/C_6D_6).

3.10.3 [Cu(IPr)(O*t*Bu)] **3***

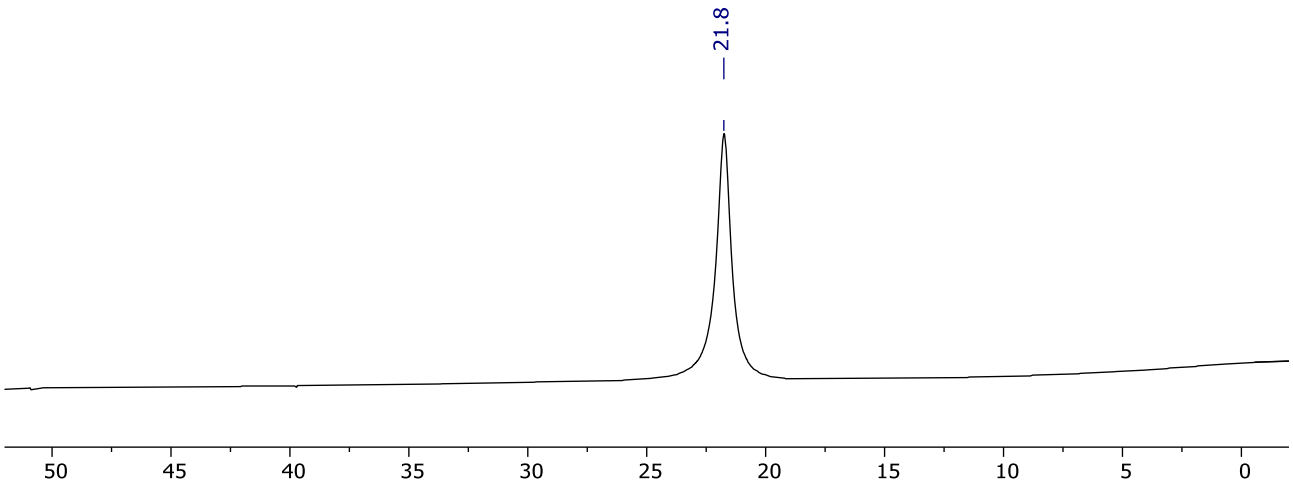

Figure S58. $^{11}B\{^{1}H\}$ NMR spectrum collected following the B_2pin_2 reduction of N_2O (3 bar gauge) using 5 mol% **3*** in toluene after 120 min (128 MHz, toluene/C_6D_6).

3.10.4 [Cu(SIMes)(O*t*Bu)] **4***

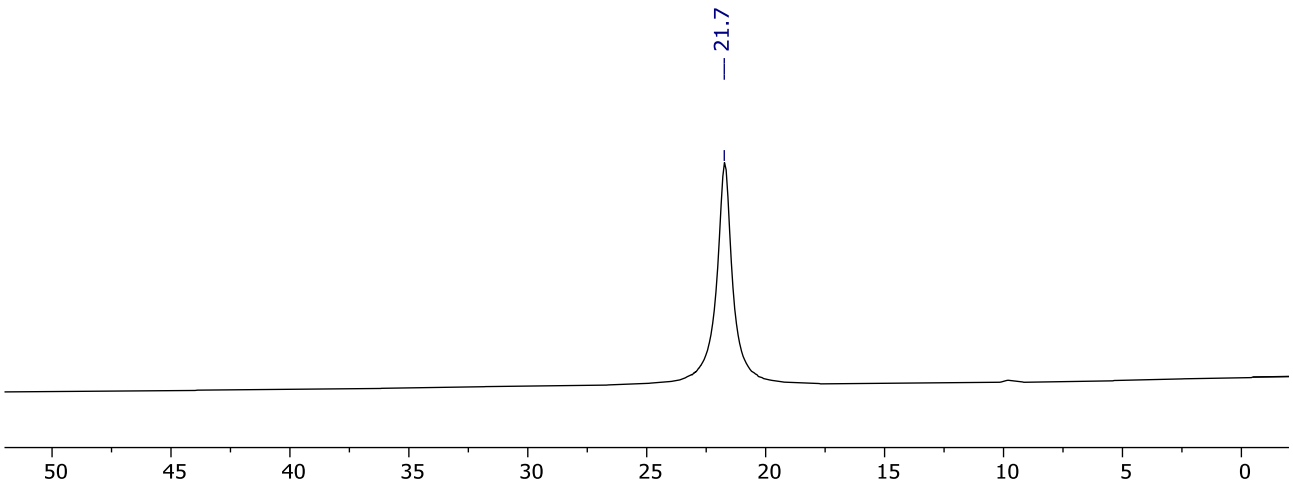

Figure S59. $^{11}B\{^{1}H\}$ NMR spectrum collected following the B_2pin_2 reduction of N_2O (3 bar gauge) using 5 mol% **4*** in toluene after 120 min (128 MHz, toluene/C_6D_6).

3.10.5 [Cu(IMes)(O*t*Bu)] **5***

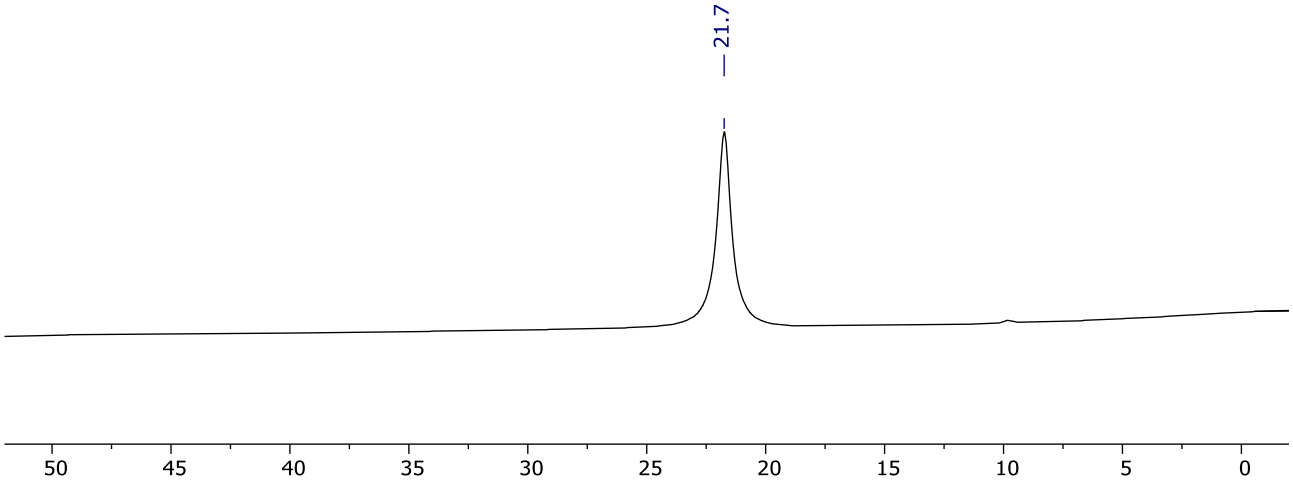

Figure S60. $^{11}B\{^{1}H\}$ NMR spectrum collected following the B_2pin_2 reduction of N_2O (3 bar gauge) using 5 mol% **5*** in toluene after 120 min (128 MHz, toluene/C_6D_6).

3.10.6 [CuO*t*Bu] **6***

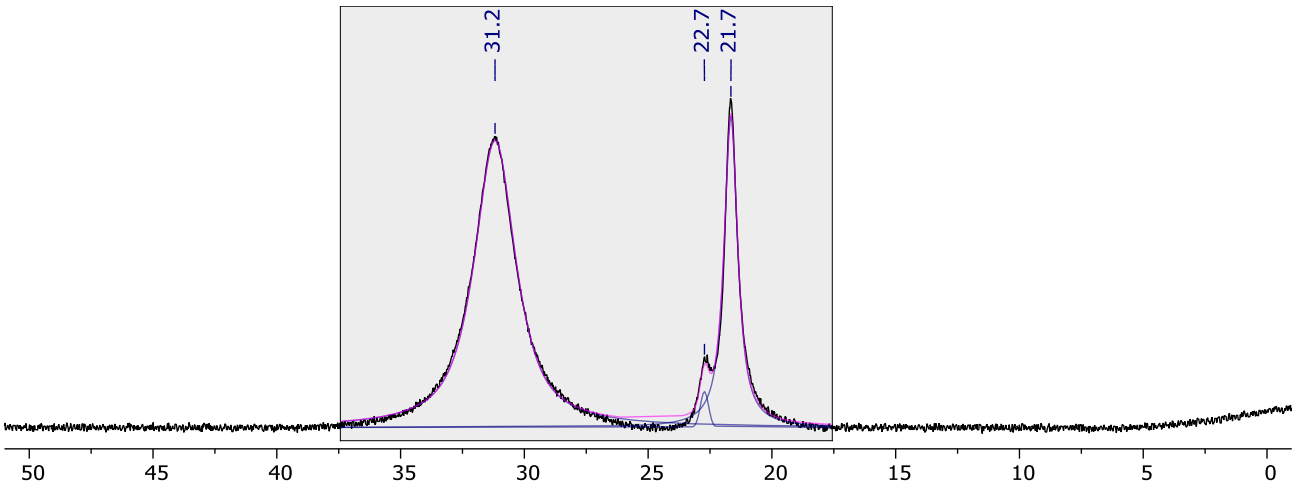

Figure S61. $^{11}B\{^{1}H\}$ NMR spectrum collected following the B_2pin_2 reduction of N_2O (3 bar gauge) using 5 mol% **6*** in toluene after 120 min (128 MHz, toluene/C_6D_6).

3.11 Data collected for entry 5b

3.11.1 No catalyst

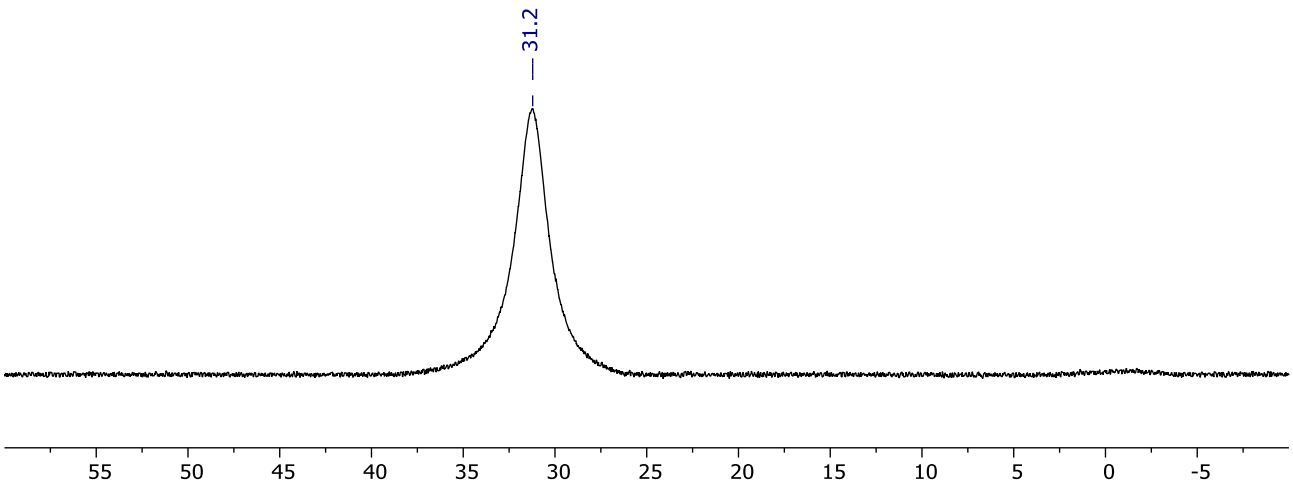

Figure S62. $^{11}B\{^{1}H\}$ NMR spectrum collected following the attempted B_2pin_2 reduction of N_2O (3 bar gauge) in toluene with no catalyst after 120 min (128 MHz, toluene/C_6D_6).

3.11.2 [Cu(SIPr)(O*t*Bu)] **2***

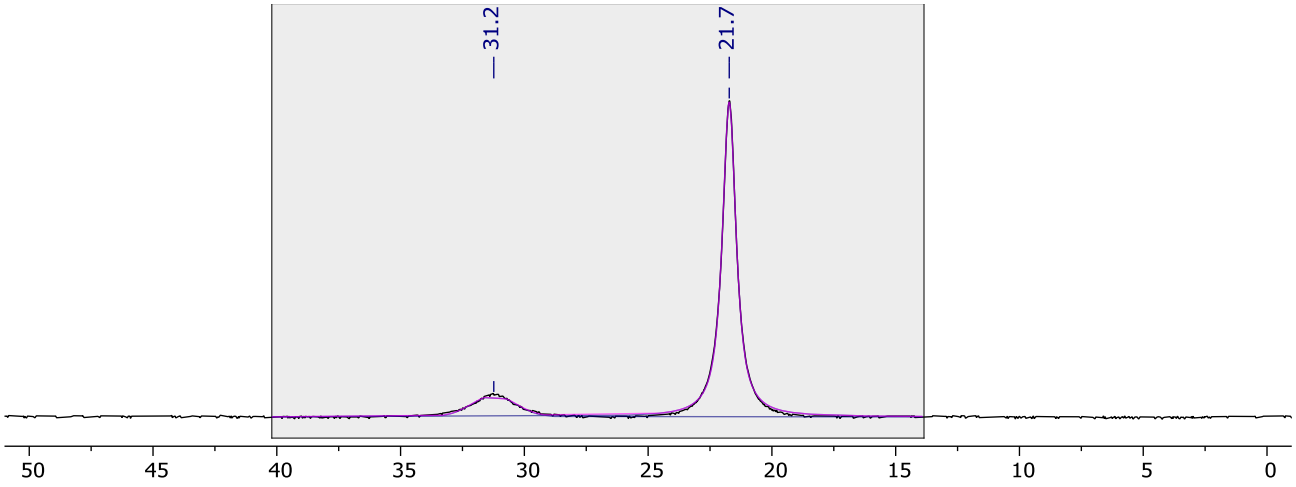

Figure S63. $^{11}B\{^{1}H\}$ NMR spectrum collected following the B_2pin_2 reduction of N_2O (3 bar gauge) using 5 mol% **2*** in toluene after 120 min (128 MHz, toluene/C_6D_6).

3.11.3 [Cu(IPr)(O*t*Bu)] **3***

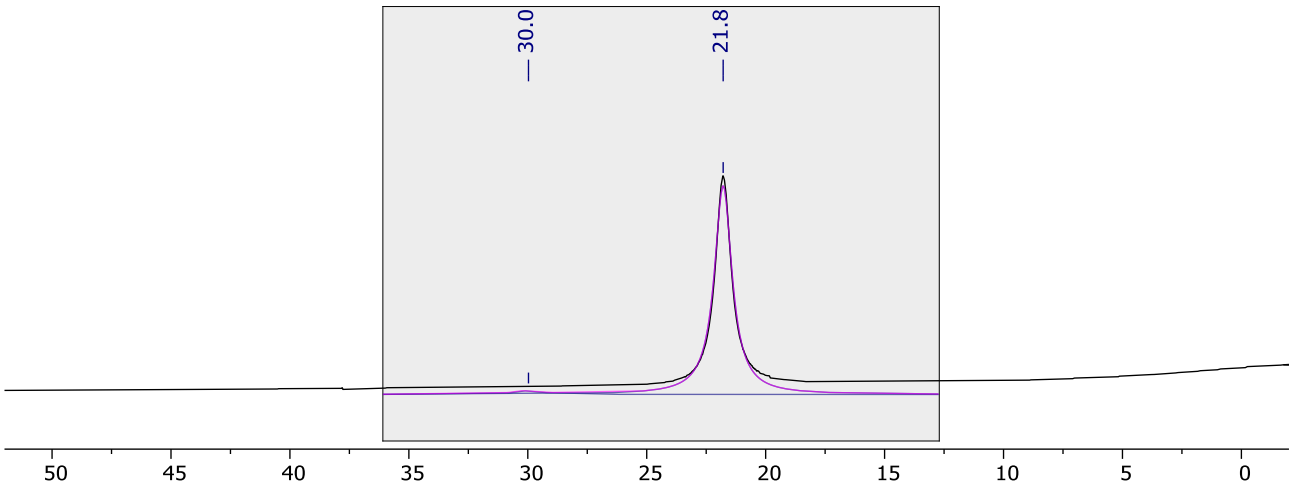

Figure S64. $^{11}B\{^{1}H\}$ NMR spectrum collected following the B_2pin_2 reduction of N_2O (3 bar gauge) using 5 mol% **3*** in toluene after 120 min (128 MHz, toluene/C_6D_6).

3.11.4 [Cu(SIMes)(O*t*Bu)] **4***

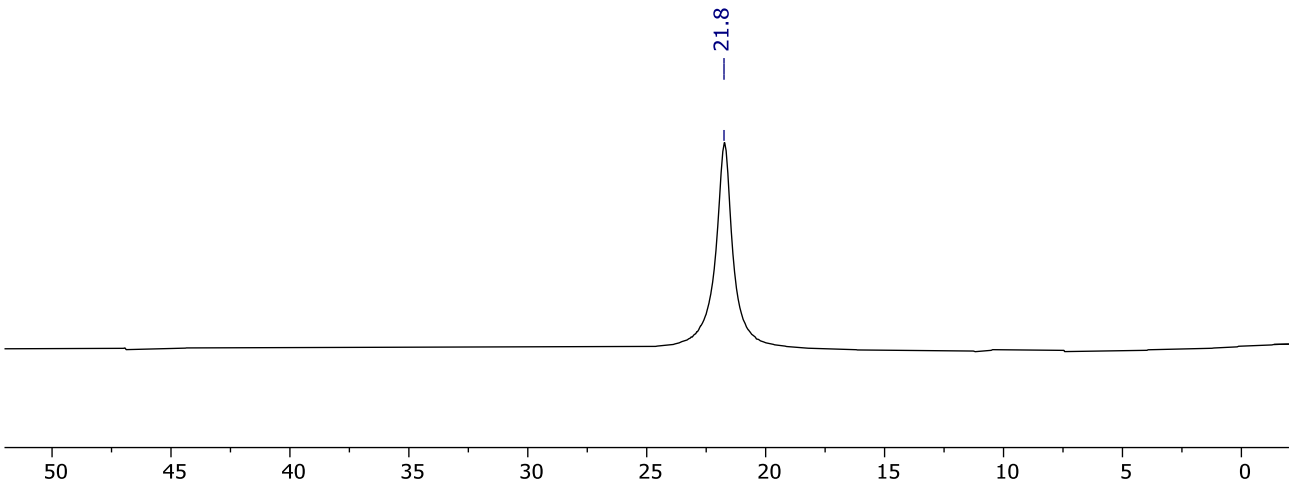

Figure S65. $^{11}B\{^{1}H\}$ NMR spectrum collected following the B_2pin_2 reduction of N_2O (3 bar gauge) using 5 mol% **4*** in toluene after 120 min (128 MHz, toluene/C_6D_6).

3.11.5 [Cu(IMes)(O*t*Bu)] **5***

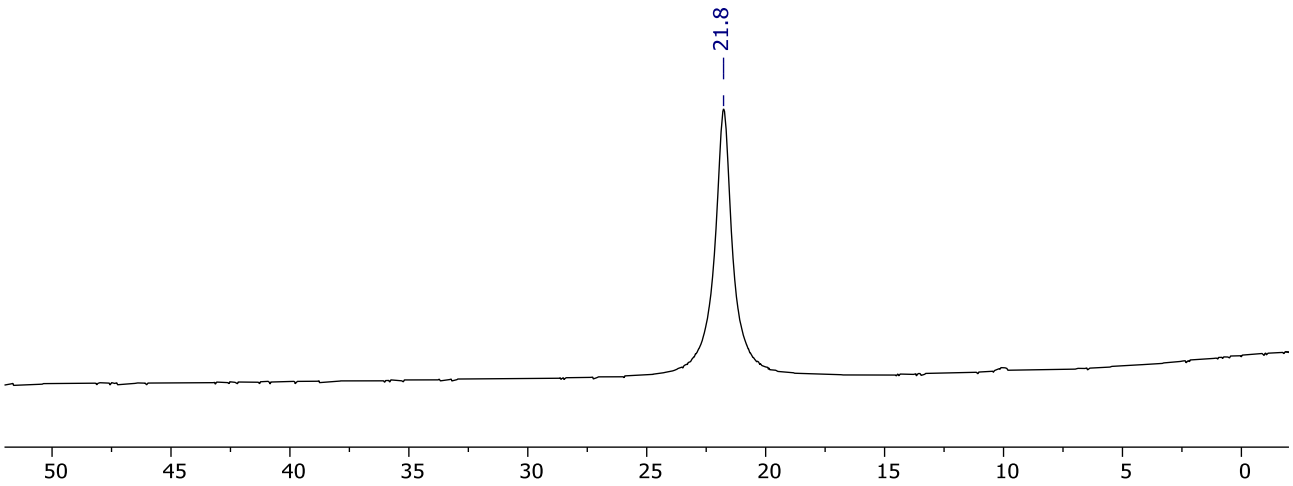

Figure S66. $^{11}B\{^{1}H\}$ NMR spectrum collected following the B_2pin_2 reduction of N_2O (3 bar gauge) using 5 mol% **5*** in toluene after 120 min (128 MHz, toluene/C_6D_6).

3.11.6 [CuO*t*Bu] **6***

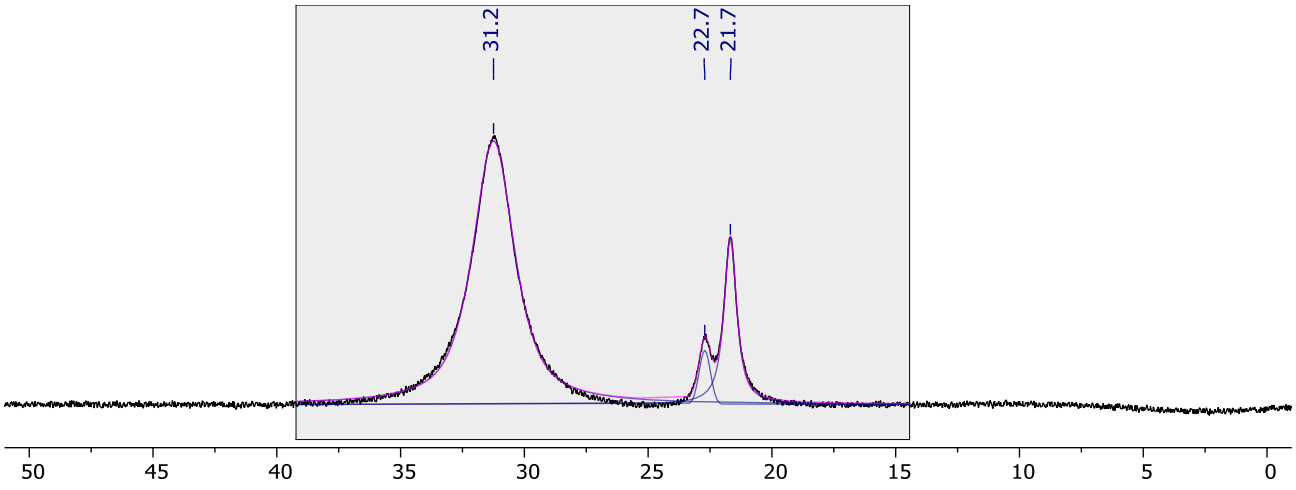

Figure S67. $^{11}B\{^{1}H\}$ NMR spectrum collected following the B_2pin_2 reduction of N_2O (3 bar gauge) using 5 mol% **6*** in toluene after 120 min (128 MHz, toluene/C_6D_6).

3.12 Data collected for entry 6a

3.12.1 [Cu(SIMes)(O*t*Bu)] **4***

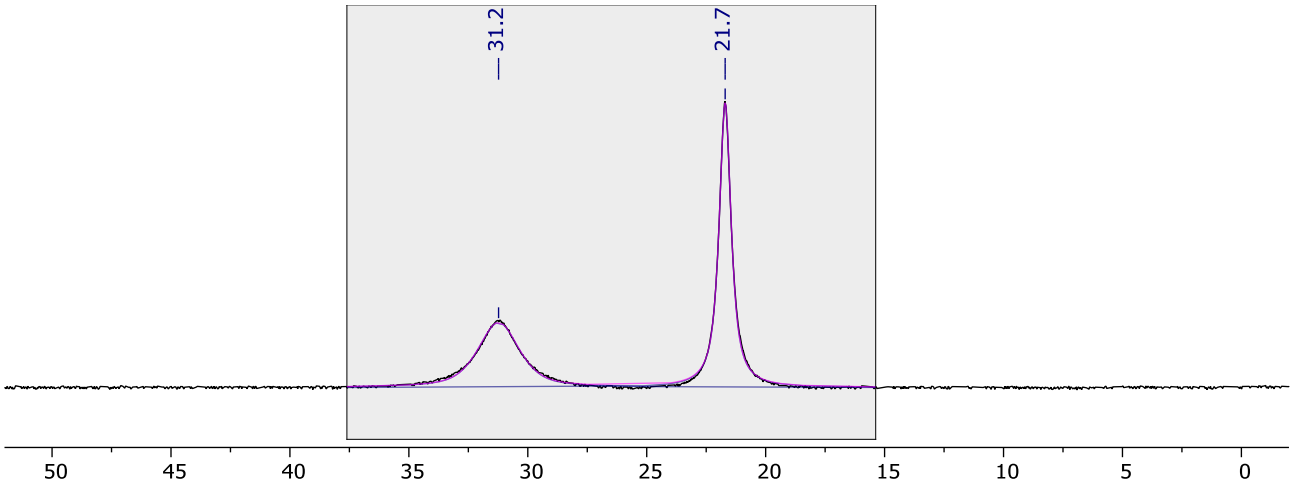

Figure S68. $^{11}B\{^{1}H\}$ NMR spectrum collected following the B_2pin_2 reduction of N_2O (3 bar gauge) using 5 mol% **4*** in toluene after 10 min (128 MHz, toluene/C_6D_6).

3.12.2 [Cu(IMes)(O*t*Bu)] **5***

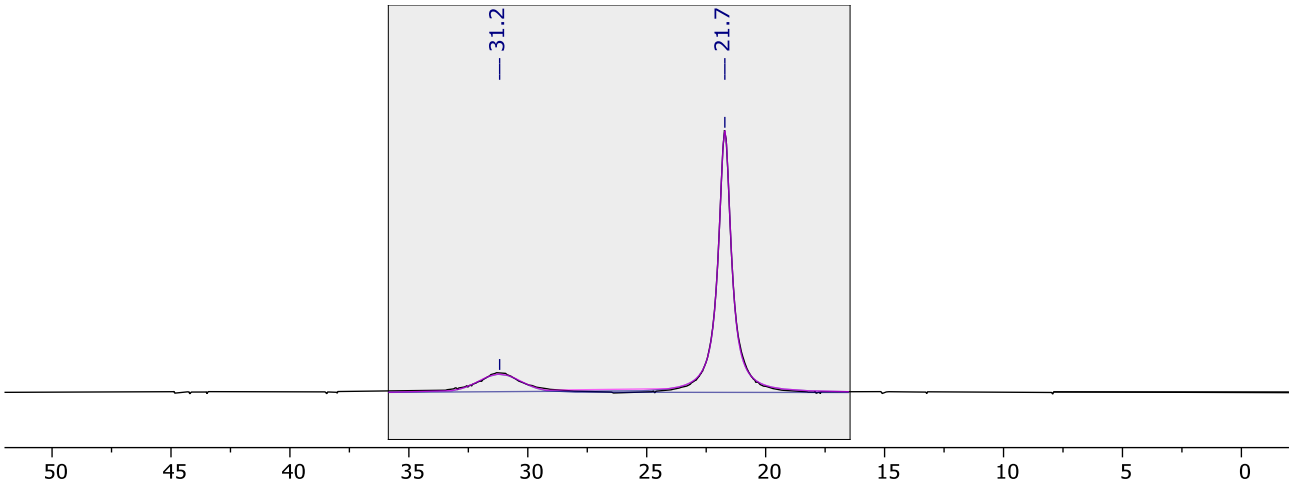

Figure S69. $^{11}B\{^{1}H\}$ NMR spectrum collected following the B_2pin_2 reduction of N_2O (3 bar gauge) using 5 mol% **5*** in toluene after 10 min (128 MHz, toluene/C_6D_6).

3.13 Data collected for entry 6b

3.13.1 [Cu(SIMes)(O*t*Bu)] **4***

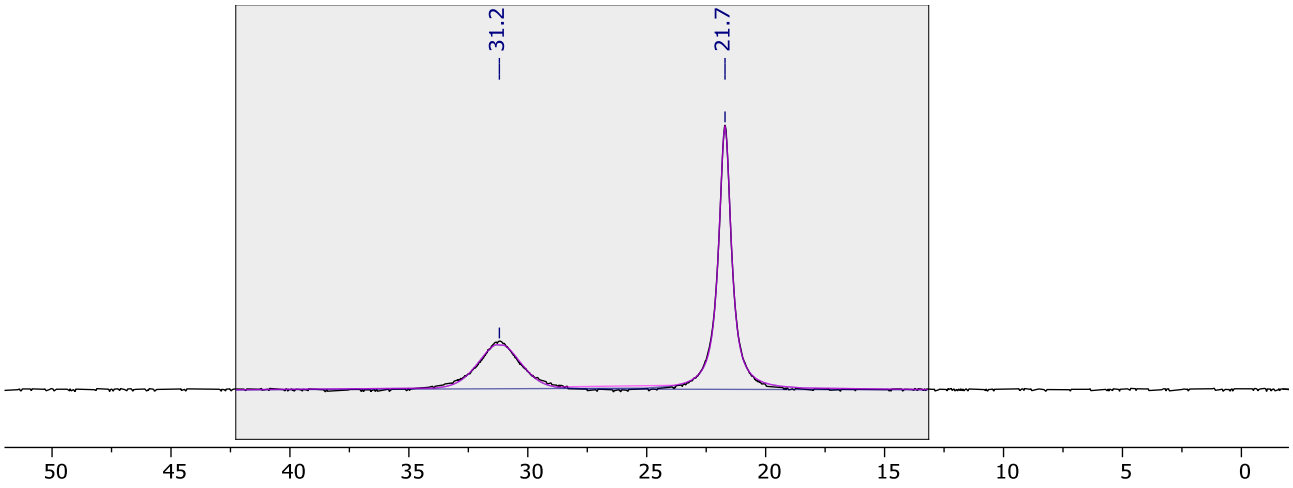

Figure S70. $^{11}B\{^{1}H\}$ NMR spectrum collected following the B_2pin_2 reduction of N_2O (3 bar gauge) using 5 mol% **4*** in toluene after 10 min (128 MHz, toluene/C_6D_6).

3.13.2 [Cu(IMes)(O*t*Bu)] **5***

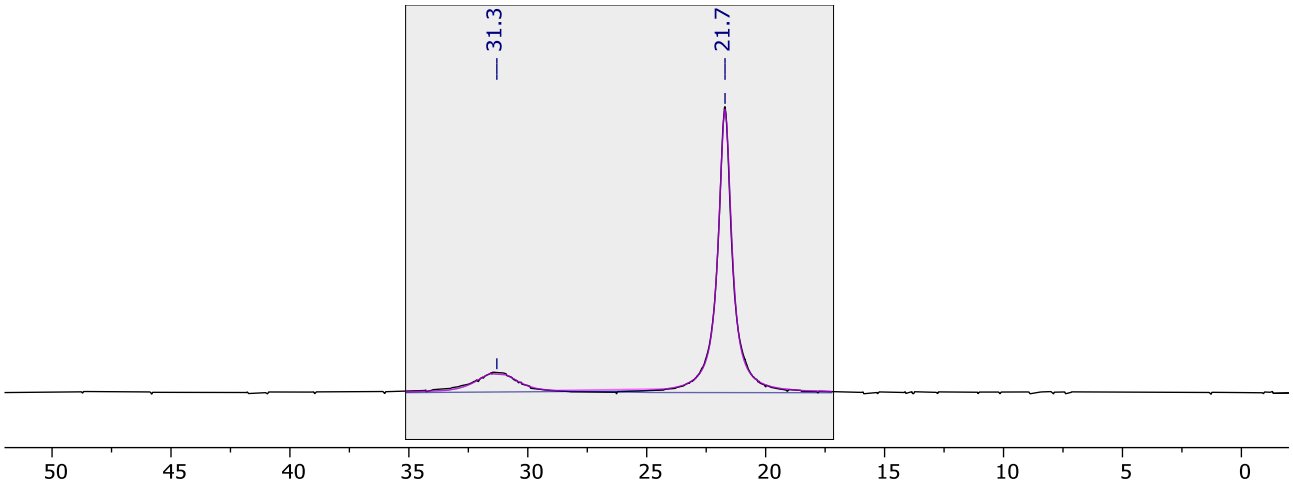

Figure S71. $^{11}B\{^{1}H\}$ NMR spectrum collected following the B_2pin_2 reduction of N_2O (3 bar gauge) using 5 mol% **5*** in toluene after 10 min (128 MHz, toluene/C_6D_6).

3.14 Data collected for entry 7a

3.14.1 [Cu(SIPr)(O*t*Bu)] **2***

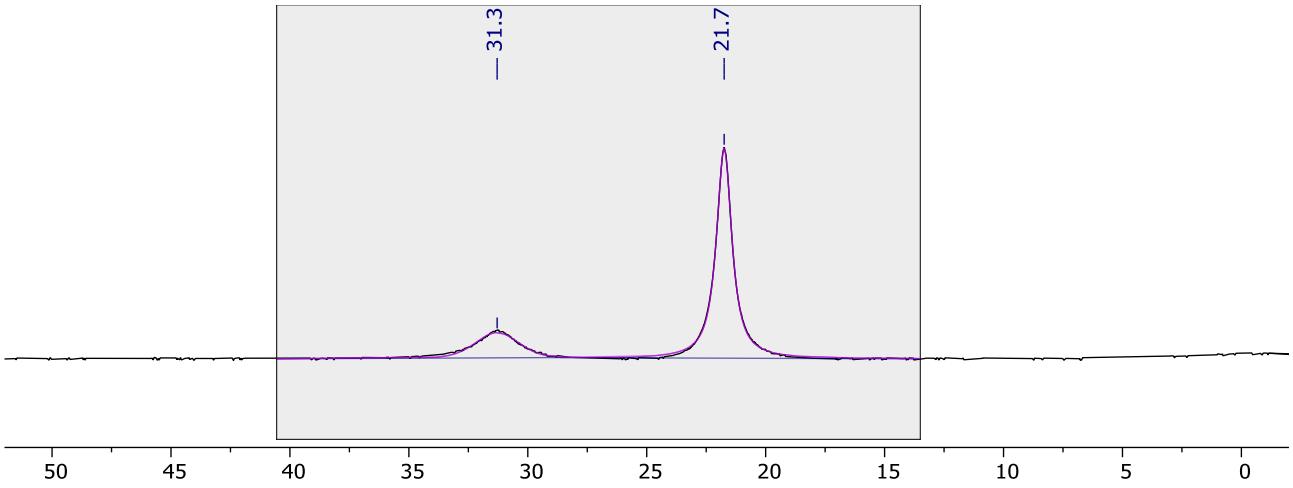

Figure S72. $^{11}B\{^{1}H\}$ NMR spectrum collected following the B_2pin_2 reduction of N_2O (1 bar gauge) using 5 mol% **2*** in toluene after 120 min (128 MHz, toluene/C_6D_6).

3.14.2 [Cu(IPr)(O*t*Bu)] **3***

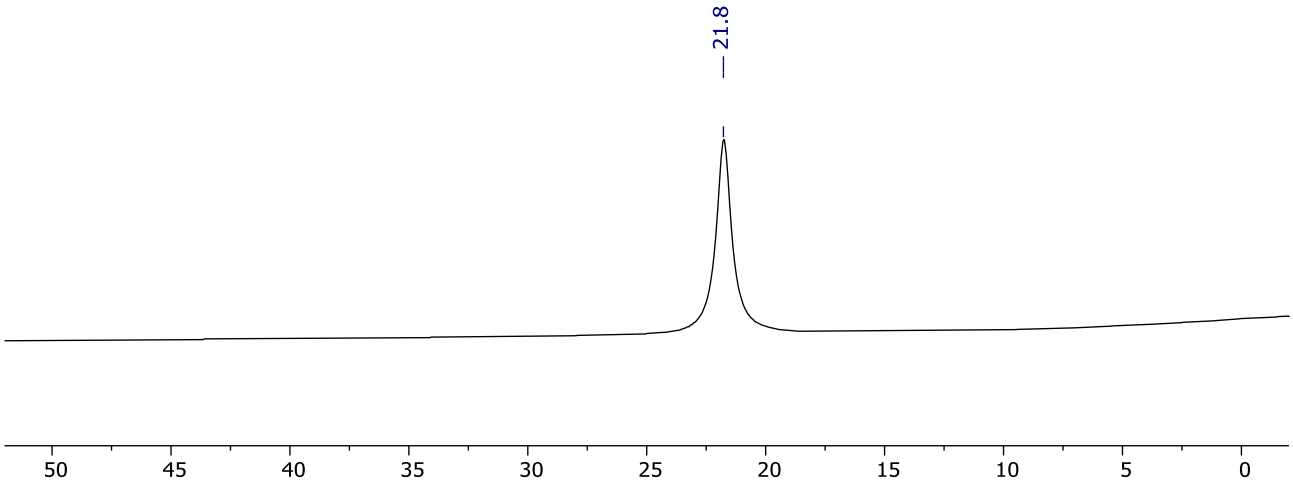

Figure S73. $^{11}B\{^{1}H\}$ NMR spectrum collected following the B_2pin_2 reduction of N_2O (1 bar gauge) using 5 mol% **3*** in toluene after 120 min (128 MHz, toluene/C_6D_6).

3.14.3 [Cu(SIMes)(O*t*Bu)] **4***

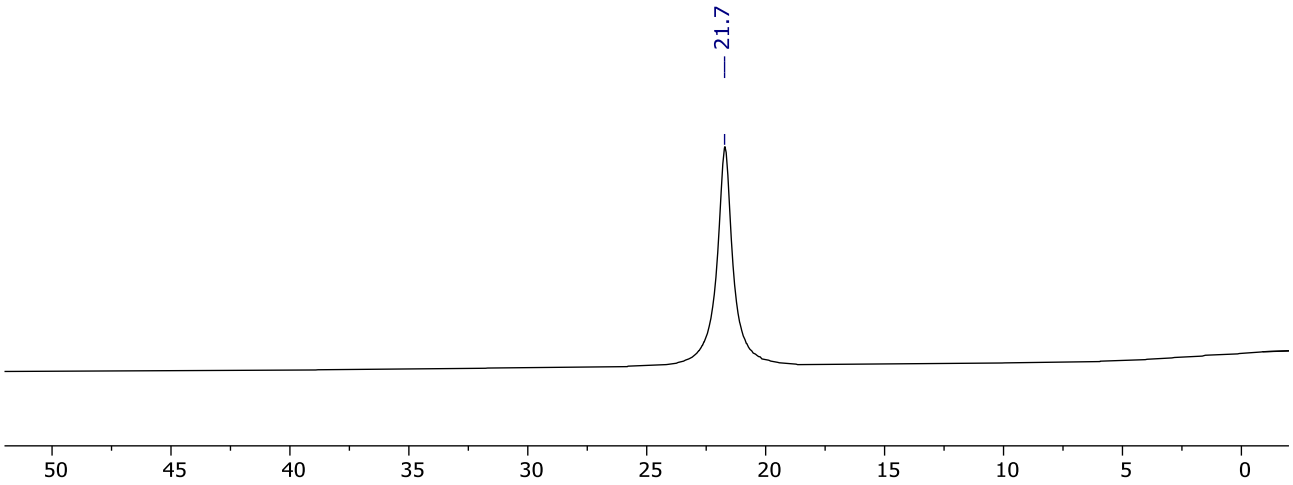

Figure S74. $^{11}B\{^{1}H\}$ NMR spectrum collected following the B_2pin_2 reduction of N_2O (1 bar gauge) using 5 mol% **4*** in toluene after 120 min (128 MHz, toluene/C_6D_6).

3.14.4 [Cu(IMes)(O*t*Bu)] **5***

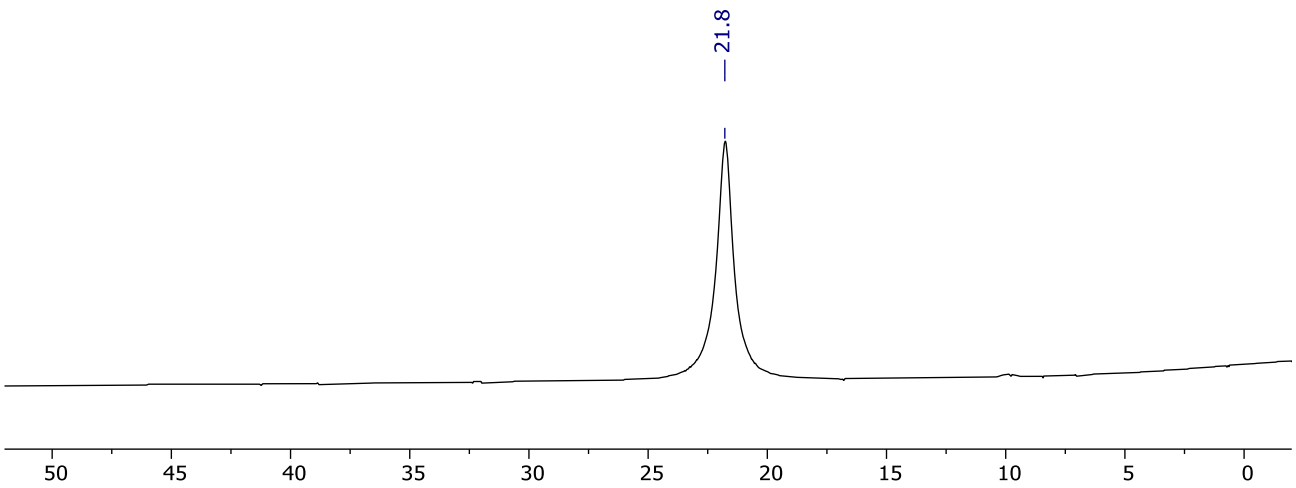

Figure S75. $^{11}B\{^{1}H\}$ NMR spectrum collected following the B_2pin_2 reduction of N_2O (1 bar gauge) using 5 mol% **5*** in toluene after 120 min (128 MHz, toluene/C_6D_6).

3.15 Data collected for entry 7b

3.15.1 [Cu(SIPr)(O*t*Bu)] **2***

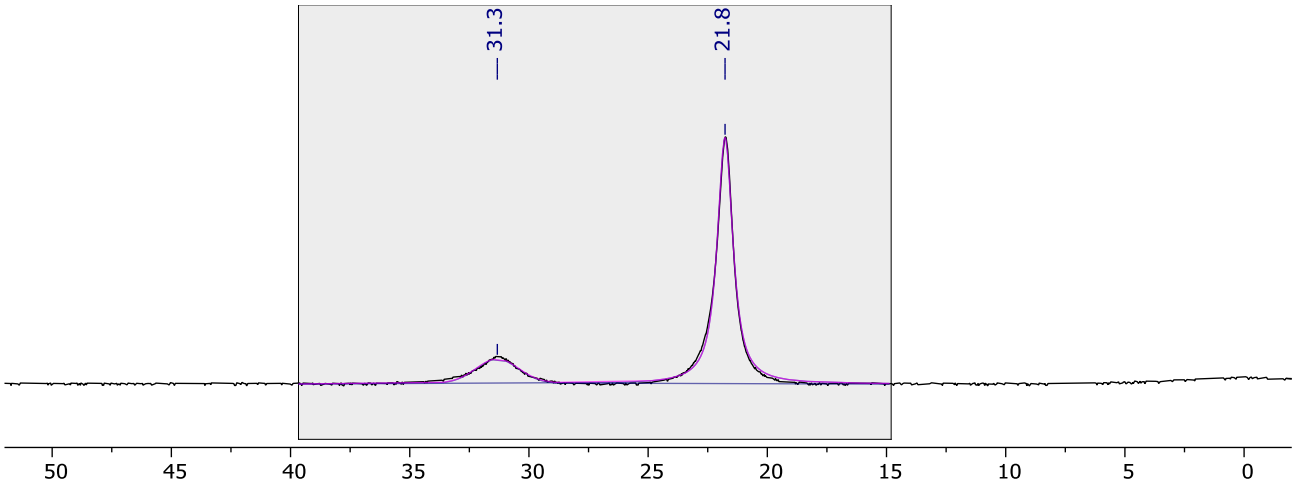

Figure S76. $^{11}B\{^{1}H\}$ NMR spectrum collected following the B_2pin_2 reduction of N_2O (1 bar gauge) using 5 mol% **2*** in toluene after 120 min (128 MHz, toluene/C_6D_6).

3.15.2 [Cu(IPr)(O*t*Bu)] **3***

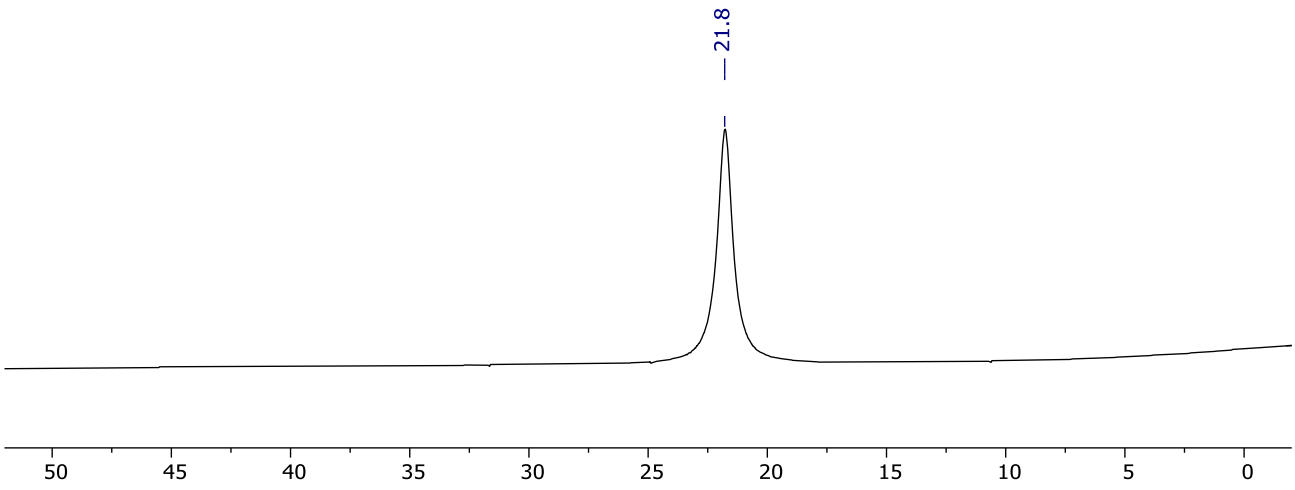

Figure S77. $^{11}B\{^{1}H\}$ NMR spectrum collected following the B_2pin_2 reduction of N_2O (1 bar gauge) using 5 mol% **3*** in toluene after 120 min (128 MHz, toluene/C_6D_6).

3.15.3 [Cu(SIMes)(O*t*Bu)] **4***

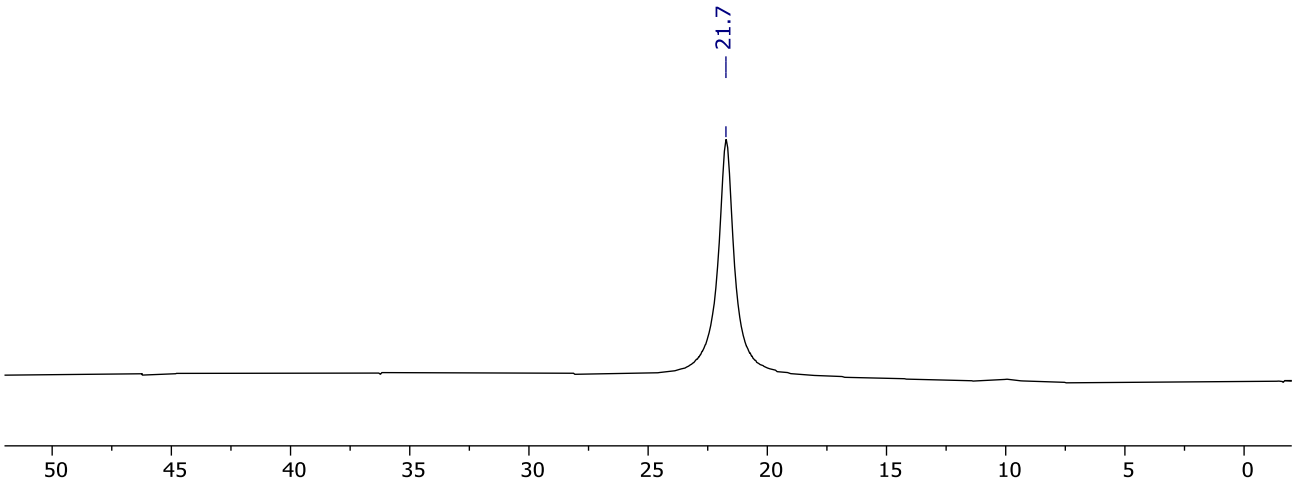

Figure S78. $^{11}B\{^{1}H\}$ NMR spectrum collected following the B_2pin_2 reduction of N_2O (1 bar gauge) using 5 mol% **4*** in toluene after 120 min (128 MHz, toluene/C_6D_6).

3.15.4 [Cu(IMes)(O*t*Bu)] **5***

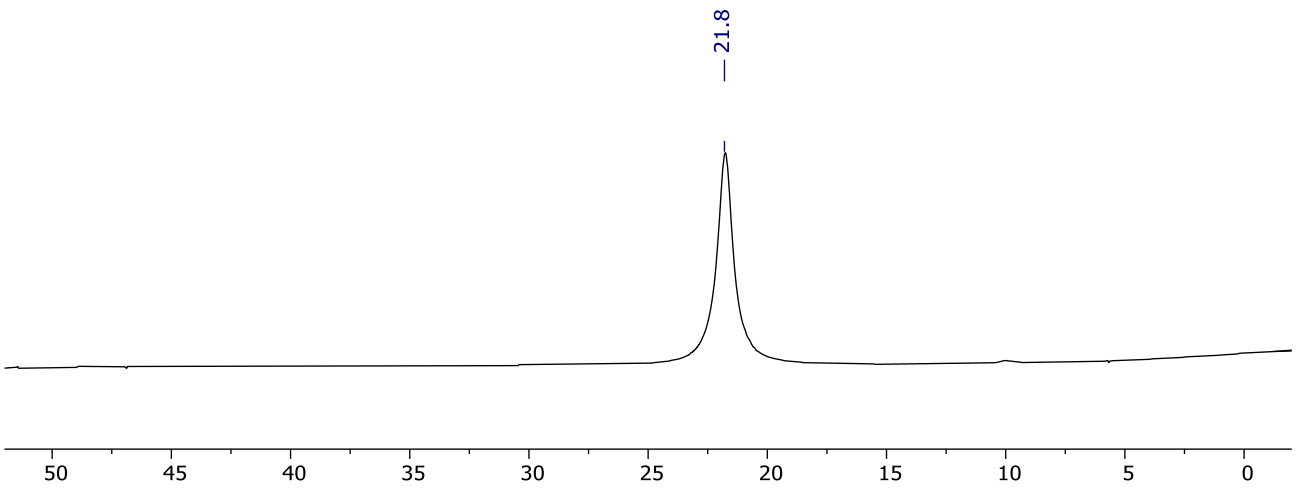

Figure S79. $^{11}B\{^{1}H\}$ NMR spectrum collected following the B_2pin_2 reduction of N_2O (1 bar gauge) using 5 mol% **5*** in toluene after 120 min (128 MHz, toluene/C_6D_6).

3.16 Data collected for entry 8a

3.16.1 [Cu(SIMes)(O*t*Bu)] **4***

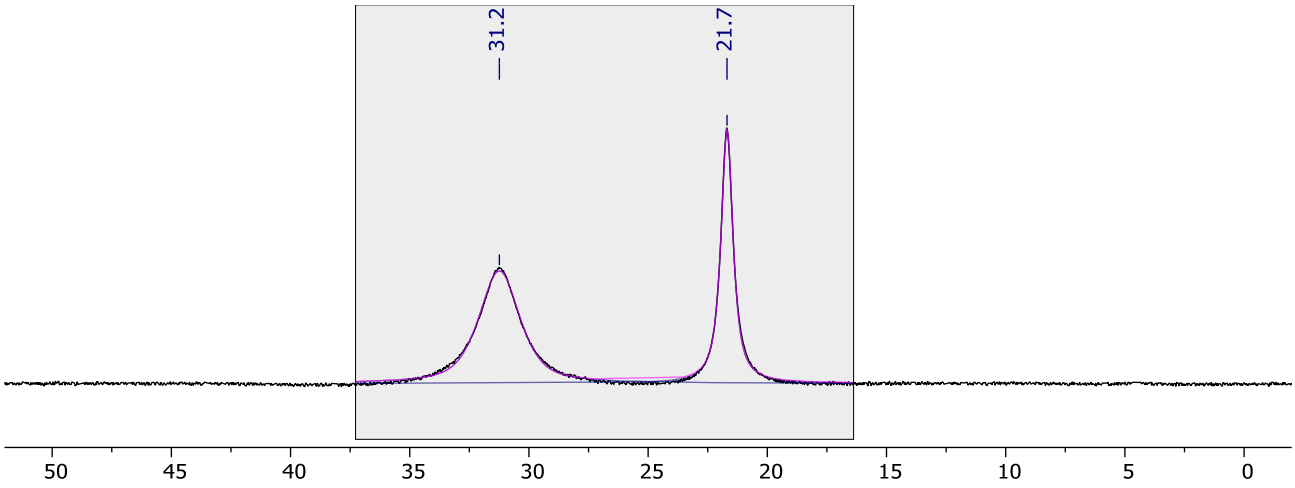

Figure S80. $^{11}B\{^{1}H\}$ NMR spectrum collected following the B_2pin_2 reduction of N_2O (1 bar gauge) using 5 mol% **4*** in toluene after 10 min (128 MHz, toluene/C_6D_6).

3.16.2 [Cu(IMes)(O*t*Bu)] **5***

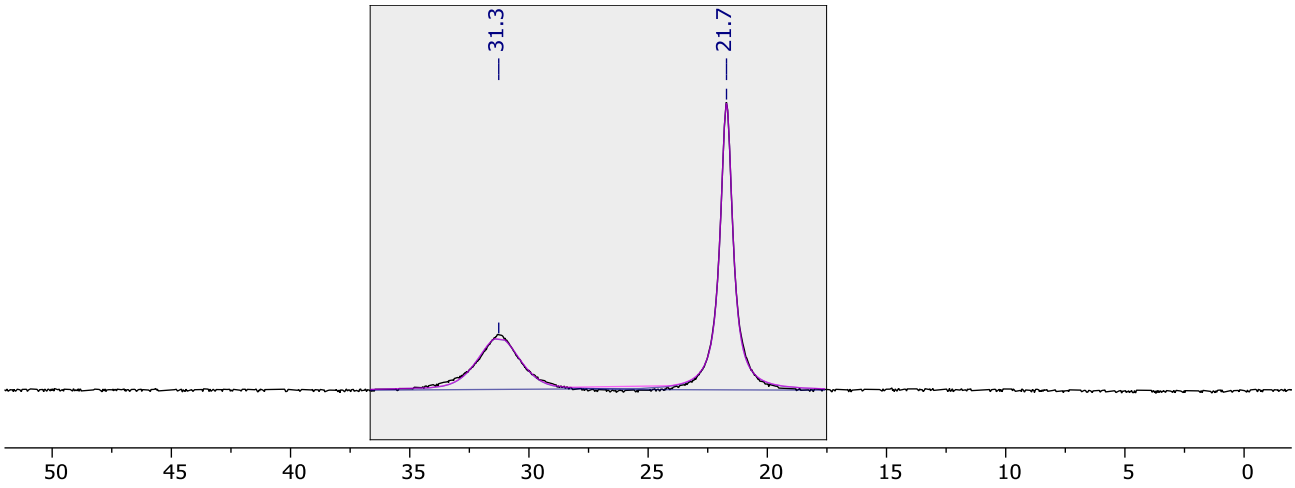

Figure S81. $^{11}B\{^{1}H\}$ NMR spectrum collected following the B_2pin_2 reduction of N_2O (1 bar gauge) using 5 mol% **5*** in toluene after 10 min (128 MHz, toluene/C_6D_6).

3.17 Data collected for entry 8b

3.17.1 [Cu(SIMes)(O*t*Bu)] **4***

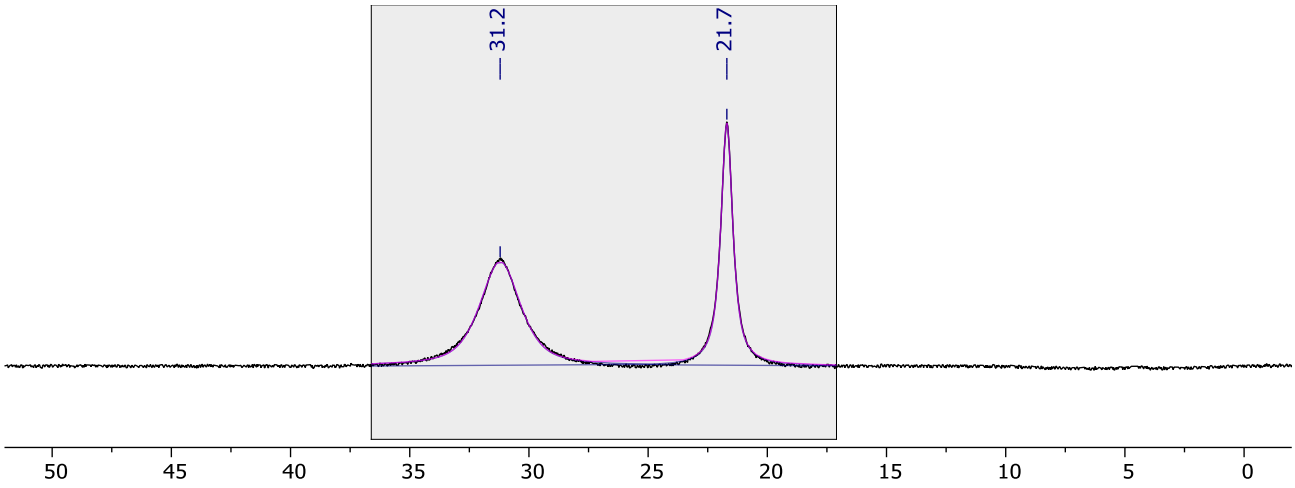

Figure S82. $^{11}B\{^{1}H\}$ NMR spectrum collected following the B_2pin_2 reduction of N_2O (1 bar gauge) using 5 mol% **4*** in toluene after 10 min (128 MHz, toluene/C_6D_6).

3.17.2 [Cu(IMes)(O*t*Bu)] **5***

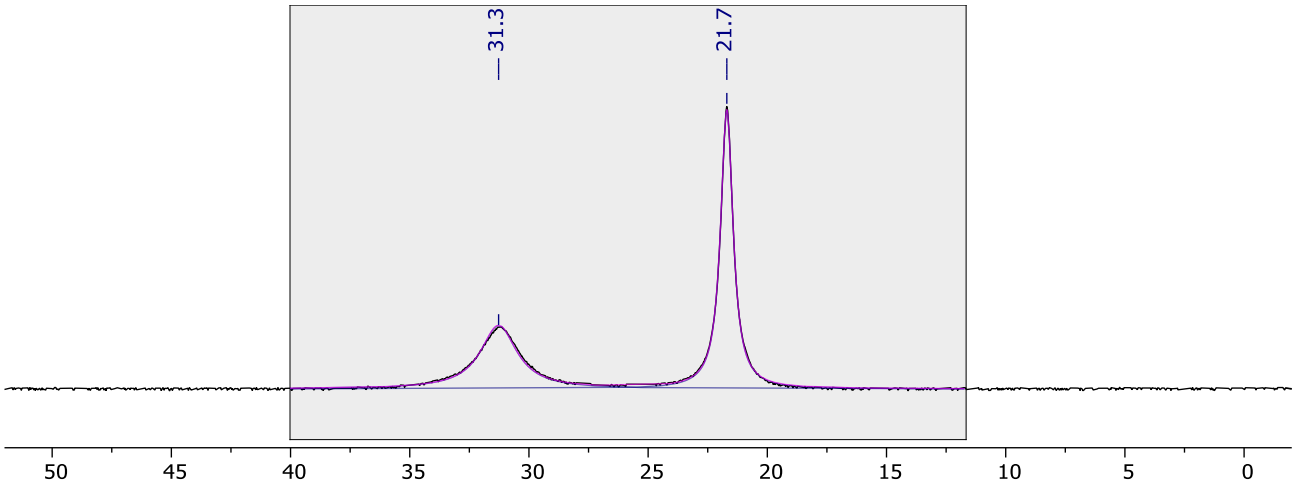

Figure S83. $^{11}B\{^{1}H\}$ NMR spectrum collected following the B_2pin_2 reduction of N_2O (1 bar gauge) using 5 mol% **5*** in toluene after 10 min (128 MHz, toluene/C_6D_6).

3.18 Data collected for entry 9a

3.18.1 No catalyst

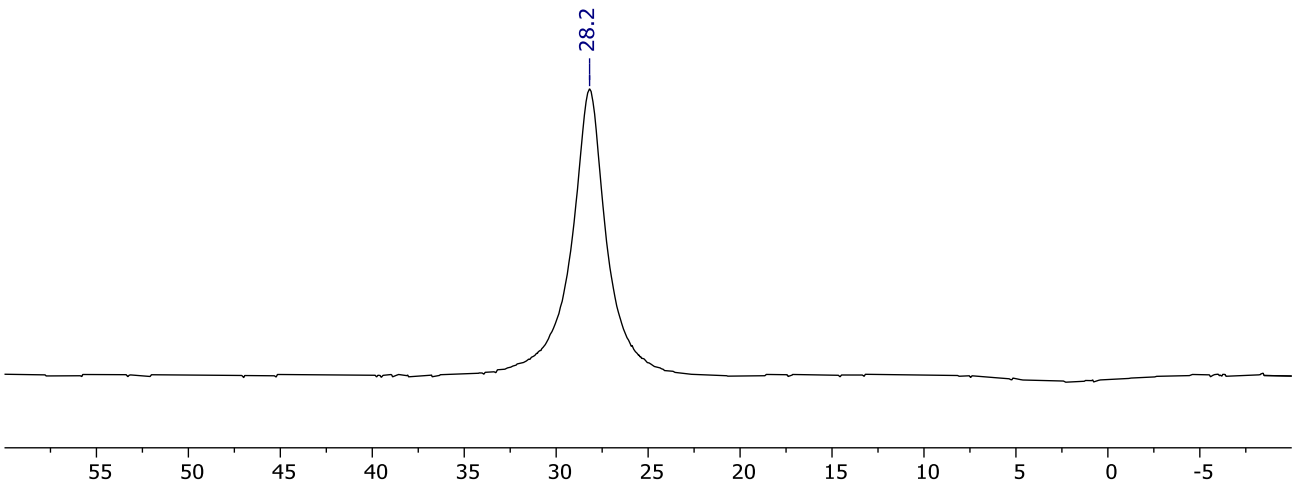

Figure S84. $^{11}B\{^{1}H\}$ NMR spectrum collected following the attempted B_2neop_2 reduction of N_2O (3 bar gauge) in THF with no catalyst after 120 min (128 MHz, THF/C_6D_6).

3.18.2 [$Rh(PEt_3)_3(OPh)$] **1***

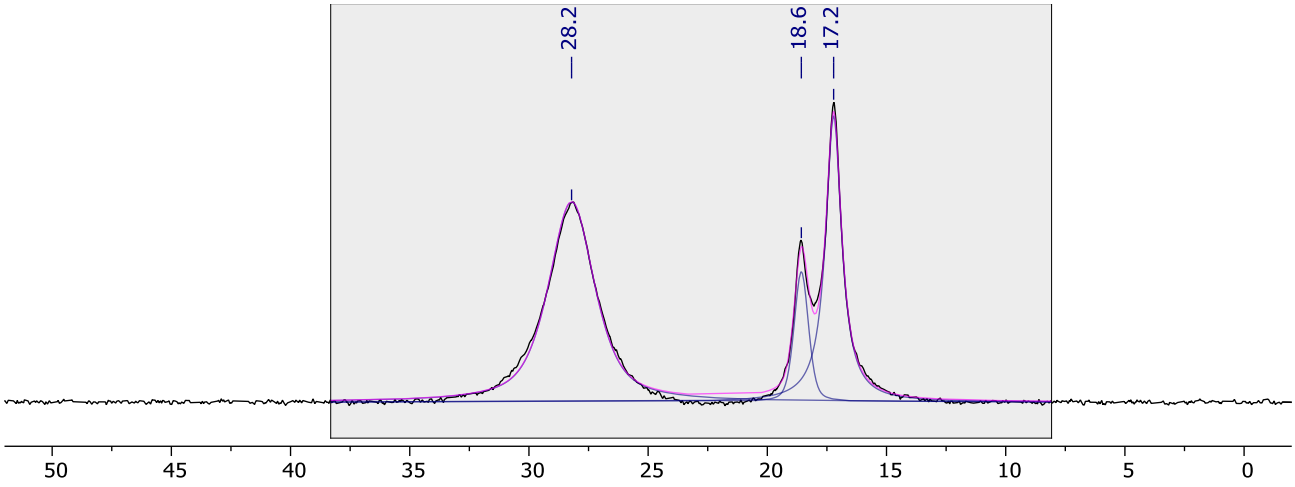

Figure S85. $^{11}B\{^{1}H\}$ NMR spectrum collected following the B_2neop_2 reduction of N_2O (3 bar gauge) using 5 mol% **1*** in THF after 120 min (96 MHz, THF/C_6D_6).

3.18.3 [Cu(SIPr)(O*t*Bu)] **2***

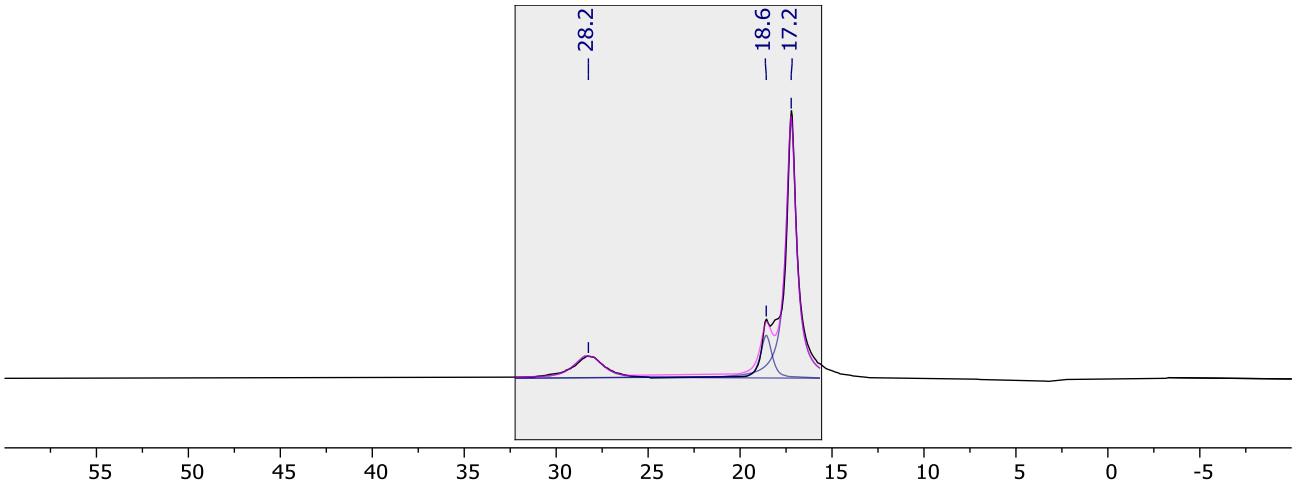

Figure S86. $^{11}B\{^{1}H\}$ NMR spectrum collected following the B_2neop_2 reduction of N_2O (3 bar gauge) using 5 mol% **2*** in THF after 120 min (128 MHz, THF/C_6D_6).

3.18.4 [Cu(IPr)(O*t*Bu)] **3***

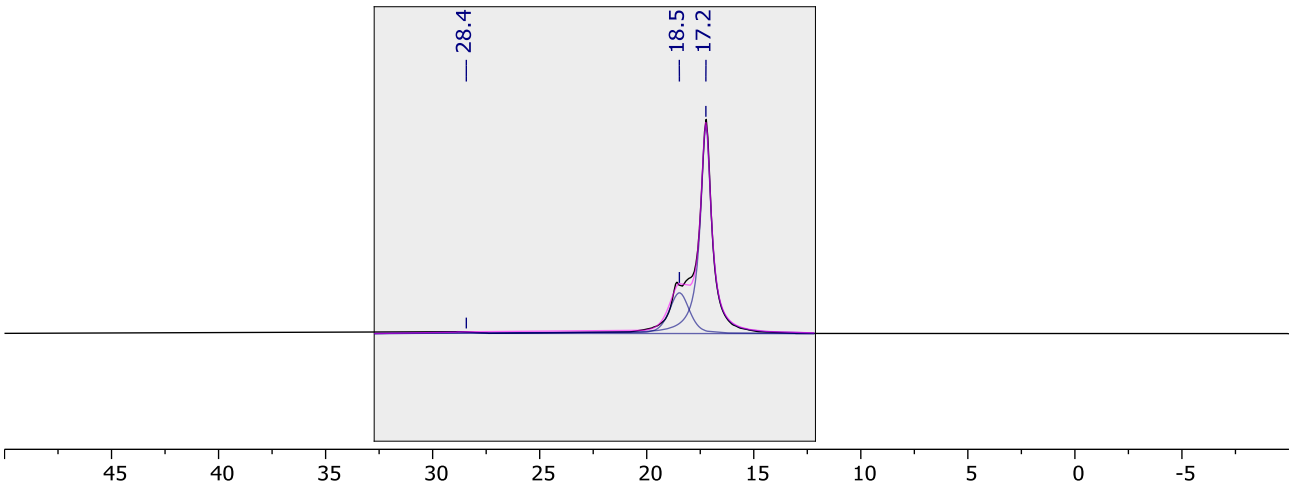

Figure S87. $^{11}B\{^{1}H\}$ NMR spectrum collected following the B_2neop_2 reduction of N_2O (3 bar gauge) using 5 mol% **3*** in THF after 120 min (128 MHz, THF/C_6D_6).

3.18.5 [Cu(SIMes)(O*t*Bu)] **4***

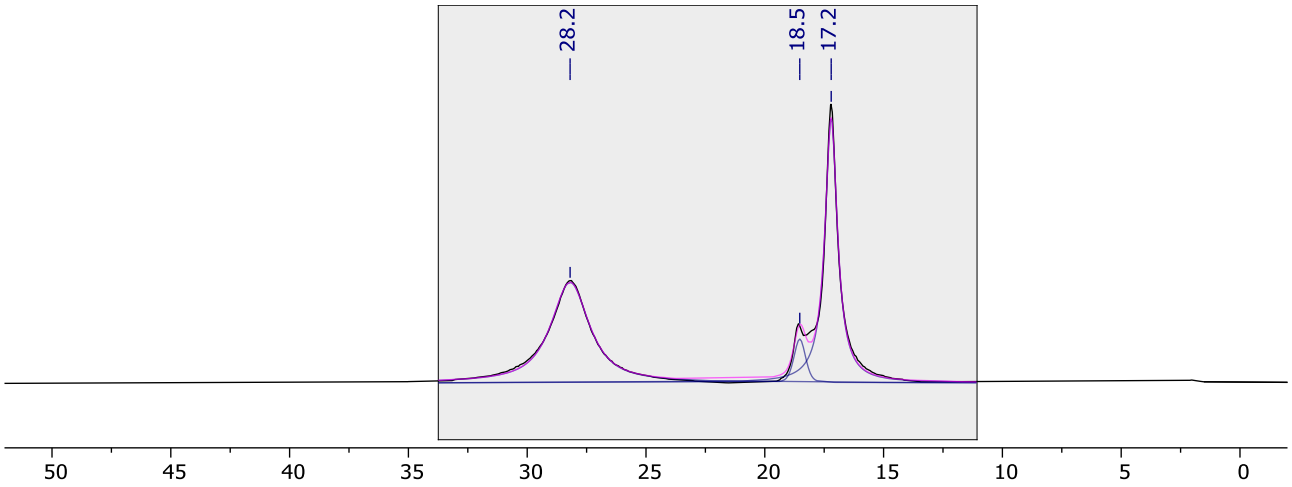

Figure S88. $^{11}B\{^{1}H\}$ NMR spectrum collected following the B_2neop_2 reduction of N_2O (3 bar gauge) using 5 mol% **4*** in THF after 120 min (128 MHz, THF/C_6D_6).

3.18.6 [Cu(IMes)(O*t*Bu)] **5***

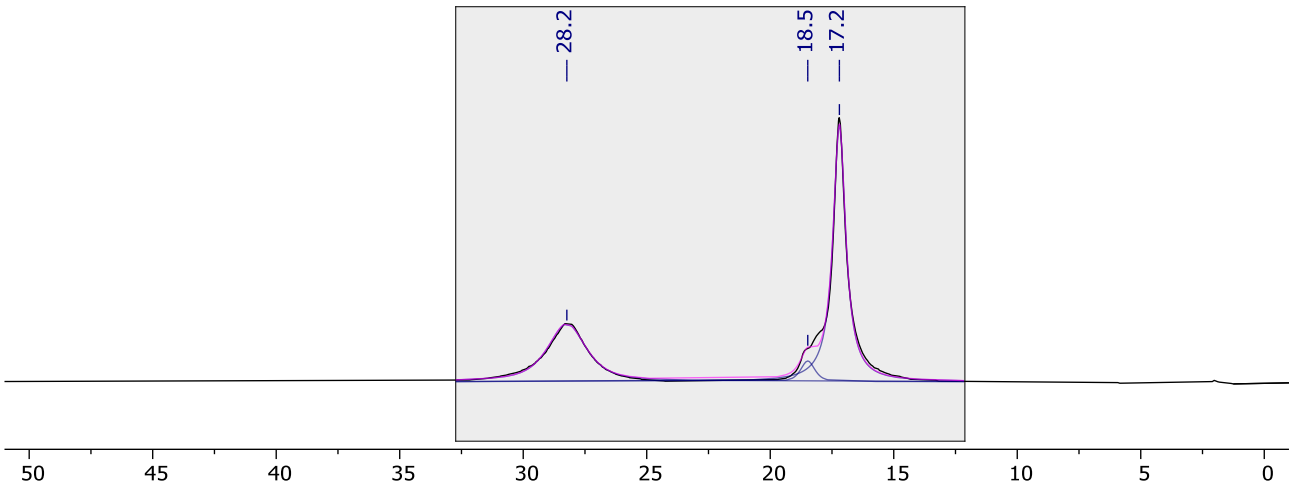

Figure S89. $^{11}B\{^{1}H\}$ NMR spectrum collected following the B_2neop_2 reduction of N_2O (3 bar gauge) using 5 mol% **5*** in THF after 120 min (128 MHz, THF/C_6D_6).

3.18.7 [CuO*t*Bu] **6***

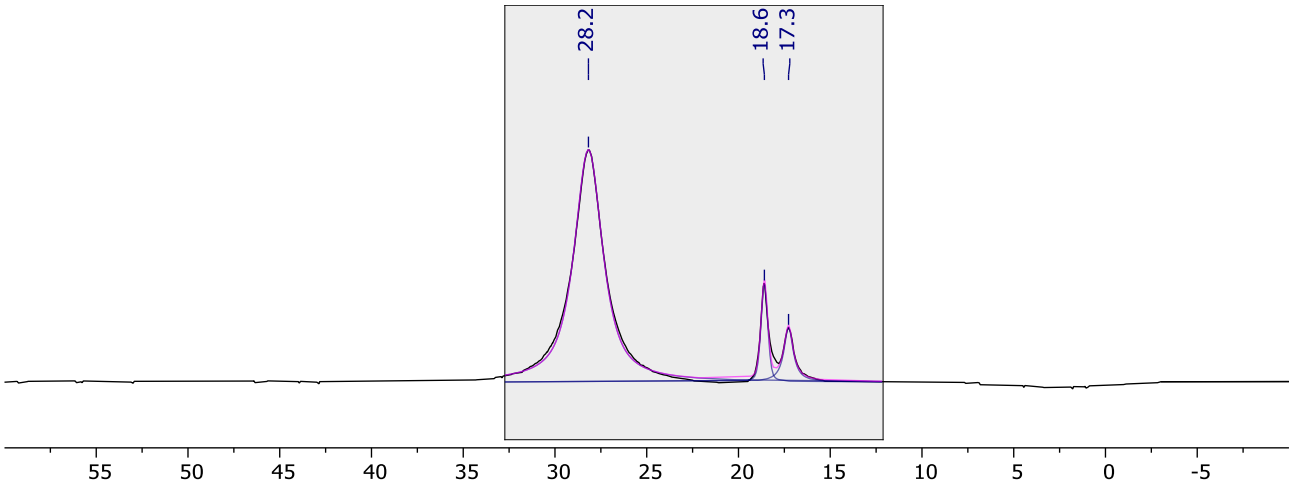

Figure S90. $^{11}B\{^{1}H\}$ NMR spectrum collected following the B_2neop_2 reduction of N_2O (3 bar gauge) using 5 mol% **6*** in THF after 120 min (128 MHz, THF/C_6D_6).

3.18.8 [Rh(PNP-*i*Pr)(OPh)] **7***

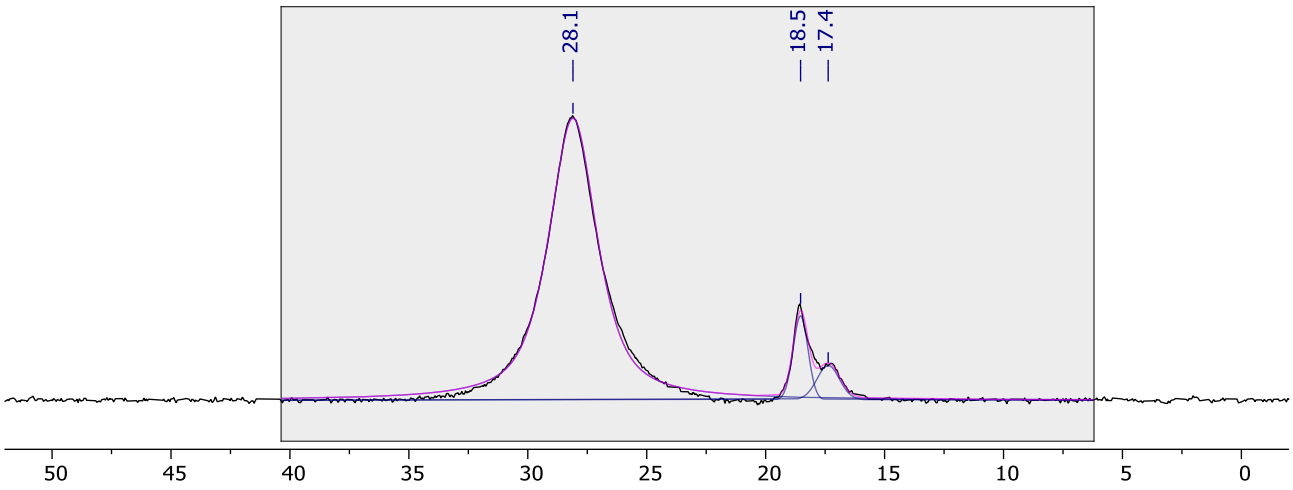

Figure S91. $^{11}B\{^{1}H\}$ NMR spectrum collected following the B_2neop_2 reduction of N_2O (3 bar gauge) using 5 mol% **7*** in THF after 120 min (96 MHz, THF/C_6D_6).

3.18.9 [Rh(PNP-*i*Pr)(OPh)] **8**

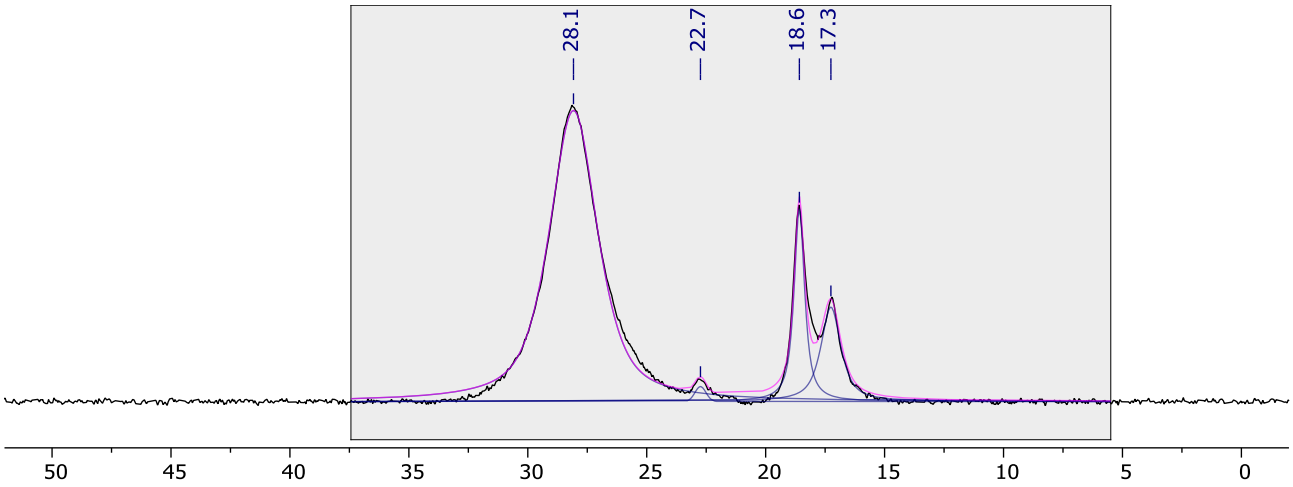

Figure S92. $^{11}B\{^{1}H\}$ NMR spectrum collected following the B_2neop_2 reduction of N_2O (3 bar gauge) using 5 mol% **8** in THF after 120 min (96 MHz, THF/C_6D_6).

3.19 Data collected for entry 9b

3.19.1 No catalyst

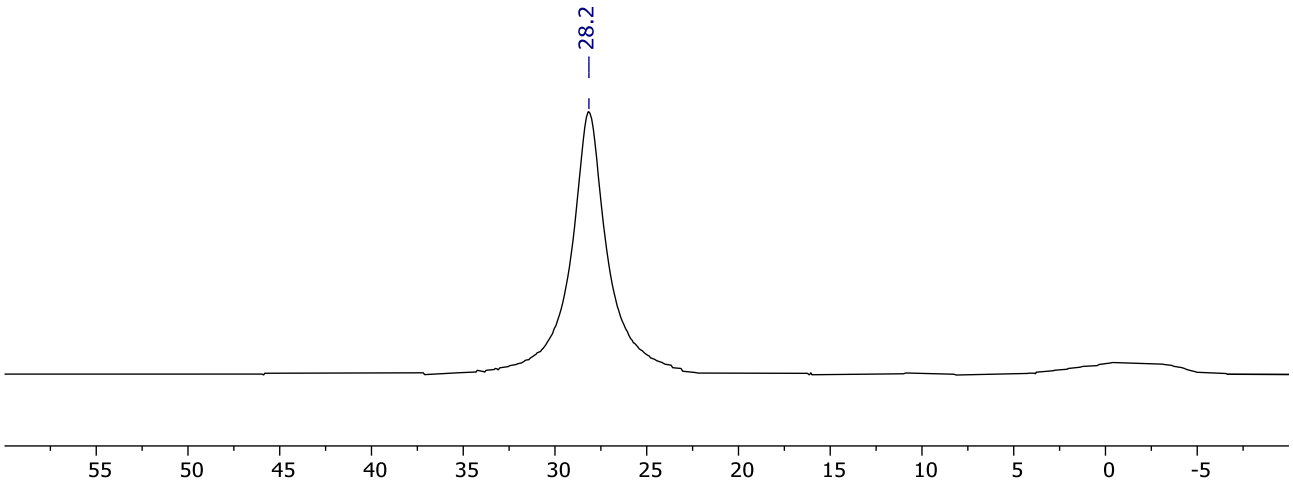

Figure S93. $^{11}B\{^{1}H\}$ NMR spectrum collected following the attempted B_2neop_2 reduction of N_2O (3 bar gauge) in THF with no catalyst after 120 min (128 MHz, THF/C_6D_6).

3.19.2 [Rh(PEt$_3$)$_3$(OPh)] **1***

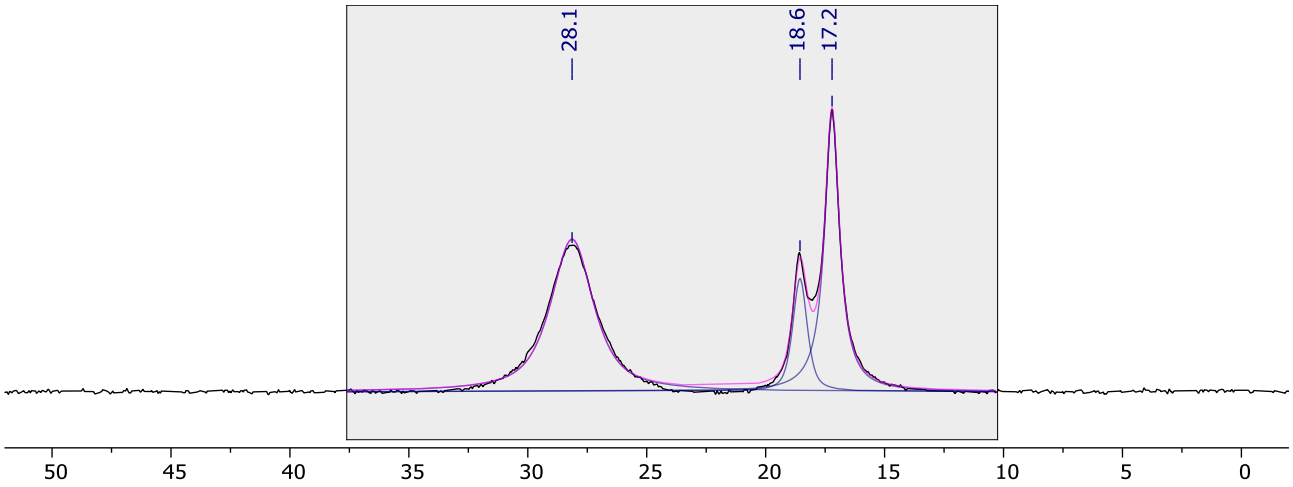

Figure S94. $^{11}B\{^1H\}$ NMR spectrum collected following the B_2neop_2 reduction of N_2O (3 bar gauge) using 5 mol% **1*** in THF after 120 min (96 MHz, THF/C_6D_6).

3.19.3 [Cu(SIPr)(O*t*Bu)] **2***

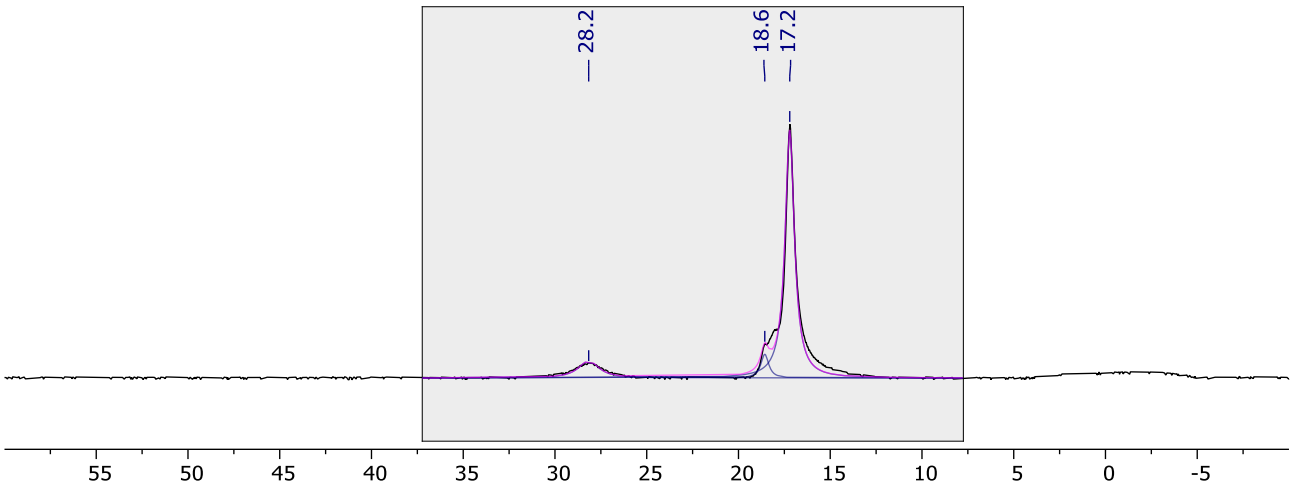

Figure S95. $^{11}B\{^1H\}$ NMR spectrum collected following the B_2neop_2 reduction of N_2O (3 bar gauge) using 5 mol% **2*** in THF after 120 min (128 MHz, THF/C_6D_6).

3.19.4 [Cu(IPr)(O*t*Bu)] **3***

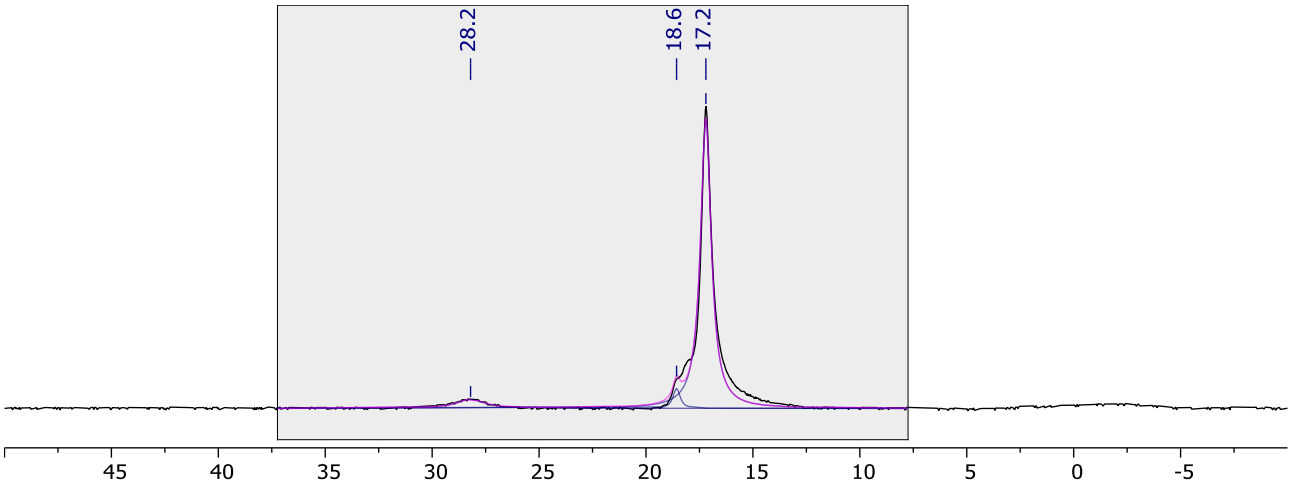

Figure S96. $^{11}B\{^{1}H\}$ NMR spectrum collected following the B_2neop_2 reduction of N_2O (3 bar gauge) using 5 mol% **3*** in THF after 120 min (128 MHz, THF/C_6D_6).

3.19.5 [Cu(SIMes)(O*t*Bu)] **4***

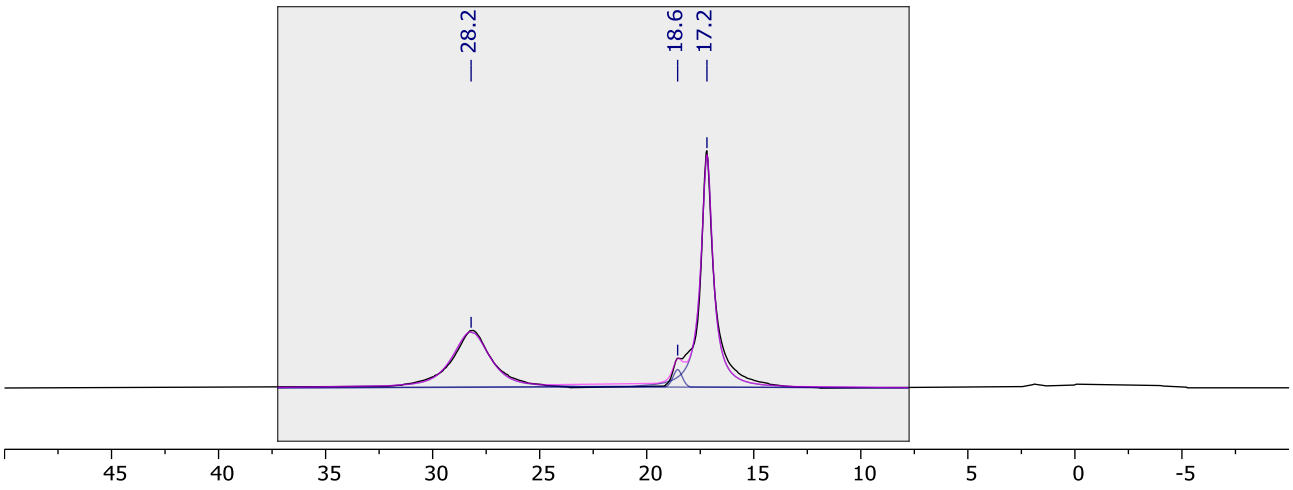

Figure S97. $^{11}B\{^{1}H\}$ NMR spectrum collected following the B_2neop_2 reduction of N_2O (3 bar gauge) using 5 mol% **4*** in THF after 120 min (128 MHz, THF/C_6D_6).

3.19.6 [Cu(IMes)(O*t*Bu)] **5***

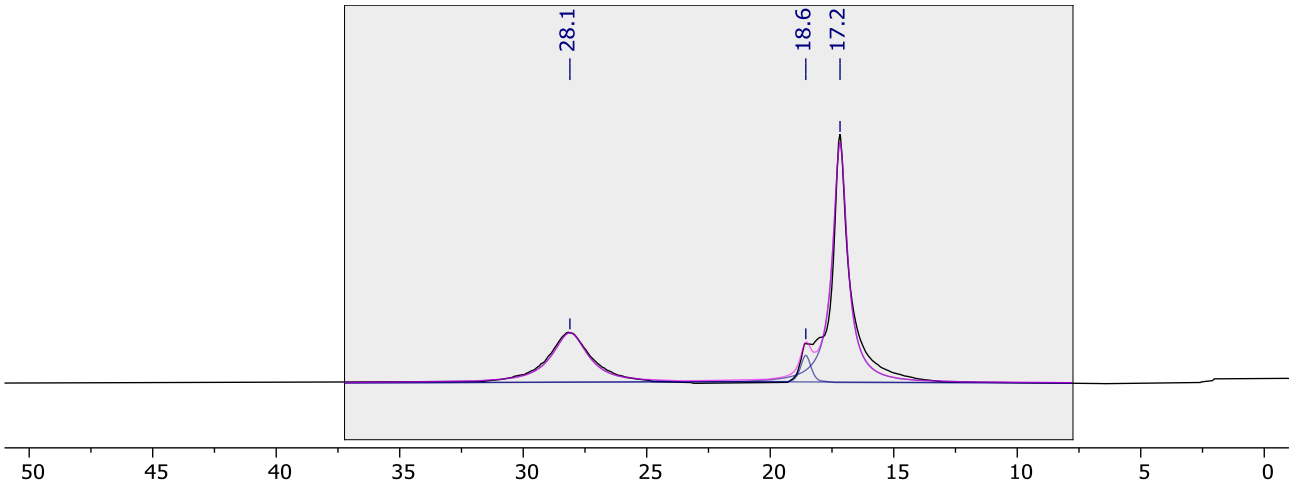

Figure S98. $^{11}B\{^{1}H\}$ NMR spectrum collected following the B_2neop_2 reduction of N_2O (3 bar gauge) using 5 mol% **5*** in THF after 120 min (128 MHz, THF/C_6D_6).

3.19.7 [CuO*t*Bu] **6***

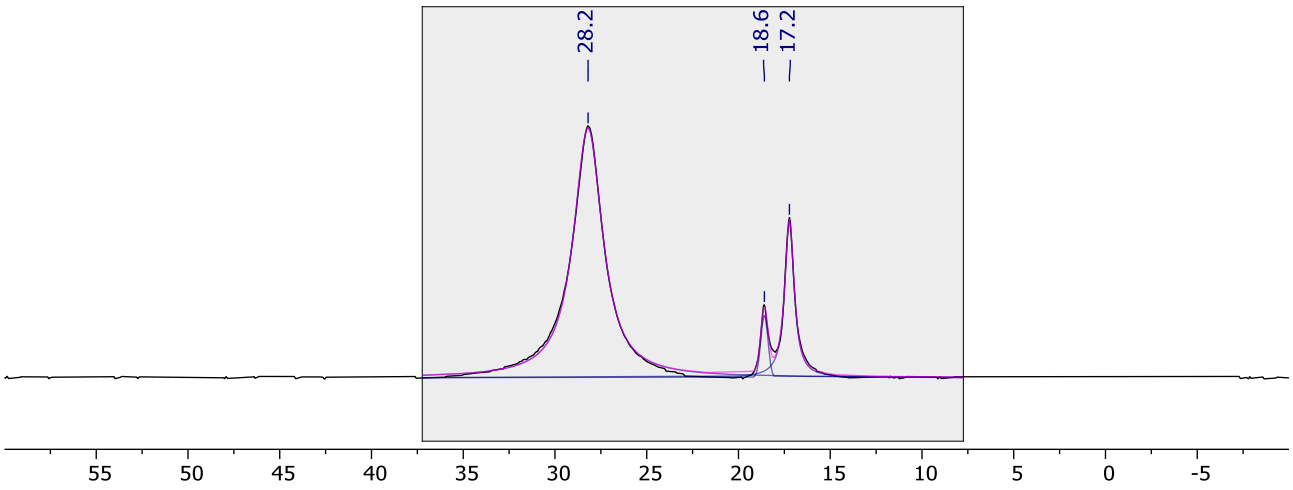

Figure S99. $^{11}B\{^{1}H\}$ NMR spectrum collected following the B_2neop_2 reduction of N_2O (3 bar gauge) using 5 mol% **6*** in THF after 120 min (128 MHz, THF/C_6D_6).

3.19.8 [Rh(PNP-*i*Pr)(OPh)] **7***

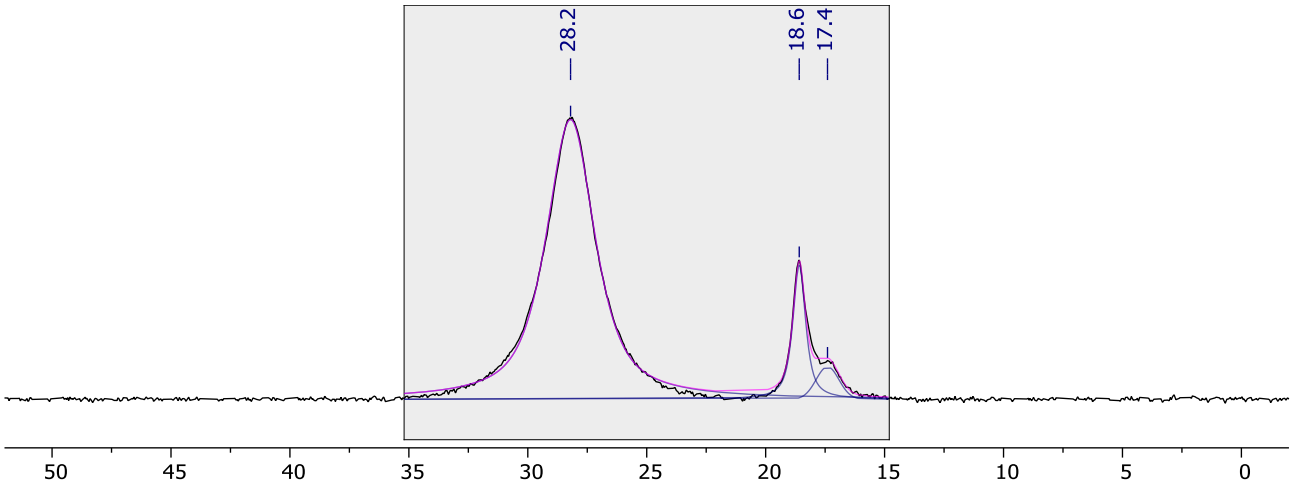

Figure S100. $^{11}B\{^{1}H\}$ NMR spectrum collected following the B_2neop_2 reduction of N_2O (3 bar gauge) using 5 mol% **7*** in THF after 120 min (96 MHz, THF/C_6D_6).

3.19.9 [Rh(POP-*i*Pr)(Bpin)] **8**

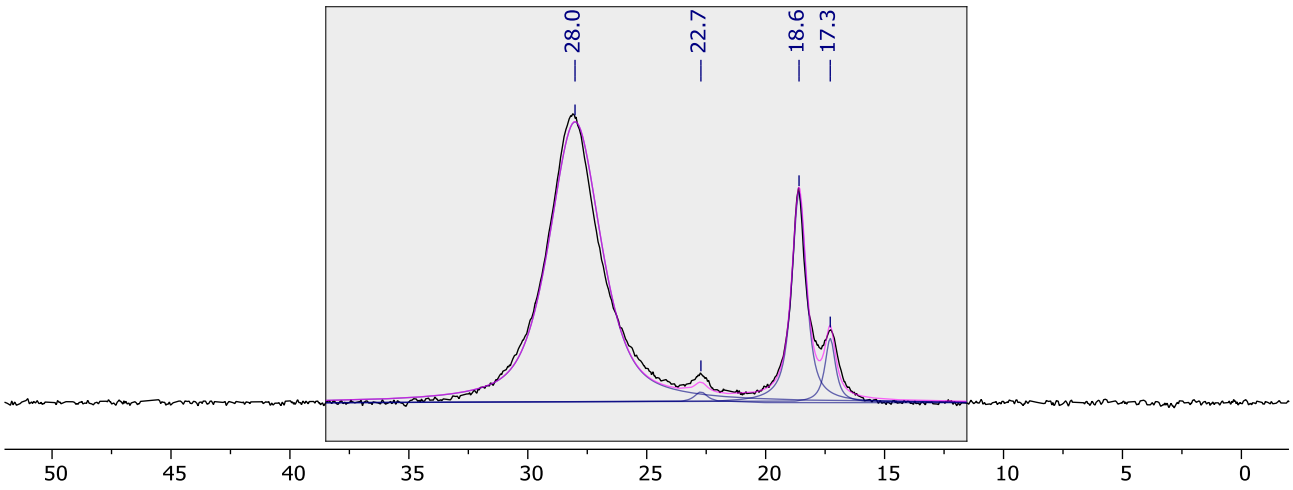

Figure S101. $^{11}B\{^{1}H\}$ NMR spectrum collected following the B_2neop_2 reduction of N_2O (3 bar gauge) using 5 mol% **8** in THF after 120 min (96 MHz, THF/C_6D_6).

3.20 Data collected for entry 10a

3.20.1 No catalyst

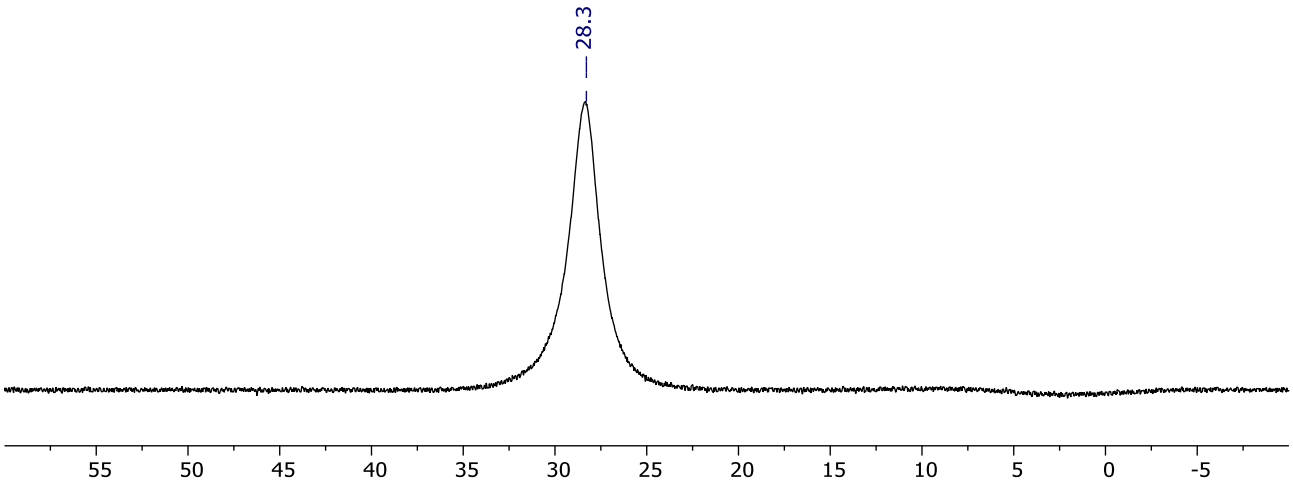

Figure S102. $^{11}B\{^{1}H\}$ NMR spectrum collected following the attempted B_2neop_2 reduction of N_2O (3 bar gauge) in toluene with no catalyst after 120 min (128 MHz, toluene/C_6D_6).

3.20.2 [Cu(SIPr)(O*t*Bu)] **2***

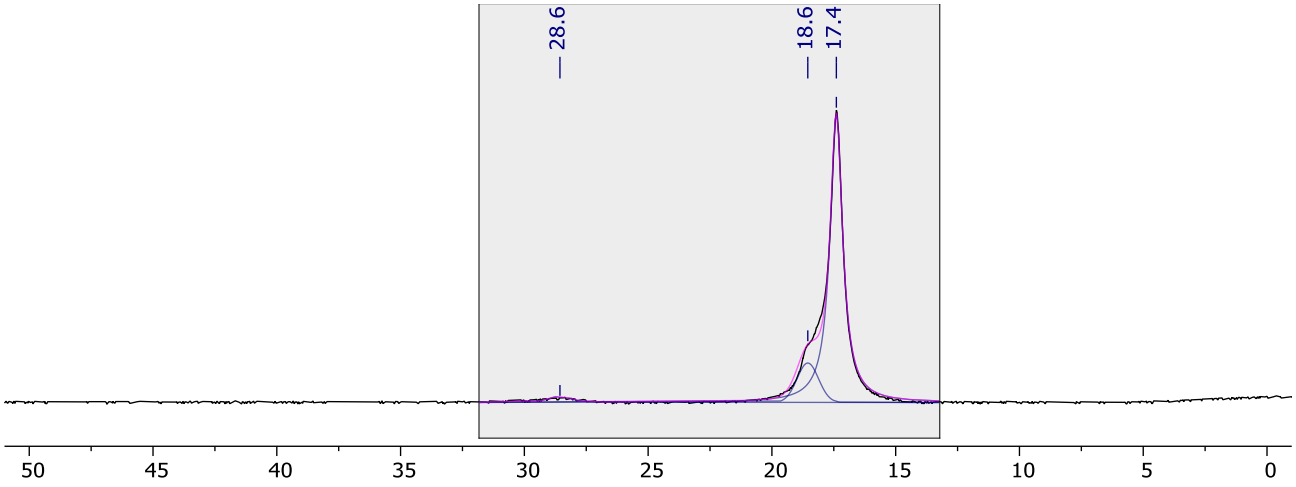

Figure S103. $^{11}B\{^{1}H\}$ NMR spectrum collected following the B_2neop_2 reduction of N_2O (3 bar gauge) using 5 mol% **2*** in toluene after 120 min (128 MHz, toluene/C_6D_6).

3.20.3 [Cu(IPr)(O*t*Bu)] **3***

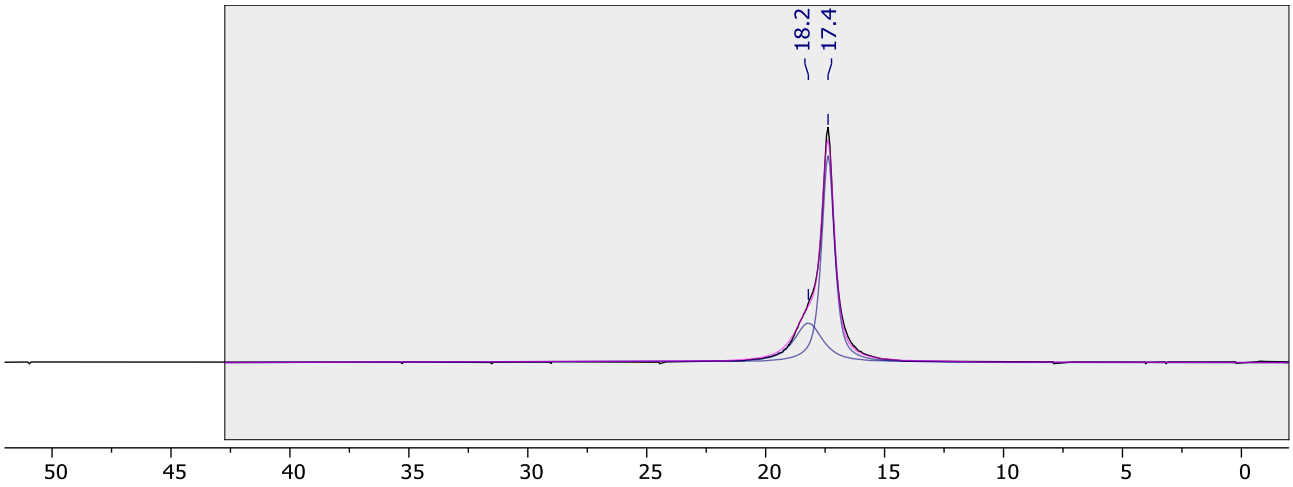

Figure S104. $^{11}B\{^{1}H\}$ NMR spectrum collected following the B_2neop_2 reduction of N_2O (3 bar gauge) using 5 mol% **3*** in toluene after 120 min (128 MHz, toluene/C_6D_6).

3.20.4 [Cu(SIMes)(O*t*Bu)] **4***

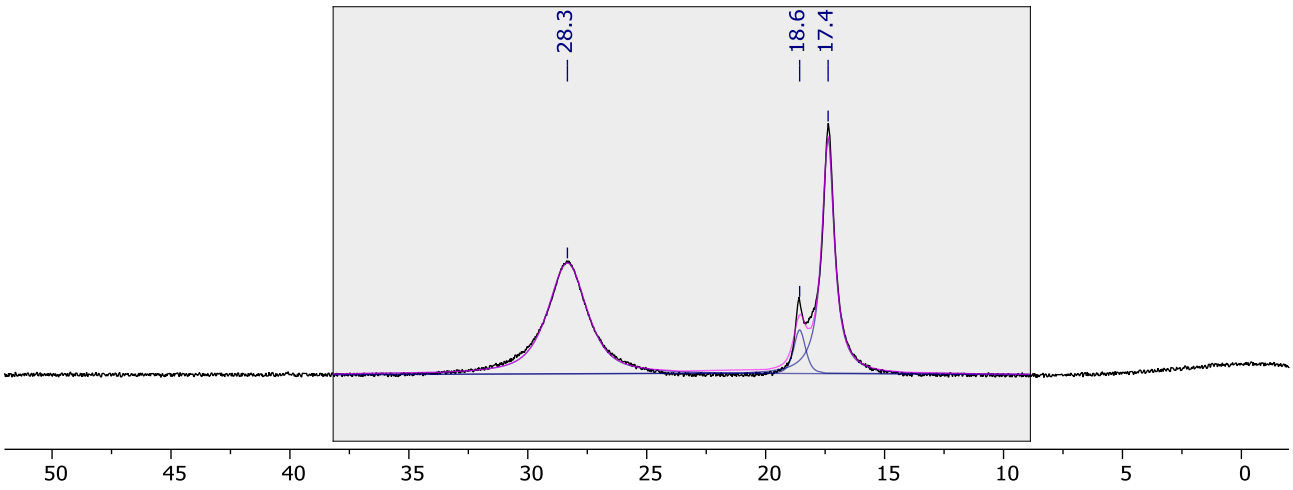

Figure S105. $^{11}B\{^{1}H\}$ NMR spectrum collected following the B_2neop_2 reduction of N_2O (3 bar gauge) using 5 mol% **4*** in toluene after 120 min (128 MHz, toluene/C_6D_6).

3.20.5 [Cu(IMes)(O*t*Bu)] **5***

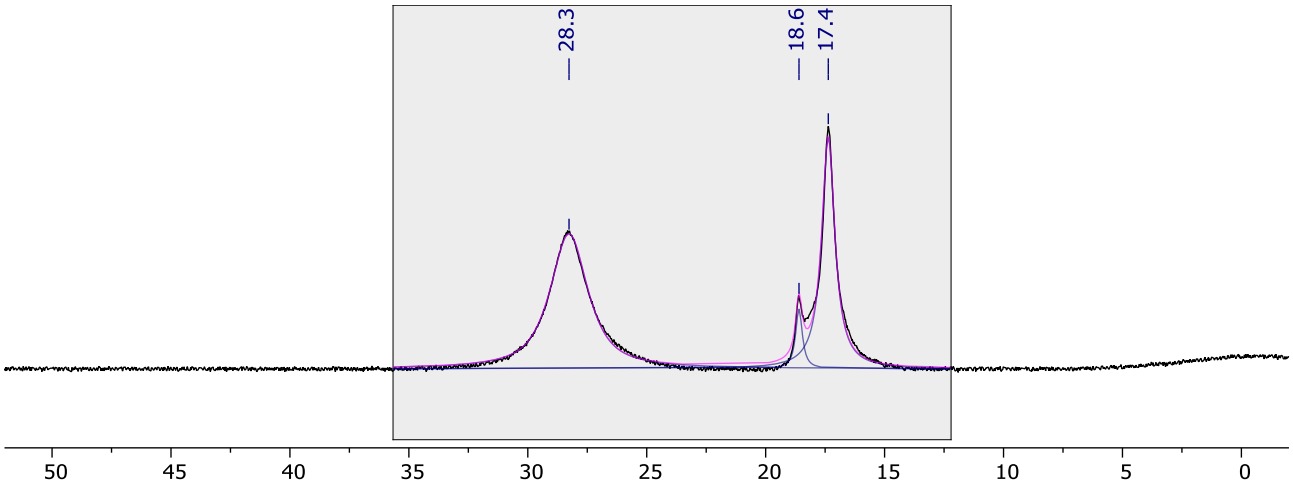

Figure S106. $^{11}B\{^{1}H\}$ NMR spectrum collected following the B_2neop_2 reduction of N_2O (3 bar gauge) using 5 mol% **5*** in toluene after 120 min (128 MHz, toluene/C_6D_6).

3.20.6 [CuO*t*Bu] **6***

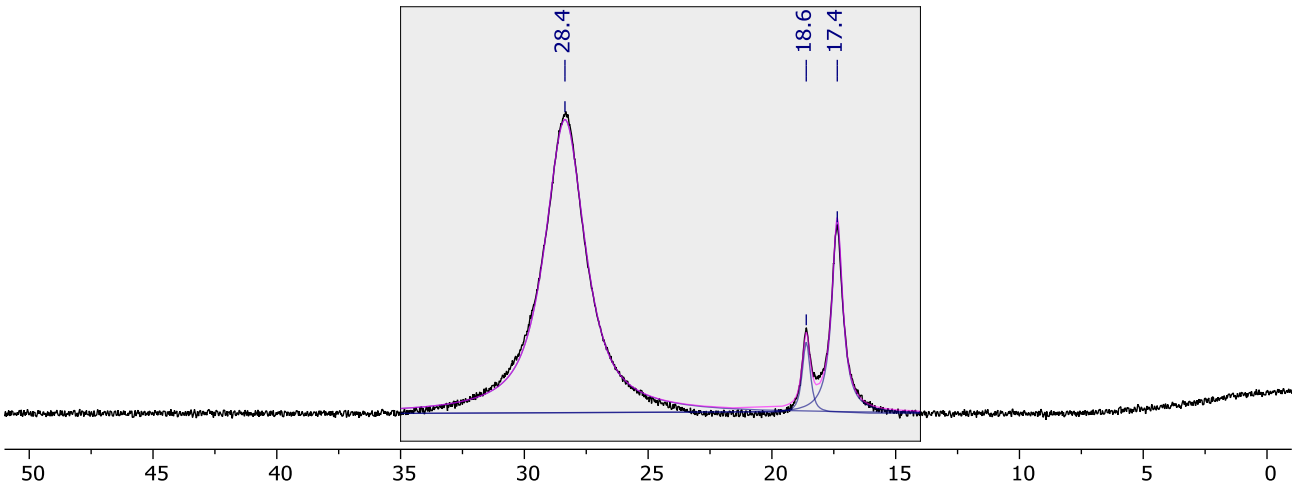

Figure S107. $^{11}B\{^{1}H\}$ NMR spectrum collected following the B_2neop_2 reduction of N_2O (3 bar gauge) using 5 mol% **6*** in toluene after 120 min (128 MHz, toluene/C_6D_6).

3.21 Data collected for entry 10b

3.21.1 No catalyst

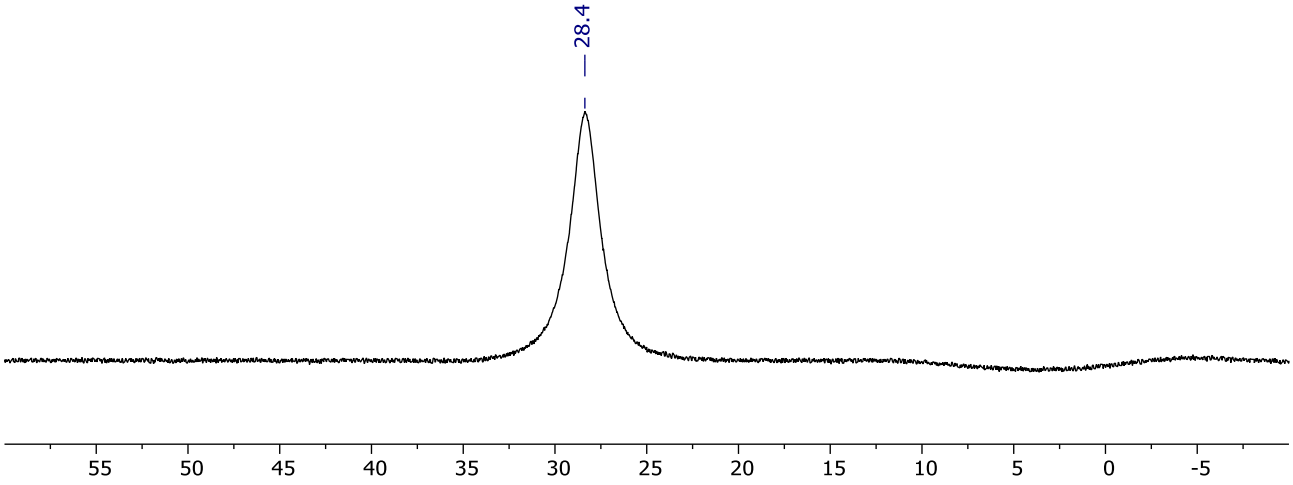

Figure S108. $^{11}B\{^{1}H\}$ NMR spectrum collected following the attempted B_2neop_2 reduction of N_2O (3 bar gauge) in toluene with no catalyst after 120 min (128 MHz, toluene/C_6D_6).

3.21.2 [Cu(SIPr)(O*t*Bu)] **2***

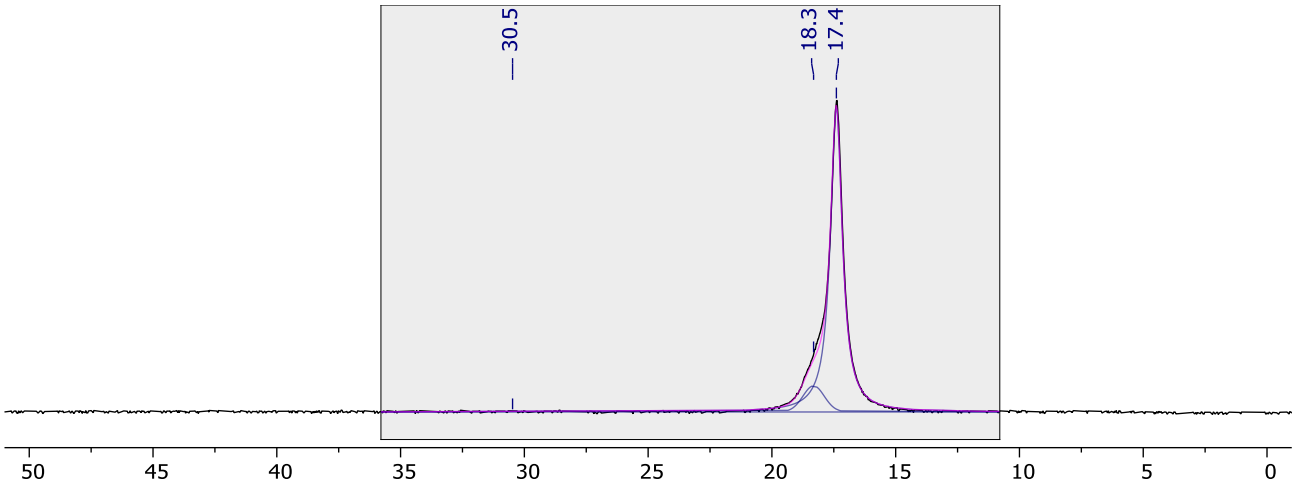

Figure S109. $^{11}B\{^{1}H\}$ NMR spectrum collected following the B_2neop_2 reduction of N_2O (3 bar gauge) using 5 mol% **2*** in toluene after 120 min (128 MHz, toluene/C_6D_6).

3.21.3 [Cu(IPr)(O*t*Bu)] **3***

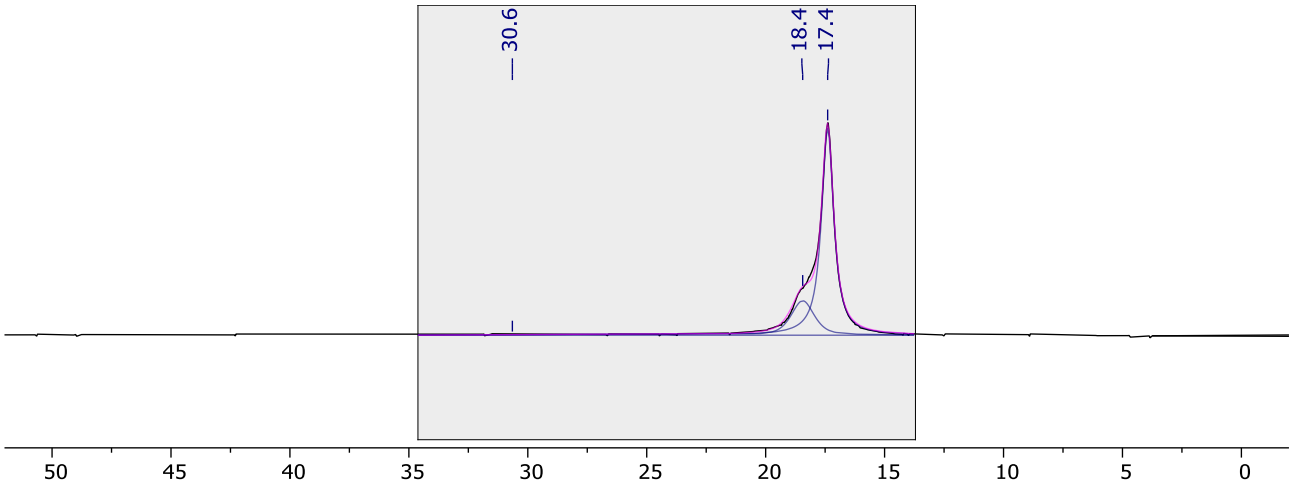

Figure S110. $^{11}B\{^{1}H\}$ NMR spectrum collected following the B_2neop_2 reduction of N_2O (3 bar gauge) using 5 mol% **3*** in toluene after 120 min (128 MHz, toluene/C_6D_6).

3.21.4 [Cu(SIMes)(O*t*Bu)] **4***

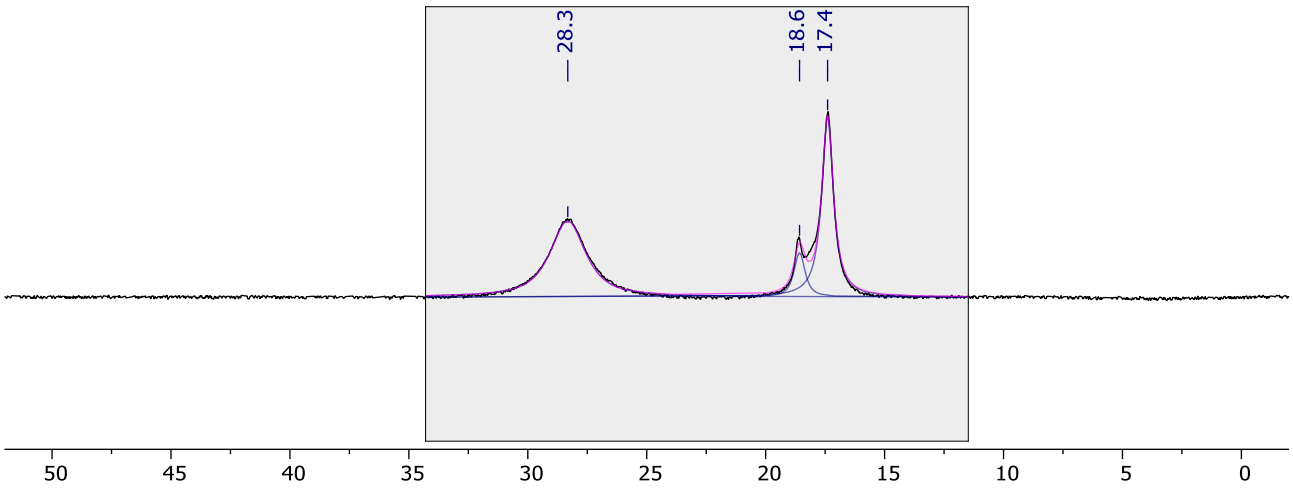

Figure S111. $^{11}B\{^{1}H\}$ NMR spectrum collected following the B_2neop_2 reduction of N_2O (3 bar gauge) using 5 mol% **4*** in toluene after 120 min (128 MHz, toluene/C_6D_6).

3.21.5 [Cu(IMes)(O*t*Bu)] **5***

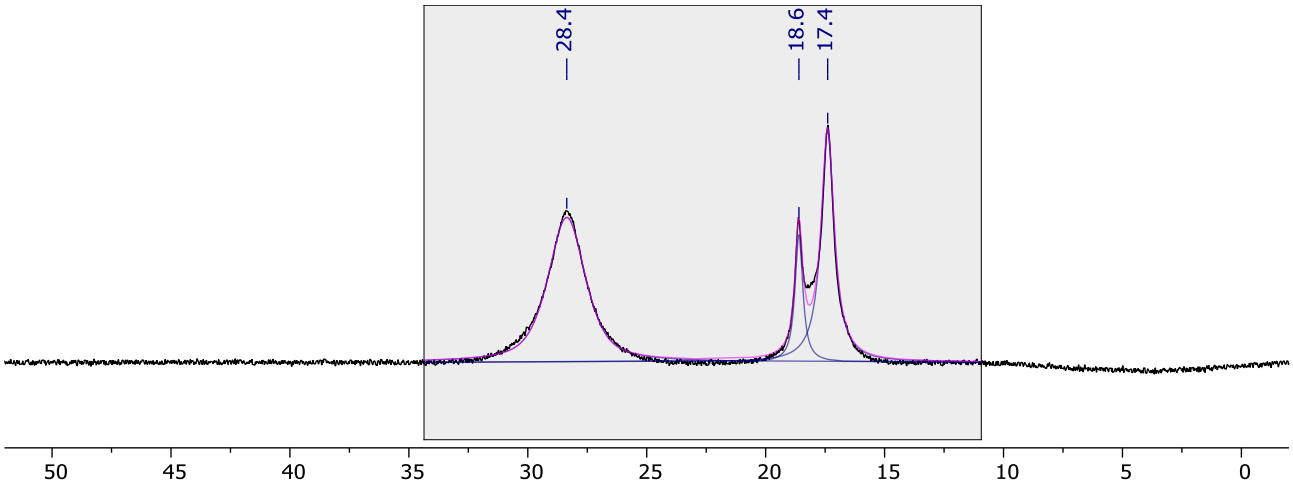

Figure S112. $^{11}B\{^{1}H\}$ NMR spectrum collected following the B_2neop_2 reduction of N_2O (3 bar gauge) using 5 mol% **5*** in toluene after 120 min (128 MHz, toluene/C_6D_6).

3.21.6 [CuO*t*Bu] **6***

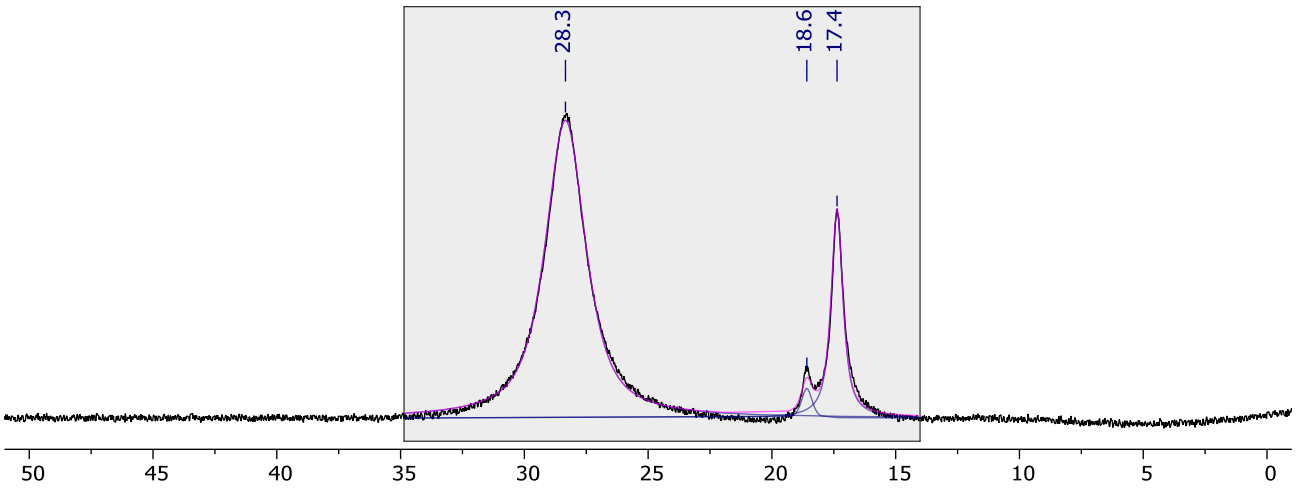

Figure S113. $^{11}B\{^{1}H\}$ NMR spectrum collected following the B_2neop_2 reduction of N_2O (3 bar gauge) using 5 mol% **6*** in toluene after 120 min (128 MHz, toluene/C_6D_6).

3.22 Data collected for entry 11a

3.22.1 No catalyst

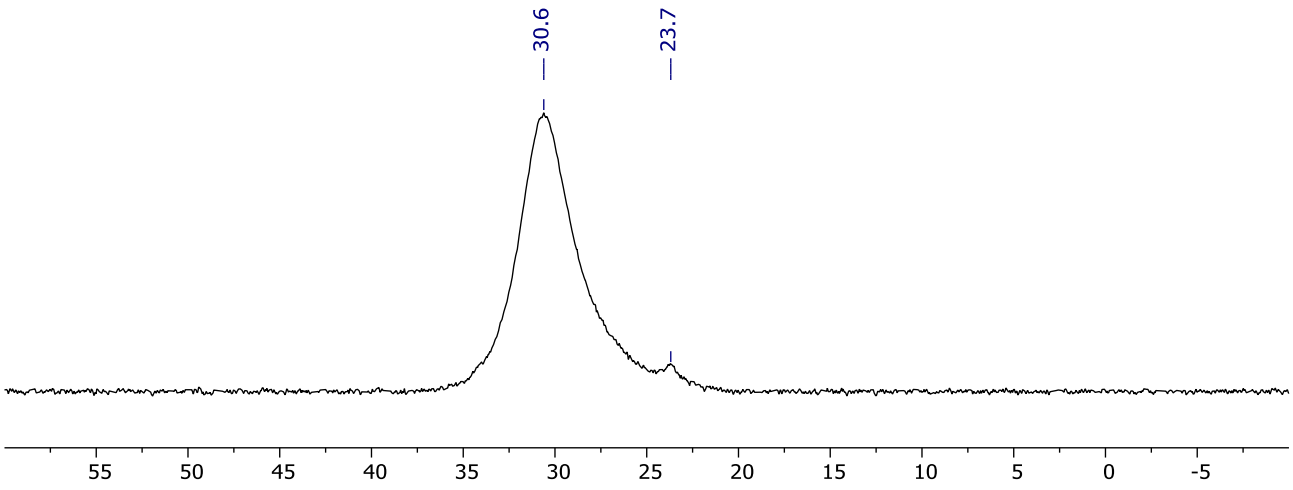

Figure S114. $^{11}B\{^{1}H\}$ NMR spectrum collected following the attempted B_2cat_2 reduction of N_2O (3 bar gauge) in THF with no catalyst after 120 min (96 MHz, THF/C_6D_6).

3.22.2 [$Rh(PEt_3)_3(OPh)$] **1***

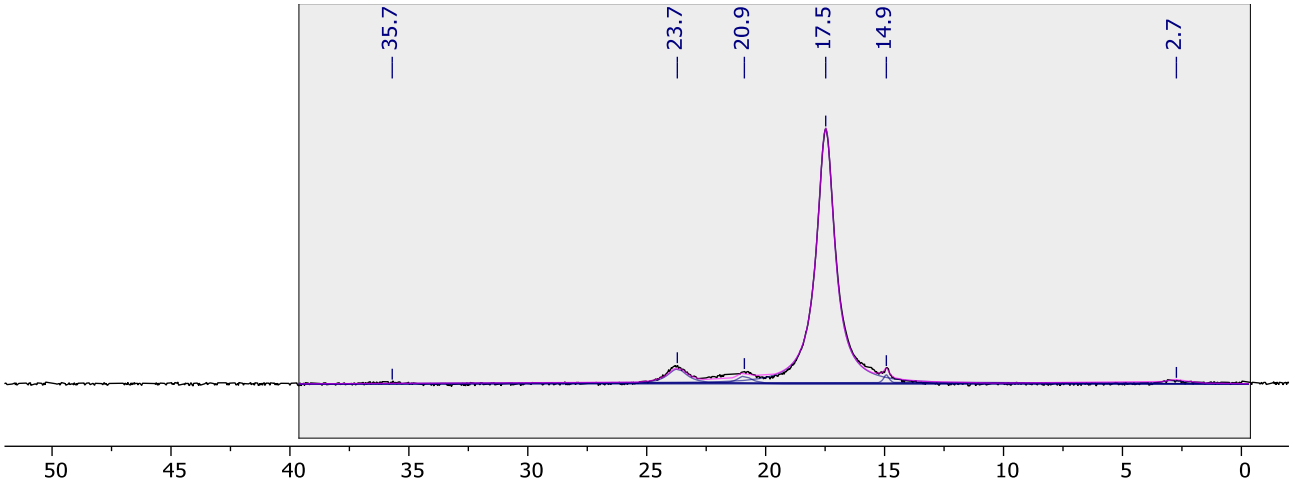

Figure S115. $^{11}B\{^{1}H\}$ NMR spectrum collected following the B_2cat_2 reduction of N_2O (3 bar gauge) using 5 mol% **1*** in THF after 120 min (128 MHz, THF/C_6D_6).

3.22.3 [Cu(SIPr)(O*t*Bu)] **2***

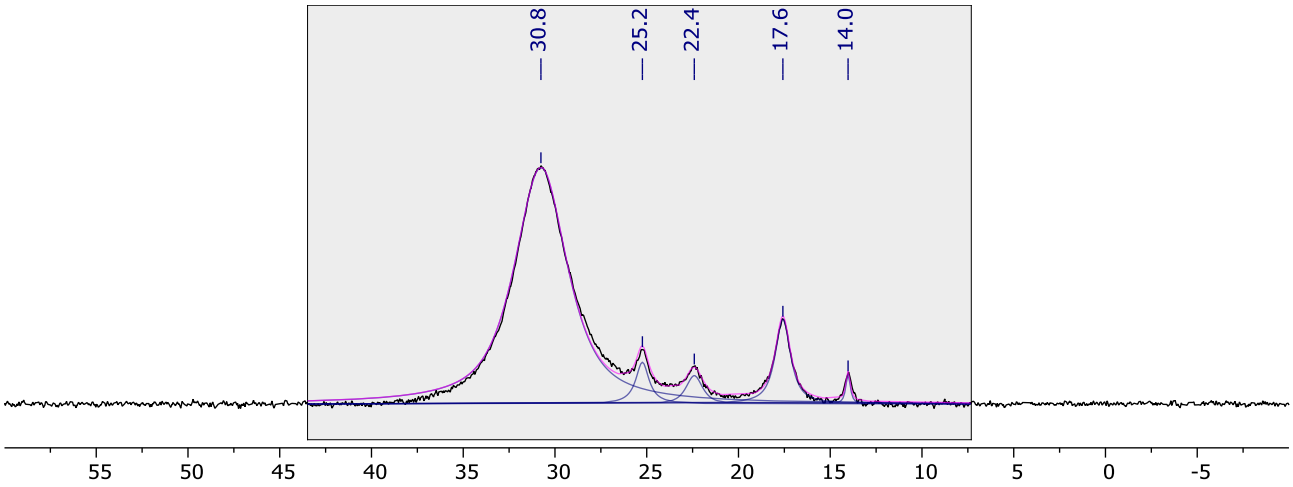

Figure S116. $^{11}B\{^{1}H\}$ NMR spectrum collected following the B_2cat_2 reduction of N_2O (3 bar gauge) using 5 mol% **2*** in THF after 120 min (96 MHz, THF/C_6D_6).

3.22.4 [Cu(IPr)(O*t*Bu)] **3***

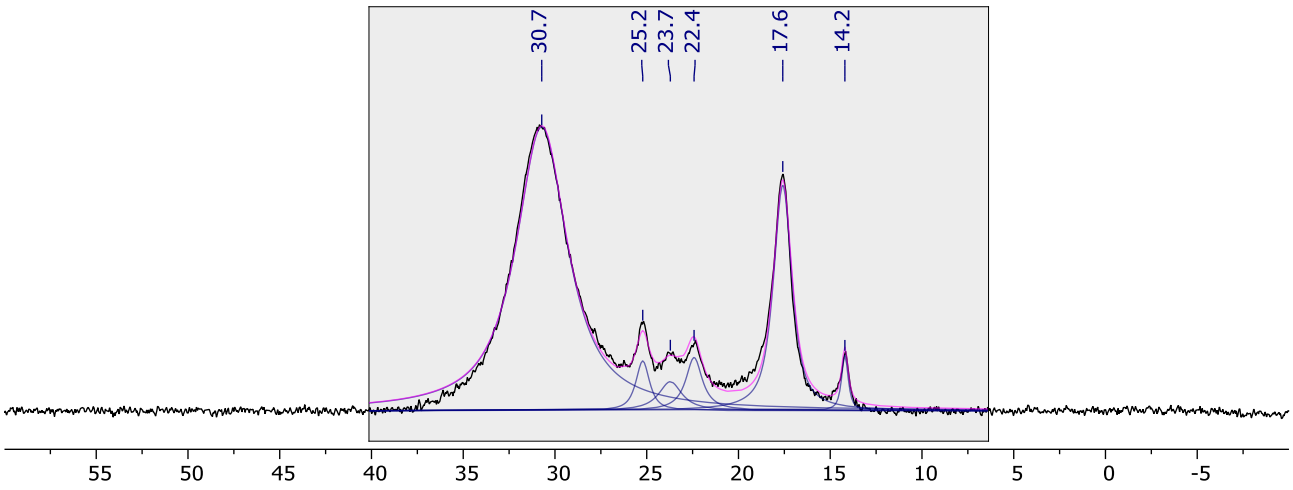

Figure S117. $^{11}B\{^{1}H\}$ NMR spectrum collected following the B_2cat_2 reduction of N_2O (3 bar gauge) using 5 mol% **3*** in THF after 120 min (96 MHz, THF/C_6D_6).

3.22.5 [Cu(SIMes)(O*t*Bu)] **4***

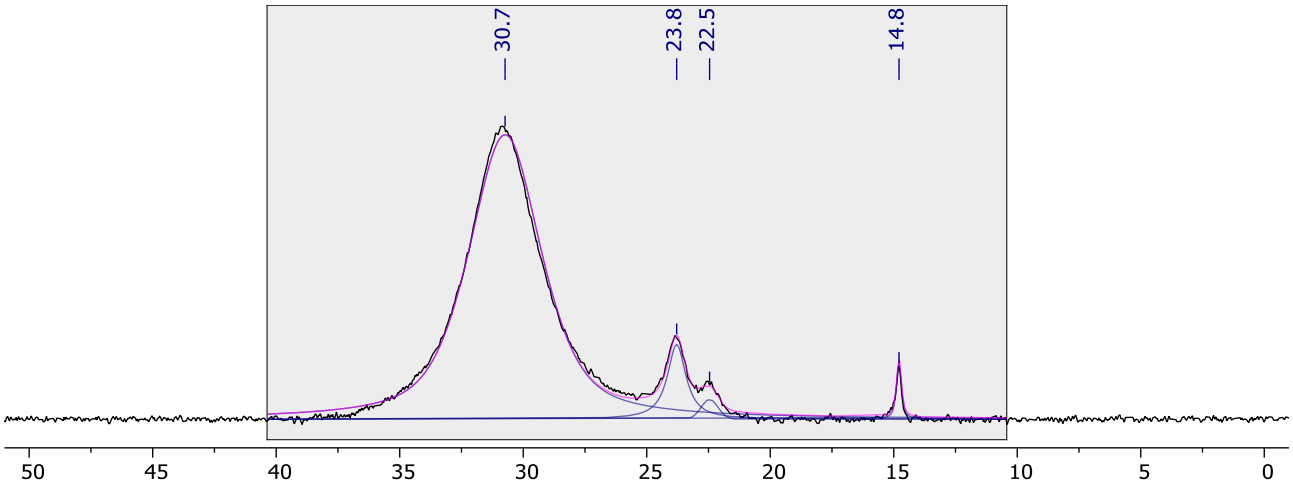

Figure S118. $^{11}B\{^{1}H\}$ NMR spectrum collected following the B_2cat_2 reduction of N_2O (3 bar gauge) using 5 mol% **4*** in THF after 120 min (96 MHz, THF/C_6D_6).

3.22.6 [Cu(IMes)(O*t*Bu)] **5***

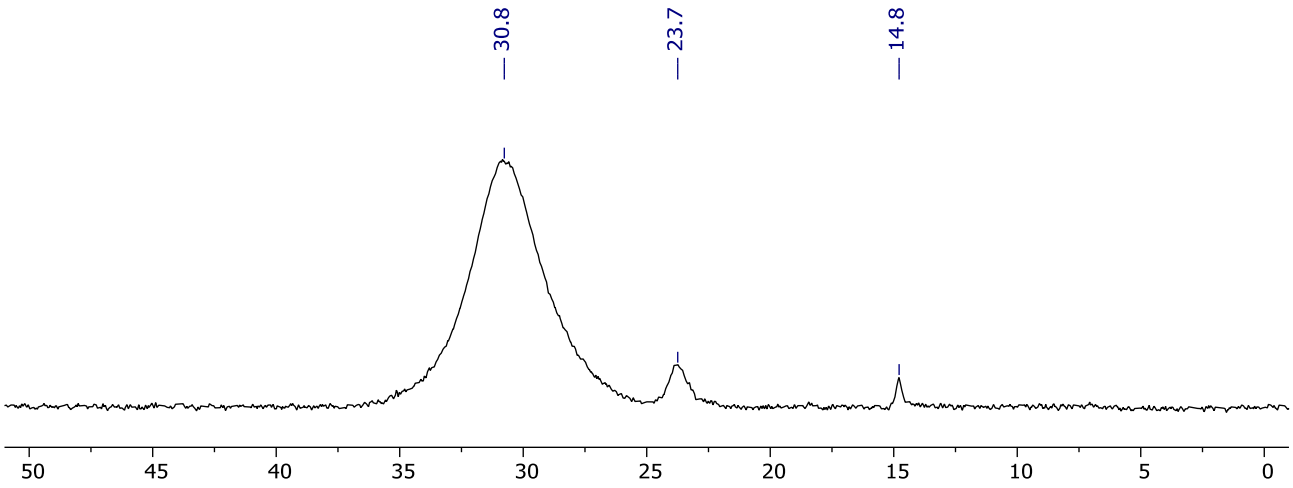

Figure S119. $^{11}B\{^{1}H\}$ NMR spectrum collected following the B_2cat_2 reduction of N_2O (3 bar gauge) using 5 mol% **5*** in THF after 120 min (96 MHz, THF/C_6D_6).

3.22.7 [CuO*t*Bu] **6***

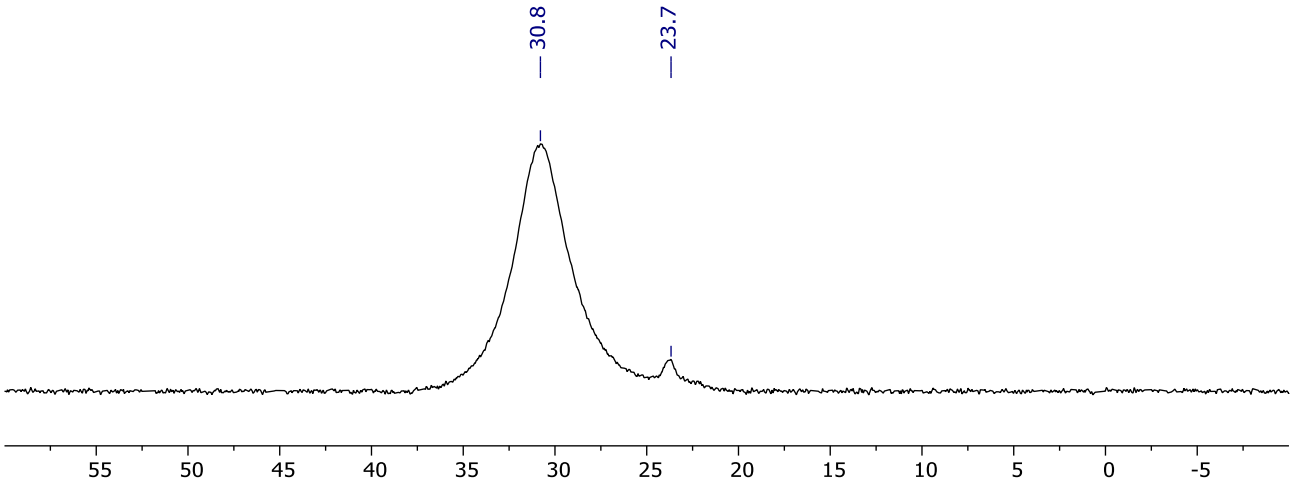

Figure S120. $^{11}B\{^{1}H\}$ NMR spectrum collected following the attempted B_2cat_2 reduction of N_2O (3 bar gauge) using 5 mol% **6*** in THF after 120 min (96 MHz, THF/C_6D_6).

3.22.8 [Rh(PNP-*i*Pr)(OPh)] **7***

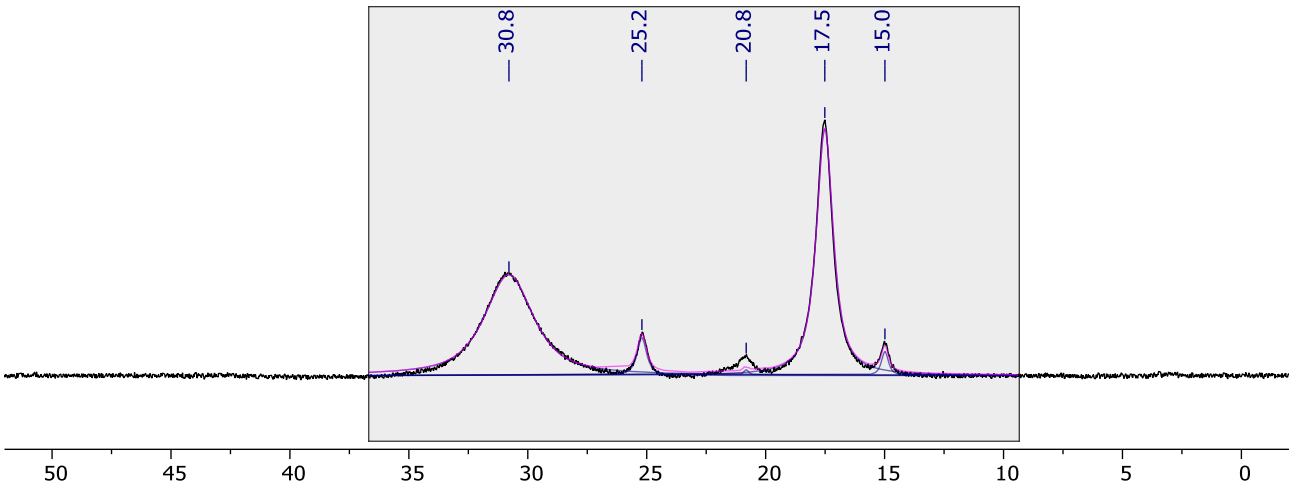

Figure S121. $^{11}B\{^{1}H\}$ NMR spectrum collected following the B_2cat_2 reduction of N_2O (3 bar gauge) using 5 mol% **7*** in THF after 120 min (128 MHz, THF/C_6D_6).

3.22.9 [Rh(PNP-*i*Pr)(OPh)] **8**

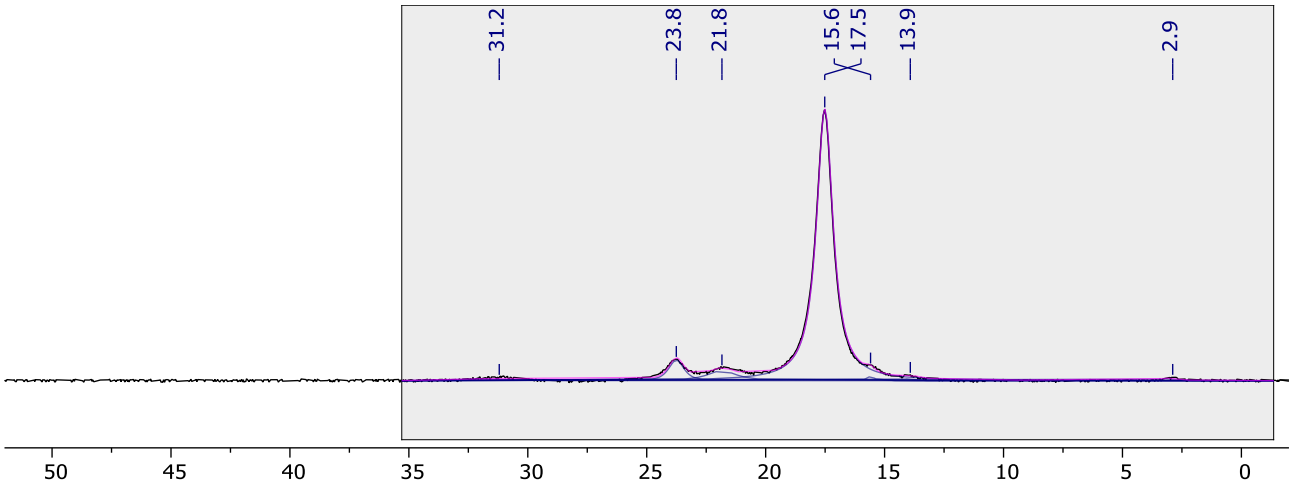

Figure S122. $^{11}B\{^{1}H\}$ NMR spectrum collected following the B_2cat_2 reduction of N_2O (3 bar gauge) using 5 mol% **8** in THF after 120 min (128 MHz, THF/C_6D_6).

3.23 Data collected for entry 11b

3.23.1 No catalyst

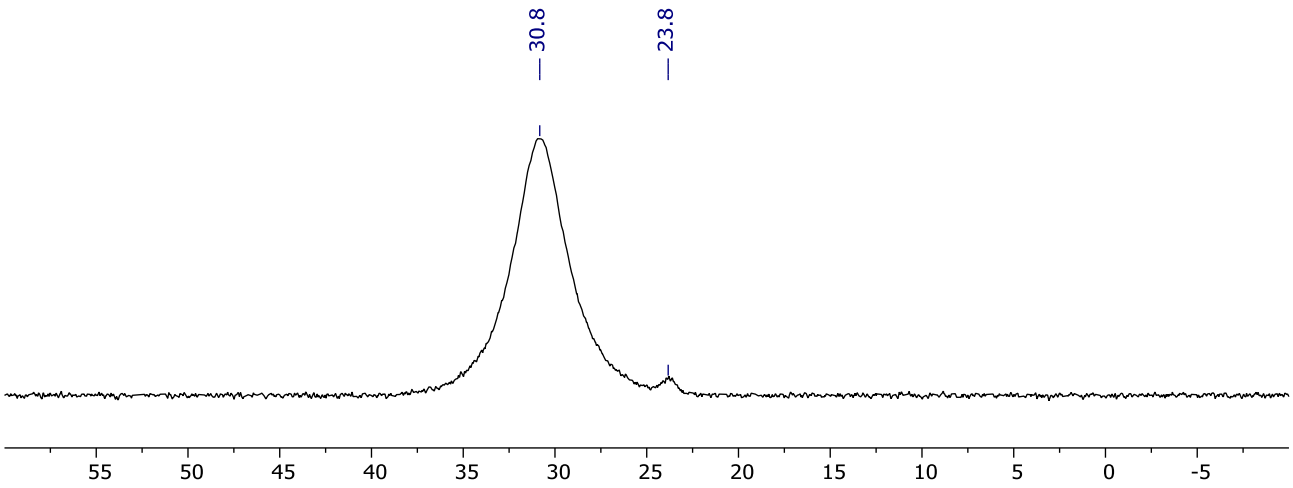

Figure S123. $^{11}B\{^{1}H\}$ NMR spectrum collected following the attempted B_2cat_2 reduction of N_2O (3 bar gauge) in THF with no catalyst after 120 min (96 MHz, THF/C_6D_6).

3.23.2 [Rh(PEt$_3$)$_3$(OPh)] **1***

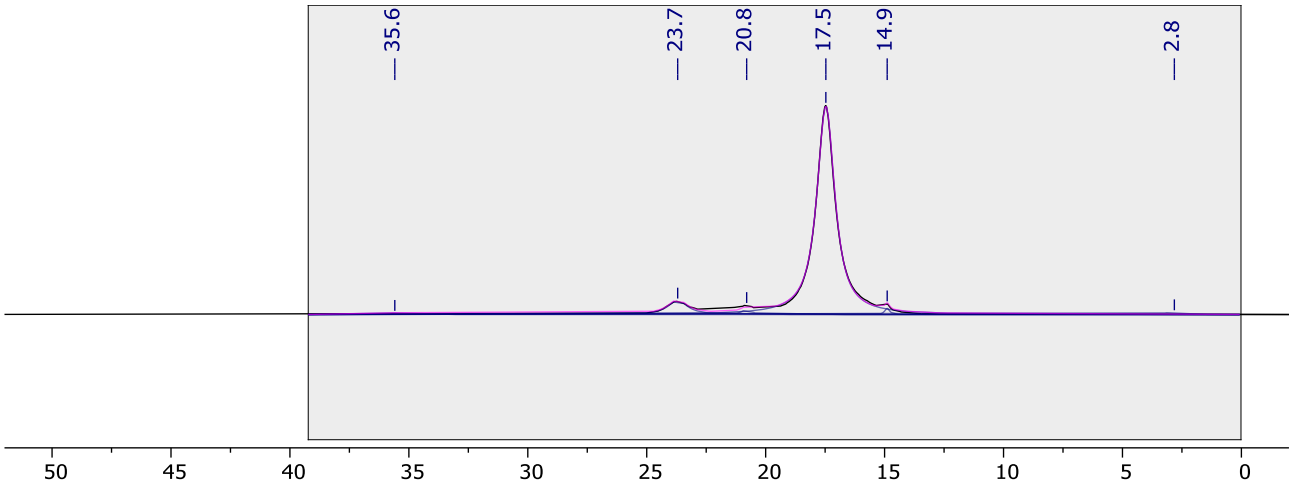

Figure S124. $^{11}B\{^1H\}$ NMR spectrum collected following the B_2cat_2 reduction of N_2O (3 bar gauge) using 5 mol% **1*** in THF after 120 min (128 MHz, THF/C_6D_6).

3.23.3 [Cu(SIPr)(O*t*Bu)] **2***

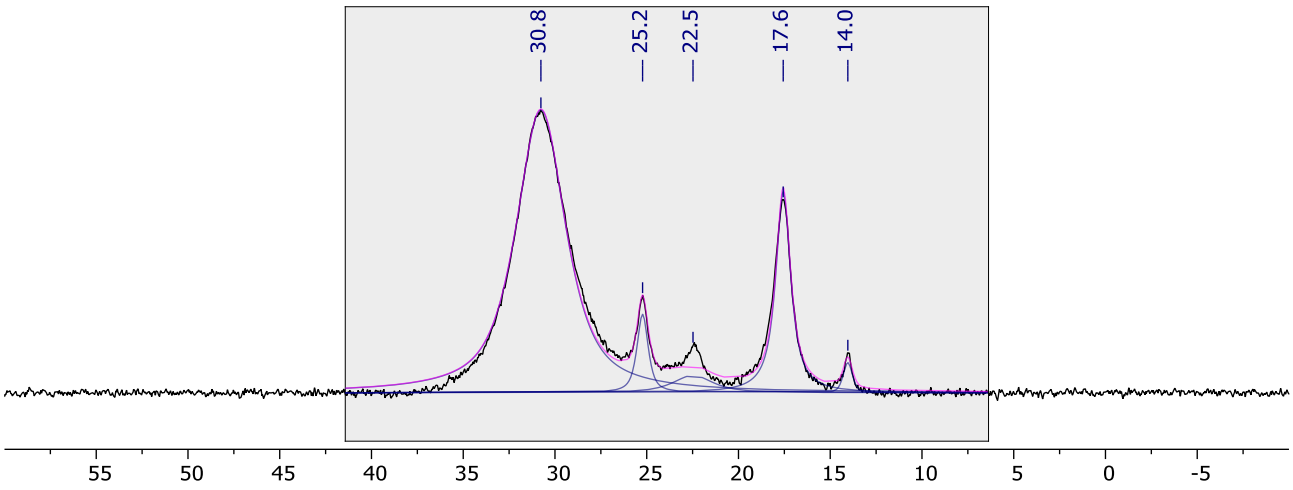

Figure S125. $^{11}B\{^1H\}$ NMR spectrum collected following the B_2cat_2 reduction of N_2O (3 bar gauge) using 5 mol% **2*** in THF after 120 min (96 MHz, THF/C_6D_6).

3.23.4 [Cu(IPr)(O*t*Bu)] **3***

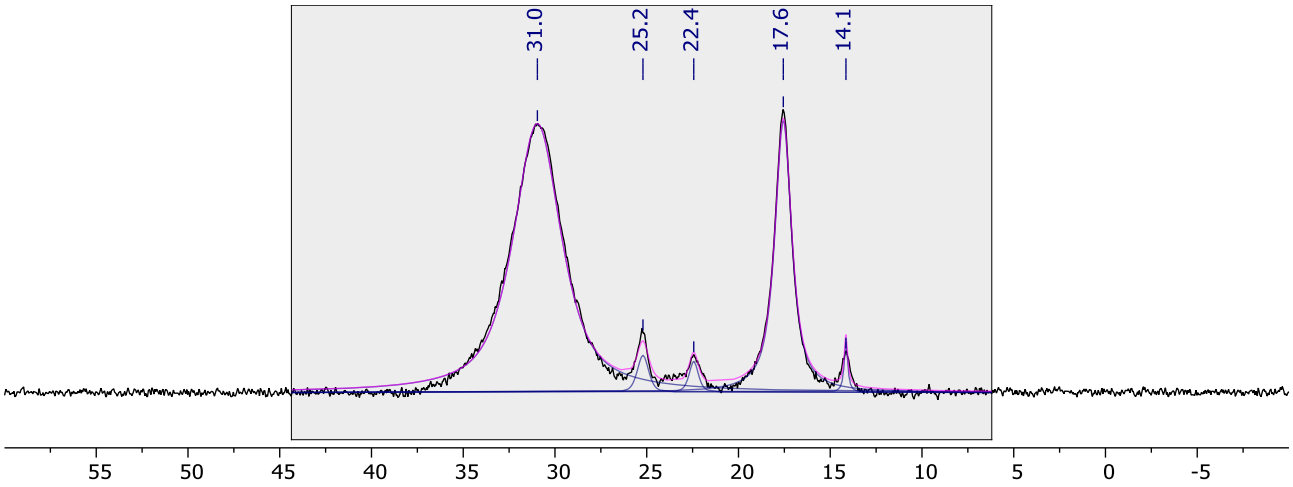

Figure S126. $^{11}B\{^{1}H\}$ NMR spectrum collected following the B_2cat_2 reduction of N_2O (3 bar gauge) using 5 mol% **3*** in THF after 120 min (96 MHz, THF/C_6D_6).

3.23.5 [Cu(SIMes)(O*t*Bu)] **4***

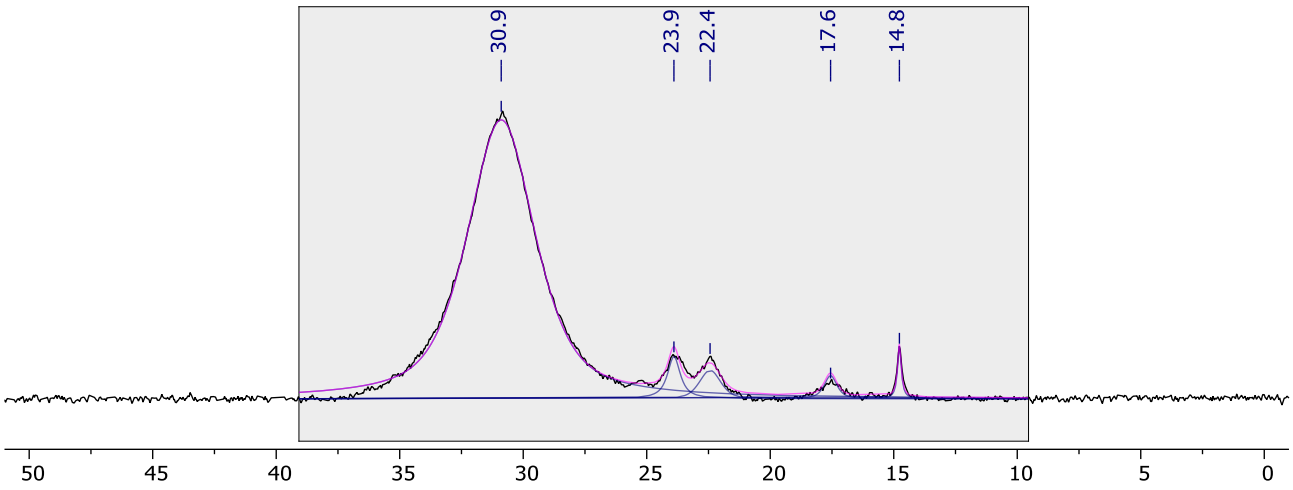

Figure S127. $^{11}B\{^{1}H\}$ NMR spectrum collected following the B_2cat_2 reduction of N_2O (3 bar gauge) using 5 mol% **4*** in THF after 120 min (96 MHz, THF/C_6D_6).

3.23.6 [Cu(IMes)(O*t*Bu)] **5***

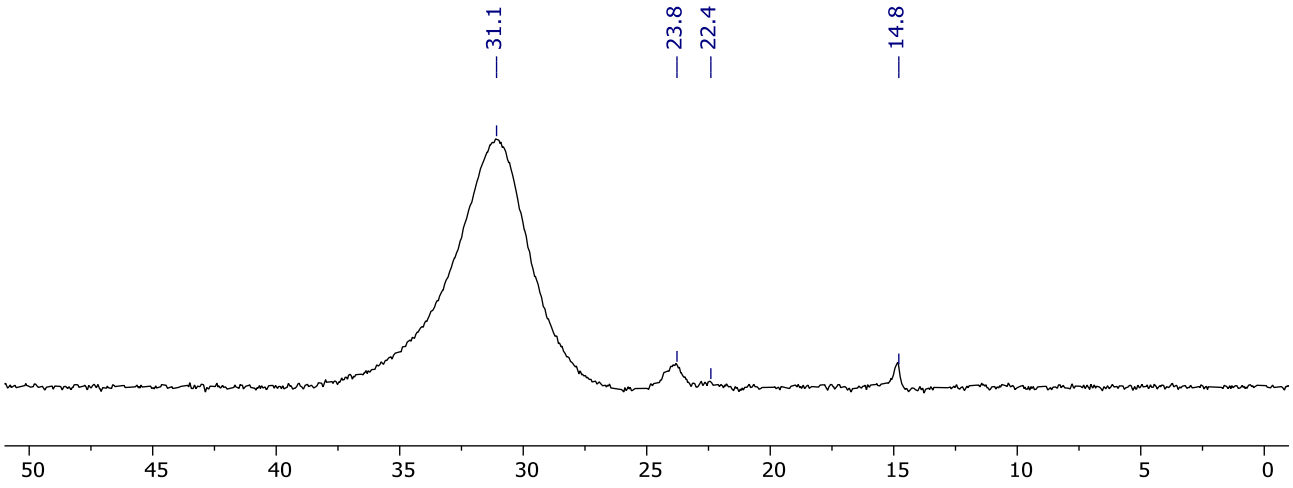

Figure S 128. $^{11}B\{^{1}H\}$ NMR spectrum collected following the B_2cat_2 reduction of N_2O (3 bar gauge) using 5 mol% **5*** in THF after 120 min (96 MHz, THF/C_6D_6).

3.23.7 [CuO*t*Bu] **6***

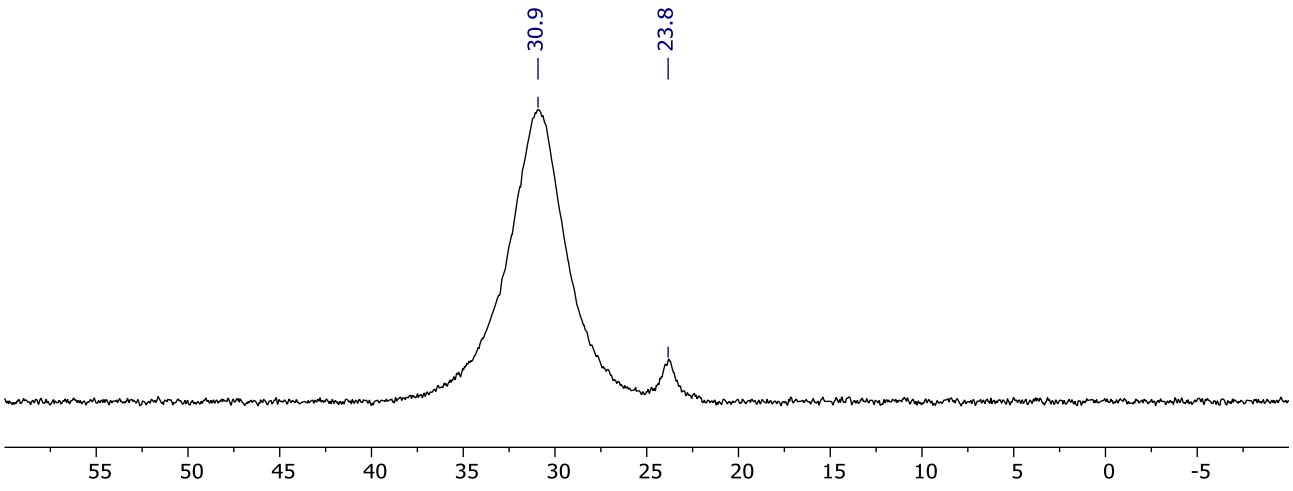

Figure S129. $^{11}B\{^{1}H\}$ NMR spectrum collected following the attempted B_2cat_2 reduction of N_2O (3 bar gauge) using 5 mol% **6*** in THF after 120 min (96 MHz, THF/C_6D_6).

3.23.8 [Rh(PNP-*i*Pr)(OPh)] **7***

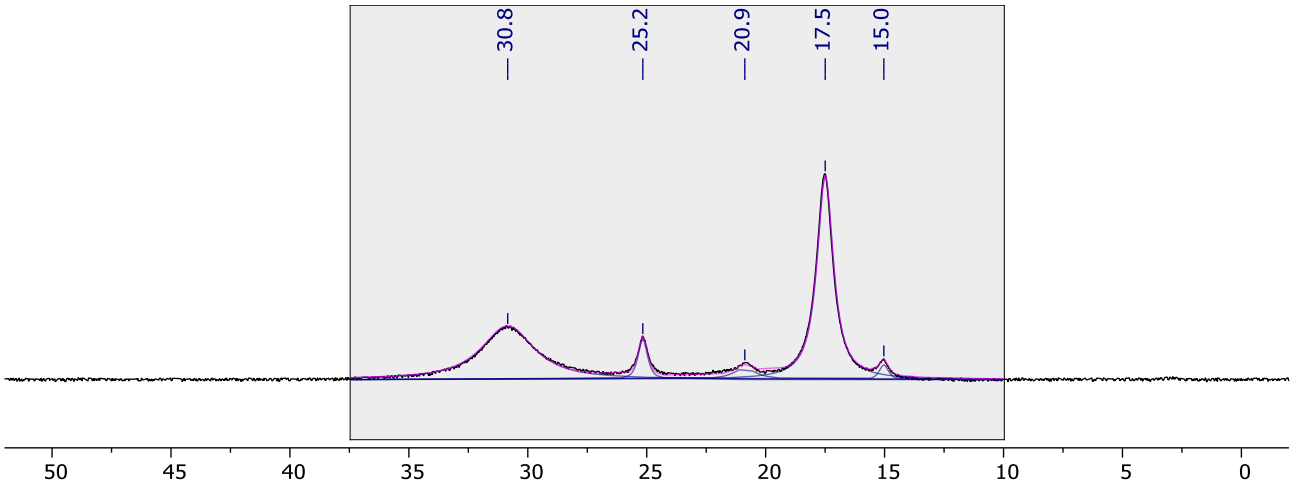

Figure S130. $^{11}B\{^{1}H\}$ NMR spectrum collected following the B_2cat_2 reduction of N_2O (3 bar gauge) using 5 mol% **7*** in THF after 120 min (128 MHz, THF/C_6D_6).

3.23.9 [Rh(POP-*i*Pr)(Bpin)] **8**

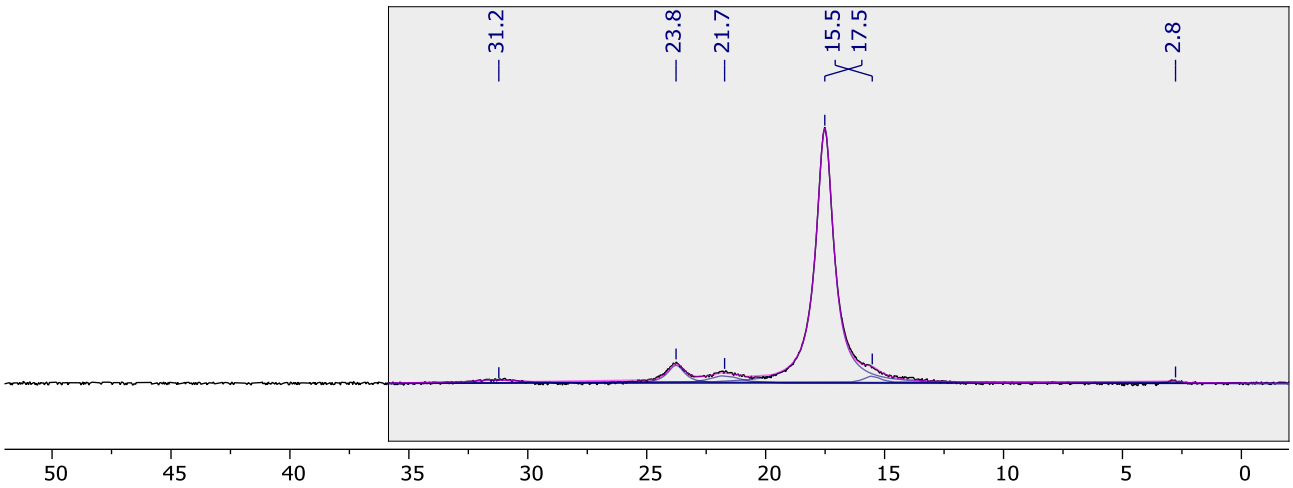

Figure S131. $^{11}B\{^{1}H\}$ NMR spectrum collected following the B_2cat_2 reduction of N_2O (3 bar gauge) using 5 mol% **8** in THF after 120 min (128 MHz, THF/C_6D_6).

3.24 Data collected for entry 12a

3.24.1 No catalyst

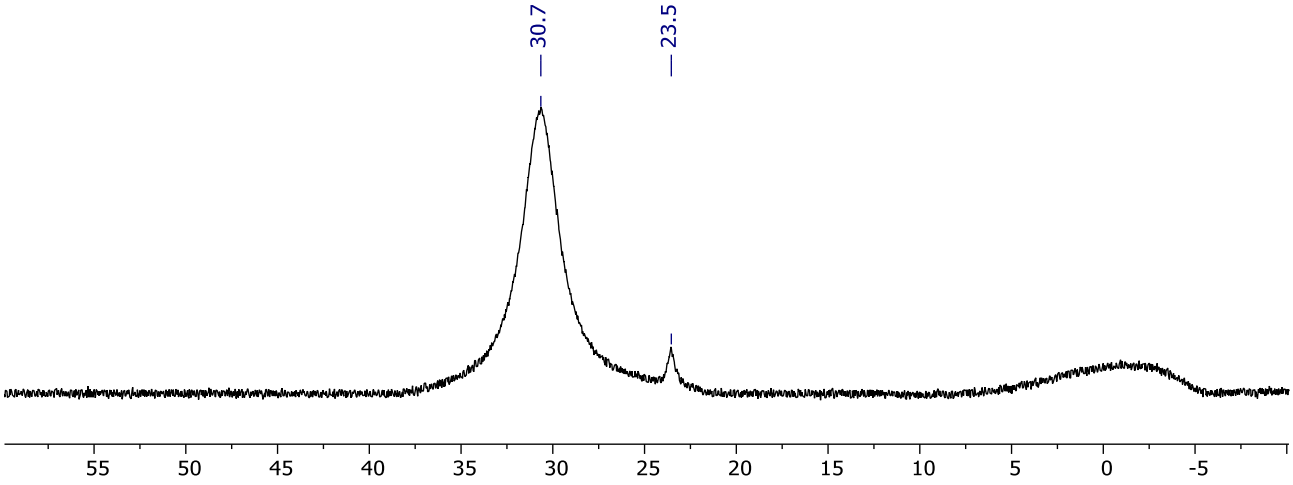

Figure S132. $^{11}B\{^{1}H\}$ NMR spectrum collected following the attempted B_2cat_2 reduction of N_2O (3 bar gauge) in toluene with no catalyst after 120 min (128 MHz, toluene/C_6D_6).

3.24.2 [Cu(SIPr)(O*t*Bu)] **2***

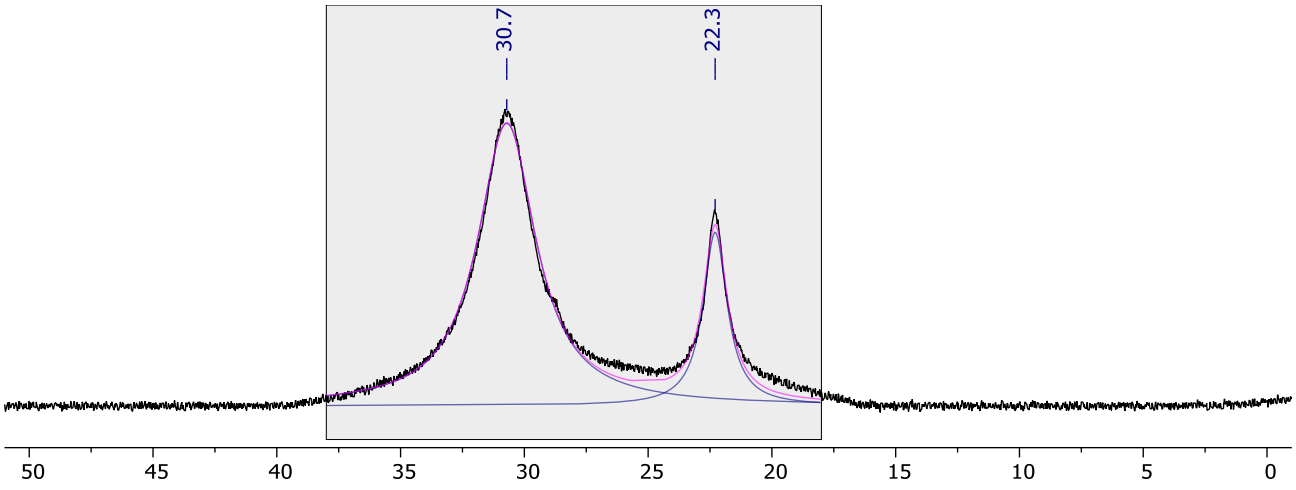

Figure S133. $^{11}B\{^{1}H\}$ NMR spectrum collected following the B_2cat_2 reduction of N_2O (3 bar gauge) using 5 mol% **2*** in toluene after 120 min (128 MHz, toluene/C_6D_6).

3.24.3 [Cu(IPr)(O*t*Bu)] **3***

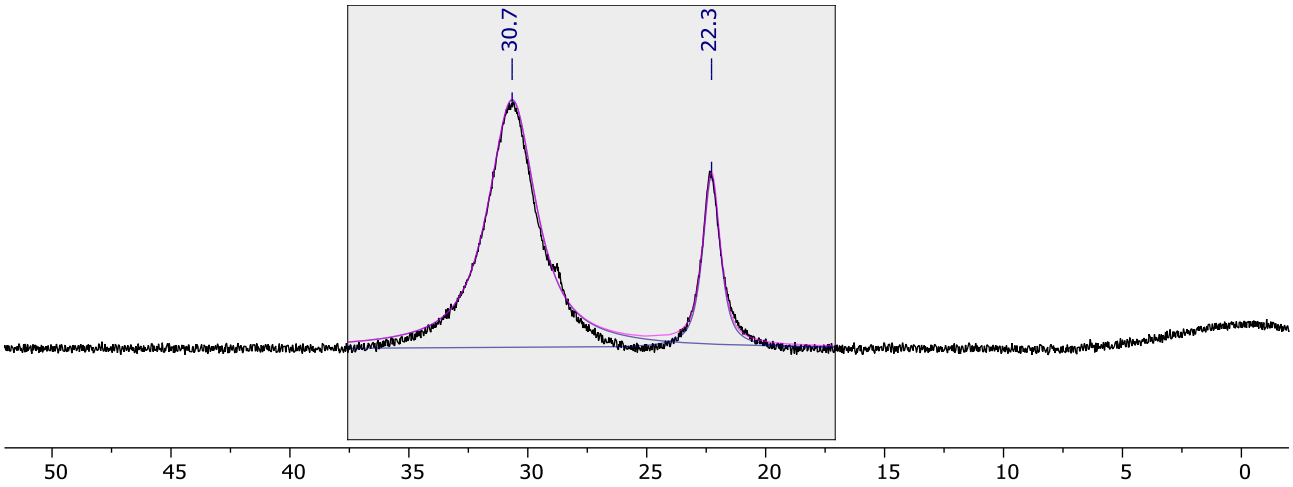

Figure S134. $^{11}B\{^{1}H\}$ NMR spectrum collected following the B_2cat_2 reduction of N_2O (3 bar gauge) using 5 mol% **3*** in toluene after 120 min (128 MHz, toluene/C_6D_6).

3.24.4 [Cu(SIMes)(O*t*Bu)] **4***

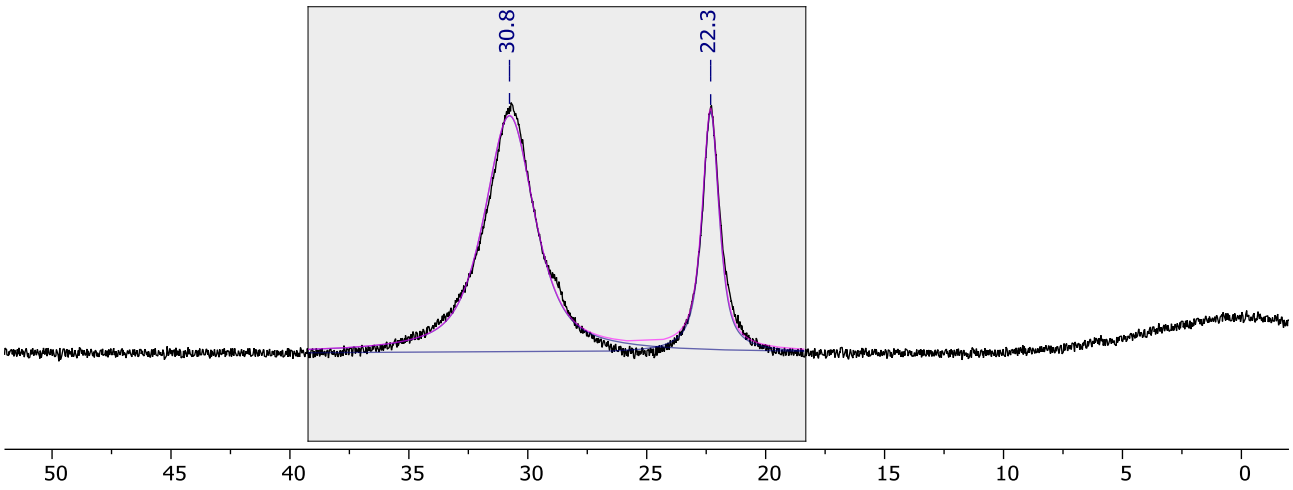

Figure S135. $^{11}B\{^{1}H\}$ NMR spectrum collected following the B_2cat_2 reduction of N_2O (3 bar gauge) using 5 mol% **4*** in toluene after 120 min (128 MHz, toluene/C_6D_6).

3.24.5 [Cu(IMes)(O*t*Bu)] **5***

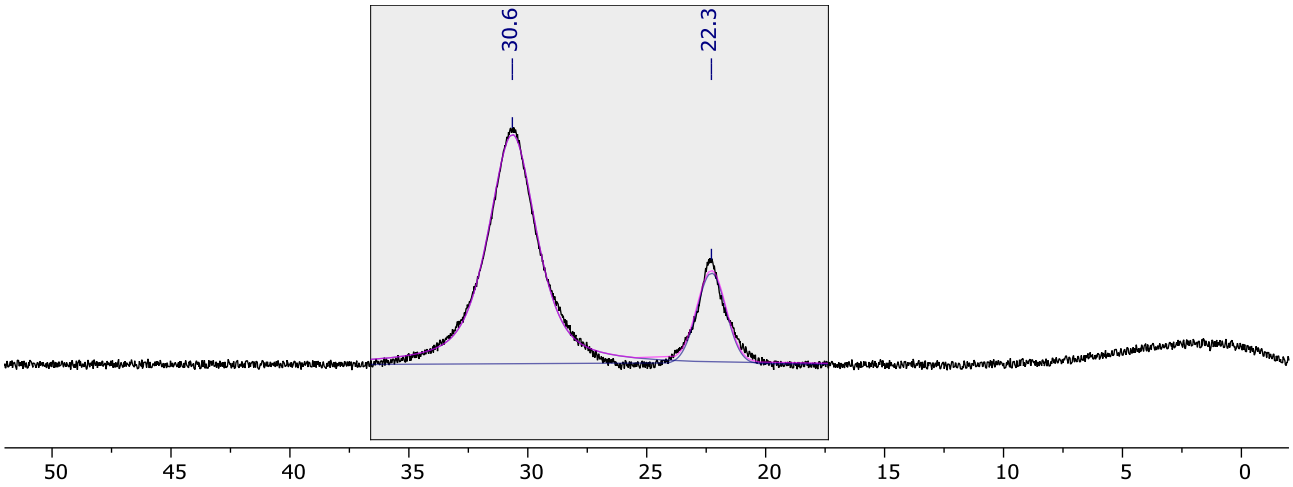

Figure S136. $^{11}B\{^{1}H\}$ NMR spectrum collected following the B_2cat_2 reduction of N_2O (3 bar gauge) using 5 mol% **5*** in toluene after 120 min (128 MHz, toluene/C_6D_6).

3.24.6 [CuO*t*Bu] **6***

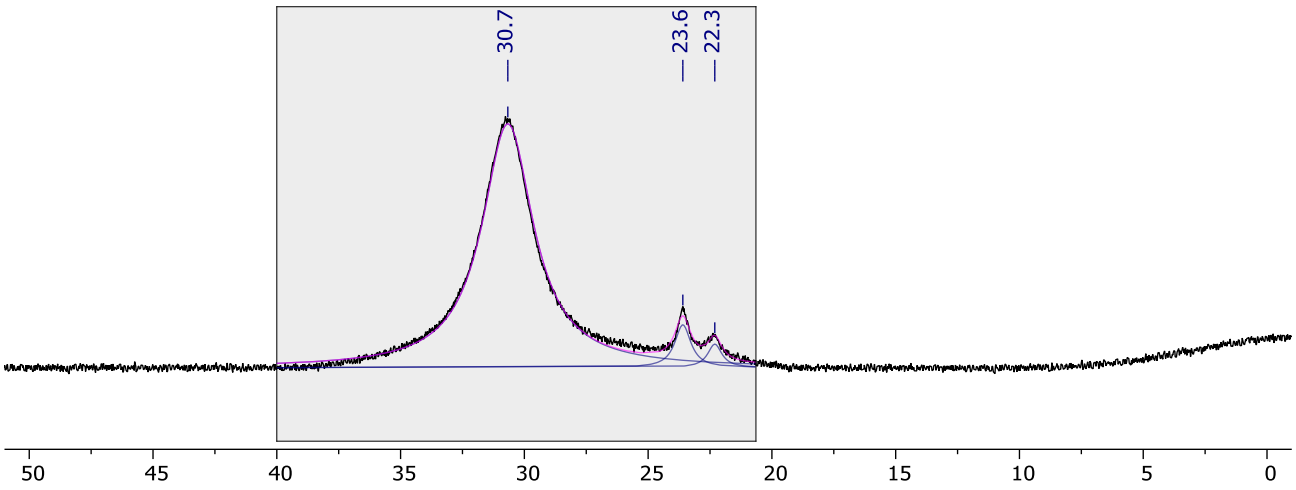

Figure S137. $^{11}B\{^{1}H\}$ NMR spectrum collected following the B_2cat_2 reduction of N_2O (3 bar gauge) using 5 mol% **6*** in toluene after 120 min (128 MHz, toluene/C_6D_6).

3.25 Data collected for entry 12b

3.25.1 No catalyst

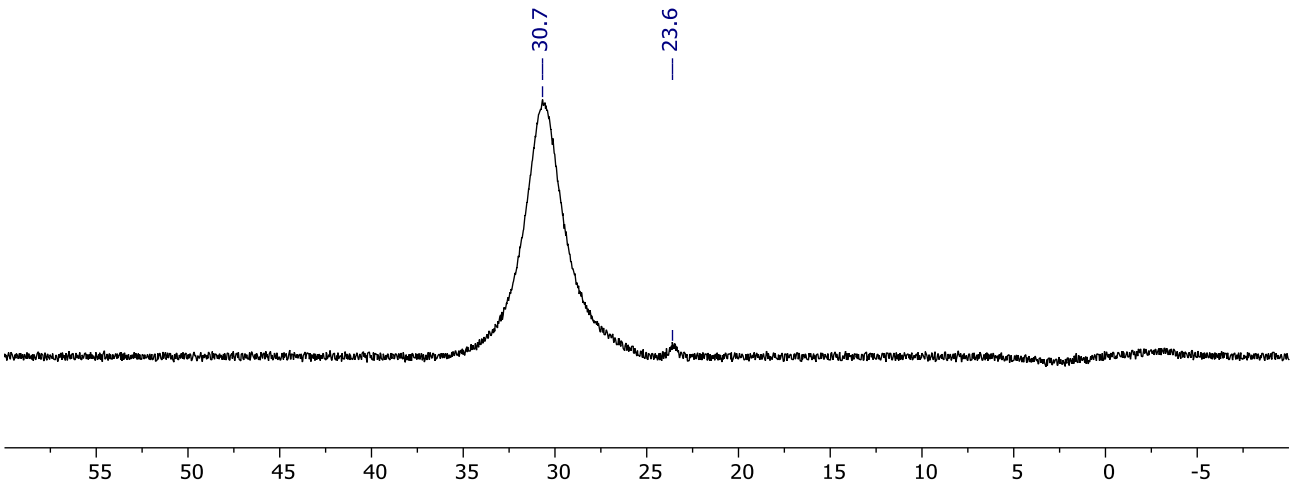

Figure S138. $^{11}B\{^{1}H\}$ NMR spectrum collected following the attempted B_2cat_2 reduction of N_2O (3 bar gauge) in toluene with no catalyst after 120 min (128 MHz, toluene/C_6D_6).

3.25.2 [Cu(SIPr)(O*t*Bu)] **2***

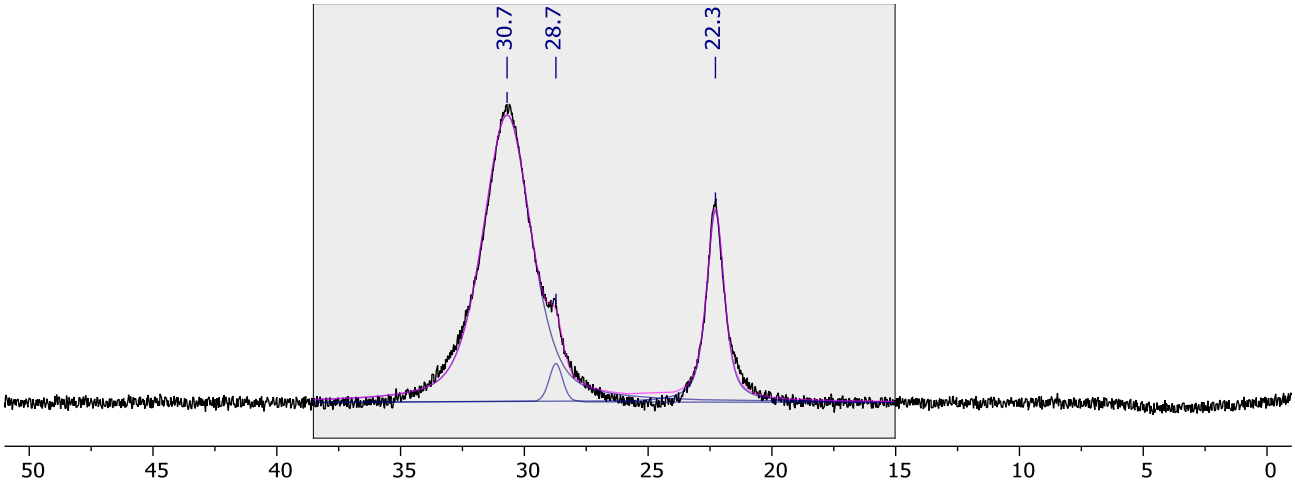

Figure S139. $^{11}B\{^{1}H\}$ NMR spectrum collected following the B_2cat_2 reduction of N_2O (3 bar gauge) using 5 mol% **2*** in toluene after 120 min (128 MHz, toluene/C_6D_6).

3.25.3 [Cu(IPr)(O*t*Bu)] **3***

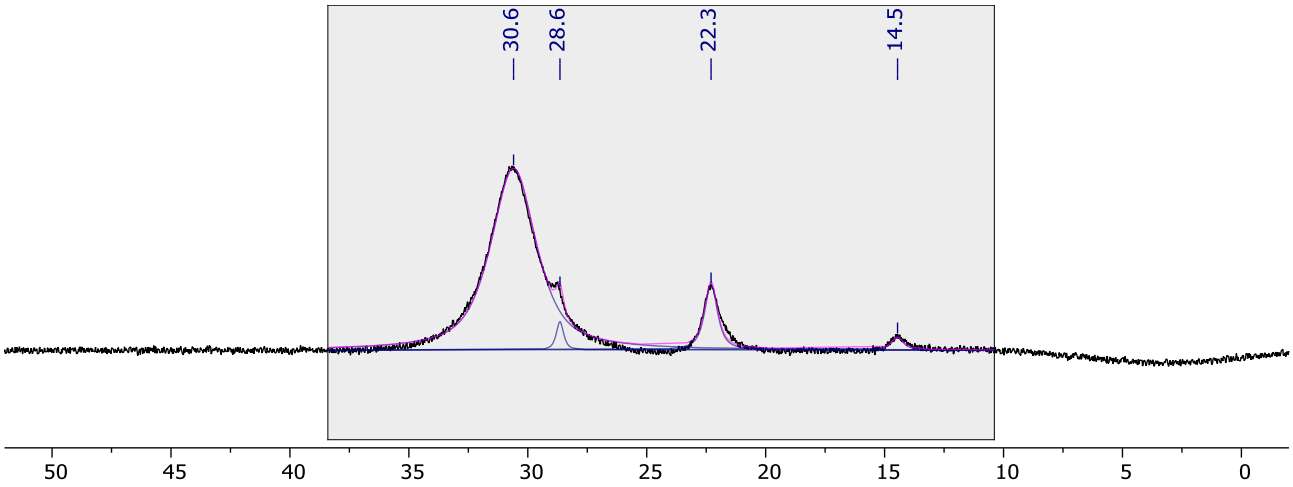

Figure S140. $^{11}B\{^{1}H\}$ NMR spectrum collected following the B_2cat_2 reduction of N_2O (3 bar gauge) using 5 mol% **3*** in toluene after 120 min (128 MHz, toluene/C_6D_6).

3.25.4 [Cu(SIMes)(O*t*Bu)] **4***

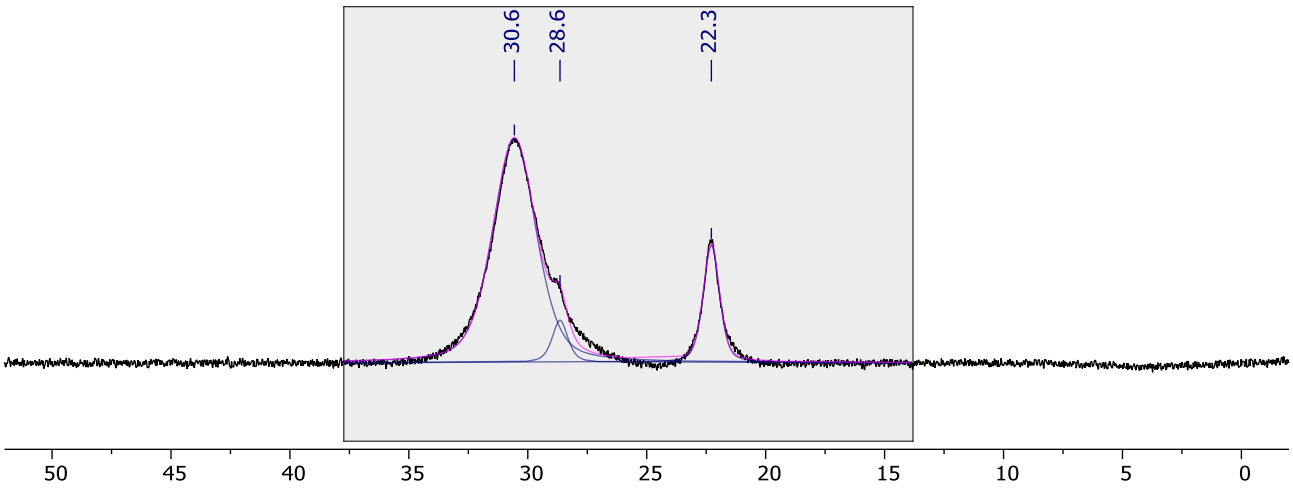

Figure S141. $^{11}B\{^{1}H\}$ NMR spectrum collected following the B_2cat_2 reduction of N_2O (3 bar gauge) using 5 mol% **4*** in toluene after 120 min (128 MHz, toluene/C_6D_6).

3.25.5 [Cu(IMes)(O*t*Bu)] **5***

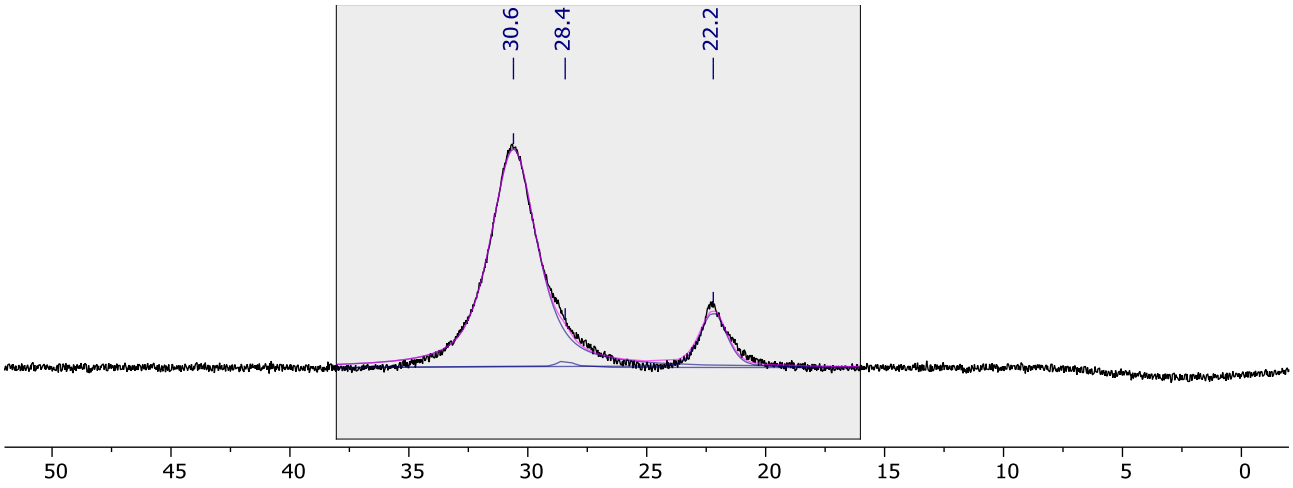

Figure S142. $^{11}B\{^{1}H\}$ NMR spectrum collected following the B_2cat_2 reduction of N_2O (3 bar gauge) using 5 mol% **5*** in toluene after 120 min (128 MHz, toluene/C_6D_6).

3.25.6 [CuO*t*Bu] **6***

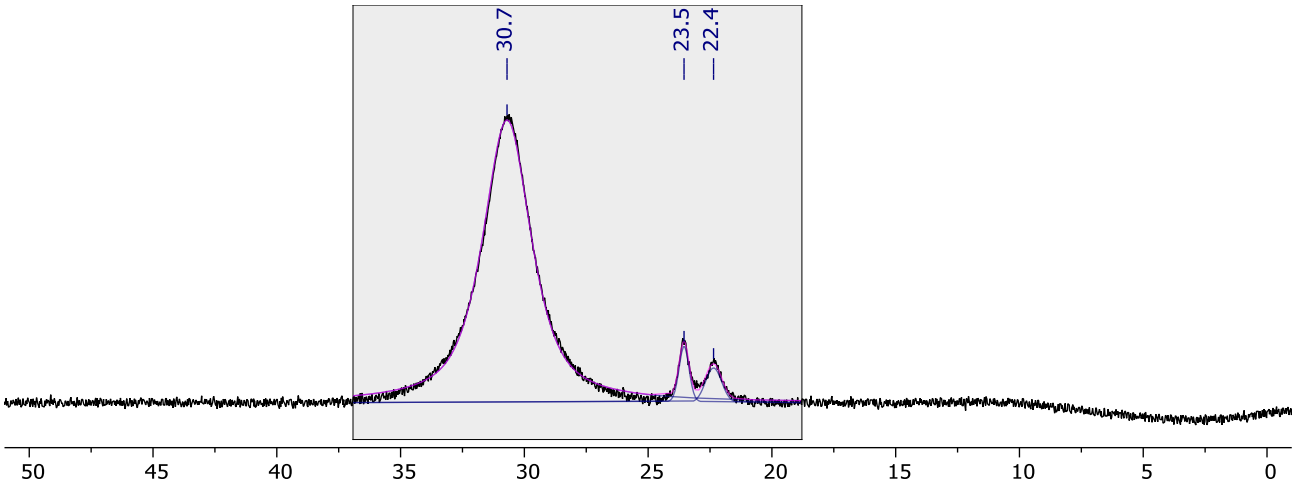

Figure S143. $^{11}B\{^{1}H\}$ NMR spectrum collected following the B_2cat_2 reduction of N_2O (3 bar gauge) using 5 mol% **6*** in toluene after 120 min (128 MHz, toluene/C_6D_6).

4 Copper(I) boryl stability investigation

4.1 General procedure: dark

A mixture of [Cu(NHC)(O*t*Bu)] (10 μmol) and B_2pin_2 (2.8 mg, 11 μmol) was dissolved in d_8-THF or d_8-toluene (0.5 mL) within an amberised J. Young valve NMR tube in the dark at room temperature and then immediately frozen (77 K). The solution was thawed to room temperature and then loaded into an NMR spectrometer. The stability of the resulting boryl derivative was monitored by ^{1}H and ^{11}B NMR spectroscopy periodically for 30 min or 24 h and the sample was kept in the spectrometer for the duration of the experiment.

4.2 General procedure: ambient light

A mixture of [Cu(NHC)(O*t*Bu)] (10 μmol) and B_2pin_2 (2.8 mg, 11 μmol) was dissolved in d_8-THF or d_8-toluene (0.5 mL) within a clear glass J. Young valve NMR tube in the dark at room temperature and then immediately frozen (77 K). The solution was thawed to room temperature, exposed to light for 1 min and then loaded into an NMR spectrometer for initial analysis. The stability of the resulting boryl derivative was thereafter monitored by ^{1}H and ^{11}B NMR spectroscopy periodically for 30 min or 24 h with constant exposure to ambient interior light between acquisition of spectra.

4.3 General procedure: direct sunlight

A mixture of [Cu(NHC)(O*t*Bu)] (10 μmol) and B_2pin_2 (2.8 mg, 11 μmol) was dissolved in d_8-THF or d_8-toluene (0.5 mL) within a clear glass J. Young valve NMR tube in the dark at room temperature and then immediately frozen (77 K). The solution was thawed to room temperature, exposed to direct sun light for 1 h and then loaded into an NMR spectrometer for initial analysis. The stability of the resulting boryl derivative was thereafter monitored by ^{1}H and ^{11}B NMR spectroscopy periodically for > 24 h with constant exposure to direct sunlight between acquisition of spectra.

4.4 Data collected for [Cu(SIPr)(Bpin)] 2

Stability was assessed following the general procedures and using **2*** (5.3 mg, 10.1 μmol). The boryl derivative **2** was characterised *in situ* using data collected in the dark at t < 5 min. Samples were either kept in the dark or exposed to light for ~ 24 h.

^{1}H NMR (600 MHz, d_8-THF): δ 7.32 (t, $^3J_{HH}$ = 7.7, 2H. *p*-Ar), 7.23 (d, $^3J_{HH}$ = 7.7, 4H, *m*-Ar), 3.93 (s, 4H, CH_2), 3.19 (app. sept, $^3J_{HH}$ = 6.9, 4H, *i*Pr{CH}), 1.41 (d, $^3J_{HH}$ = 6.9, 12H, *i*Pr{CH_3}), 1.32 (d, $^3J_{HH}$ = 7.0, 12H, *i*Pr{CH_3}), 0.81 (s, 12H, pin).

^{1}H NMR (600 MHz, d_8-toluene): δ 7.07–7.12 (obscured t, 2H, *p*-Ar), 7.02 (d, $^3J_{HH}$ = 8.1, 4H, *m*-Ar), 3.28 (s, 4H, CH_2), 3.06 (app. sept, $^3J_{HH}$ = 6.8, 4H, *i*Pr{CH}), 1.53 (d, $^3J_{HH}$ = 6.9, 12H, *i*Pr{CH_3}), 1.21 (d, J = 7.0 Hz, 12H, *i*Pr{CH_3}), 0.98 (s, 12H, pin).

^{11}B{^{1}H} NMR (193 MHz, d_8-THF): δ 42.0 (vbr, fwhm ~ 620 Hz).

^{11}B{^{1}H} NMR (193 MHz, d_8-toluene): δ 42.4 (vbr, fwhm ~ 750 Hz).

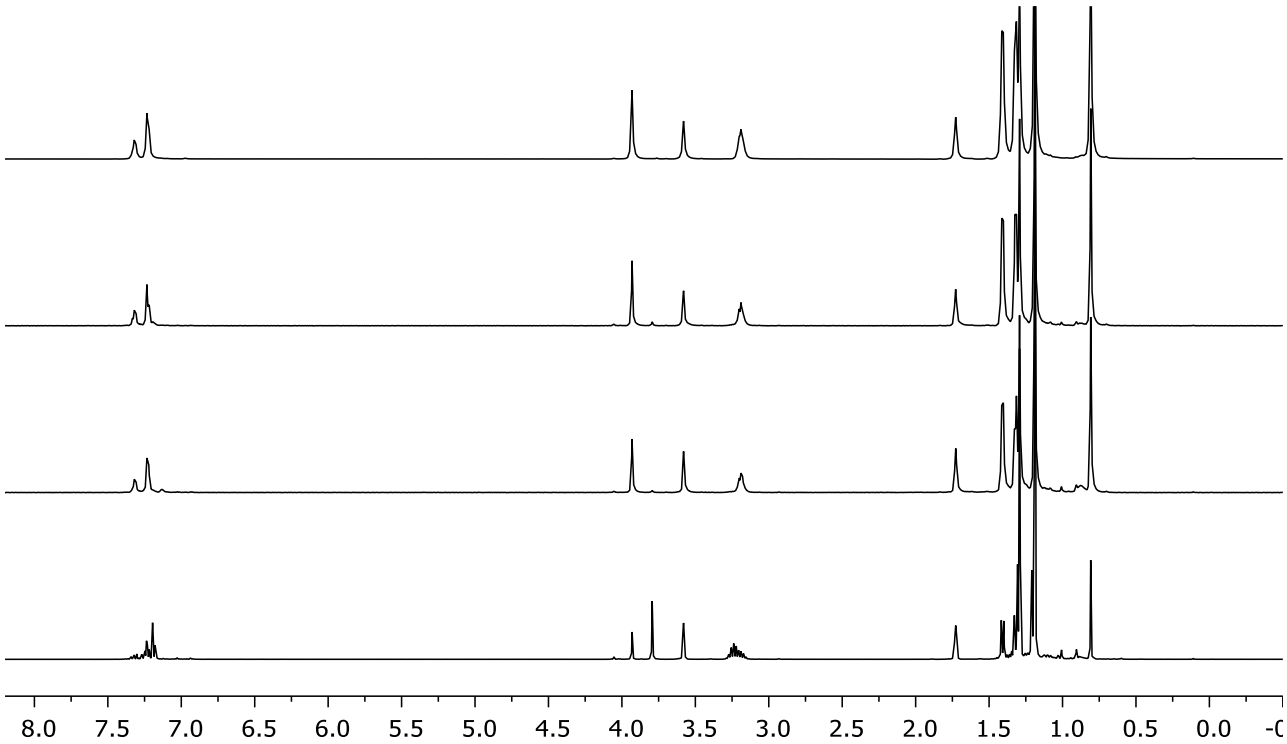

Figure S144. ^{1}H NMR spectra of **2***+B_2pin_2 recorded after < 5 min in the dark (top), 24 h in the dark (middle top), 24 h exposed to ambient light (middle bottom), and > 24 h exposed to direct sunlight (bottom) (600 MHz, d_8-THF).

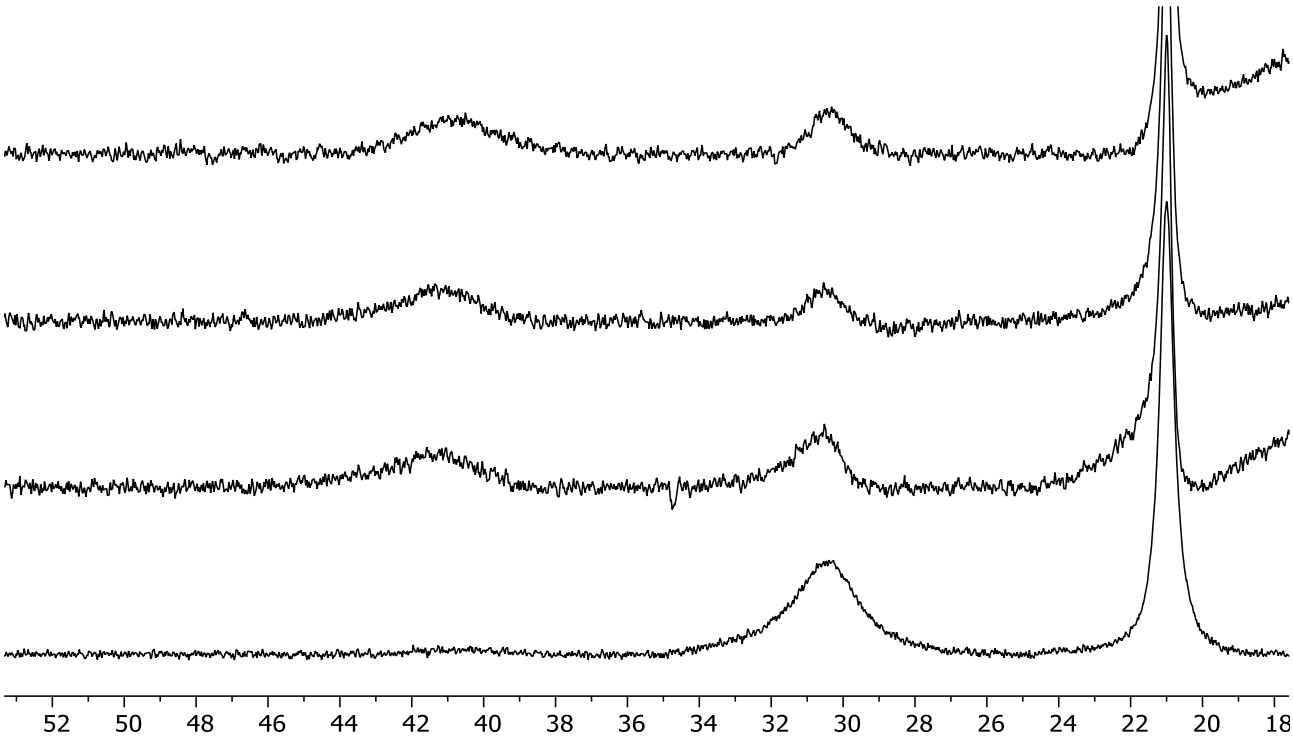

Figure S145. ^{11}B{^{1}H} NMR spectra of **2***+B_2pin_2 recorded after < 5 min in the dark (top), 24 h in the dark (middle top), 24 h exposed to ambient light (middle bottom), and > 24 h exposed to direct sunlight (bottom) (193 MHz, d_8-THF).

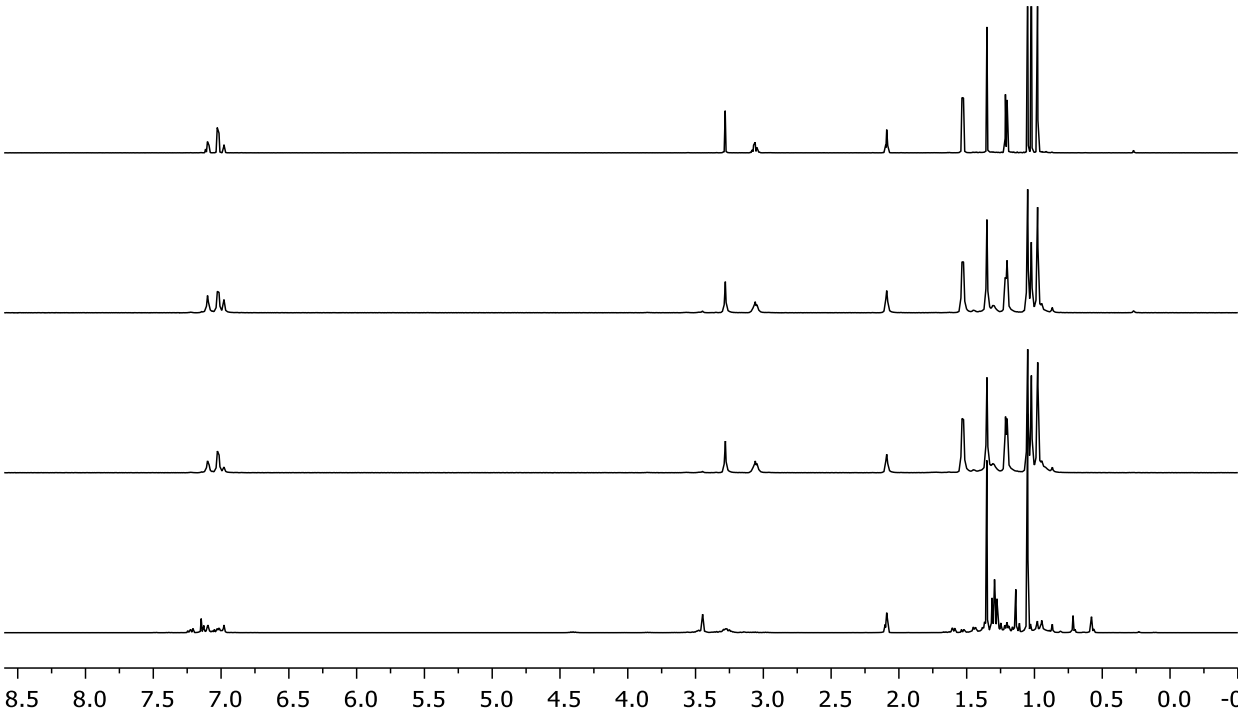

Figure S146. ^{1}H NMR spectra of **2***+B_2pin_2 recorded after < 5 min in the dark (top), 24 h in the dark (middle top), 24 h exposed to ambient light (middle bottom), and > 24 h exposed to direct sunlight (bottom) (600 MHz, d_8-toluene).

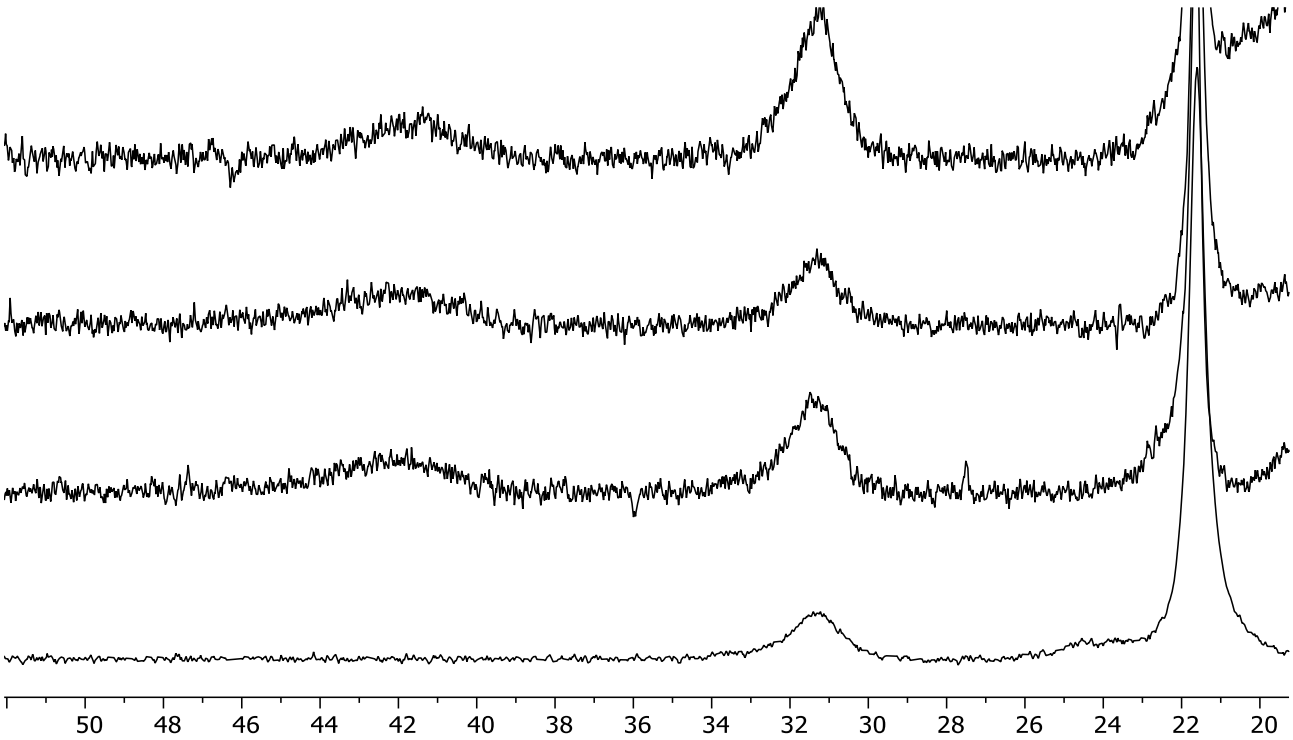

Figure S147. ^{11}B{^{1}H} NMR spectra of **2***+B_2pin_2 recorded after < 5 min in the dark (top), 24 h in the dark (middle top), 24 h exposed to ambient light (middle bottom), and > 24 h exposed to direct sunlight (bottom) (193 MHz, d_8-toluene).

4.5 Data collected for [Cu(IPr)(Bpin)] 3

Stability was assessed following the general procedures and using **3*** (5.3 mg, 10.1 μmol). The boryl derivative **3** was characterised *in situ* using data collected in the dark at t < 5 min. Samples were either kept in the dark or exposed to light for ~ 24 h.

^{1}H NMR (600 MHz, d_8-THF): δ 7.43 (t, $^3J_{HH}$ = 7.8, 2H, *p*-Ar), 7.27–7.33 (m, 6H, *m*-Ar+CH), 2.70 (app. sept, $^3J_{HH}$ = 7.1, 4H, *i*Pr{CH}), 1.34 (d, $^3J_{HH}$ = 6.9, 12H, *i*Pr{CH_3}), 1.20 (d, $^3J_{HH}$ = 7.0, 12H, *i*Pr{CH_3}), 0.84 (s, 12H, pin).

^{1}H NMR (600 MHz, d_8-toluene): δ 7.14 (t, $^3J_{HH}$ = 7.7, 2H, *p*-Ar), 7.04 (d, $^3J_{HH}$ = 7.8, 4H, *m*-Ar), 6.31 (s, 2H, CH), 2.65 (app. sept, $^3J_{HH}$ = 7.0, 4H, *i*Pr{CH}), 1.44 (d, $^3J_{HH}$ = 6.9, 12H, *i*Pr{CH_3}), 1.09 (d, $^3J_{HH}$ = 6.9 Hz, 12H, *i*Pr{CH_3}), 1.01 (s, 12H, pin).

^{11}B{^{1}H} NMR (193 MHz, d_8-THF): δ 41.7 (vbr, fwhm ~ 600 Hz).

^{11}B{^{1}H} NMR (193 MHz, d_8-toluene) δ 42.3 (vbr, fwhm ~ 600 Hz).

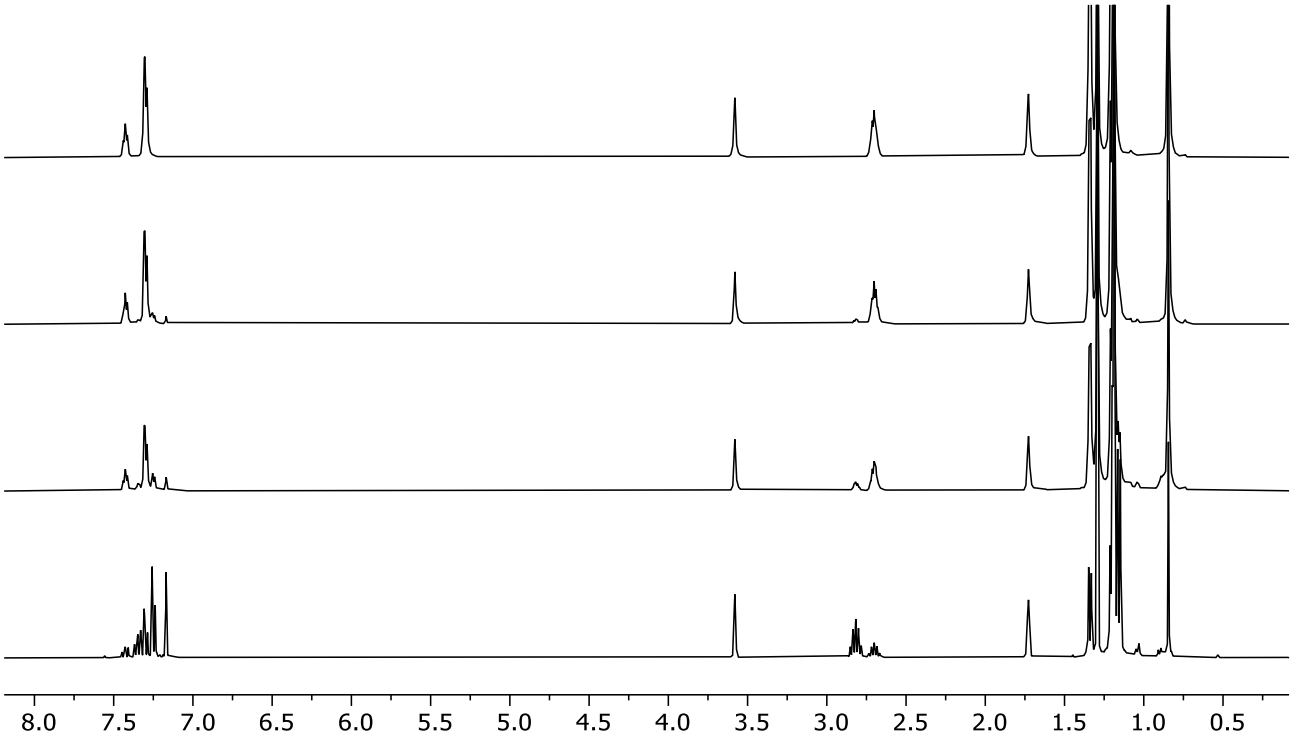

Figure S148. ^{1}H NMR spectra of **3***+B_2pin_2 recorded after < 5 min in the dark (top), 24 h in the dark (middle top), 24 h exposed to ambient light (middle bottom), and > 24 h exposed to direct sunlight (bottom) (600 MHz, d_8-THF).

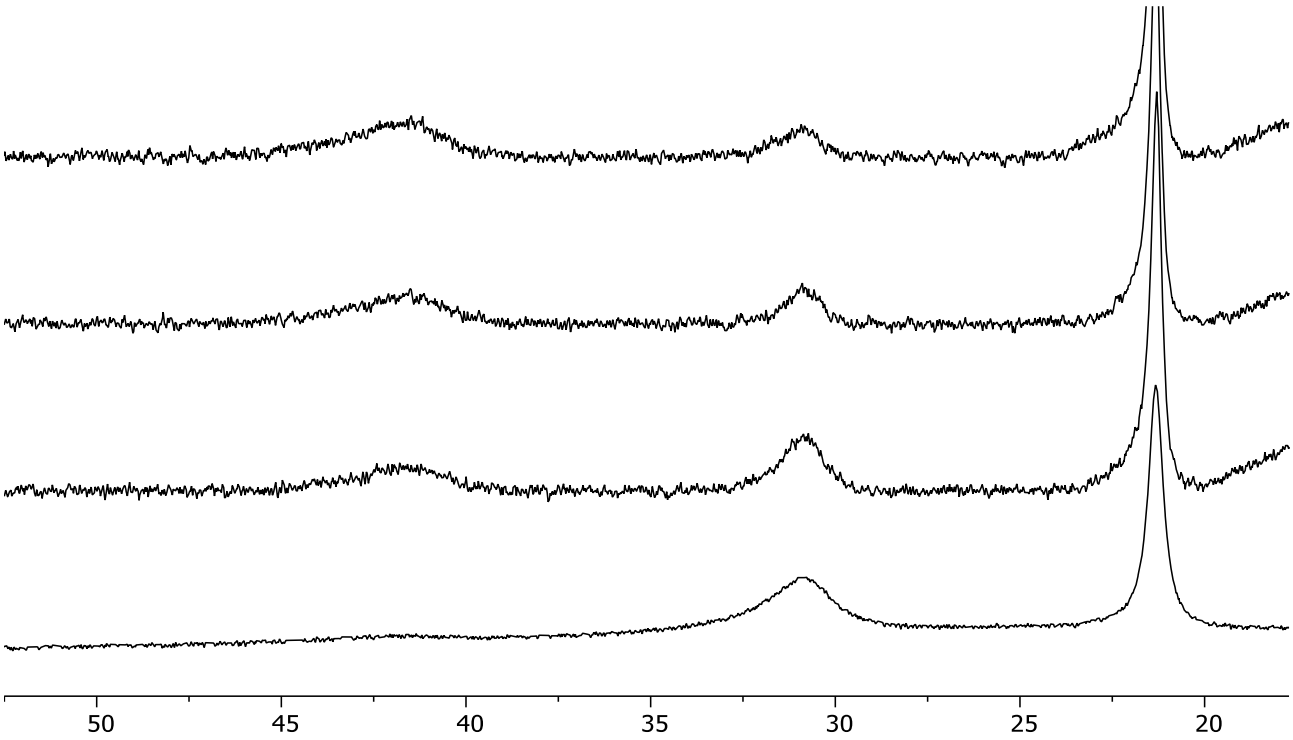

Figure S149. $^{11}B\{^{1}H\}$ NMR spectra of **3***+B_2pin_2 recorded after < 5 min in the dark (top), 24 h in the dark (middle top), 24 h exposed to ambient light (middle bottom), and > 24 h exposed to direct sunlight (bottom) (193 MHz, d_8-THF).

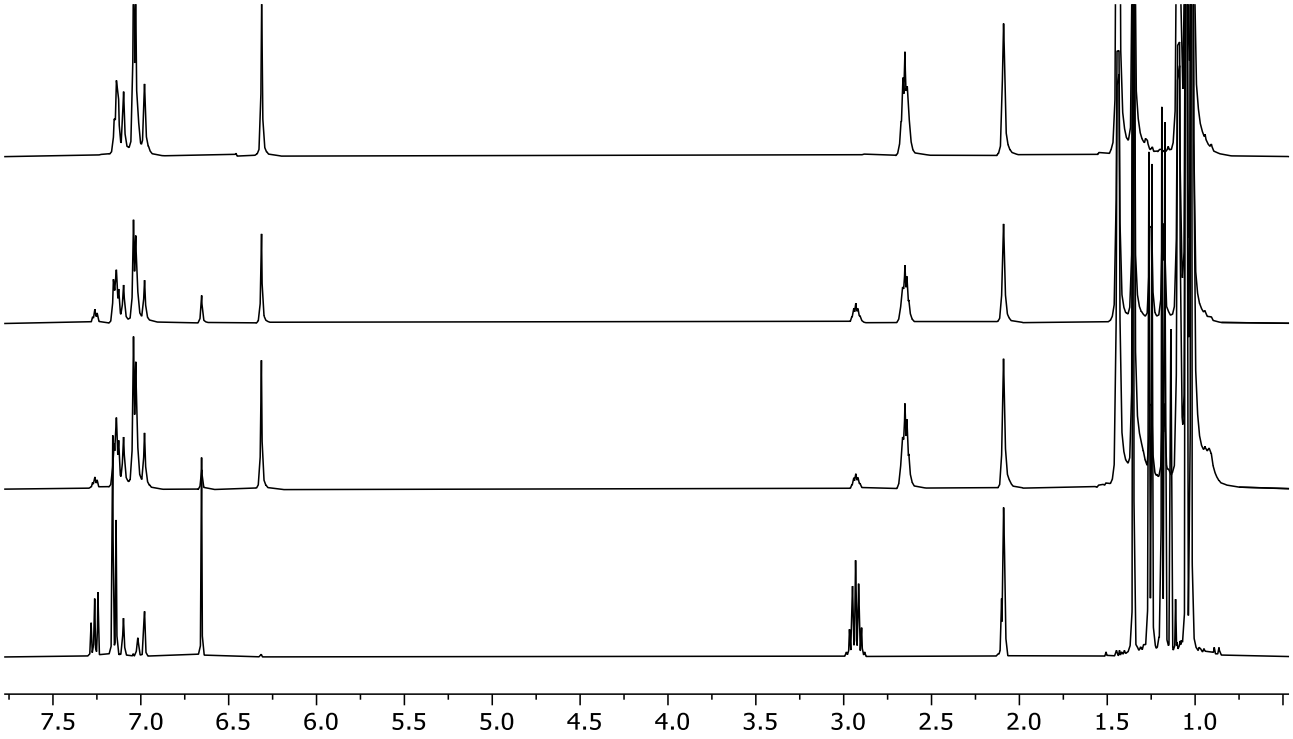

Figure S150. ^{1}H NMR spectra of **3***+B_2pin_2 recorded after < 5 min in the dark (top), 24 h in the dark (middle top), 24 h exposed to ambient light (middle bottom), and > 24 h exposed to direct sunlight (bottom) (600 MHz, d_8-toluene).

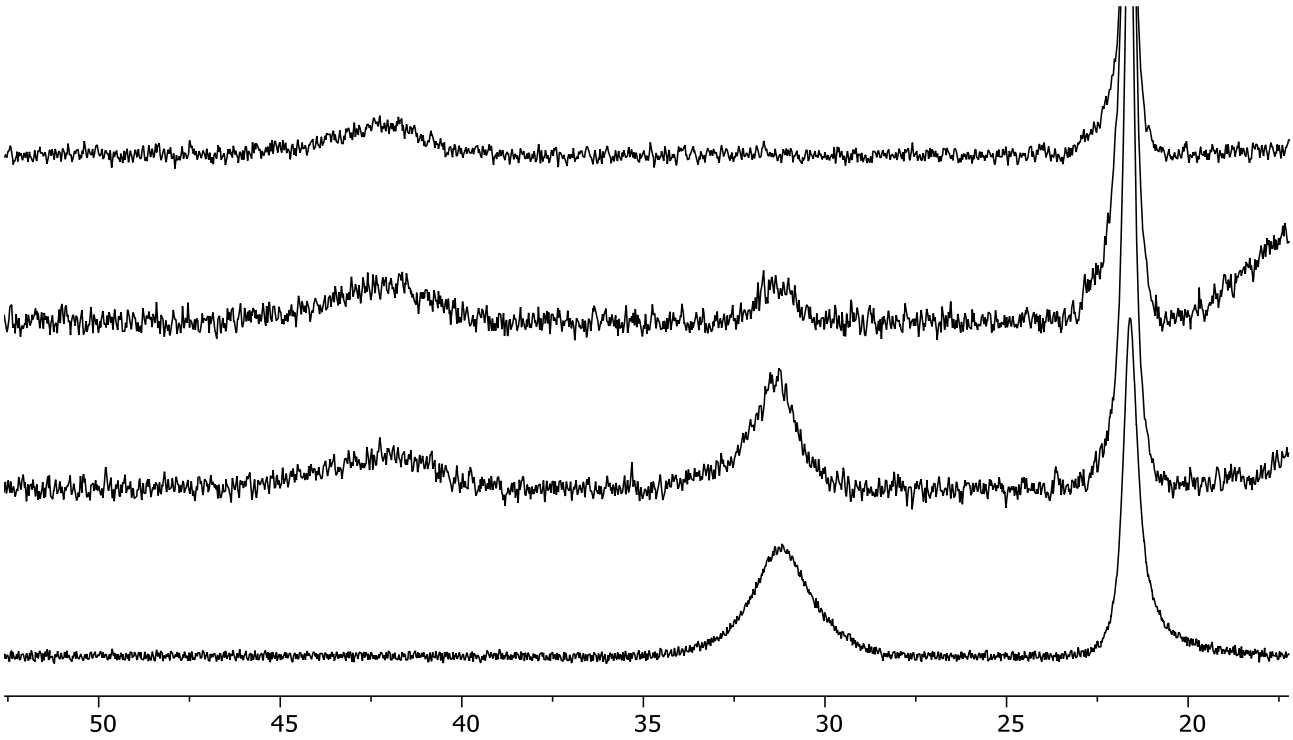

Figure S151. $^{11}B\{^1H\}$ NMR spectra of **3***+B_2pin_2 recorded after < 5 min in the dark (top), 24 h in the dark (middle top), 24 h exposed to ambient light (middle bottom), and > 24 h exposed to direct sunlight (bottom) (193 MHz, d_8-toluene).

4.6 Data collected for [Cu(SIMes)(Bpin)] 4

Stability was assessed following the general procedures and using **4*** (4.4 mg, 10.1 μmol). The boryl derivative **4** was characterised *in situ* using data collected in the dark at t < 5 min. Samples were either kept in the dark or exposed to ambient light for ~ 30 min.

^{1}H NMR (600 MHz, d_8-THF): δ 6.92 (s, 4H, Ar), 3.85 (s, 4H, CH_2), 2.34 (s, 12H, CH_3), 2.27 (s, 6H, CH_3), 0.86 (s, 12H, pin).

^{1}H NMR (600 MHz, d_8-toluene): δ 6.64 (s, 4H, Ar) 3.04 (s, 4H, CH_2), 1.00 (s, 12H, pin). The CH_3 resonances were not unambiguously located.

$^{11}B\{^1H\}$ NMR (193 MHz, d_8-THF): δ 41.4 (vbr).

$^{11}B\{^1H\}$ NMR (193 MHz, d_8-toluene): δ 42.2 (vbr).

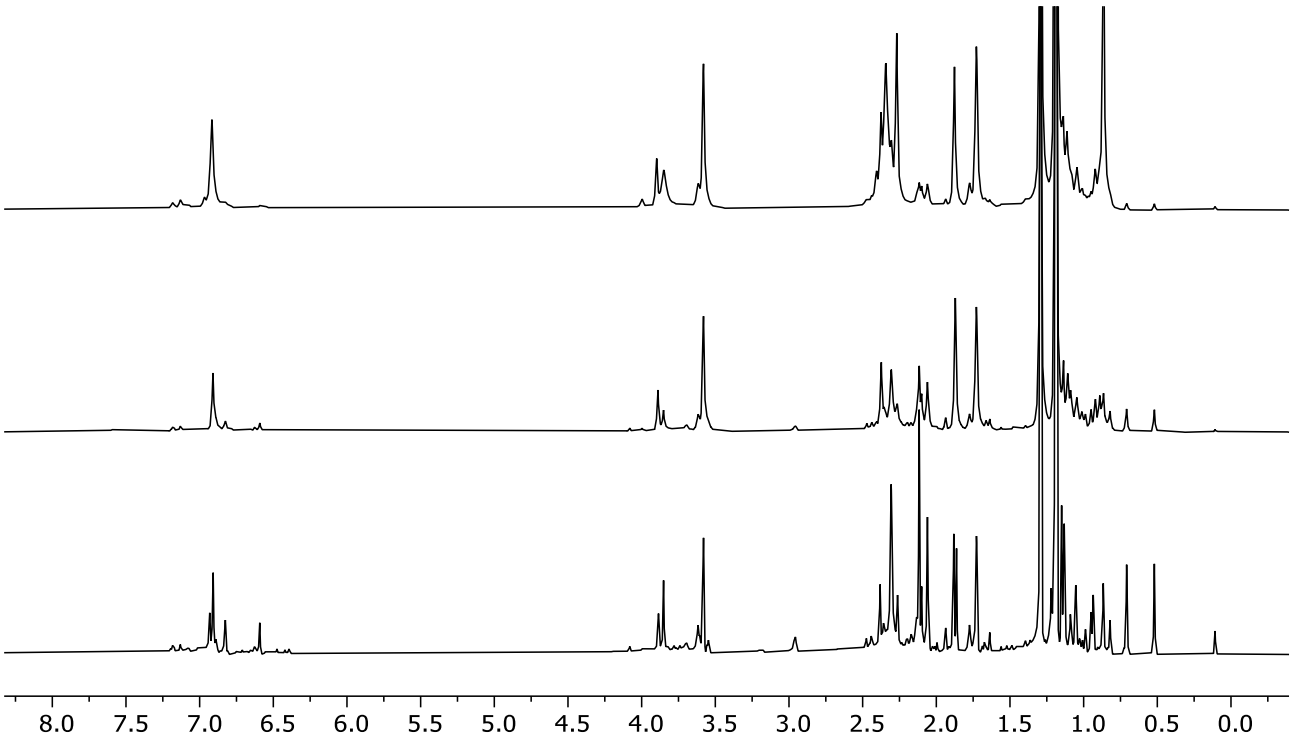

Figure S152. ^{1}H NMR spectra of **4***+B_2pin_2 recorded after < 5 min in the dark (top), 30 min in the dark (middle), and 10 min exposed to ambient light (bottom) (600 MHz, d_8-THF).

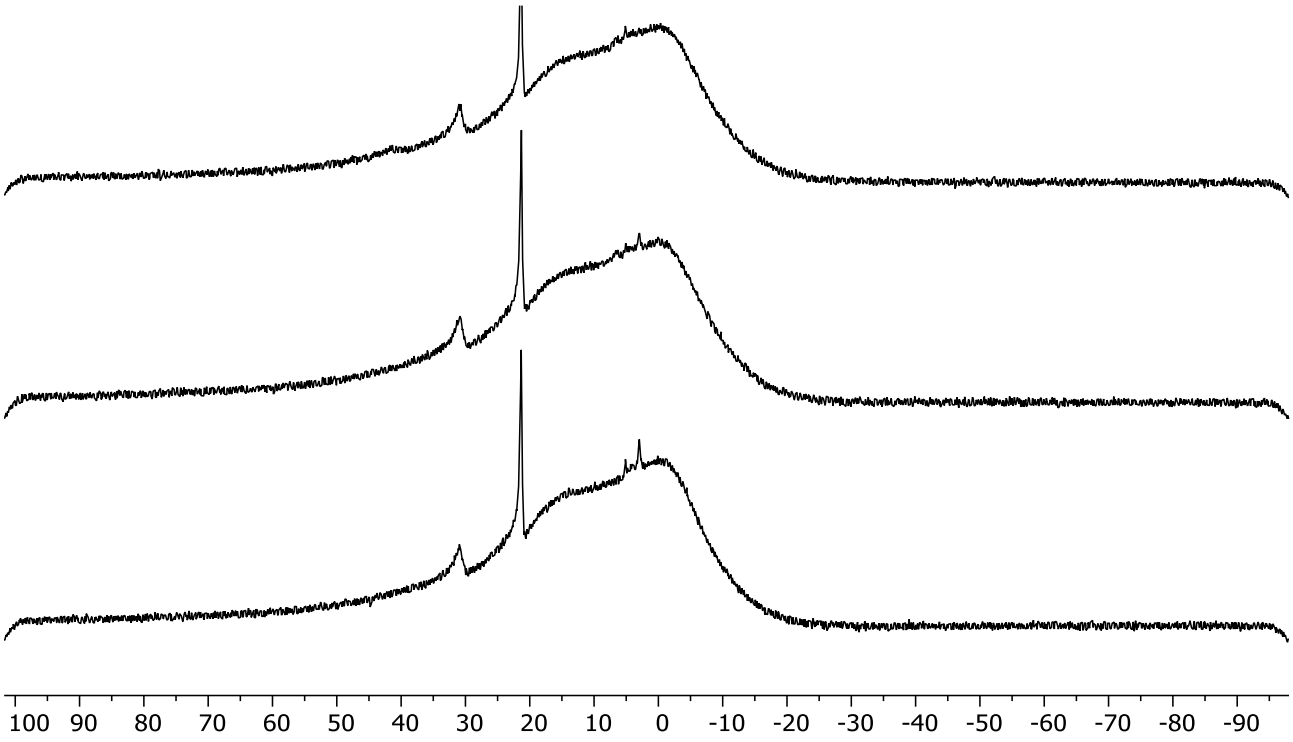

Figure S153. ^{11}B{^{1}H} NMR spectra of **4***+B_2pin_2 recorded after < 5 min in the dark (top), 30 min in the dark (middle), and 10 min exposed to ambient light (bottom) (193 MHz, d_8-THF). Uncorrected spectra presented as the boryl resonance is lost upon baseline correction.

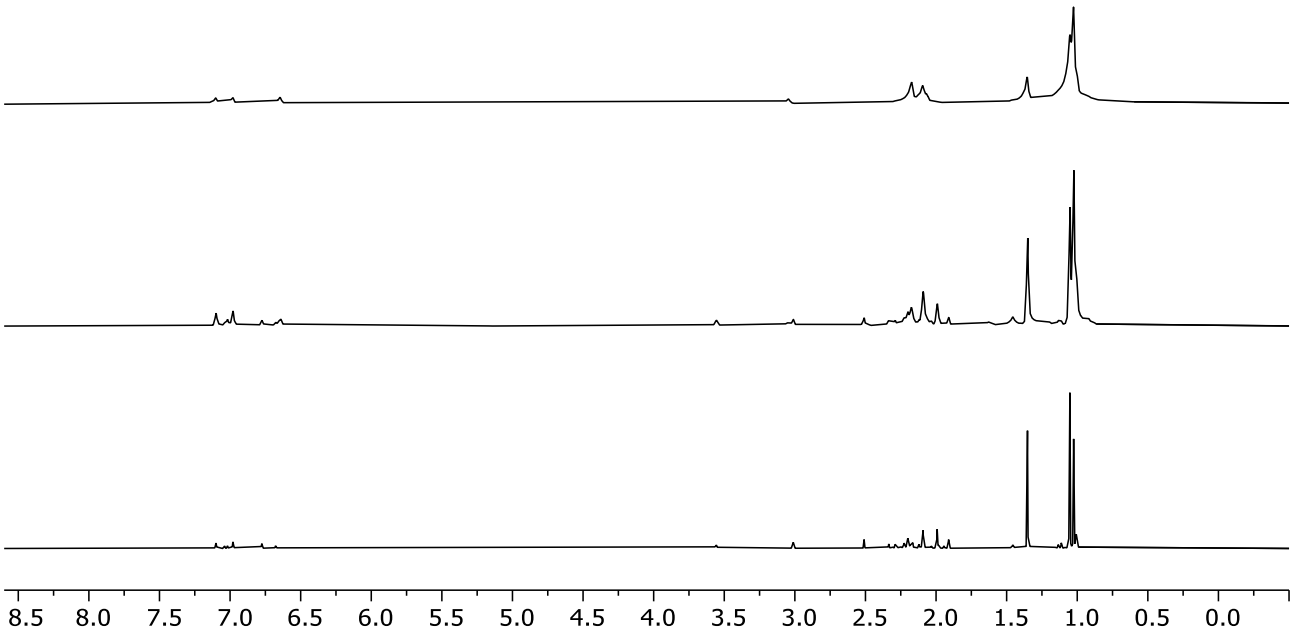

Figure S154. ^{1}H NMR spectra of **4***+B_2pin_2 recorded after < 5 min in the dark (top), 30 min in the dark (middle), and 5 min exposed to ambient light (bottom) (600 MHz, d_8-toluene).

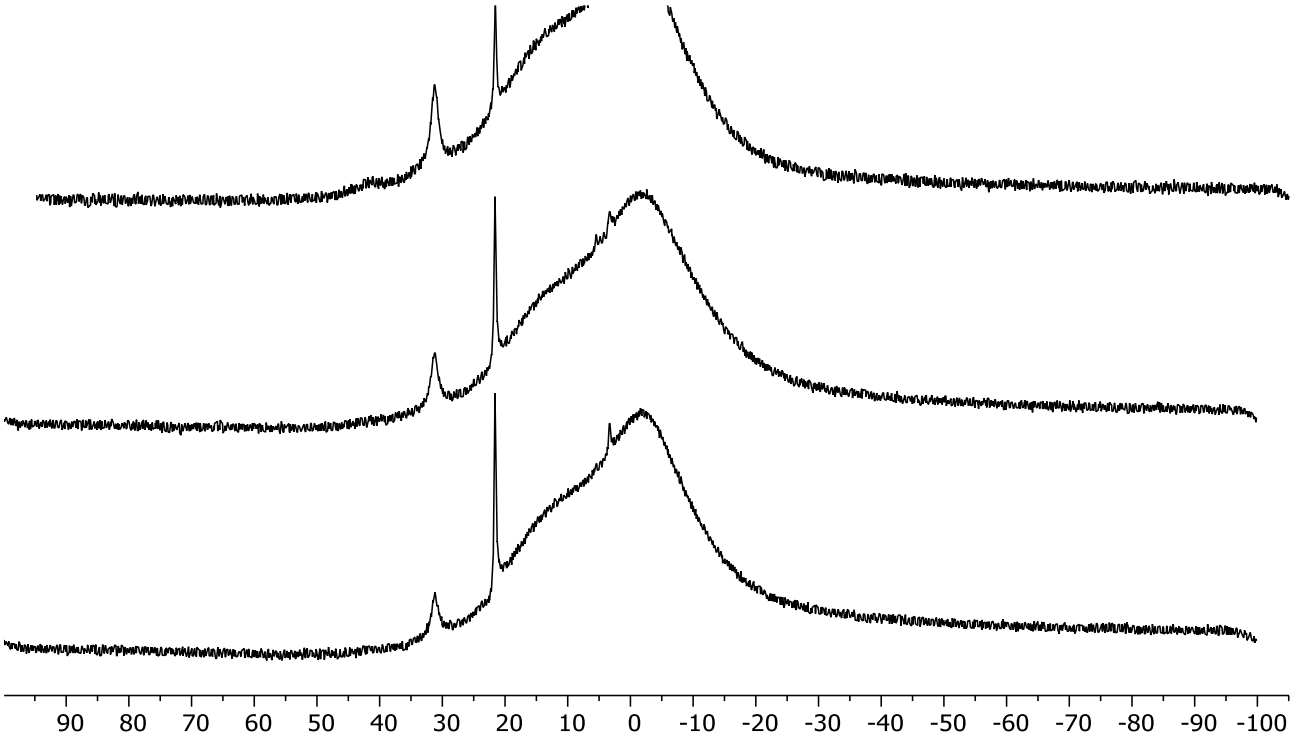

Figure S155. ^{11}B{^{1}H} NMR spectra of **4***+B_2pin_2 recorded after < 5 min in the dark (top), 30 min in the dark (middle), and 5 min exposed to ambient light (bottom) (193 MHz, d_8-toluene). Uncorrected spectra presented as the boryl resonance is lost upon baseline correction.

4.7 Data collected for [Cu(IMes)(Bpin)] 5

Stability was assessed following the general procedures and using **5*** (4.4 mg, 10.1 μmol). The boryl derivative **5** was characterised *in situ* using data collected in the dark at t < 5 min. Samples were either kept in the dark or exposed to ambient light for ~ 30 min. The ^{1}H NMR resonances of **5** could not be unambiguously assigned.

^{11}B{^{1}H} NMR (193 MHz, d_8-THF): δ ~ 42 (vbr).

^{11}B{^{1}H} NMR (193 MHz, d_8-toluene): δ ~ 42 (vbr).

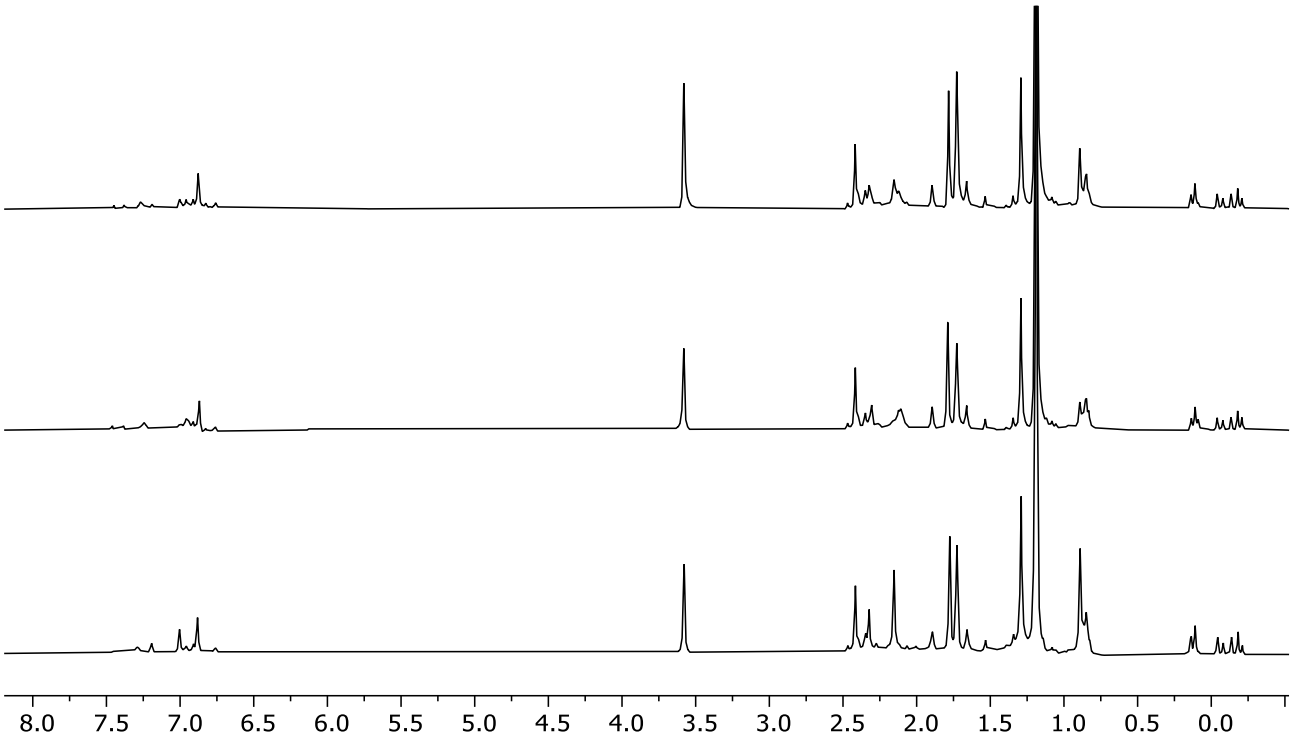

Figure S156. ^{1}H NMR spectra of **5***+B_2pin_2 recorded after < 5 min in the dark (top), 10 min in the dark (middle), and 1 min exposed to ambient light (bottom) (600 MHz, d_8-THF).

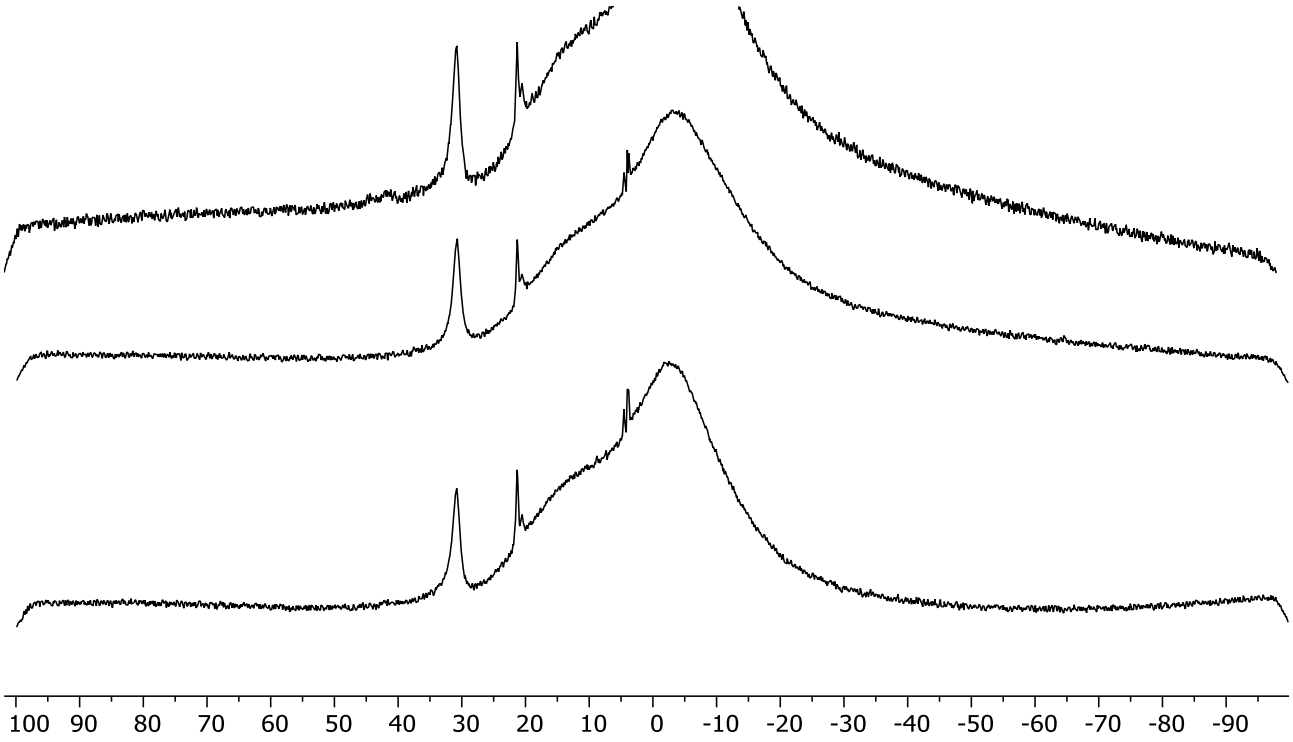

Figure S157. $^{11}B\{^{1}H\}$ NMR spectra of **5***+B_2pin_2 recorded after < 5 min in the dark (top), 10 min in the dark (middle), and 1 min exposed to ambient light (bottom) (193 MHz, d_8-THF). Uncorrected spectra presented as the boryl resonance is lost upon baseline correction.

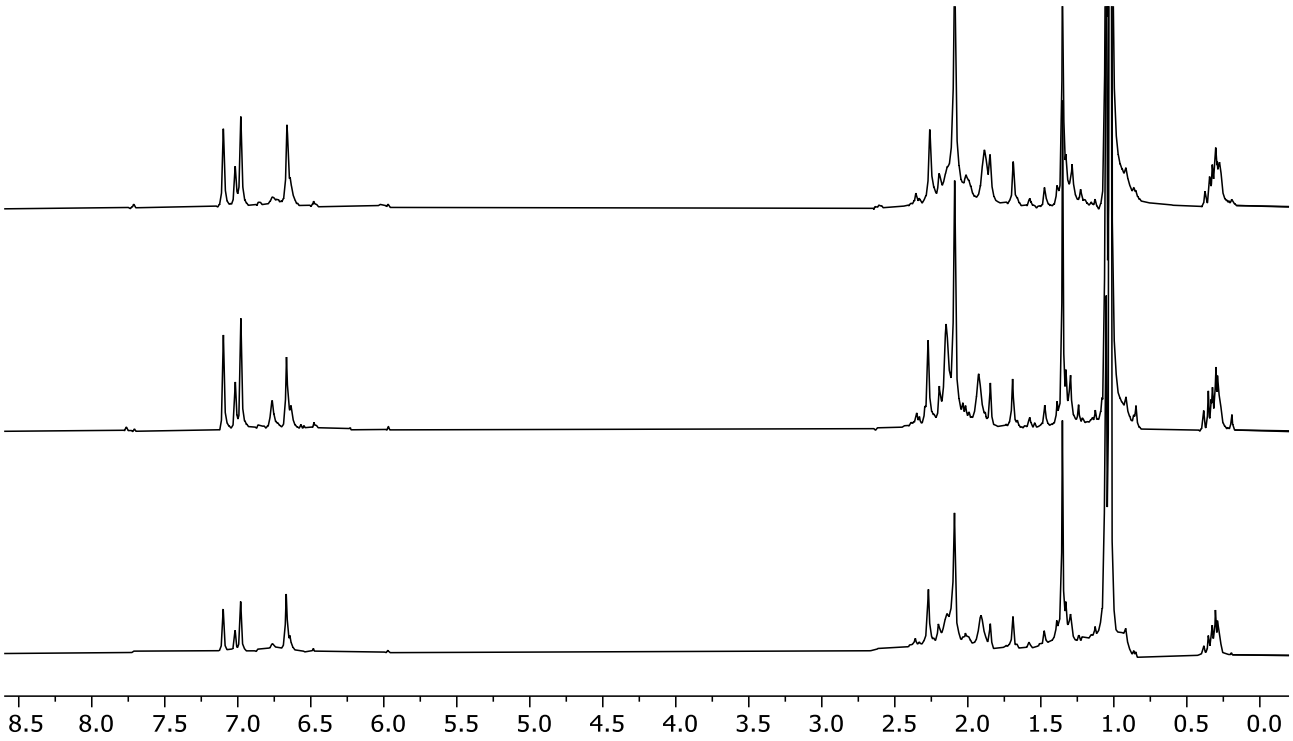

Figure S158. ^{1}H NMR spectra of **5***+B_2pin_2 recorded after < 5 min in the dark (top), 10 min in the dark (middle), and 1 min exposed to ambient light (bottom) (600 MHz, d_8-toluene).

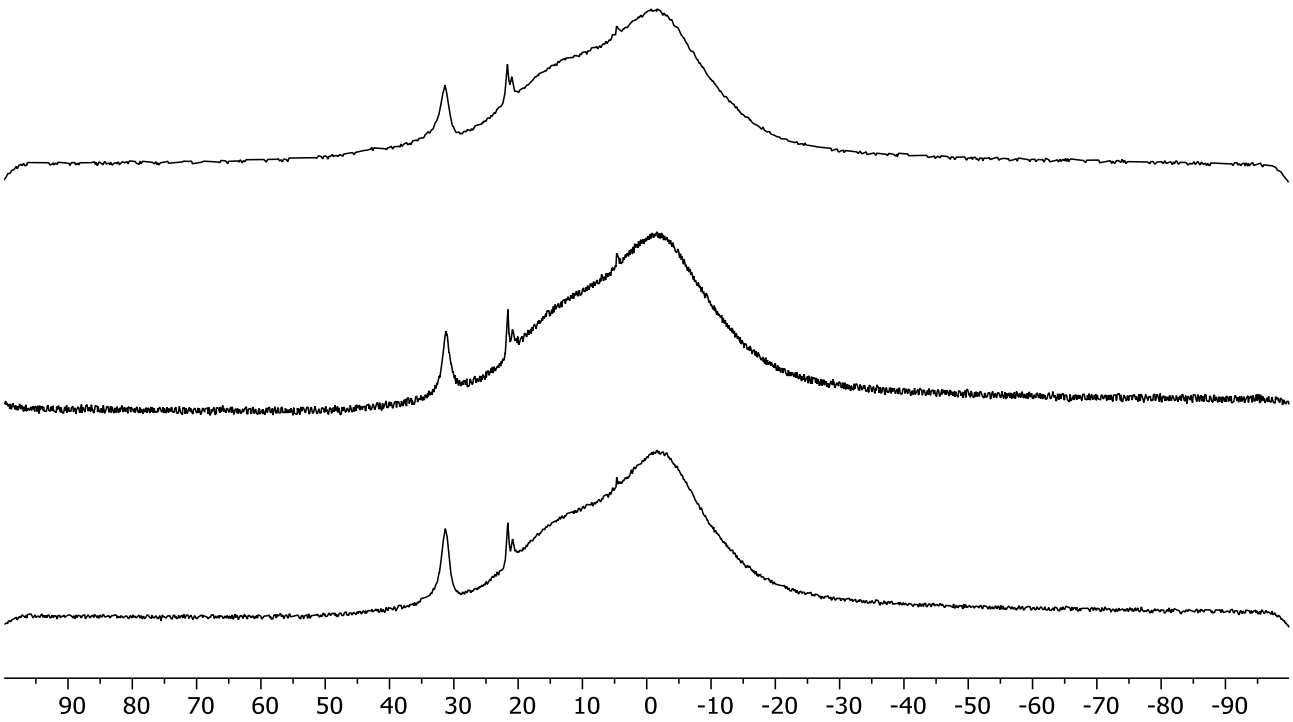

Figure S159. $^{11}B\{^{1}H\}$ NMR spectra of **5***+B_2pin_2 recorded after < 5 min in the dark (top), 10 min in the dark (middle), and 1 min exposed to ambient light (bottom) (193 MHz, d_8-toluene). Uncorrected spectra presented as the boryl resonance is lost upon baseline correction.

5 Catalyst productivity

5.1 General procedure: dark

In an argon-filled glovebox, amberised vials were charged with precatalyst (0.1 mg, 0.23 μmol) and a solution of B_2pin_2 (127 mg, 0.5 mmol) in THF (5 mL) in the dark. The vials were sealed in a stainless-steel reactor within a 4-well aluminium insert, pressurised with N_2O (1 bar gauge), and stirred for 20 h at room temperature in the dark. A sample of the headspace was taken for analysis by GC-TCD and then the reactor was depressurised, opened to air and exposed to light. Aliquots were quickly taken from each vial (0.5 mL), loaded into a J. Young valve NMR tube, and immediately frozen (77 K) before being analysed by ^{11}B NMR spectroscopy at room temperature.

5.2 General procedure: light

In an argon-filled glovebox, a Büchiglass tinyclave glass pressure reactor (Figure S160) was charged with precatalyst (0.1 mg, 0.23 μmol) and a solution of B_2pin_2 (127 mg, 0.5 mmol) in THF (5 mL) in ambient light. The reactor was pressurised with N_2O (1 bar gauge) and stirred for 20 h at room temperature in ambient light. The reactor was depressurised and opened to air. An aliquot (0.5 mL) was taken immediately, loaded into a J. Young valve NMR tube, and frozen (77 K) before being analysed by ^{11}B NMR spectroscopy at room temperature.

Figure S160. Büchiglass tinyclave glass pressure reactor.

Table S2. Evaluation of **4*** and **5*** (0.05 mol%) as catalysts for the B_2pin_2 reduction of N_2O.

Entry	**Conditions**					**Conversion %**	
	mol%	Solvent	Light/Dark	p_{N2O} / bar	time / h	**4***	**5***
1	0.05	THF	Dark	1	20	97	98
2	0.05	THF	Dark	1	20	98	95
3	0.05	THF	Light	1	20	5	4

5.3 Data collected for entries 1 and 2

5.3.1 [Cu(SIMes)(O*t*Bu)] **4***

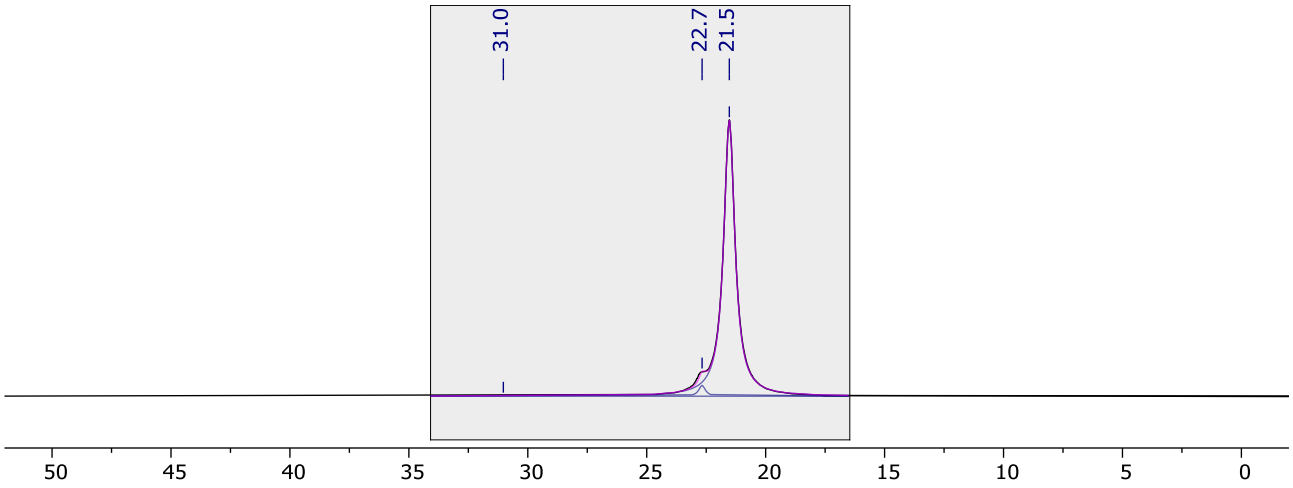

Figure S161. $^{11}B\{^1H\}$ NMR spectrum collected following the B_2pin_2 reduction of N_2O (1 bar gauge) using 0.05 mol% **4*** in THF after 20 h in the dark (128 MHz, THF/C_6D_6).

5.3.2 [Cu(IMes)(O*t*Bu)] **5***

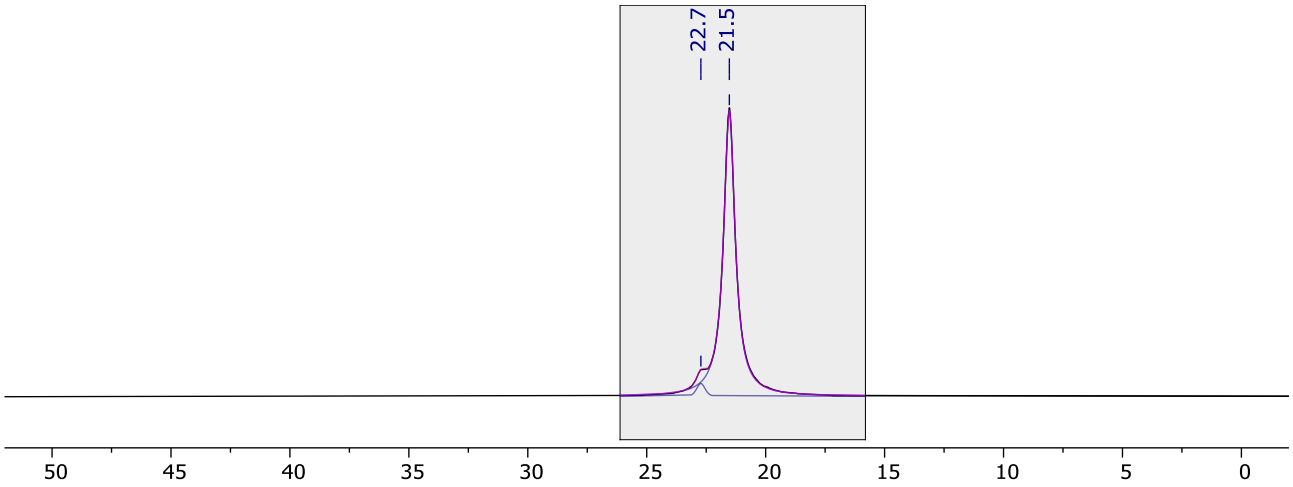

Figure S162. $^{11}B\{^{1}H\}$ NMR spectrum collected following the B_2pin_2 reduction of N_2O (1 bar gauge) using 0.05 mol% **5*** in THF after 20 h in the dark (128 MHz, THF/C_6D_6).

5.3.3 [Cu(SIMes)(O*t*Bu)] **4***

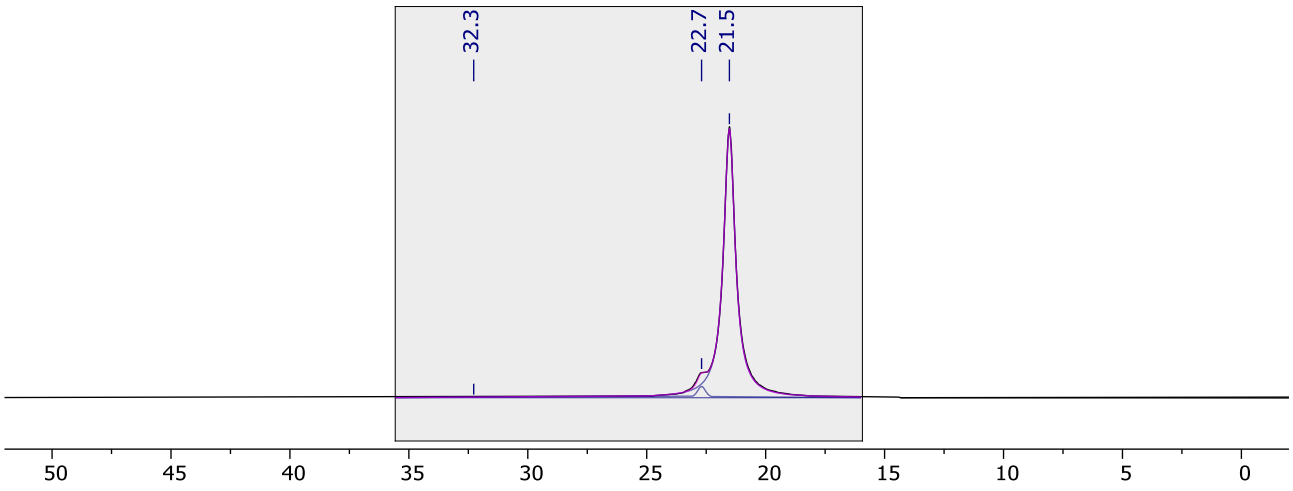

Figure S163. $^{11}B\{^{1}H\}$ NMR spectrum collected following the B_2pin_2 reduction of N_2O (1 bar gauge) using 0.05 mol% **4*** in THF after 20 h in the dark (128 MHz, THF/C_6D_6).

5.3.4 [Cu(IMes)(O*t*Bu)] **5***

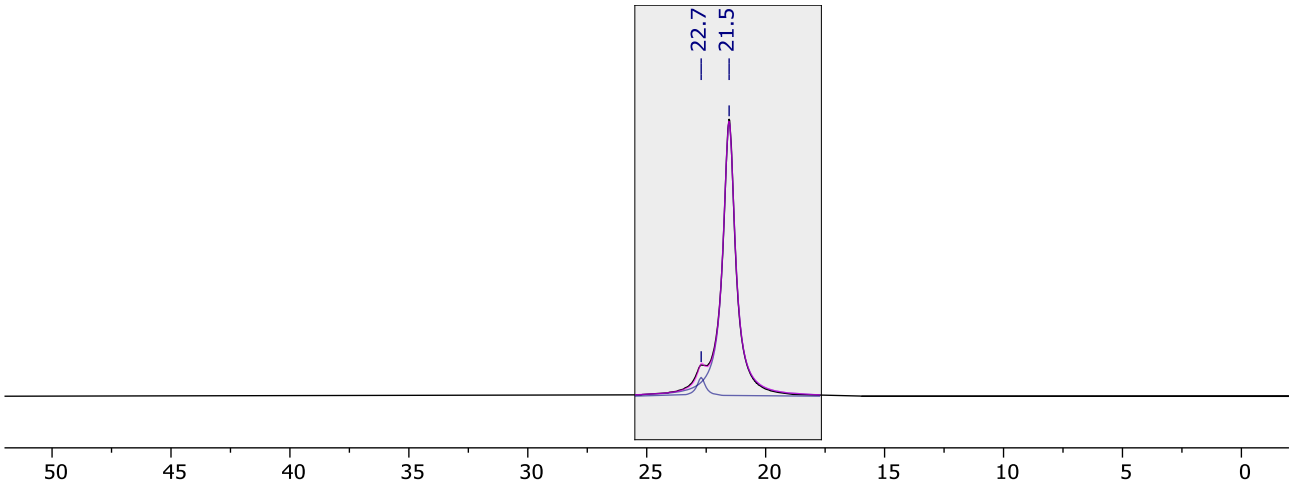

Figure S164. $^{11}B\{^{1}H\}$ NMR spectrum collected following the B_2pin_2 reduction of N_2O (1 bar gauge) using 0.05 mol% **5*** in THF after 20 h in the dark (128 MHz, THF/C_6D_6).

5.3.5 GC-TCD analysis of the reactor headspace

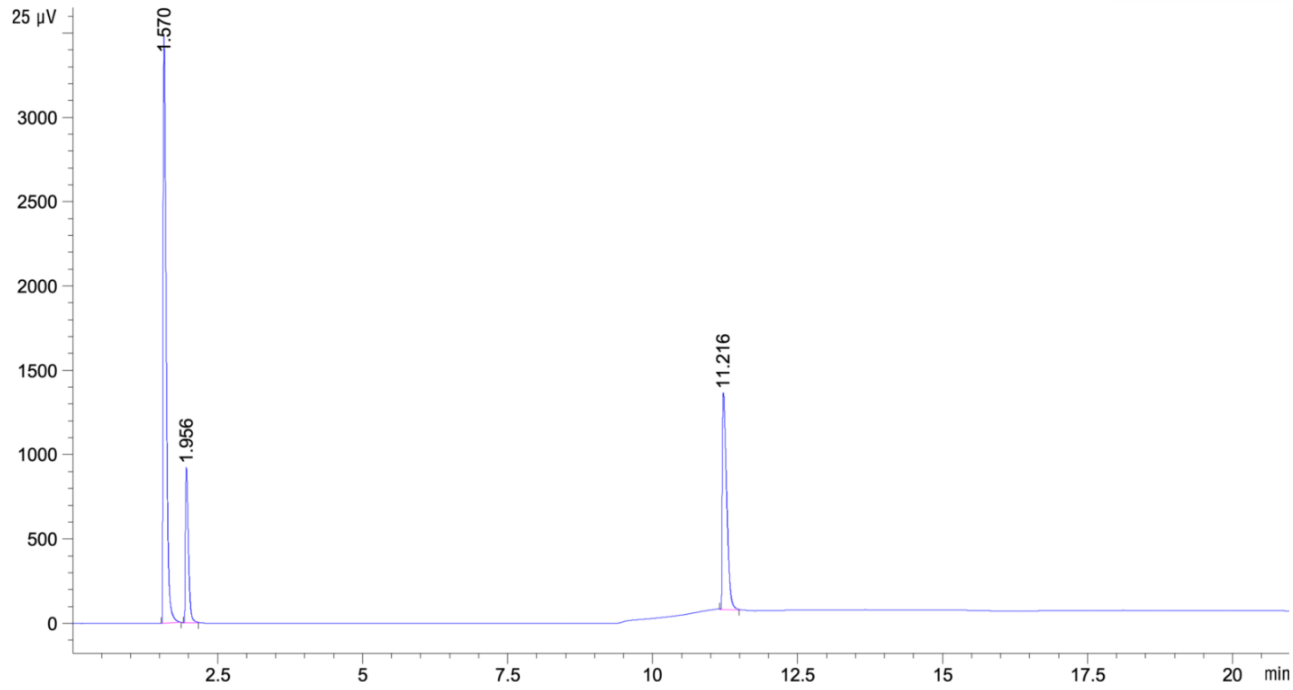

Figure S165. GC-TCD trace collected for following the B_2pin_2 reduction of N_2O (1 bar gauge) using 0.05 mol% **4***/**5*** in THF after 20 h in the dark, showing presence of Ar (1.6 min), N_2 (2.0 min) and N_2O (11.2 min). Ratio N_2:N_2O = 1:2.

5.4 Data collected for entry 3

5.4.1 [Cu(SIMes)(O*t*Bu)] **4***

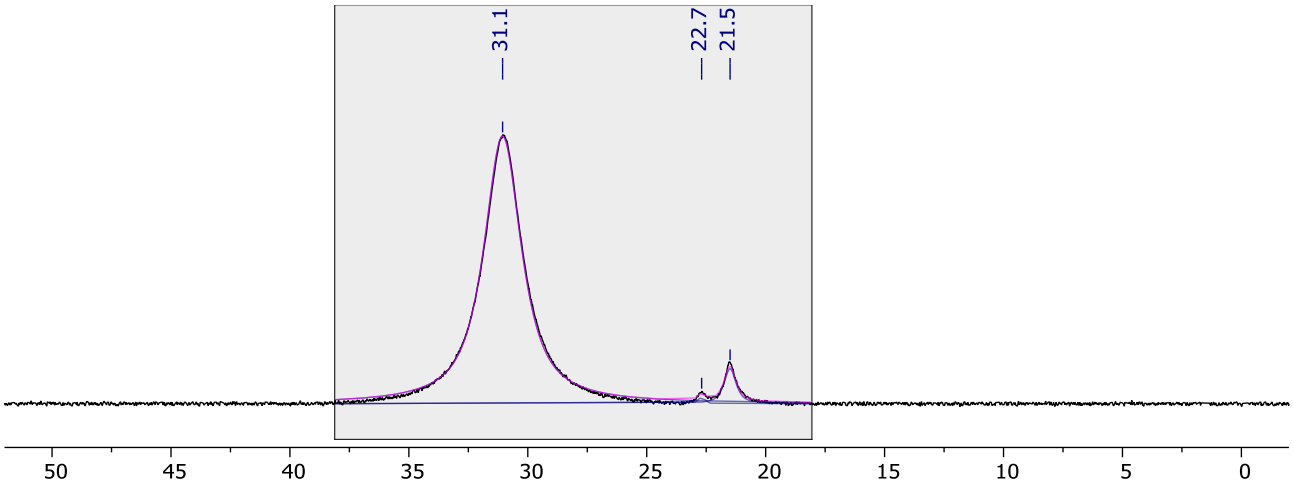

Figure S166. $^{11}B\{^{1}H\}$ NMR spectrum collected following the B_2pin_2 reduction of N_2O (1 bar gauge) using 0.05 mol% **4*** in THF after 20 h exposed to ambient light (128 MHz, THF/C_6D_6).

5.4.2 [Cu(IMes)(O*t*Bu)] **5***

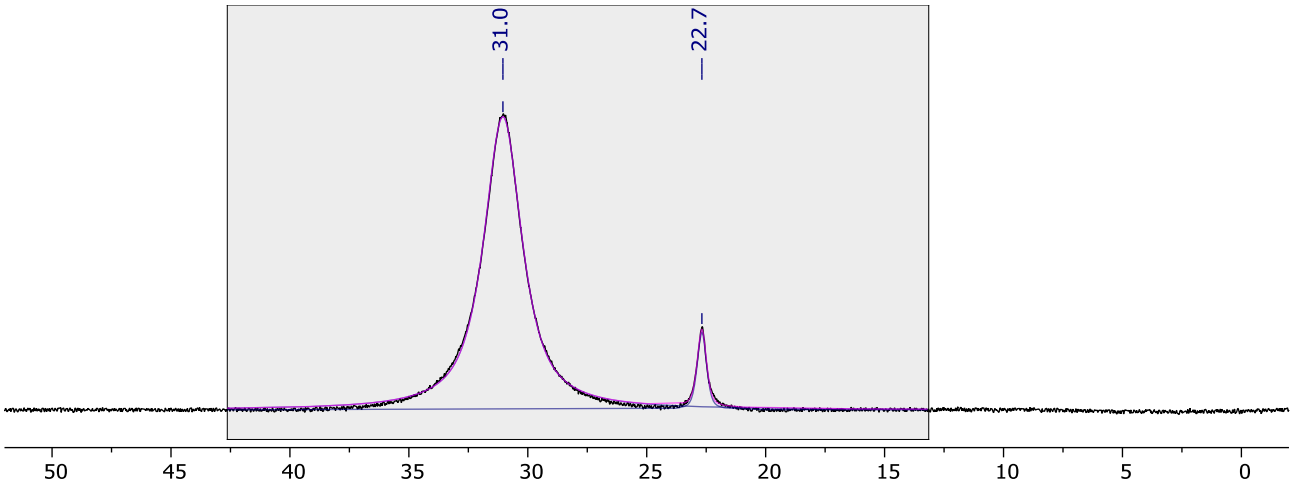

Figure S167. $^{11}B\{^{1}H\}$ NMR spectrum collected following the B_2pin_2 reduction of N_2O (1 bar gauge) using 0.05 mol% **5*** in THF after 20 h exposed to ambient light (128 MHz, THF/C_6D_6).

6 Computational details

All electronic structure calculations presented in this paper were carried out using the Gaussian 16 (revision C.01)[16] and ORCA 6.1.0[17] program suites at the DFT level of theory, with the former used to explore the potential energy surfaces of all reactions. Geometries of all species were fully optimised without imposing symmetry constraints, employing the BP86[18] functional. The def2-SVP basis sets developed by Weigend and Ahlrichs[19] were applied to all atoms. Optimised stationary points were characterised by analysis of their analytical second derivatives, with minima having only positive eigenvalues and transition states having exactly one imaginary eigenvalue. Optimised geometries of all structures are provided in .xyz format. Dispersion effects were accounted for by applying Grimme's van der Waals correction (D3 parameterization with Becke-Johnson damping) during geometry optimizations of all stationary points.[20] In order to identify the minima linked by each transition state for **2**, either intrinsic reaction co-ordinate (IRC) calculations were performed (TS_O, TS_{ON2}, TS_{N2O}, TS_{SBM}), or subsequent geometry optimisations were performed in both forward and reverse direction of the displacement vector of the transition state coordinate ($TS2_{ON2}$, $TS3_{ON2}$). Single point energies were computed on BP86-D3(BJ)/def2-SVP optimised geometries of all molecules using the B3LYP functional[21] while the triple-zeta quality def2-TZVP basis set[19] was applied to all atoms. Thermal and entropic corrections to the SCF energies in the gas phase at T = 298.15 K and p = 1 atm were obtained from the frequency calculations at the BP86-D3(BJ)/def2-SVP level of theory. Effects due to the presence of a solvent were treated implicitly with a polarisable dielectric model, using the IEFPCM formalism in conjunction with Truhlar's SMD model.[22]

The NBO program (version 6.0)[23] was used to perform Natural Bond Orbital analyses on the optimised structures and generate Wiberg Bond Indices.[24] The topology of the electron density was analysed using QTAIM (quantum theory of atoms in molecules),[25] as implemented in the AIMALL package.[26] Both NBO and QTAIM used wavefunctions obtained from the B3LYP-D3(BJ)/def2TZVP level of theory. EDA-NOCV analysis[27] was performed using the ORCA 6.1.0 software package at the B3LYP-D3(BJ)/def2TZVP theory level.

All structures were visualised using the ChemCraft tool.[28] Computational resources were provided by LuxProvide Euro High Peformance Cluster (Euro HPC) Meluxina architecture based in Luxemburg, a cluster system of 573 nodes, where each node has 2× 64-core 2.6 GHz AMD Rome processors, 512 GB of RAM, a 1.92 TB local SSD scratch allocation and each node is connected to the InfiniBand network. All calculations were run in parallel on a single node using 32 cores.

6.1 Reaction profiles for O-atom transfer to 2

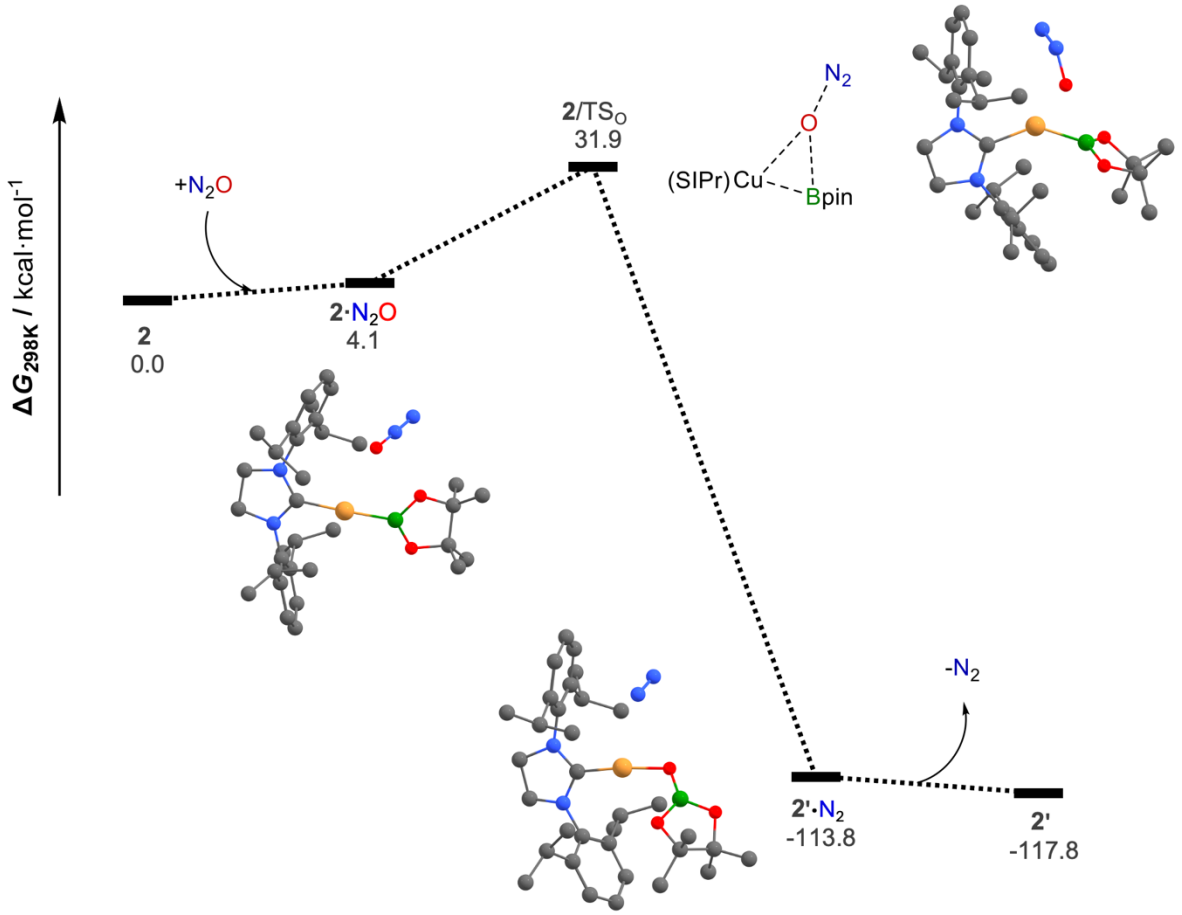

Figure S168. Concerted O-atom transfer reaction between **2** and N_2O. Energies corrected for benzene solvent and H-atoms omitted for clarity. Species **2**·N_2O (concerted pathway) and **2'**·N_2 (concerted pathway) are non-bonding encounter complexes.

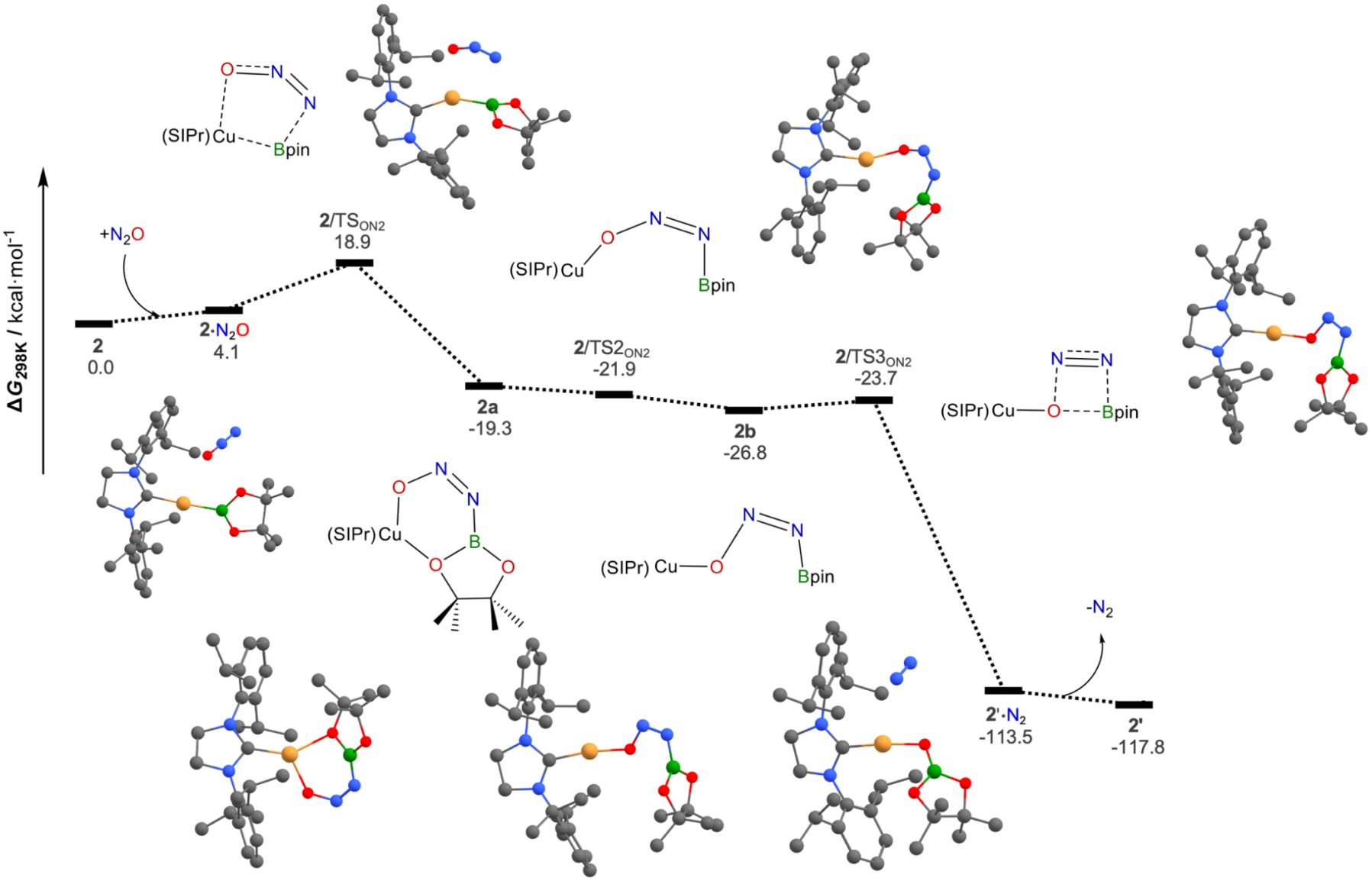

Figure S169. O-atom transfer reaction between **2** and N_2O proceeding *via* $CuON_2B$ addition. Energies corrected for benzene solvent and H-atoms omitted for clarity. Species **2**·N_2O and **2'**·N_2 (alternative addition) are non-bonding encounter complexes.

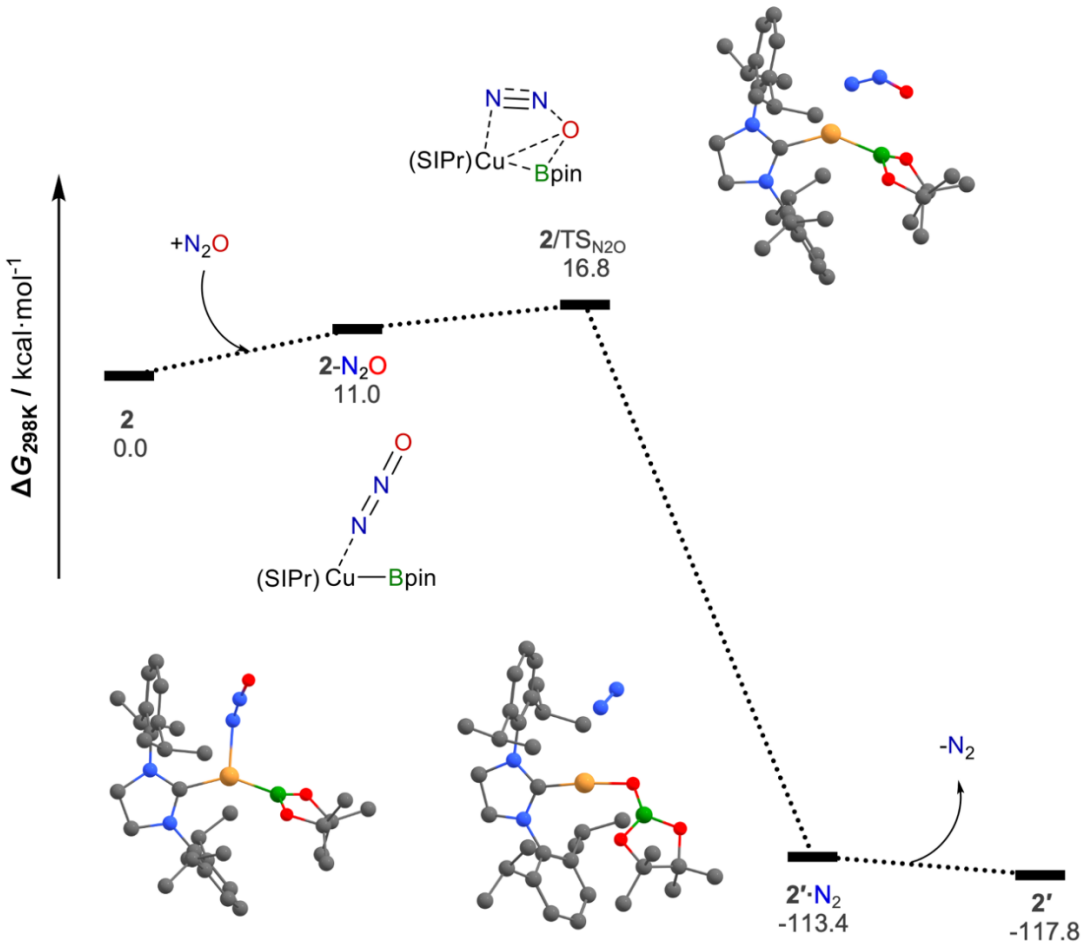

Figure S170. O-atom transfer reaction between **2** and N_2O proceeding *via* CuN_2OB addition mechanism. Energies corrected for benzene solvent and H-atoms omitted for clarity. Species **2**-N_2O is coordination complex; **2'**·N_2 is a non-bonding encounter complex.

6.2 Wiberg bond indices for O-atom transfer to 2

Table S3. Wiberg bond indices (and interatomic distances / Å) for interactions of interest for reactions between **2** and N_2O.

Species	N–N	NN–O	NNO	Cu–NNO	Cu–ONN	Cu–B	B–ONN	B–NNO
N_2	3.0314 (1.1124)	-	-	-	-	-	-	-
N_2O	2.3893 (1.1416)	1.5528 (1.1825)	0.6493 (2.3240)	-	-	-	-	-
2	-	-	-	-	-	0.7871 (1.9945)	-	-
2/TS_O	2.4489 (1.1578)	0.9723 (1.4191)	0.3156 (2.4188)	0.1061 (3.6193)	0.3191 (1.9469)	0.5240 (2.0233)	0.2032 (2.4270)	0.1211 (4.4959)
2/TS_{ON2}	2.2870 (1.1647)	1.4451 (1.2183)	0.5364 (2.3044)	0.0420 (3.2706)	0.1060 (2.4233)	0.6582 (2.0256)	0.0239 (3.2451)	0.1739 (2.4563)
2a	1.6690 (1.2718)	1.3160 (1.3108)	0.2383 (2.2223)	0.0168 (3.1803)	0.2910 (1.9983)	0.0304 (2.7287)	0.0369 (2.7839)	1.0755 (1.4270)
2/$TS2_{ON2}$	1.8751 (1.2492)	1.1065 (1.3840)	0.2083 (2.2239)	0.0191 (3.4662)	0.3822 (1.8465)	0.0115 (3.2967)	0.0462 (2.5231)	0.9178 (1.4680)
2b	1.8954 (1.2462)	1.0762 (1.4024)	0.2026 (2.1785)	0.0276 (3.8738)	0.3812 (1.8247)	0.0046 (3.9937)	0.0917 (2.2874)	0.8779 (1.4887)
2/$TS3_{ON2}$	1.9862 (1.2326)	0.9675 (1.4676)	0.1820 (2.1564)	0.0256 (3.8349)	0.3565 (1.8293)	0.0070 (3.5994)	0.2639 (1.9692)	0.8045 (1.5328)
2-N_2O	2.2906 (1.1567)	1.5294 (1.1984)	0.5782 (2.3500)	0.2554 (2.1448)	0.0343 (4.0669)	0.7682 (2.0001)	0.0147 (4.6706)	0.0366 (3.3264)
2/TS_{N2O}	2.0820 (1.1897)	1.4424 (1.2284)	0.4716 (2.2787)	0.4024 (1.9862)	0.0535 (3.3597)	0.6030 (2.0305)	0.1136 (2.6650)	0.1538 (2.8386)

6.3 QTAIM analysis of 2-N_2O

Bond critical points are located between the Cu, N, and O centres of the N_2O moiety. The low value of the electron density ρ(r) at BCP1 (0.001 e/a_0^3), combined with a positive value of the Laplacian $\nabla^2\rho$(r) (+0.241 e/a_0^5) and the small negative total energy density $H(r)$ (–0.007 E_h/a_0^3) are diagnostic of a bonding interaction. The delocalisation index for the Cu1–N1 linkage (0.375) is smaller than the formal bond order but support the above assignment. The parameters associated with the BCPs of the N_2O moiety are slightly reduced relative to the uncoordinated counterpart, due to the perturbation of the bonds upon coordination.

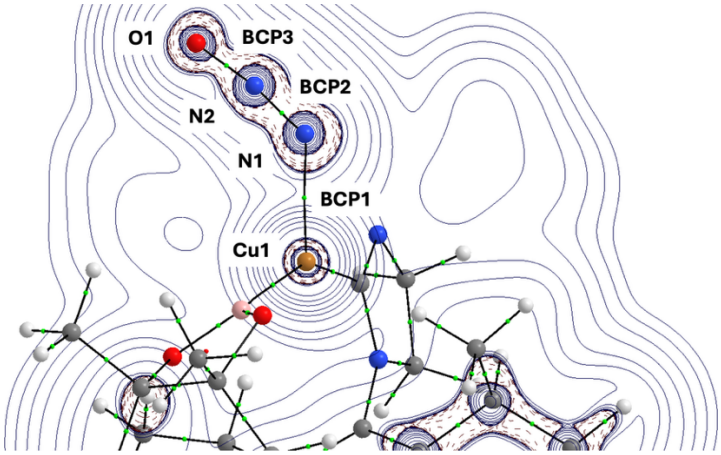

Figure S171. Molecular graph overlaid with the negative Laplacian of the electron density in the plane containg Cu1, N1, N2 and O1 for **2**-N_2O. The Dipp subsituent of the supporting NHC ligand has been omitted for clarity.

Table S4. Selected QTAIM properties of the BCPs in **2**-N_2O and free N_2O, where $\rho(r)$ is the electron density (e/a_0^3), $\nabla^2\rho(r)$ is the Laplacian of the electron density (e/a_0^5), ε is the bond ellipticity, δ(A|B) the delocalisation index, and $V(r)$, $G(r)$ and $H(r)$ represent the potential, kinetic and total energy density, respectively (E_h/a_0^3).

	BCP	$\rho(r)$	$\nabla^2\rho(r)$	ε	δ(A|B)	$V(r)$	$G(r)$	$H(r)$
2-N_2O	Cu1–N1	0.057	+0.241	0.076	0.375	–0.074	+0.067	–0.007
	N1–N2	0.551	–1.535	0.021	2.319	–1.463	+0.540	–0.923
	N2–O1	0.521	–1.182	0.002	1.729	–1.171	+0.438	–0.734
N_2O	N1–N2	0.572	–1.681	0.000	2.445	–1.611	+0.596	–1.016
	N2–O1	0.544	–1.314	0.000	1.771	–1.261	+0.466	–0.795

6.4 EDA-NOCV analysis of 2/TS_O, 2/TS_{ON2} and 2/TS_{N2O}

Interaction between **2** and N_2O in these transition states is charactered by charge transfer from the Cu–B σ-bonding/boryl lone pair orbitals into π* orbitals of N_2O. Values of ΔE_{prep} decrease in the order **2**/TS_O > **2**/TS_{N2O} > **2**/TS_{ON2}, mirroring the extent to which N_2O is distorted from linearity in these transition states, are offset most effectively in the $CuON_2B$ and CuN_2OB addition pathways. The larger value of ΔE_{orb} invoked along the CuN_2OB vs $CuON_2B$ addition pathway may be attributed to the higher oxophilicity of boron relative to copper.

Table S5. EDA-NOCV results for {**2**}{N_2O} fragmentation of **2**/TS_O, **2**/TS_{ON2} and **2**/TS_{N2O} (kcal·mol^{-1})

Energy	**2**/TS_O	**2**/TS_{ON2}	**2**/TS_{N2O}
ΔE_{int}	-27.07	-9.45	-25.68
ΔE_{disp}[a]	-7.72 (28.5%)	-8.14 (86.1%)	-8.23 (32.0%)
$\Delta E_{int\ (rest)}$[a]	-19.35 (71.5%)	-1.31 (13.9%)	-17.45 (68.0%)
ΔE_{Pauli}	+150.15	+64.15	+127.31
ΔE_{elstat}[b]	-97.12 (57.3%)	-45.89 (70.1%)	-86.88 (60.0%)
ΔE_{orb}[b]	-72.38 (42.7%)	-19.57 (29.9%)	-57.88 (40.0%)
ΔE_{σ}[c]	-60.55 (83.7%)	-13.80 (70.5%)	-45.43 (78.5%)
ΔE_{rest}[c]	-11.83 (16.3%)	-5.77 (29.5%)	-12.45 (21.5%)
ΔE_{prep}	+49.80	+17.67	+32.85
ΔE ($-D_e$)	+22.73	+8.22	+7.17

[a] Percentage contribution to ΔE_{int} in parentheses. [b] Percentage contribution to total attractive interactions (ΔE_{elstat} + ΔE_{orb}) in parentheses. [c] Percentage contribution to ΔE_{orb} for the dominant NOCV orbital pairs in parentheses.

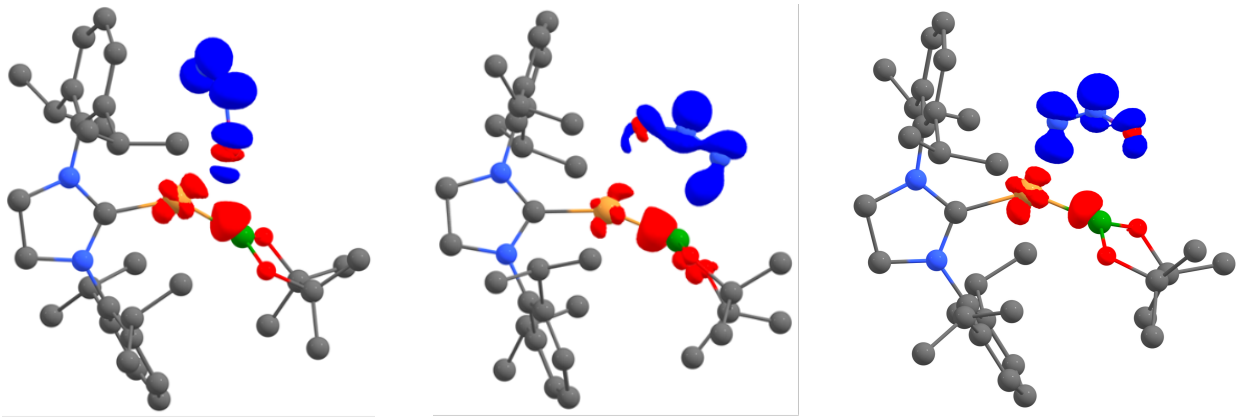

2/TS_O $|v_1|$ = 0.99 **2**/TS_{ON2} $|v_1|$ = 0.54 **2**/TS_{N2O} $|v_1|$ = 0.83

Figure S172. Deformation densities for {**2**}{N_2O} fragmentation. Charge flow from red to blue.

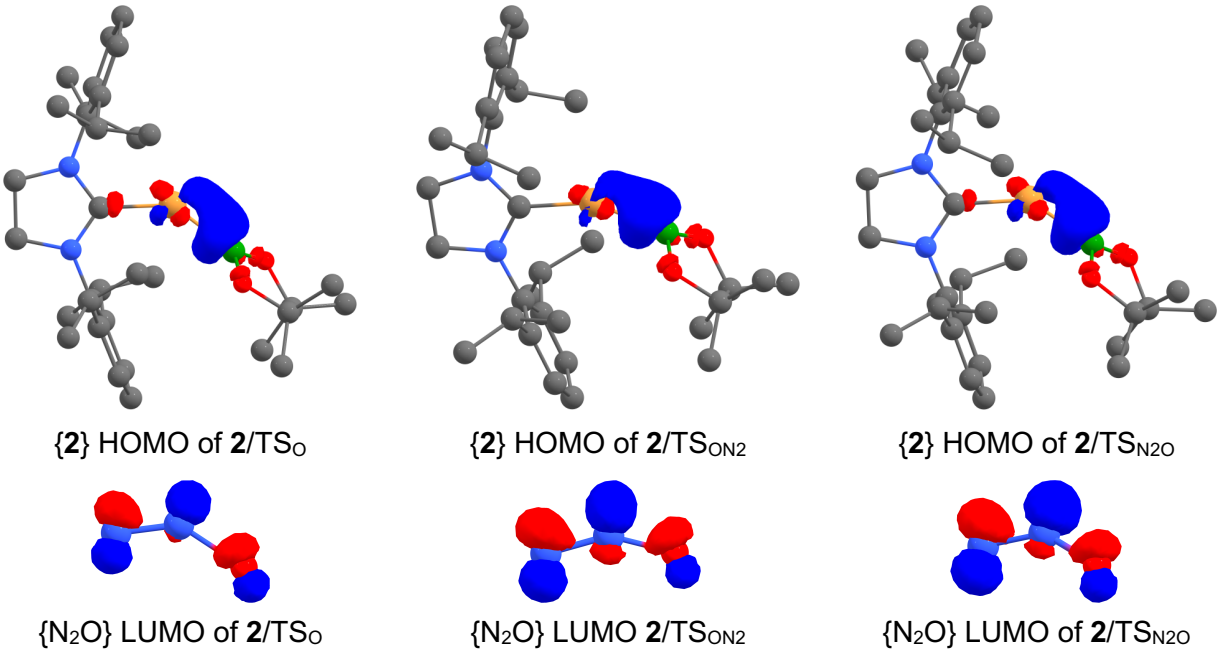

Figure S173. Frontier molecular orbitals of the {**2**} and {N_2O} fragments. Red/blue depicting phase.

6.5 Reaction profile for sigma bond metathesis between 2′ and B_2pin_2

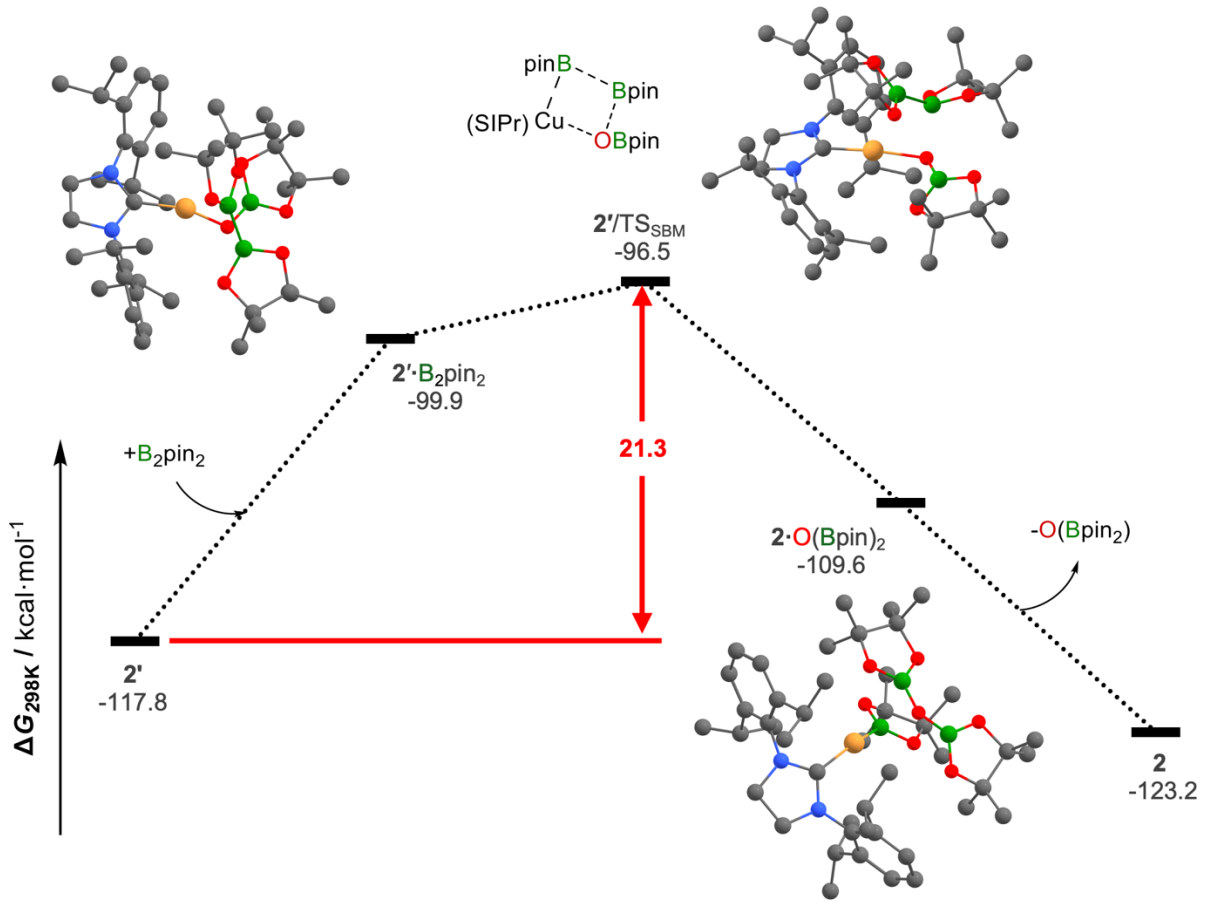

Figure S174. Sigma bond metathesis between **2'** and B_2pin_2. Energies corrected for benzene solvent and H-atoms omitted for clarity. Species **2'**·B_2pin_2 and **2**·$O(Bpin)_2$ are non-bonding encounter complexes.

6.6 Activation barriers for N_2O deoxygenation reactions catalysed by 2–5

Table S6. Calculated activation barriers for O-atom transfer ($\Delta G^{\ddagger}_{298K}$ / kcal·mol^{-1})

Int.	Concerted via TS_O			$CuON_2B$ addition via TS_{ON2}			CuN_2OB addition via TS_{N2O}		
	Benzene	**THF**	**Toluene**	**Benzene**	**THF**	**Toluene**	**Benzene**	**THF**	**Toluene**
2	31.9	31.0	31.8	18.9	19.3	18.8	16.8	16.0	16.7
3	31.5	30.8	31.4	20.6	21.0	20.5	17.1	16.4	17.0
4	32.4	31.3	32.3	20.6	20.8	20.5	18.0	17.4	17.9
5	32.8	32.0	32.7	20.0	20.5	20.0	19.1	18.6	19.0

Table S7. Calculated activation barriers for sigma bond metathesis ($\Delta G^{\ddagger}_{298K}$ / kcal·mol^{-1}).

Int.	Benzene	THF	Toluene
2'	21.3	23.0	21.2
3'	18.4	19.9	18.4
4'	18.3	20.0	18.3
5'	18.7	20.3	18.7

12 References

1 M. Teltewskoi, J. A. Panetier, S. A. Macgregor and T. Braun, *Angew. Chem. Int. Ed.*, 2010, **49**, 3947–3951.

2 D. S. Laitar, *PhD thesis, Massachusetts Institute of Technology* (USA), 2006, pp 43.

3 N. P. Mankad, D. S. Laitar and J. P. Sadighi, *Organometallics*, 2004, **23**, 3369–3371.

4 G. G. Dubinina, J. Ogikubo and D. A. Vicic, *Organometallics*, 2008, **27**, 6233–6235.

5 O. Santoro, F. Lazreg, Y. Minenkov, L. Cavallo and C. S. J. Cazin, *Dalton Trans.*, 2015, **44**, 18138–18144;

6 Y. M. Badiei and T. H. Warren, *Inorg. Synth*. 2010, **35**, 51.

7 G. M. Parker, S. Lau, B. Leforestier and A. B. Chaplin, *Eur. J. Inorg. Chem*. 2019, 3791–3798.

8 A. van der Ent, A. L. Onderdelinden and R. A. Schunn, *Inorg. Synth.*, 1990, **28**, 90–92.

9 G. Asensio, A. B. Cuenca, M. A. Esteruelas, M. Medio-Simón, M. Oliván, and M. Valencia, *Inorg. Chem.*, 2010, **49**, 8665–8667.

10 T. R. Hoye, B. M. Eklov and M. Voloshin, *Org. Lett.*, 2004, **6**, 2567–2570.

11 P. S. Pregosin, *NMR in Organometallic Chemistry*, Wiley-VCH, 2012, pp 251–254.

12 W. P. Leung, Q. W. Y. Ip, S. Y. Wong and T. C. W. Mak, *Organometallics*, 2003, **22**, 4604–4609.

[13] J. J. Gair, Y. Qiu, N. H. Chan, A. S. Filatov and J. C. Lewis, *Organometallics*, 2017, **36**, 4699–4706.

[14] M. A. Esteruelas, M. Oliván and A. Vélez, *Inorg. Chem.*, 2013, **52**, 5339–5349.

[15] M. A. Esteruelas, M. Oliván and A. Vélez, *Organometallics*, 2015, **34**, 1911–1924.

[16] Gaussian 16, Revision C.01, M. J. Frisch, G. W. Trucks, H. B. Schlegel, G. E. Scuseria, M. A. Robb, J. R. Cheeseman, G. Scalmani, V. Barone, G. A. Petersson, H. Nakatsuji, X. Li, M. Caricato, A. V. Marenich, J. Bloino, B. G. Janesko, R. Gomperts, B. Mennucci, H. P. Hratchian, J. V. Ortiz, A. F. Izmaylov, J. L. Sonnenberg, D. Williams-Young, F. Ding, F. Lipparini, F. Egidi, J. Goings, B. Peng, A. Petrone, T. Henderson, D. Ranasinghe, V. G. Zakrzewski, J. Gao, N. Rega, G. Zheng, W. Liang, M. Hada, M. Ehara, K. Toyota, R. Fukuda, J. Hasegawa, M. Ishida, T. Nakajima, Y. Honda, O. Kitao, H. Nakai, T. Vreven, K. Throssell, J. A. Montgomery, Jr., J. E. Peralta, F. Ogliaro, M. J. Bearpark, J. J. Heyd, E. N. Brothers, K. N. Kudin, V. N. Staroverov, T. A. Keith, R. Kobayashi, J. Normand, K. Raghavachari, A. P. Rendell, J. C. Burant, S. S. Iyengar, J. Tomasi, M. Cossi, J. M. Millam, M. Klene, C. Adamo, R. Cammi, J. W. Ochterski, R. L. Martin, K. Morokuma, O. Farkas, J. B. Foresman, and D. J. Fox, Gaussian, Inc., Wallingford CT, 2016.

[17] F. Neese, *WIRES Comput. Molec. Sci.*, 2025, **15**, e70019.

[18] J. P. Perdew, *Phys. Rev. B.,* 1986, **33**, 8822–8824; A. D. Becke, *Phys. Rev. A.,* 1988, **38**, 3098–3100.

[19] F. Weigend and R. Ahlrichs, *Phys. Chem. Chem. Phys.,* 2005, **7**, 3297–3305; F. Weigend, *Phys. Chem. Chem. Phys.,* 2006, **8**, 1057–1065.

[20] S. Grimme, J. Antony, S. Ehrlich and H. Krieg, *J. Chem. Phys.*, 2010, **132**, 154104; S. Grimme, S. Ehrlich and L. Goerigk, *J. Comp. Chem.*, 2011, **32**, 1456–1465.

[21] S. H. Vosko, L. Wilk, and M. Nusair, *Can. J. Phys.,* 1980, **58**, 1200–1211; C. Lee, W. Yang, and R. G. Parr, *Phys. Rev. B.,* 1988, **37**, 785–789; A. D. Becke, *J. Chem. Phys.*, 1993, **98**, 5648–5652.

[22] A. V. Marenich, C. J. Cramer and D. G. Truhlar, *J. Phys. Chem. B*, 2009, **113**, 6378–6396.

[23] Glendening, E. D.; Landis, C. R.; Weinhold, F. *J. Comput. Chem.*, 2013, **34**, 1429–1437.

[24] I. Mayer, *J. Comput. Chem.*, 2007, **28**, 204–221.

[25] R. F. W. Bader, *Acc. Chem. Res.*, 1985, **18**, 9–15.

[26] T. A. Keith, AIMAll (Version 19.10.12), 2019.

[27] M. P. Mitoraj, A. Michalak, and T. Ziegler, *J. Chem. Theory Comput.,* 2009, **5**, 962–975; M. P. Mitoraj, *J. Phys. Chem. A,* 2011, **115**, 14708–14716; P. Vermeeren, S. C. C. van der Lubbe, C. F. Guerra, F. M. Bickelhaupt and T. A. Hamlin, *Nature Protocols*, 2020, **15**, 649-667.

[28] G. A. Zhurko, D. A. Zhurko and G. A. Andrienko, Chemcraft Version 1.8 (Build 726b).